Skeletal Morbidity and Its Determinants in Type 1 Diabetes

Dr Suet Ching Chen
MBChB, MRCPCH

Submitted in fulfilment
of the requirements for the degree of
Doctor of Medicine

College of Medical, Veterinary and Life Sciences

March 2019

Abstract

Adults, and more recently, children with T1D have been found to have a significantly increased risk of fractures compared to the general population. The increased fracture risk is disproportioned to the marginal reduction in bone mineral density (BMD) observed in T1D suggesting that factors other than bone mineral status contribute to skeletal fragility. The National Institute of Health (NIH) Consensus Development Panel on Osteoporosis highlighted that bone strength is in fact dependent on two main factors: bone density and bone quality. Recognising the importance of bone quality as a factor determining bone health, this work set out to examine bone microarchitecture using novel imaging techniques of high-resolution magnetic resonance imaging (HR-MRI). Furthermore, HR-MRI enables the use of magnetic resonance spectroscopy (MRS) to quantify the amount of bone marrow fat, providing invaluable insight into the relationship between bone marrow adiposity and skeletal fragility. The background to this work, the current body of evidence and the rationale for the studies are therefore laid out in Chapter 1. All the methodology used in the thesis is summarised in Chapter 2, including the laboratory techniques carried out.

The clinical study was conducted in children with T1D as not only have these children been shown to have increased fracture risk, but also given that childhood and adolescence are important physiological periods for optimal bone development, it is therefore possible that they may be especially predisposed to abnormalities of bone health. The use of MRI as a research tool in children is relatively new, so I started this work exploring the practicality of this technique in children and using data from a previous HR-MRI study to determine the feasibility of partial set analysis of the images, the latter detailed in Chapter 3. This straight-forward exercise confirmed that partial MRI data sets can reliably represent a larger complete set of images when assessing trabecular bone microarchitecture parameters.

The overall objective of this thesis is to assess the bone health of children with Type 1 diabetes, by using HR-MRI to study the trabecular bone microarchitecture, in addition to bone mineral density and bone turnover status as detailed in Chapter 4. A cross-sectional case control study was conducted in 32 children with T1D and compared to 26 healthy age- and gender- matched controls. The primary hypothesis of the study was proven, in that children with T1D were found to have poorer bone microarchitecture with lower trabecular bone volume compared to the controls. Children with T1D also had lower number of trabeculae and the trabeculae were spaced further apart from one another. Although this study demonstrated that children with T1D fracture more than children without the

condition, it did not however show any relationship between the compromised bone microarchitecture to fracture. In fact, the children with T1D who fractured were found to have significantly lower bone mineral density and poorer glycaemic control. There was also no significant disparity in the bone marrow adiposity between the two groups.

In parallel, I performed one year of laboratory-based experiments to study the differentiation of mesenchymal stem cells (MSCs), which are the precursors to bone (osteoblasts) and fat cells (adipocytes), as detailed in Chapter 5. My main aim was to study the effects of metformin, a drug increasingly used in patients with T1D, on the MSC differentiation in order to determine if metformin may have a therapeutic bone protective role. My studies successfully demonstrated *in vitro* that metformin exerted reciprocal control over the osteogenic transcription factor Runx2, and the adipogenic transcription factor, PPARγ; promoting osteogenesis through an increase in Runx2 transcriptional activities, independently of Runx2 protein expression, and suppressing adipogenesis, through suppression of PPARγ protein expression and activity. I proceeded to study the underlying molecular mechanisms of the metformin action, starting with AMP-activated protein kinase (AMPK) given that metformin is a known AMPK activator. To our fascination, the study found that the suppression of adipogenesis by metformin appeared to be independent of AMPK activation but rather through the suppression of the mTOR/$p70^{S6K}$ signalling pathway.

Chapter 6 summarised all my work for this thesis, highlighting its strengths and limitations as well as providing my perspectives into the future directions of this work.

Table of Contents

List of Tables

List of Figures

Scientific Outputs Arisen from this Thesis

Publications **(Attached in Appendices)**

Chen SC, Shepherd S, McMillan M, McNeilly J, Foster J, Wong SC, Robertson KJ, Ahmed SF. Skeletal Fragility & Its Clinical Determinants in Children with Type 1 Diabetes. *J Clin Endocrinol Metab*. 2019 Mar 8. pii: jc.2019-00084. doi: 10.1210/jc.2019-00084

Chen SC, Brooks R, Houskeeper J, Bremner SK, Dunlop J, Viollet B, Logan PJ, Salt IP, Ahmed SF, Yarwood SJ. Metformin Suppresses Adipogenesis through Both AMP-activated Protein Kinase (AMPK)-dependent and AMPK-independent Mechanisms. *Mol Cell Endocrinol* 2017;440:57-68

Abdalrahman N, **Chen SC**, Wang JR, Ahmed SF. An Update on Diabetes related Skeletal Fragility. *Expert Review of Endocrinology & Metabolism* 2015;10:193-210

Abstracts

Chen SC, Shepherd S, McMillan M, McNeilly J, Foster J, Wong SC, Robertson KJ, Ahmed SF. The Determinants of Skeletal Fragility in Children with Type 1 Diabetes Mellitus. *Proceedings from the 57th Annual European Society for Paediatric Endocrinology (ESPE), Athens, Sep 2018. Horm Res Paediatr 2018;90(Suppl 1):pp111 [Oral RFC 11.5]*

Chen SC, Brooks R, Houskeeper J, Bremner SK, Dunlop J, Viollet B, Logan PJ, Salt IP, Ahmed SF, Yarwood SJ. Metformin Suppresses Adipogenesis through Both AMP-activated Protein Kinase (AMPK)-dependent and AMPK-independent Mechanisms. *Proceedings from the 55th Annual European Society for Paediatric Endocrinology (ESPE), Paris, Sep 2016. Horm Res Paediatr 2016;86(Suppl 1):pp39 [Oral FC 5.1]*

Chen SC, Shepherd S, McMillan M, McNeilly J, Robertson KJ, Wong SC, Ahmed SF. Fractures in Children with Type 1 Diabetes are Associated with Poorer Bone Mineral Status and Glycaemic Control. *Proceedings from the 55th Annual European Society for Paediatric Endocrinology (ESPE), Paris, Sep 2016. Horm Res Paediatr 2016;86(Suppl 1):pp187 [Poster P2-160]*

Chen SC, Brooks R, Ahmed SF, Yarwood SJ. Metformin regulates the differentiation of murine mesenchymal stem cells via AMPK-independent suppression of p70s6-kinase. *Diabetes UK Professional Conference, Glasgow, Mar 2016. Diabetic Medicine*. 2016;33(*Suppl 1:pp32) [Oral A77, Poster P38]*

Chen SC, Brooks R, Ahmed SF, Yarwood SJ. Metformin regulates the differentiation of murine mesenchymal stem cells via AMPK-independent suppression of p70s6-kinase. *1st European Bone Marrow Adiposity Meeting, Lille, France. Aug 2015. Oral*

Chen SC, Abdalrahaman N, McComb C, Foster J, Ahmed SF. The Precision of Partial Image Analysis of Trabecular Bone Microarchitecture by High-resolution Magnetic Resonance Imaging (HR-MRI). *7th International Conference on Children's Bone Health (ICCBH), Salzburg, Jun 2015. Bone Abstracts 4 Poster P178*

Chen SC, Brooks R, Ahmed SF, Yarwood SJ. Metformin regulates the differentiation of murine mesenchymal stem cells via AMPK-independent suppression of p70s6-kinase. *43nd Meeting of the British Society for Paediatric Endocrinology and Diabetes (BSPED), Sheffield, Nov 2014. Endocrine Abstracts 39 Poster EP16*

Chen SC, Brooks R, Ahmed SF, Yarwood SJ. The Role of AMPK Pathway in Mediating the Effects of Metformin on Mesenchymal Stem Cell Differentiation. *42nd Meeting of the British Society for Paediatric Endocrinology and Diabetes (BSPED), Winchester, Nov 2014. Endocrine Abstracts 36 Oral OC6.4*

Chen SC, Brooks R, Ahmed SF, Yarwood SJ. The Role of AMPK in Mediating the Effects of Metformin on Mesenchymal Stem Cell Differentiation. *Yorkhill Research Day, University of Glasgow, Nov 2014. Oral OC16*

Achievement and Awards for this Work

Shortlisted for Nick Hales Young Investigator Award – Metformin regulates the differentiation of murine mesenchymal stem cells via AMPK-independent suppression of p70s6-kinase. *Diabetes UK Professional Conference, 2016*

Best Abstract Award - The Role of AMPK Pathway in Mediating the Effects of Metformin on Mesenchymal Stem Cell Differentiation. *42nd Meeting of the British Society for Paediatric Endocrinology and Diabetes, 2014*

Best Oral Presentation – The Role of AMPK in Mediating the Effects of Metformin on Mesenchymal Stem Cell Differentiation. *Yorkhill Research Day, 2014*

Clinical Research Fellowship Award (£65,000) for the research proposal – *Glasgow Children's Hospital Charity, 2013*

Dedicated to my husband, Douglas, and my daughter, Annabel, for their love, understanding and support; as well as my parents, who have always believed in me.

Acknowledgement

This thesis would not have come to fruition without the support and encouragement from my principal supervisor Professor Faisal Ahmed, whose foresight made this work possible and attention to detail provided my drive to excel.

I am also indebted to Dr Stephen Yarwood who supervised my laboratory work, for his invaluable advice and guidance. I am incredibly grateful to the members of Dr Yarwood and Dr Ian Salt's laboratory, in particular to Euan Parnell and Julia Dunlop, for their patience in guiding me through the laboratory techniques involved.

I would also like to express my utmost gratitude to Dr Guftar Shaikh, for being a constant source of motivation and his confidence in me to complete the writing of this thesis. This work would also not have been possible without the support of the Paediatric Diabetes Service in Glasgow, spearheaded by Dr Kenneth Robertson.

My sincere thanks to Dr Christie McComb for her expertise in the MRI pulse sequence determination and the MRI radiographers Tracey Steedman, Rosemary Woodward, Caroline Crosbie and Evonne McLennan for their assistance with image acquisition. The help of Dr Sheila Shepherd with the DXA scans and analysis support is very much appreciated. I would also like to thank Dr Jane McNeilly and Martin McMillan for their assistance in the processing of the biochemical samples.

I am also grateful to Glasgow Children's Hospital Charity (previously known as Yorkhill Children's Charity) for my clinical fellowship award, and to Tenovus Scotland and the British Society of Paediatric Endocrinology and Diabetes for funding the study.

Finally, I could not thank enough my husband, family and friends, for spurring me on and their moral support to the very end. A special thanks to my cousin, Hooi Ching, for providing in-house help and endless hours of entertainment for my little one to facilitate the writing of this thesis.

Author's Declaration

I declare, except where reference is made to the contribution of others that all work presented in this thesis was performed entirely by myself and has not been submitted for any other degree at the University of Glasgow, or any other institution.

Dr Suet Ching Chen

I certify that the work reported in this thesis has been performed by Dr Suet Ching Chen and that during the period of study, she has fulfilled the conditions of the ordinances and regulations governing the Degree of Doctor of Medicine, University of Glasgow.

Prof S Faisal Ahmed

Abbreviations

aBMD	areal bone mineral density
ACC	acetyl co-A carboxylase
AGD	ascorbic acid, β-glycerolphosphate, dexamethasone
AGEs	advanced glycation end-products
AICAR	5-aminoimidazole-4-carboxamide riboside
ALS	acid labile subunits
AMP	adenosine monophosphate
AMPK	AMP-activated protein kinase
AP	alkaline phosphatase
APN	adiponectin
appBV/TV	apparent bone volume to total volume ratio
appTbN	apparent trabecular number
appTbSp	apparent trabecular spacing
appThTh	apparent trabecular thickness
ATP	adenosine triphosphate
BA	bone area
BAP	bone alkaline phosphatase
BMA	bone marrow adiposity
BMAD	bone mineral apparent density
BMC	bone mineral content
BMD	bone mineral density
BMF	bone marrow fat
BMI	body mass index
BMMSCc	bone-marrow-derived mesenchymal stem cells
BMPs	bone morphogenic proteins
C/EBP	CCAAT-enhancer binding protein
CI	confidence interval
CSA	cross sectional area
CSII	continuous subcutaneous insulin infusion
CT	computed tomography
CTX	cross-linked C-terminal telopeptide of Type 1 collagen
CV	coefficient of variation
DKA	diabetic ketoacidosis
DKK-1	dipkoff-1
DM	diabetes mellitus
DMEM	Dulbecco’s modified eagle medium
DNA	deoxyribonucleic acid
DPP-4	dipeptidyl peptidase-4

Dpyr	deoxypyridoline
DXA	dual energy X-ray absorptiometry
ELISA	enzyme-linked immunosorbent assay
FEA	finite element analysis
FF	fat fraction
FGF	fibroblast growth factor
FN	femoral neck
FOV	field of view
FRAX	fracture risk assessment tool
GH	growth hormone
GLP-1	glycogen-like peptide 1
HbA1c	haemoglobin A1c
hMSC	human mesenchymal stem cell
HPro	hydroxyproline
HR-MRI	high resolution magnetic resonance imaging
HR-pQCT	high resolution peripheral quantitative computed tomography
IBMX	3-isobutyl-1-methylxanthine
IFN	interferon
IGF	insulin-like growth factor
IGFBP	insulin-like growth factor -binding protein
IID	insulin, IBMX, dexamethasone
IL	interleukin
IM	images
IR	insulin receptor
KO	knock out
LBM	lean body mass
LS	lumbar spine
LWR	lipid to water ratio
MCP	monocyte chemoattractant protein
MDI	multiple daily (insulin) injections
MIL	mean intercept length
miRNA	micro-ribonucleic acid
MRI	magnetic resonance imaging
mRNA	messenger ribonucleic acid
MRS	magnetic resonance spectroscopy
MSCs	mesenchymal stem cells
mTOR	mammalian target of rapamycin
MVD	microvascular diseases
NMV	net magnetisation vector
OC	osteocalcin

OI	osteogenesis imperfecta
OPG	osteoprotegerin
OR	odds ratio
ORO	oil red O
PHV	peak height velocity
PIO	pioglitazone
PPARγ	peroxisome proliferator-activated receptor gamma
pQCT	peripheral quantitative computed tomography
PREF-1	pre-adipocyte factor-1
PRESS	point-resolved spectroscopy sequence
PTH	parathyroid hormone
PVDF	polyvinylidene difluoride
Pyr	pyridoline
QCT	quantitative computed tomography
QUS	quantitative ultrasound
RANK	receptor activator of nuclear factor κβ
RANKL	receptor activator of nuclear factor κβ ligand
RCT	randomised controlled trial
RF	radiofrequency
ROI	region of interest
ROS	reactive oxygen species
RR	relative risk
Runx	Runt-related proteins
Runx2	Runt-related transcription factor 2
SDS	standard deviation score
SDS-PAGE	sodium dodecyl sulfate-polyacrylamide gel electrophoresis
SGLT-2	sodium/glucose con-transporter 2
SNR	signal-to-noise ratio
STZ	streptozocin
T1D	Type 1 diabetes mellitus
T2D	Type 2 diabetes mellitus
TB	total body
TBLH	total body less head
TBS	tris-buffered saline
TBST	tris-buffered saline with Tween20
TE	echo time
TGFβ	transforming growth factors-β
TNFα	tumour necrosis factors-α
TR	repetition time
TrueFISP	true fast imaging with steady state precession

TZDs	thiazolidinediones
TUNEL	terminal deoxynucleotidyl transferase dUTP nick end labeling
vBMD	volumetric BMD
VF	vertebral fracture
WT	wild type

1 Introduction

1.1 Background to the thesis

T1D affects 300,000 people in the UK, of which 35,000 are children. The incidence of T1D is 1:4000, with peak age at diagnosis between 9-14 years old. In addition to the many target organs that are typically associated with dysfunction in diabetes mellitus, the skeleton has now been recognised as another organ adversely affected in diabetes mellitus. The effects on bone health manifest clinically as early osteoporosis and fragility fractures, with increased incidence of hip fractures particularly in patients with T1D compared to age-matched non-diabetics (Vestergaard 2007, Hothersall *et al.* 2014). In addition, this increased risk is also evident in young adults (Hothersall *et al.* 2014). Given that childhood and adolescence are important physiological periods for optimal bone development, it is possible that children and adolescents with T1D may be especially predisposed to abnormalities of bone health.

In adults, patients with T1D have a modest 10% lower BMD than the general population (Vestergaard 2007) which generates an estimated relative hip fracture risk of 1.4-fold (Table 1.1) but instead, a meta-analysis of several large cohort studies demonstrated a disproportionately higher risk of hip fractures by 7-folds (Figure 1.1) (Janghorbani *et al.* 2007). Such disparities between dual x-ray absorptiometry (DXA)-derived BMD and actual fracture risk in T1D suggest that factors other than BMD need to be considered more comprehensively. This is acknowledged by the National Institute of Health (NIH) Consensus Development Panel on Osteoporosis which recognises the importance of bone microarchitecture as a factor determining bone health (NIH Consensus Development Conference Panel 1993) High resolution MRI provides the necessary information of cortical and trabecular microarchitecture, analogous to high resolution computed-tomography (CT) but without the radiation (Seeman and Delmas 2006, Wehrli 2007). In addition, spectroscopic imaging in MRI also enables evaluation of bone marrow adiposity (BMA) (Wehrli *et al.* 2000), an issue which is gaining increasing attention in the field of osteoporosis because of the connection between adipogenesis and osteogenesis (Fazeli *et al.* 2013).

Table 1.1 Observed changes in BMD and expected change in fracture risk

Type of diabetes	**Spine Z-score**	**Hip z-score**
T1D	-0.22 ± 0.01	-0.37± 0.16
T2D	0.41± 0.01	0.27± 0.01
Expected relative fracture risk	**Any fracture**	**Hip fracture**
T1D	1.09	1.42
T2D	0.85	0.77

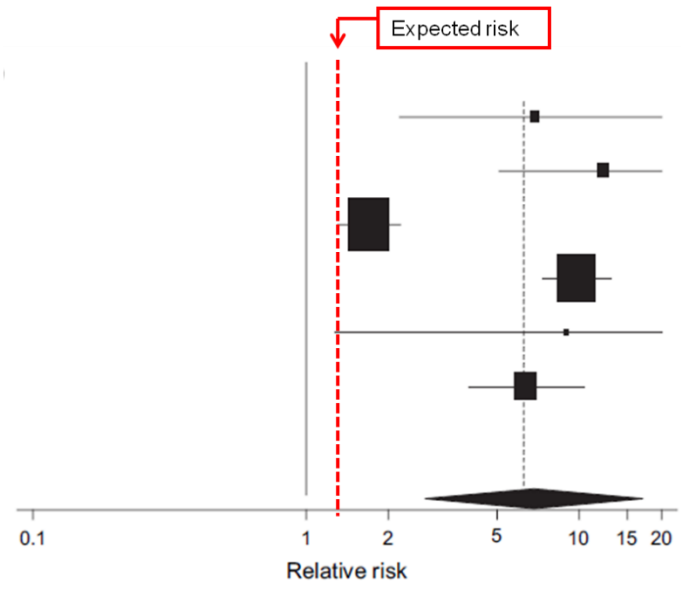

Figure 1.1 Meta-analysis of the association between T1D and risk of hip fracture. Results from 6 studies showed that adults with T1D have an almost 7-fold increase in relative risk of hip fracture compared to that of the general population. This is disproportionately high for the expected risk of fracture predicted from the marginal reduction in bone mineral density (see Table 1.1). [Adapted from (Janghorbani *et al.* 2007)]

NHS Greater Glasgow and Clyde Paediatric Diabetes Service is one of the largest paediatric diabetes centre in the UK looking after over 750 children with Type 1 diabetes. In 2015 the Royal Hospital for Children in Glasgow moved to one of the largest biomedical campuses in Europe with a dedicated £10million clinical research facility and state-of-the-art MRI imaging facilities. This provided me an ideal opportunity to carry out a comprehensive multi-modality assessment looking at the bone health of children with Type 1 diabetes, without radiation exposure.

Evidence suggests that diabetic bone loss involves a complex interplay of chronic hyperglycaemia, insulin deficiency, increased marrow adiposity, inflammation and vasculopathy, although the exact underlying pathogenesis remains unclear. *In vitro* and *in vivo* studies in T1D point towards a defect in bone formation (Rico *et al.* 1989, Verhaeghe *et al.* 1990, Pater *et al.* 2010), in contrast to bone resorption which is the underlying mechanism of age-related osteoporosis. Importantly, this highlights therapeutic implications for treating diabetic bone loss with bisphosphonates, which is current practice for age-related osteoporosis and fragility fracture, as it will not be mechanistically sound. The anti-diabetic drug metformin, however, may have a bone protective effect as reduction in fracture risks has been noted in Type 2 diabetes mellitus (T2D) patients on this medication (Vestergaard *et al.* 2005, Zinman *et al.* 2010). Metformin is also increasingly used in T1D to improve insulin sensitivity and glycaemic control (Vella *et al.* 2010), so it would be advantageous to

ascertain the underlying mechanisms by which metformin protects bones. This led me to a one-year laboratory research at the Institute of Molecular, Cell and Systems Biology, University of Glasgow, studying the effects of metformin on mesenchymal stem cell differentiation into bone (osteoblasts) and fat cells (adipocytes).

I hope that this work will contribute to a better understanding of the extent of skeletal morbidity in children with Type 1 diabetes and its relationship to the disease. I further hope that it will not only elucidate the causes, but also provide evidence for measures to protect bone health in this cohort of children from an early age. Based on my laboratory research, I hope to establish the bone protective mechanisms of metformin as a therapeutic potential for use in diabetic osteopathy.

1.2 Bone development and its components

Bone is a mineralised connective tissue with an impressive hierarchical organisation from a macroscopic to microscopic level. This confers it a combination of stiffness and toughness allowing it to perform its multifunctional role from locomotion, support and protection of vital organs such as heart, lungs and brain, to mineral homeostasis and haematopoiesis. More recent discoveries revealed that bone also has an endocrine function, in particular through osteocalcin and its role in glucose metabolism. Circulating undercarboxylated osteocalcin, itself regulated by insulin acts on pancreatic β-cells to further increase β-cell mass and subsequent insulin secretion in a feed-forward loop (Ducy *et al.* 1996, Lee *et al.* 2007, Ferron *et al.* 2010).

1.2.1 Bone architecture

On a macroscopic level, bone is made up of two main entities: cortical and trabecular bone, giving rise to four distinct surfaces called skeletal envelopes which are morphologically distinct with different roles: periosteal, endocortical, trabecular and intracortical envelopes (Figure 1.2).

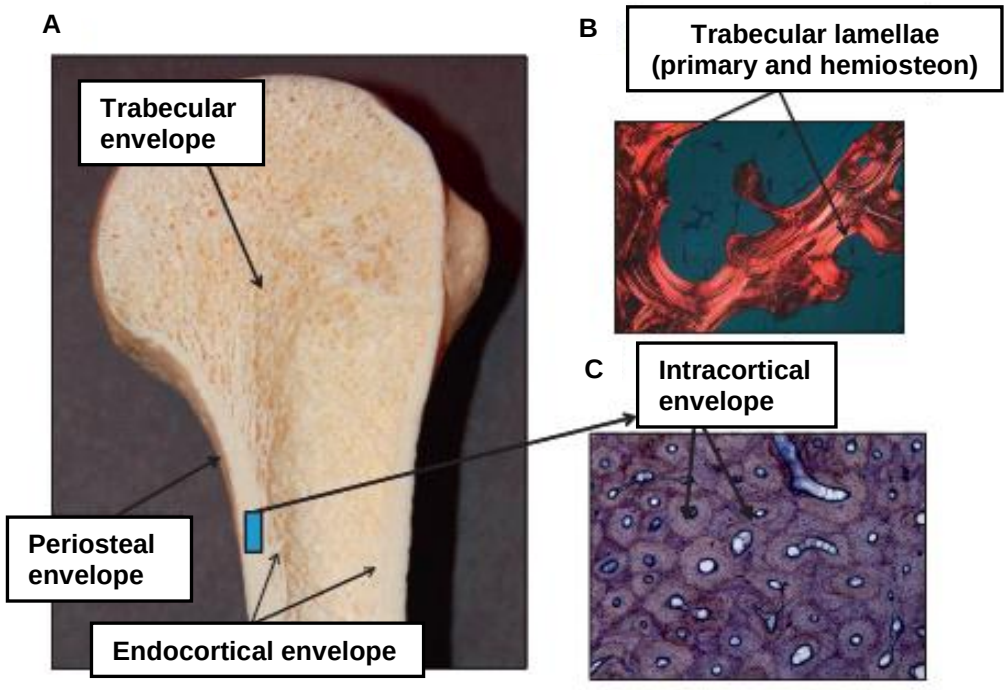

Figure 1.2 Bone structure. (A) Macroscopically, bone appears as either lace-like trabecular bone or denser cortical bone. These create four different kinds of surfaces. called envelopes, upon which bone cells act. (B) Trabeculae in the cancellous bone compartment consist mostly of primary lamellae. However remodelled areas (areas in which bone has been resorbed and reformed) can also form hemiosteons, similar to half osteons). (C) The intracortical envelope in humans is packed with secondary osteons, or Haversian systems. [Adapted from (Burr and Akkus 2014)].

The adult skeleton is composed of 80% cortical bone and 20% trabecular bone (Eriksen *et al.* 1994). The ratio of cortical to trabecular bone varies in different bones and skeletal sites. Whilst the radial diaphysis is 95:5 cortical to trabecular bone, the vertebra is only 25:75 with trabecular predominance. Within the long bone, the hollow shaft, or diaphysis, is composed primarily of cortical bone whereas the metaphysis and epiphyses are composed of mainly trabecular bone with only a thin shell of cortical bone. Both cortical and trabecular bones are composed of osteons.

1.2.1.1 Cortical bone

Cortical bone is the dense and solid thick outer shell of bones, also known as the "compact" bone. Although it constitutes 80% of the total bone mass, cortical bone has a substantially smaller surface area than trabecular bone (Weatherholt *et al.* 2012). Osteons are the basic units in the cortical bone orientated along the long axis of the bone with a central Haversian canal, together forming the Haversian system. They are cylindrical in shape with circumferential bands of bone where collagen and mineral exist in discrete sheets (known as concentric lamellae) in the walls of the Haversian system, as shown in Figure 1.3. The collagen fibres of the concentric lamellae are orientated in alternating directions to give strength to the tissue.

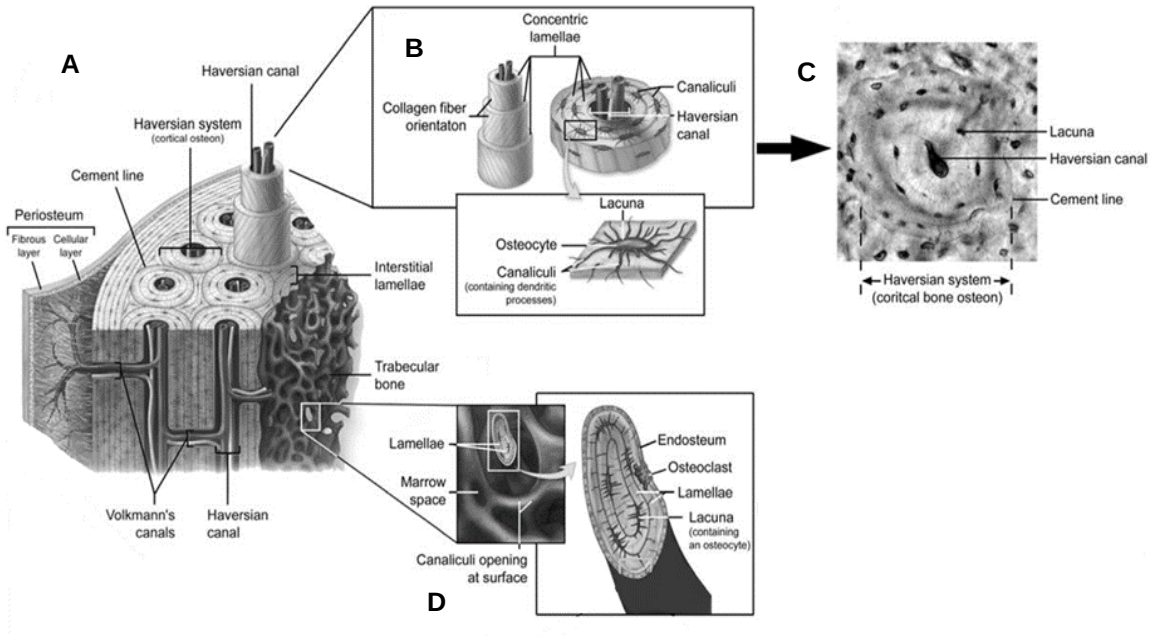

Figure 1.3 The hierarchical organisation of bone on a microscopic level. (A) Schematic diagram of a bone microstructure. (B) Cortical bone osteon or Haversian system with a central Haversian canal, with concentric lamellae and uniformly spaced lacunae. (C) Cross section of a cortical bone osteoid under light microscopy. (D) Trabeculae shown in cross section with lamellae of bone, lacunae and outer covering of endosteum. [Adapted from (Weatherholt *et al.* 2012)]

There are many interconnected canals (lacunae and canaliculi) through which bone cells communicate and receive vascular supply. These canals give rise to the low 3-5% of porosity in cortical bone (Burr and Akkus 2014). Increased cortical remodeling causes an increase in cortical porosity and decrease in cortical bone mass (reduction in cortical volumetric bone mineral density (vBMD) (Clarke 2008).

Cortical bone has an outer periosteal surface and an inner endosteal surface. On the periosteal surface, bone formation exceeds resorption, hence bone increases in diameter (appositional growth) with aging. On the endosteal surface, the opposite is true with bone resorption typically exceeding formation, so the marrow space expands with aging. Higher remodelling activity takes place on the endosteal surface, with greater biomechanical strain and greater inflammatory exposure from the adjacent marrow (Clarke 2008). Trabecular bone loss begins first, in early adulthood for both sexes, before cortical bone which begins during middle age for women, though much later in men (after age 75 years) (Riggs *et al.* 2008). By age 50 years, approximately 40% of total lifetime trabecular loss has occurred, in contrast to only 15% of cortical bone lost (Riggs *et al.* 2008).

1.2.1.2 Trabecular bone

Trabecular bone, also known as the "spongy" bone, or cancellous bone, is the honeycomb-like network of plate and rod-like structures found predominantly in the metaphyses of long bones, vertebrae and ribs (Figure 1.4A). Trabecular bone constitutes 20% of the total bone mass in the skeleton. Unlike the cortical osteons, the trabecular osteons are *hemi*osteons without central Harversian canal due to bone remodelling on the longer surface of the trabeculae. The lamellae are arranged parallel to this longer trabecular surface (Burr and Akkus 2014). Trabecular bone has 50-90% higher porosity relative to the cortical bone (Weatherholt *et al.* 2012).

The porosity helps trabecular bone to be light yet add strength to the skeleton by providing a honeycomb scaffolding to reinforce the ends of long bones, close to the joints, which are often subjected to mechanical stresses from the sides. The trabecular bones help to channel the mechanical stresses imposed on it to the stronger, and more solid cortical bones. In the vertebrae, it helps to cushion axial loading forces on the skeleton.

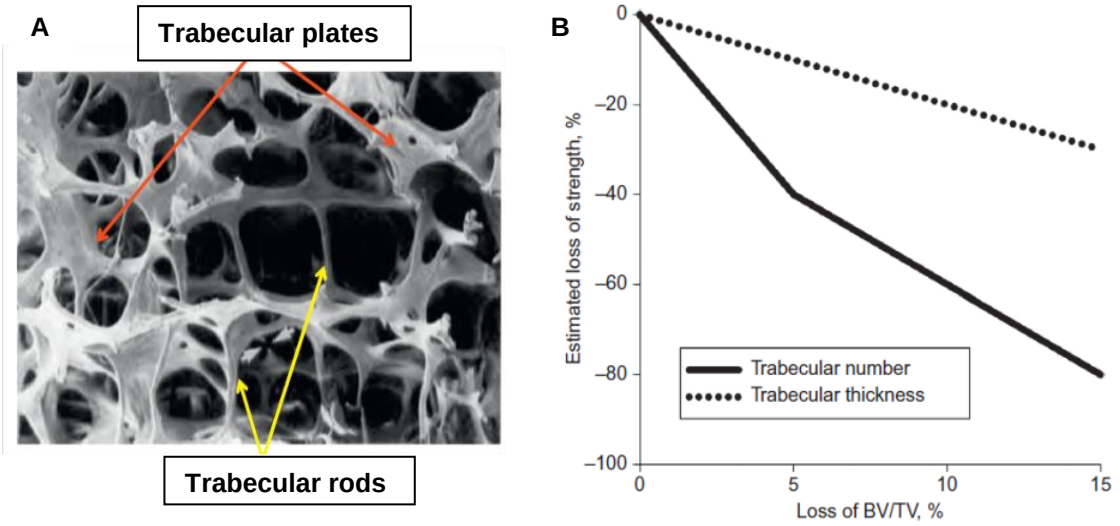

Figure 1.4 Trabecular bone. (A) Trabecular bone is composed of broader plates and thinner rods When bone is lost, more of the trabecular plates convert to being rod-like. (B) Impact of trabecular number and trabecular thickness on bone strength. Reduction in trabecular number has a greater negative impact on bone strength than does the loss of an equal amount of bone through trabecular thinning [Adapted from (Mosekilde 1990), (Burr and Akkus 2014)]

In healthy humans, the trabeculae tend to be shaped as plates rather than circular or elliptical rods. The architecture of the trabecular bone can be characterised by the number of trabeculae (TbN), how thick they are (TbTh), and how far apart they are (TbSp) all contributing to the overall trabecular bone volume (BV). TbTh ranges between 50-400µm, averaging about 200µm in adults (Eriksen *et al.* 1994) and 150µm in children up to 16 years (Glorieux *et al.* 2000), with an estimated total trabecular area of $7m^2$ (Clarke 2008).

The ideal relationship between TbN and TbTh is not only dependent on the site, but also the primary direction of the loading forces (Burr and Akkus 2014). Most importantly, TbN have a bigger impact on the strength of the bone than TbTh, with the loss of a complete trabeculae (reduced TbN) weakening the bone by 2-3 folds more compared to losing the same amount through thinning of the trabeculae (reduced TbTh) (Figure 1.4B). This highlights the importance of connectivity within the trabecular architecture. The loss of connectivity can also occur when trabecular bone plates become more rod-like, as with the case in osteoporosis. Trabecular bone is also preferentially lost; earlier and at a greater rate than cortical bone during aging resulting in skeletal fragility at trabecular rich sites such as distal radius (Riggs *et al.* 2008) and femoral head (Li and Aspden 1997, Ciarelli *et al.* 2000).

1.2.2 Bone cells and matrix

Bone is a living tissue made up of minerals, organic matrix, water and lipids, as seen in Figure 1.5. The organic matrix is 90% **Type 1 collagen** with a trace amount of Type III and V collagen, providing bone its elasticity and flexibility (Clarke 2008). The collagen fibres are made up of triple helixes of three polypeptide chains, connected by different kinds of cross-links. which can alter the material properties of the tissue, and ultimately the mechanical behaviour of the whole bone. These cross links, such as pyridinoline and deoxypyridinoline, can be formed through enzymatic processes, or through non-enzymatic glycation, creating advanced glycation end products (AGEs) such as pentosidine.

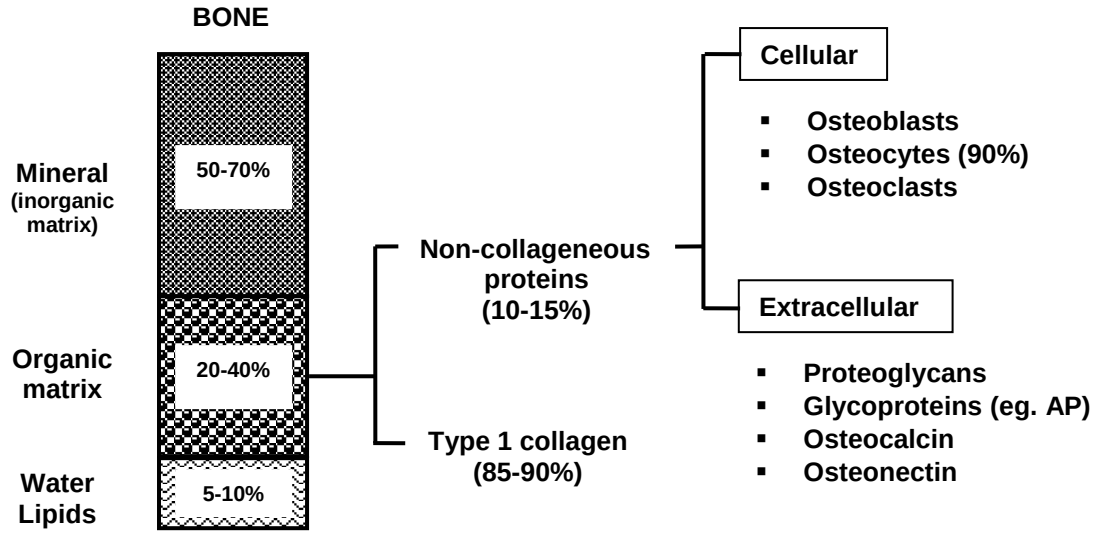

Figure 1.5 Bone composition. Bone is comprised predominantly of calcium hydroxyapatite mineral, with Type I collagen making up most of the organic matrix.

The inorganic matrix is predominantly **calcium hydroxyapatite** which is interspersed with the collagen fibres conferring bone the mechanical rigidity and load-bearing strength to bone. Human bones are 60% mineralised (Seeman and Delmas 2006). The balance of distribution between collagen and mineral is crucial to ensure bone is stiff enough to provide mechanical support yet has the flexibility to absorb and redistribute loading stresses. Alteration in this balance with aging and with diseases can therefore compromise the structural integrity of bone resulting in increased susceptibility to fracture. In diabetes, especially when free sugar is in abundance due to poor glycaemic control, AGEs accumulate in the extracellular matrix (Yamamoto *et al.* 2001). The increased cross linking increases the stiffness of the bone ultimately making it too brittle resulting in fragility fracture (Vashishth *et al.* 2001).

There are three distinct types of cells found within bone: i) the **Osteoblasts** (3-4% of the cells in bone) which synthesise and regulate the deposition and mineralisation of the extracellular matrix of bone. These cells are derived from pluripotent mesenchymal stem cells, as described in detail in section 1.3, and have a lifespan of up to 8 weeks in humans, during which time they lay down osteoid (including proteoglycans, glycoproteins and collagen fibres) before becoming embedded in their own calcified matrix and developing morphologically into an osteocyte. ii) **Osteocytes**, are the most abundant bone cells (90-95%) and the longest lived with a life span of up to 25 years (Capulli *et al.* 2014). Although derived from osteoblasts, they are distinctively different in function. These spider-shaped cells have long and branched cellular processes that extend throughout bone aiding cell to cell communication and intracellular transport of small signalling molecules. iii) **Osteoclasts** are derived from haematopoetic stem cells, although their formation (osteoclastogenesis) remains dependent on osteoblasts and osteoblast precursors. The osteoblasts secrete receptor activator of nuclear factor-ƙB ligand (RANKL) and macrophage colony-stimulating factor (CSF) to recruit and activate the differentiation of osteoclast precursors into osteoclasts (Figure 1.6). Osteoprotegerin (OPG), also produced by osteoblasts, is a competitive inhibitor of RANKL binding to RANK receptor so the ratio of RANKL:OPG determines osteoclastogenesis. Functionally, osteoclasts are the only cells capable of resorbing mineralised bone.

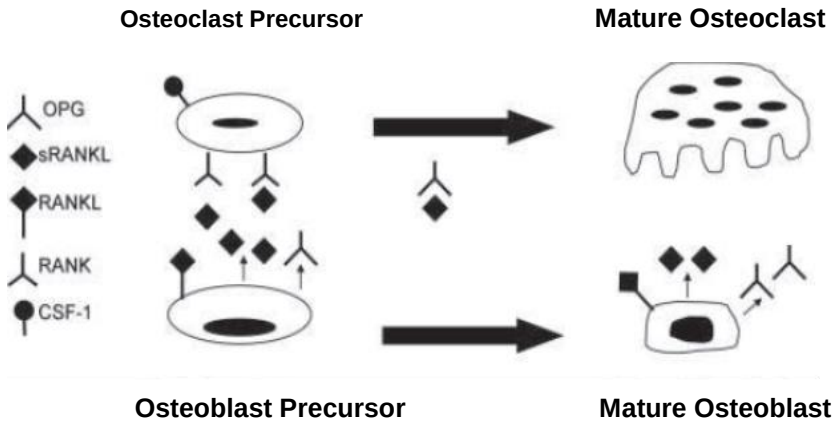

Figure 1.6 Regulation of Osteoclastogenesis by RANKL and OPG. Osteoclasts are derived from haematopoetic stem cells although their formation remains dependent on osteoblasts. Osteoblasts and osteoblast precursors produce two forms of RANKL which stimulate osteoclast recruitment and activation. The membrane-bound form directly interacts with membrane-bound RANK molecules on adjacent osteoclast precursors. The soluble form diffuses through the intercellular space and interacts with the membrane-bound RANK molecules on nearby osteoclast precursors. Osteoprotegerin (OPG) acts as a decoy receptor (inhibitor) to prevent RANKL or sRANKL from interacting with RANK. The ratio between RANKL and OPG produced determines osteoclastogenesis. [Adapted from (Clarke 2008)]

1.2.3 Bone growth, modelling and remodelling

Bone is a highly dynamic and metabolically active tissue, which undergoes constant growth, modelling and remodelling. Longitudinal growth occurs at the growth plates during childhood and adolescence to allow for growth and attainment of peak bone mass. Cartilages proliferate in the epiphyseal and metaphyseal areas of long bones, before undergoing mineralisation to form primary new bone. Modelling is the process by which bones change their overall shape to accommodate for skeletal loading and radial growth, which continues throughout life although less frequent in adulthood. During bone modelling, bone formation and resorption are *not* tightly coupled, in that osteoblasts and osteoclasts act independently in response to biomechanical forces. Bones normally widen with age when bone formation at the periosteal envelope exceeds bone resorption at the endosteal surface (Clarke 2008).

Bone remodelling is the process whereby old bone is replaced by newly formed bone, which allows self-repair in both childhood and adulthood. More acutely, remodelling also helps to maintain calcium homeostasis. The process of remodelling occurs at all four skeletal envelopes: endocortical, intracortical and trabecular, with a lesser extent on the periosteal envelope. It involves four sequential phases: *activation*, *resorption*, *reversal* and *formation*, as shown in Figure 1.7. Osteocytes are thought to sense bone deformation or microdamage (Han *et al.* 2004), initiating the need for remodelling during which bone resorption by osteoclasts precedes bone formation by osteoblasts. The osteocytes, through their long cytoplasmic processes, relay the information to the osteoblast lining-cells and osteoblast precursors, which in turn *activates* osteoclastogenesis (as described in Section 1.2.2) and is believed to orchestrate the bone remodelling process (Verborgt *et al.* 2000, Parfitt 2002). The mononuclear monocyte-macrophage osteoclast precursors recruited from the circulation lift off the bone-lining cells from the endosteum, fuse to form multinucleated osteoclasts underneath, then bind to the matrix *resorb*ing old bone before undergoing apoptosis at the end. Osteoclast-mediated bone resorption takes only approximately 2-4 weeks during each remodelling cycle. Bone resorption transitions to bone formation in the *reversal* phase, where monocytes, osteocytes released from bone matrix and the osteoblast precursors from the same multicellular remodelling unit migrate to the resorption cavities, under the influence of several growth factors such as TGFβ, IGF-1 and BMPs (Hock *et al.* 1988, Bonewald and Mundy 1990). The osteoblast precursors then mature to become osteoblasts promoting bone *formation*, through synthesis of new collagenous organic matrix and regulation of the matrix mineralisation by releasing small membrane-bound matrix vesicles

that concentrate calcium and phosphate. Bone formation takes longer, up to 4-6 months to complete (Clarke 2008).

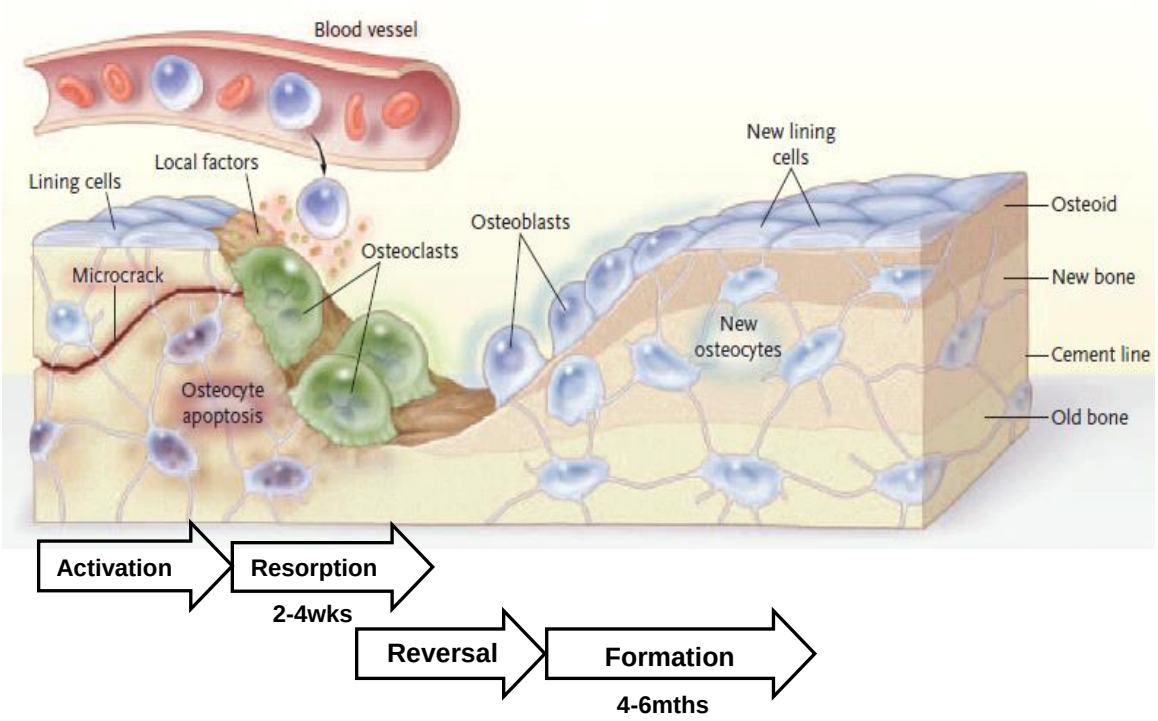

Figure 1.7 Sequential Bone Remodelling Processes on a Trabecula. When microcracks sever canaliculi, the osteocytes sense the damage and signals the osteoblast lining cells to activate osteoclastogenesis (activation phase). The activated osteoclast binds to the matrix and resorbs old bone and the microcrack (resorption phase), taking 2-4 weeks to complete, following which osteoclasts undergo apoptosis and osteoblast precursors migrate to the area under the influence of growth factors (reversal phase). These osteoblast precursors mature into osteoblasts and begin synthesizing new collagenous organic matrix bone formation, laying down osteoid which becomes mineralised over the next 4-6 months (formation phase). [Adapted from (Seeman and Delmas 2006)]

The remodeling process begins before birth and continues until death. The rate, however, decreases as longitudinal growth ceases with epiphyseal closure (Parfitt *et al.* 2000). Bone remodelling, in particular bone resorption, increases with age in both men and women, although more marked in the latter especially in peri-menopausal and early postmenopausal women, accounting for the higher rate of osteoporosis and fragility fracture in this group.

Bone turnover is the process of bone remodelling, where bone formation and bone resorption are tightly coupled in space and time (Delmas 1991). Biochemical markers of bone formation and resorption enable the assessment of bone turnover as described above. This can allow insight into the effects of diseases on bone health in childhood. Interpretation of the results, however, can be challenging as they depend on age, gender, pubertal stage, nutritional status and other hormonal regulation. Skeletal growth and puberty can lead to substantial changes in raw levels of bone formation and resorption markers with age, as seen with their correlation with growth velocity (van Coeverden *et al.* 2002). In children, there is

added variability and reduced specificity as these markers are released into the circulation during the process of growth in length, when the actions of osteoclasts and osteoblasts are not coupled. Some markers can also be affected by circadian variation and day-to-day fluctuations. This can be further compounded by methodologic issues with assay sensitivity and specificity.

1.2.3.1 Bone formation markers

The commonly used serum markers for bone formation are bone-specific alkaline phosphatase (BAP) and osteocalcin (OC), which are released at different stages of osteoblast proliferation and differentiation (Calvo *et al.* 1996).

1.2.3.1.1 Bone Alkaline Phosphatase (BAP)

Serum total alkaline phosphatase (AP) is a combination of four isoenzymes; liver/bone, placental, intestinal and germ cell. The first two, liver and bone isoenzymes, differ only by post-translational glycosylation. Current immunoassays for BAP therefore possess a low cross-reactivity (16%) with the circulating liver isoenzyme (Delmas 1995). It has a relatively long half-life of 1 to 2 days and no circadian variation (Yang and Grey 2006). BAP is produced by osteoblasts and is involved in the initialisation process of osteoid mineralisation.

BAP is a very sensitive diagnostic tool in adults where a small increase is easily detectable and indicating possible pathology (Delmas 1995). In infants, BAP increases after birth due mainly to skeletal growth and is less predictive of bone mineral accrual. In rapidly growing children and adolescents, BAP increases until mid-puberty and decreases in late puberty (after menarche in girls) (Magnusson *et al.* 1995, Tobiume *et al.* 1997) (Figure 1.8), correlating positively and significantly with height velocity in both genders. BAP is about 10 times higher than adult values in pubertal girls in contrast to liver AP which remains within normal adult values (Blumsohn *et al.* 1994). BAP increase has been shown to correlate with the increase in bone mineral density in growth hormone-treated children (Tobiume *et al.* 1997).

1.2.3.1.2 Osteocalcin

Osteocalcin (OC) is a sensitive and specific marker for bone formation. It is produced almost exclusively by the osteoblasts during the matrix mineralisation phase and incorporated directly into the bone matrix (Delmas 1995). Circulating OC has a short half-life and is

rapidly (5mins) cleared by the kidneys. In adults, one third of the circulating OC is an intact molecule, one third is a large N-terminal mid-region fragment and the rest is N-terminal midregion and C-terminal fragments (Garnero *et al.* 1994). The distribution of these immunoreactive forms of OC is unknown in children. Serum OC results can vary considerably depending on which immunoreactive forms (intact molecules or OC fragments) the immunoassay measures. Assays that measure the intact molecule and large N-terminal fragment aremore robust as well as sensitive.

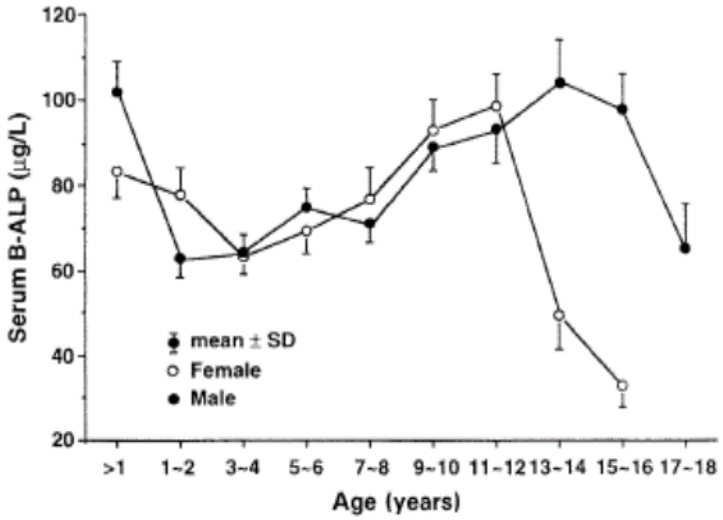

Figure 1.8 Serum bone alkaline phosphatase (BAP) in children and adolescents. Females had their peak serum BAP levels during puberty about two years earlier than males [Adapted from (Tobiume *et al.* 1997).

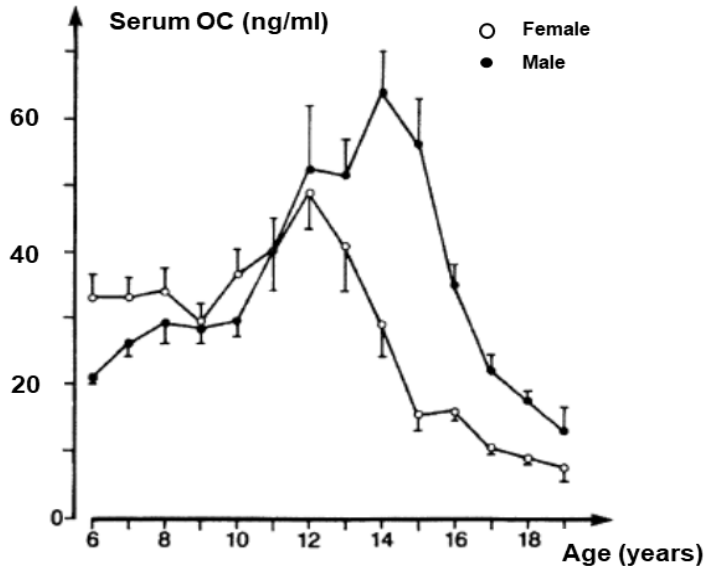

Figure 1.9 Serum osteocalcin levels in children and adolescents. Values are presented as mean and standard error of mean. [Adapted from (Johansen *et al.* 1988)]

Similar to BAP, circulating OC varies with age and pubertal stage in children as shown in Figure 1.9 (Johansen *et al.* 1988). The concentration is 10-20 times higher in growing children compared to pre-menopausal women (Matikainen *et al.* 1999). Additionally, there is also a circadian rhythm to OC production with the highest levels in the morning (Heuck *et al.* 1998). Circulating OC detectable in urine also demonstrates a similar diurnal variation (Taylor *et al.* 1990, Matikainen *et al.* 1999).

1.2.3.2 Bone resorption markers

The commonly used bone resorption markers are urinary hydroxyproline (HPro), pyridinoline (Pyr) and deoxypyridinoline (Dpyr) released during matrix resorption into the blood and excreted in the urine. They reflect bone resorption as they are not reutilised in collagen synthesis. Urinary bone markers have several limitations including the practical difficulties associated with serial urine collection, units of expression which may need size correction and expression in concentration relative to creatinine which itself is subjected to age-related changes due to muscle mass variation (Forbes and Bruining 1976, Rauch *et al.* 1994). Hence, the measurement of serum bone resorption marker, C-terminal telopeptide of type I collagen (CTX), in particular, is preferred.

1.2.3.2.1 Cross-linked Telopeptides (CTX)

During bone resorption, osteoclasts cleave off short fragments of the N- and C-terminal domains of collagen molecules into the circulation. The level of circulating CTX is highest in neonates and then markedly decreased in children after 1 year of age. The second peak was observed in girls 11-13 years old and in boys who were 14-17 years old (Crofton *et al.* 2002, Rauchenzauner *et al.* 2007), again demonstrating the effects of puberty, as seen in Figure 1.10. Urinary crosslinks show diurnal variation; highest in the morning and lowest late evening although this has not been shown in serum CTX.

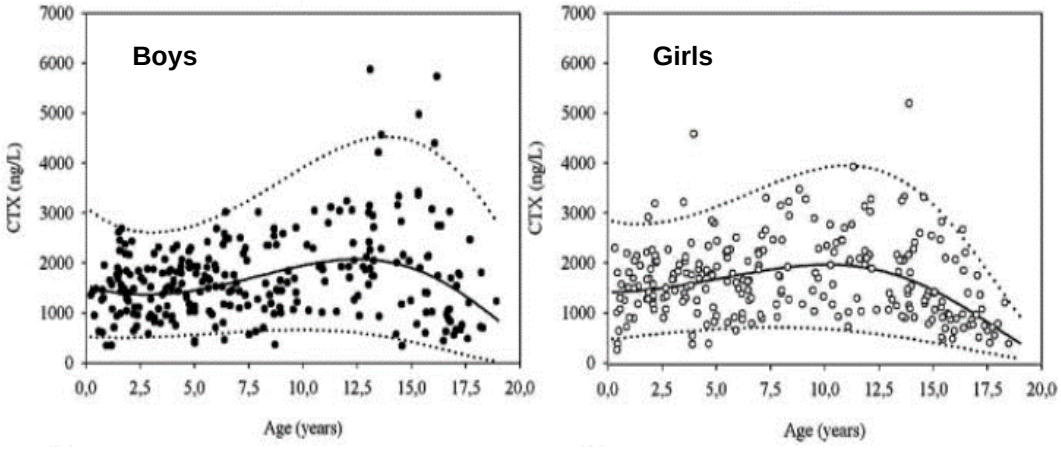

Figure 1.10 Reference curves for CTX resorption markers in childhood and adolescence. Curves represent the 50th centile (solid line) and 3rd/97th centile (dotted lines) [Adapted from (Rauchenzauner *et al.* 2007)]

1.2.3.3 Other markers

1.2.3.3.1 Sclerostin

Sclerostin is the product of *SOST* gene, secreted by osteocytes, and expressed almost exclusively in bone (Bellido T 2014). It is an inhibitor of the Wnt signalling pathway and thus inhibits bone formation. Sclerostin competes with Wnt ligands to bind to LRP5/6 co-receptors resulting in degradation of the intracellular β-catenin and hence impair osteoblast differentiation and function (Li *et al.* 2005, Bellido T 2014). Mechanical loading in rats and mice suppresses sclerostin level resulting in greater bone formation (Robling *et al.* 2008) whilst immobilisation in humans increases sclerostin levels leading to bone loss (Gaudio *et al.* 2010). These strongly suggest sclerostin as the crucial link between osteocytic mechanosensing and osteoblastic bone formation. Sclerostin level rises from early childhood and peaks at mid puberty (Tanner stage 3), and diminishes thereafter (Tsentidis *et al.* 2016). Boys have higher sclerostin levels than girls (Tsentidis *et al.* 2016). Most importantly, sclerostin has been shown to be an independent predictor of fracture risks (Ardawi *et al.* 2012, Starup-Linde *et al.* 2016).

1.2.4 Bone marrow and its composition

Bone marrow occupies approximately 85% of the medullary cavity, surrounded by a network of trabecular bone. In addition to the mesenchymal stem cells (described in section 1.3), it contains haematopoietic elements (red marrow) and a variable amount of fat (yellow marrow). At birth, the bone cavities are filled mainly with haematopoietic marrow, which is gradually replaced by fatty yellow marrow during childhood. By early adulthood, approximately 50% of the bone marrow volume is yellow marrow confined primarily in the appendicular skeleton, whilst the red marrow is concentrated to the axial skeleton (including proximal humerus and femur).

This physiological conversion occurs in a centripetal fashion from the distal to the more proximal appendicular skeleton (Vande Berg *et al.* 1998).Within the long bones, the fatty marrow conversion begins in the epiphyses at the onset of epiphyseal ossification and is completed within 6-8 months, followed by the diaphysis before extending to the metaphyses (Vogler and Murphy 1988, Jaramillo *et al.* 1991). The conversion also occurs concurrently from the central medullary canal to the endosteum. In the tibia specifically, the conversion begins in the diaphysis between age 1-5, and is completed by age 10-15 years (Vande Berg *et al.* 1998). The marrow conversion continues throughout adult life, although at a slower pace than during childhood (Vogler and Murphy 1988, Vande Berg *et al.* 1998) resulting in a positive correlation between bone marrow adiposity (BMA) and age (Meunier *et al.* 1971, Wehrli *et al.* 2000).

There is no gender differences in the rate of marrow conversion during childhood (Dooms *et al.* 1985, Waitches *et al.* 1994), although males have 6-10% more fat than females between the ages 20-60 years. This gender difference in BMA is reversed in adults >60 years. Vertebral bone fat increases sharply in females in the post-menopausal years between ages 55-65 years and stays approximately 10% higher in males thereafter (Kugel *et al.* 2001, Griffith *et al.* 2012).

1.3 Mesenchymal stem cells and bone biology

1.3.1 Origins

Bone marrow was thought to be the home of the haematopoetic stem cells, until the German pathologist Cohnheim elucidated the presence of non-haematopoetic stem cells as the source of fibroblasts within the same compartment in the late 1800s (Prockop 1997). It was not until the 1970s when Friedenstein discovered that the whole bone marrow he cultured in petri dishes, after discarding the haematopoetic cells, could differentiate into colonies of spindly-shaped fibroblasts and small deposits of bone or cartilage, suggesting that these marrow cells were multi-potential (Friedenstein *et al.* 1976). Since then, it has been established that the non-haematopoetic stem cells, now referred to as mesenchymal stem cells (MSCs) or marrow stromal cells, are capable of: i) *self-renewing*, *i.e.* proliferating in the undifferentiated form, and ii) *pluripotency*, *i.e.* differentiating into 'committed' progenitor cells such as osteoblasts, chondrocytes, adipocytes and even myoblasts, to give rise to the mesenchymal tissues bone, cartilage, adipose tissue and muscle respectively (Figure 1.11).

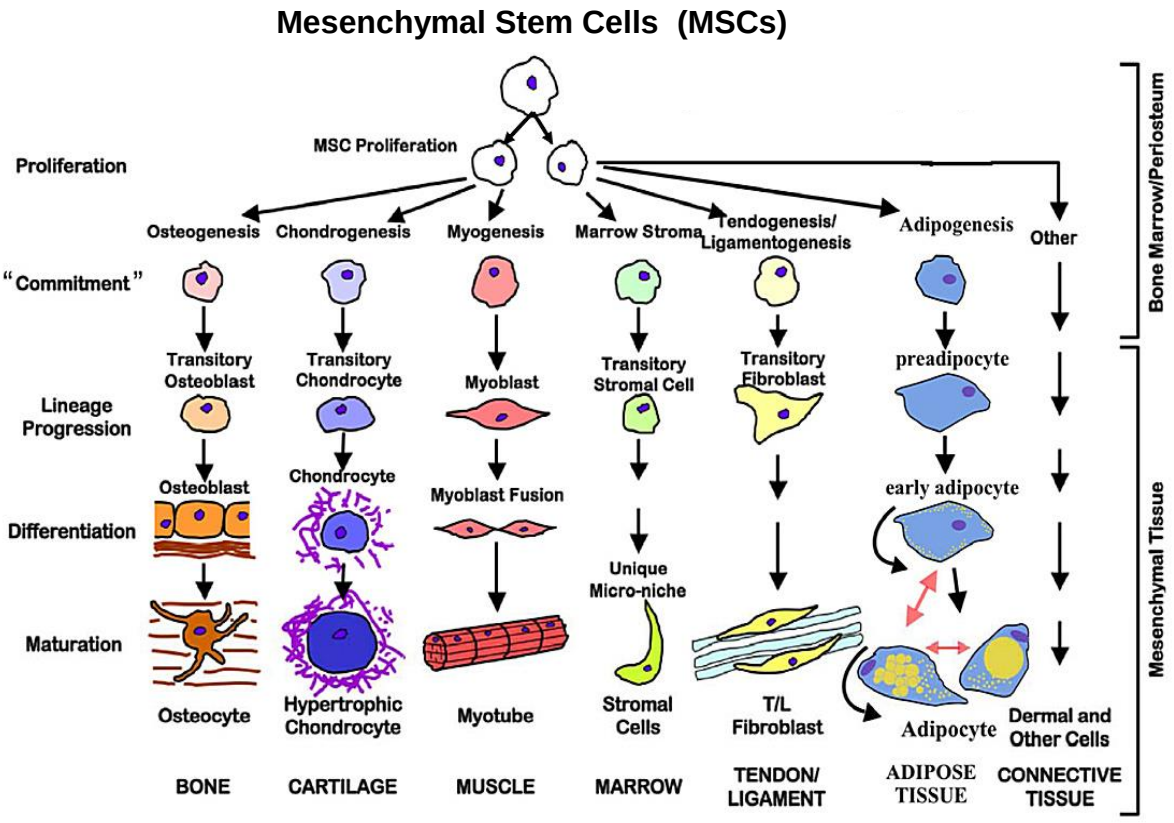

Figure 1.11 The differentiation of mesenchymal stem cells (MSCs). MSCs are pluripotent cells capable of differentiating into bone, muscle, fat and other connective tissues. [Adapted from image source: frontiersin.org]

Apart from the bone marrow, MSCs can also be isolated from periosteum, adipose tissue, amniotic fluid, and fetal tissues (Nakahara *et al.* 1991, Zuk *et al.* 2002, Anker *et al.* 2003). These are sometimes referred to as mesenchymal precursor cells which can be phenotypically similar to MSCs but exhibit heterogeneity in differentiation potential compared to the more traditional bone marrow-derived MSCs (Anker *et al.* 2003). Indeed, cultured human MSCs can have differentiation capacity not present in primary fibroblasts, which are mature mesenchymal cells (Pittenger *et al.* 1999).

Importantly, bone-marrow-derived MSCs (BMMSCs) express signature cell markers such as CD29, CD44, CD73, CD105 and CD166 and are negative for haematopoietic markers, specifically CD45, CD34, CD14 or CD11 (Chamberlain *et al.* 2007). The gene expression of MSCs continues to shift once induced to commit to a specific lineage, during differentiation and until the phenotype is characteristic of the target cell, for instance the expression of CD24, CD29 and CD36 among others in lipid-laden mature adipocytes (Berry and Rodeheffer 2013, Vroegrijk *et al.* 2013).

1.3.2 MSC Differentiation and signalling cascades involved

Pluripotent MSCs undergo "commitment" to a more lineage-specific cell line before differentiating into its respective mesenchymal tissue (Figure 1.12). This process of "commitment" happens under the influence of factors/cytokines that activate the expression of certain genes, or proteins which direct the MSCs down a designated cell line (Davis *et al.* 1987, Tang *et al.* 2004b). It is less well understood compared to the differentiation process of the more committed progenitor cells.

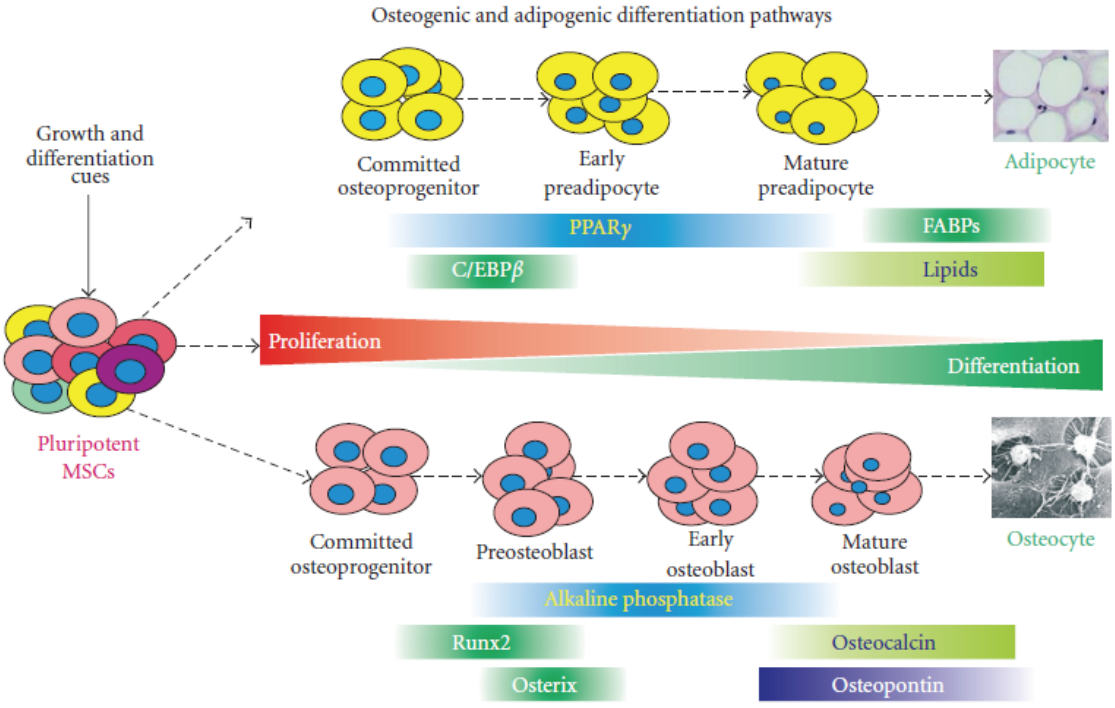

Figure 1.12 Osteogenic and adipogenic commitment and differentiation pathways in mesenchymal stem cells (MSCs). MSCs are pluripotent progenitor cells capable of differentiating into adipocytes and osteocytes, depending upon the stimulation cues. The lineage-specific differentiation is a multiple stage and well coordinated process regulated by master regulators such as PPARγ and C/EBPβ for adipogenesis and Runx2 and Osterix for osteogenesis. Osteogenic differentiation can be staged by measuring alkaline phosphatase (early marker) and osteocalcin and osteopontin (late markers). Expression of FABPs and production of lipids are indicators of terminal adipogenic differentiation. [Adapted from (Wagner *et al.* 2010)]

The differentiation of MSCs to adipocytes is not completely understood as yet. It can be broadly categorised into two phases: the *determination* phase and the *terminal differentiation* phase (Muruganandan *et al.* 2009). The determination phase is when multipotent MSCs commit to the adipocyte lineage, becoming pre-adipocytes which have a fibroblastic phenotype morphologically but are not readily distinguishable from their MSC precursors. This phase is believed to be ligand-dependent, with endogenous molecules such as fatty acids (Schopfer *et al.* 2005) and exogenous ligands such as thiazolidinediones which are

potent peroxisome proliferator-activated receptor γ (PPARγ) agonists (Lehmann *et al.* 1995), although some studies have shown otherwise (Walkey and Spiegelman 2008). In the terminal differentiation phase, pre-adipocytes become mature adipocytes with distinctive gene expression markers and new functions including lipid synthesis, storage and adipocyte-specific protein production. This is a sequentially and temporally ordered process involving multiple signalling cascades that converges at PPARγ transcriptional activity.

Similarly in MSC differentiation to osteoblasts, the process starts with commitment of osteoprogenitor cells and differentiation into pre-osteoblasts, which eventually develop into mature osteoblasts (Neve *et al.* 2011). The development of an immature osteoblast into a mature one involves proliferation, maturation, matrix synthesis and mineralisation before becoming entombed in osteoid to turn into an osteocyte. Osteoblast differentiation requires the key transcription factors runt-related transcription factor 2 (Runx2) as described above, but also others such as BMPs.

The differentiation of MSC towards an adipogenic or osteogenic cell fate depends on a variety of transcription factors and signalling cascades. The two main lineage-specific transcription factors are Runx2 for osteogenesis and PPARγ for adipogenesis. Due to its common precursor from the pluripotent MSC, *in vitro* evidence exist to suggest a mutually exclusive and reciprocal lineage selection of one or the other, whereby adipogenesis occur at the expense of osteogenesis and vice versa (Figure 1.13) (Beresford *et al.* 1992, Yang *et al.* 2008). Typically, increased expression of one is associated with downregulation of the other (Li *et al.* 2003, Zhang *et al.* 2006), further affirming the bone-fat balance hypothesis.

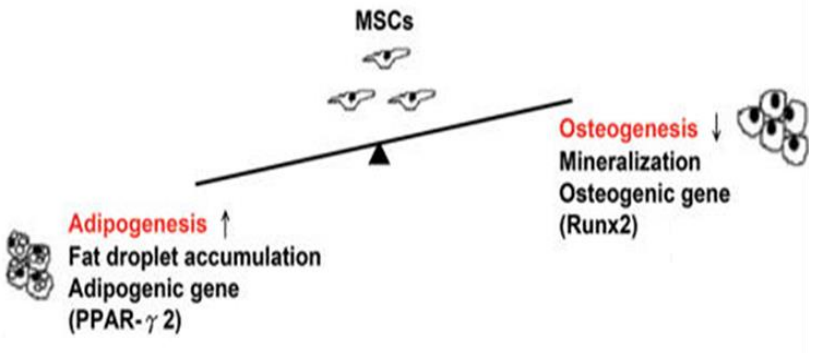

Figure 1.13 Bone-fat balance. Osteogenesis and adipogenesis are proposed to be mutually exclusive given that osteoblasts and adipocytes originate from the common progenitor mesenchymal stem cells. PPARγ is the key regulator of adipogenesis whilst Runx2 activation determines osteogenesis. [Adapted from (Yang *et al.* 2008)]

1.3.2.1 PPARγ: The master regulator of adipogenesis

Peroxisome proliferator-activated receptors (PPAR) are members of steroid/thyroid hormone receptor gene superfamily with three structural analogs: PPARα, PPARδ and PPARγ. All three are expressed during adipogenesis, but PPARγ expression is exclusive to adipocytes and increases more rapidly during early adipogenesis (Wagner *et al.* 2010). PPARγ is expressed in two isoforms, PPARγ1 and PPARγ2, generated by alternative splicing, during adipogenesis. In response to PPARγ activators, such as thiazolidinediones (TZDs) and free fatty acid molecules, PPARγ heterodimerises with the nuclear receptor, retinoid X receptor (RXR) to form a transcription complex that can bind to DNA and regulate transcription of the adipogenic genes (Figure 1.14).

PPARγ plays a very diverse role in different tissues including its function in adipogenesis, atherosclerosis, inflammation and insulin sensitisation (Kliewer *et al.* 1995, Lehmann *et al.* 1995, Takeda *et al.* 2000). It is considered the master regulator of adipogenesis as no other factor can rescue adipocyte formation when PPARγ is knocked out. Selective deletion of PPARγ in murine adipose tissue leads to a loss of both brown and white adipocytes (Rosen and MacDougald 2006). PPARγ-deficient (-/-) embryonic stem cells from genetically manipulated mice failed to differentiate into adipocytes, and instead differentiated into osteoblasts (Tzameli *et al.* 2004). In addition, cells derived from PPARγ$^{+/-}$ mice demonstrated a reduced ability to differentiate into adipocytes with increased osteoblastogenesis instead.

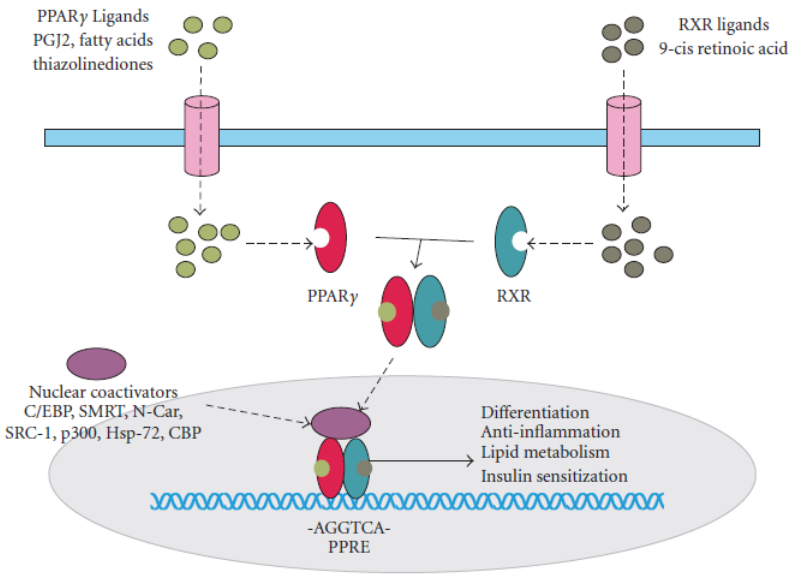

Figure 1.14 Mode of action for PPARγ. PPARγ and RXR form a heterodimer which is activated by the respective ligands. The activated PPARγ/RXR heterodimer will be translocated into the nucleus and regulates downstream target genes in concert with nuclear receptor co-activators. [PGJ2 prostaglandin J2; Adapted from (Wagner *et al.* 2010)]

1.3.2.2 Runx2: The master regulator of osteogenesis

The Runx family consists of three distinct proteins: Runx1-3 which share a common β subunit, but a different α subunit (Ogawa *et al.* 1993). Runx proteins have a DNA-binding domain, known as Runt, homologous to that identified in the *Drosophila melanogaster*. Similar to PPARy, Runx proteins form a heterodimer with core binding factor β (Cbfβ), a co-transcriptional factor, which displaces the inhibitory domain and allows binding to DNA to effect downstream targets. Runx have distinct tissue-specific expression and their functions are dependent on cellular context as summarised in Table 1.2 (Ito *et al.* 2015).

Phosphorylated Runx proteins are very susceptible to degradation (Biggs *et al.* 2006, Shen *et al.* 2006). Runx genes are intimately linked to carcinogenesis so its protein levels need to be tightly regulated in order to switch between tumour suppressive and oncogenic functions. Runx1 aberrations have been associated with leukaemia, Runx2 with osteosarcoma and Runx3 with stomach, colon and bladder cancers to name a few (Nomoto *et al.* 2008, Mangan and Speck 2011, Martin *et al.* 2011). They are expressed interdependently and often, more than one Runx family member is expressed in the same cell. Levels of Runx1 and Runx2 mRNAs are inversely correlated in skeletal development (van der Deen *et al.* 2012). Importantly, Runx protein levels oscillate during cell differentiation with Runx2 expression in osteoblasts highest at G0-G1 phases (early differentiation) of the cell cycle and downregulated during G1-S transition (mid differentiation) (Galindo *et al.* 2005). Runx have the ability to exert opposite effects on transcription due to its complex post-translational modifications, which modulate its interactions with DNA.

Table 1.2 Function of Runx proteins

Protein	Function	Phenotype
Runx1	Haematopoeisis	Haematopoeitic stem cell maintenance
	Immune response	T-cell and B-cell development
Runx2	Skeletal development	Differentiation of osteoblasts and chondrocytes Directs MSCs to the osteoblast lineage
	Alveolar cell maturation in mammary glands	Regulates mammary epithelial progenitors during pregnancy Necessary for the specification of luminal progenitor cells
Runx3	Stomach	Required for proper differentiation
	Nervous system	Involved in neuronal cell fate
	Immune response	Required for macrophage and T-cell differentiation, and dendritic cell maturation

In the mesenchymal stem cells, Runx participates in the decision to proliferate or differentiate. Specifically, Runx2 directs MSCs to the osteoblast lineage for bone development. Runx2 level, however, must be tightly regulated in osteogenesis. Its expression increases at the onset of quiescence in preparation for differentiation, but must reduce in time for osteoblast maturation as overexpression results in the accumulation of a larger immature osteoblast population (Pratap *et al.* 2003, Komori 2010). Heterozygous mutation of Runx2 ($Runx2^{+/-}$) causes hypoplastic clavicles and open fontanelles in a condition called cleidocranial hypoplasia (Mundlos *et al.* 1997) whilst $Runx2^{-/-}$ mice die soon after birth from respiratory failure due to lack of bone ossification in the thoracic cage (Komori *et al.* 1997). Due to defective osteoblast differentiation, the skeleton of $Runx2^{-/-}$ mice are cartilaginous with the complete absence of mineralisation, with the exception of very mild calcification at tibia, fibula, radius and ulna detectable on Alizarin staining. It has been noted that Runx2-/- mesenchymal stem cells are capable of differentiating into adipocytes and chondrocytes, but completely lack the potential to differentiate into osteoblasts indicating its key role in skeletal development (Kobayashi *et al.* 2000).

1.3.2.3 Signalling pathways in MSC differentiation

In addition to the transcription factors, many complex signalling pathways are involved in the commitment and differentiation of MSC towards adipocytes or osteocytes. There are several pro-osteogenic/anti-adipogenic signalling pathways including (i) β-catenin dependent Wnt signalling (as well as the non-canonical β-catenin Wnt signalling) (Taipaleenmaki *et al.* 2011, D'Alimonte *et al.* 2013), (ii) Hedgehog signalling (Fontaine *et al.* 2008, James *et al.* 2010) and (iii) NEL-like protein 1 (NELL-1) signalling (James *et al.* 2011, James *et al.* 2012). The β-catenin-dependent Wnt signalling pathway is the most well-established one involved in both bone formation. β-catenin plays a direct role in the regulation of osteoblasts with deficiency causing arrest in pre-osteoblast development at an early stage and impaired maturation and mineralisation in more committed osteoblasts, and consequent embryonic skeletal defects (Day *et al.* 2005, Holmen *et al.* 2005, Chen and Long 2013). There is also an antagonistic effect on osteoclastogenesis with suppression of bone resorption through the canonical β-catenin/Wnt signalling pathway (through upregulation of OPG expression and down-regulation of RANKL expression) and increased bone resorption through activation of the non-canonical pathway (Takahashi *et al.* 2011). Accordingly, trials involving antibody against sclerostin, which is a Wnt inhibitor, have shown promising results in phase II clinical trials demonstrating increased bone mineral density (Padhi *et al.* 2011). Its reciprocal anti-adipogenic effect is exerted through several members of the Wnt

family, such as Wnt10b and Wnt3a, which inhibits adipogenesis mainly through suppression of PPARγ and/or C/EBP-α expressions (Ross *et al.* 2000, Kawai *et al.* 2007).

Contradicting the bone-fat balance, there are signalling cascades which demonstrate dual pro-osteogenic and pro-adipogenic effects, namely (i) BMP signalling and (ii) IGF signalling. The precise determinant that governs the cell fate of BMP signalling is not well understood. Studies in mouse MSCs have shown a lower concentration of BMP-2 favouring adipogenesis and a higher concentration directing MSCs towards osteogenic differentiation (Wang *et al.* 1993).The effects of different BMP receptor expression on the lineage differentiation of MSCs have also been shown (Chen *et al.* 1998).

The identification of the genes/proteins involved in the signalling pathway for these commitment and differentiation steps in MSC differentiation is crucial as it may lead to potential targets for therapeutic interventions, as seen with the anti-sclerostin described above. Of note, MSC differentiation can also be influenced by many micro-environmental factors such as mechanical forces (Kelly and Jacobs 2010), electrical currents (Hronik-Tupaj *et al.* 2011) and magnetic fields (Yan *et al.* 2010).

1.3.3 C3H10T1/2 Mesenchymal stem cell model

Human bone-marrow-derived MSCs (BMMSCs) are ideal for *in vitro* studies investigating their own multi-lineage differentiation potential (Pittenger *et al.* 1999) and the various signalling pathways involved. This attractive cell source, however, can be difficult to obtain, usually dependent on invasive marrow aspirates of volunteer donors or samples obtained during orthopaedic surgery for an unrelated reason. In addition, BMMSCs can show variable heterogeneity in colony sizes, colony-forming rates and cell morphology during cell isolation/expansion (Bianco *et al.* 2001) which may have a false positive or false negative impact on study findings.

In contrast, the mouse mesenchymal stem cells C3H10T1/2, which are commercially available, have a homogenous population and do not undergo spontaneous differentiation under normal culture conditions making it an ideal alternative. The C3H10T1/2 cell line was established in 1973 from 14-17 day old C3H mouse embryos (Reznikoff *et al.* 1973). These cells display a fibroblastic morphology under normal culture conditions and are functionally similar to mesenchymal stem cells in their ability to develop into osteoblasts, chondrocytes and adipocytes with specific inductions (Katagiri *et al.* 1990, Tang *et al.* 2004a). It is worth noting that the C3H10T1/2 cell line has been reported to have a lower adipogenic differentiation potential of only 10% compared to 70% in primary BMMSCs (Zhao *et al.* 2009).

1.4 Bone fragility

1.4.1 Normal bone mineral accrual

The skeleton grows, in length, in breadth and in mass, as the body grows. Skeletal health is largely regulated by genetic factors, which determine up to 70% of peak bone mass (Gortz and Fassbender 2001) with other key environmental factors such as body composition (Baxter-Jones *et al.* 2003, Farr *et al.* 2014a), physical activity (Bailey *et al.* 1999, Baxter-Jones *et al.* 2008) and nutrition (Whiting *et al.* 2004, Vatanparast *et al.* 2005) affecting its accrual. Bone mass increases substantially in the first two decades of life, reaching a plateau in the late-teens or young adulthood before declining after the age of about 50 years (Figure 1.15). The actions of sex steroids, growth hormone (GH) and insulin-like growth factors released and active during the adolescent growth periods (Saggese *et al.* 2002) also contribute significantly to bone mineral acquisition and skeletal changes, underpinning the effects of puberty and the accompanying growth spurt on bone health.

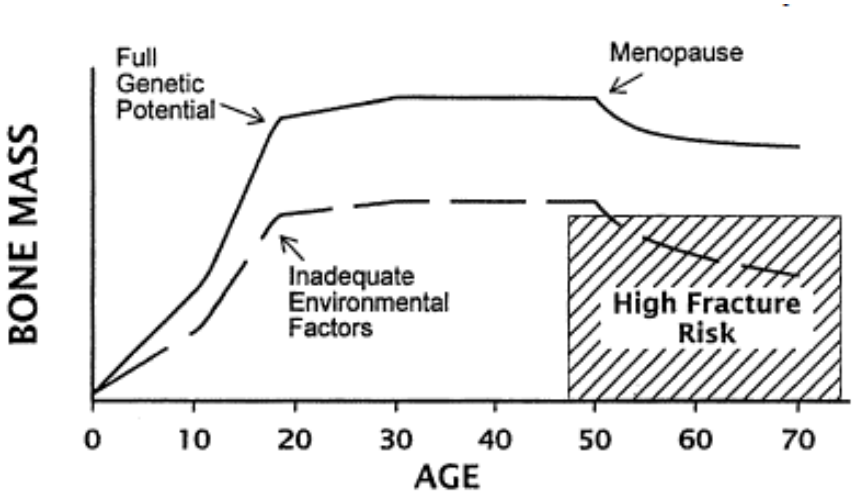

Figure 1.15 Bone mass accrual throughout life. Diagramatic representation of the bone mass accrual in individuals who achieve their full genetic potential (solid line) and in those who did not (dashed line), with the latter having lower peak bone mass predisposing to skeletal fragility in later years. [Adapted from (Heaney *et al.* 2000)]

As captured in a comprehensive longitudinal study, bone first plateaus in bone area, and then roughly 1 to 2 years later, plateaus in mineralisation (Baxter-Jones *et al.* 2011). Peak bone mass is reached approximately 7 years after peak height velocity (PHV), in both genders, at an approximate chronological age of 18.8 in females and 20.5 years in males (Baxter-Jones *et al.* 2011). The attainment of peak bone mass varied with skeletal site - femoral neck peak bone mass is attained first, 3 years after PHV, before that of lumbar spine at 5 years after PHV (Baxter-Jones *et al.* 2011). Similarly in another study in males, peak bone mass occurred by 18-20 years at the femoral neck, lumbar spine and total body but had not yet

been reached at the distal radius and tibia (Lorentzon *et al.* 2005). Depending on site, 33-46% of the total adult bone mineral content is accrued in the adolescent growth period within the 5 years surrounding PHV (Baxter-Jones *et al.* 2011). In females, this represents double the amount of bone mineral that will be subsequently lost during the post-menopausal years from 50-80 years of age (Arlot *et al.* 1997). As bone mass tracks throughout life (Slemenda *et al.* 1990, Ferrari *et al.* 1998, Loro *et al.* 2000), achieving a higher peak bone mass is therefore crucial in the protection against later-life fragility fracture. Pre-pubertal children at the high end of the bone mass distribution gained the most bone across puberty and remained at the high end of the distribution 2 years later (Loro *et al.* 2000).

In the same way that adolescence is a critical window for laying down bone, it is also a time of crucial vulnerability. Any interruption to the normal physiology by either illness (period of immobilisation, chronic inflammatory diseases, interruption to normal reproductive hormone production, eating disorders) and/or lifestyle factors (smoking, inadequate dietary intake, particularly of calcium or vitamin D, oral contraceptive use) may lead to a significantly lower peak bone mass constituted for by the genetic potential. There is a controversy that combined oral contraceptive, especially very low dose ethinyl oestradiol, during adolescent age can be detrimental to the acquisition of peak bone mass, although subsequent prospective studies and RCT have shown otherwise (Cromer *et al.* 2004, Cibula *et al.* 2012, Gargano *et al.* 2008). Additionally, medication such as glucocorticoids and anti-epileptics, necessary for the treatment in many childhood diseases, are detrimental to skeletal health. Young people affected by any of these factors will enter adulthood with low bone mass, and will have a higher long-term risk of fracture even if they lose only a modest amount of bone thereafter. Hence, optimal skeletal development during growth is protective against osteoporosis and fragility fracture in adulthood.

1.4.2 Determinants of bone strength and its clinical implications

The mechanical competence, or strength, of any structure is dependent on a combination of the mass, the physical properties of the component materials, and their geometric arrangement in space (Figure 1.16). This is no different when it comes to bone. Bone strength is determined by the whole bone – bone mass, architecture and geometry.

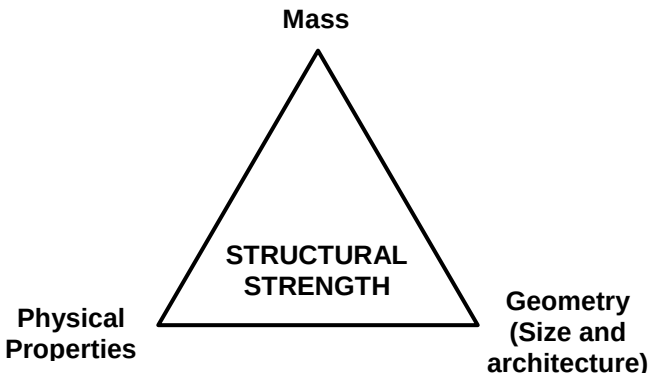

Figure 1.16 Determinants of mechanical competence or strength, of a structure. The strength of any structure is determined by the triad of the mass, physical properties of its components and the geometric arrangements of the structure.

Bone mass is an important determinant of bone strength, accounting for approximately 60-70% of the variation in bone strength (Cheng *et al.* 1997). The relationship between bone mass and structural strength holds at all ages, with a clear positive association between bone mass and fracture throughout life (Heaney *et al.* 2000). For the last several decades, as bone mass became measurable *in vivo*, quantified as bone mineral density by DXA, BMD has been used as the main surrogate for bone strength. However, when: i) useful anti-osteoporosis medications produced a reduction in fracture risk with only marginal change in BMD (SR *et al.* 1996), and ii) BMD values of subjects with and without osteoporotic fracture imbricated (Siris *et al.* 2001, Schuit *et al.* 2004), there is an increasing realisation that bone fragility is not only dependent on bone mineral mass (bone quantity) but also alterations in bone quality including bone geometry and microarchitecture.

Some of the important parameters of bone quality include bone size and shape, trabecular bone microarchitecture and cortical bone thickness and porosity. Trabecular and cortical bone parameters were found to be more discriminatory of men and women with and without fractures (Chang *et al.* 2015) compared to BMD. It also became clear from studying the microarchitecture of osteoporotic subjects and bone specimens that there was a predominance of cortical over trabecular bone loss in peripheral sites (Zebaze *et al.* 2010),

which helped explain why most fractures in old age are non-vertebral (Riggs *et al.* 1981). The study found a significant increase in cortical porosity which was poorly captured by densitometry (Zebaze *et al.* 2010). Increased porosity reduces bone strength as a 4% rise in porosity increases crack propagation through bone by 84% (Diab and Vashishth 2005), with a 10% rise in porosity halving the maximum load before fracture occur (Martin and Burr 1989). As well as disruption to the lace-like trabecular scaffolding, another important finding of the paper from studying the post-mortem bone specimens was the presence of cortical remnants, or trabecularisation of the cortex, which can mislead cortical and trabecular quantification by non-invasive imaging methods. In addition, the apparent trabecular bone volume (BV/TV) was found to be the best morphometric predictor of bone strength amongst the trabecular parameters (Thomsen *et al.* 1998). The intrinsic material properties of bone including the matrix mineralisation and collagen cross-linking can also affect bone stiffness compromising bone strength.

As there is currently no accurate measure of overall bone strength, fracture prediction may be more accurate when measures of bone mass and microarchitecture parameters can all be incorporated together. Advances in non-invasive imaging techniques such as HR-pQCT and micro-MRI can now provide information on bone quality that was not previously available to enhance the assessment of fracture risk and skeletal health in a variety of diseases related to bone abnormalities, which cannot be fully studied by DXA alone.

1.4.3 Osteoporosis in Adults

Osteoporosis is a skeletal disorder characterised by the loss of bone mass (bone quantity), and deterioration of bone microarchitecture (bone quality) resulting in compromised bone strength and increased risk of fractures (NIH Consensus Development Panel on Osteoporosis Prevention and Therapy 2001, Camacho *et al.* 2016). A comparison of the bone microarchitecture of a normal vertebra and one with osteoporotic deficit is shown in Figure 1.17.

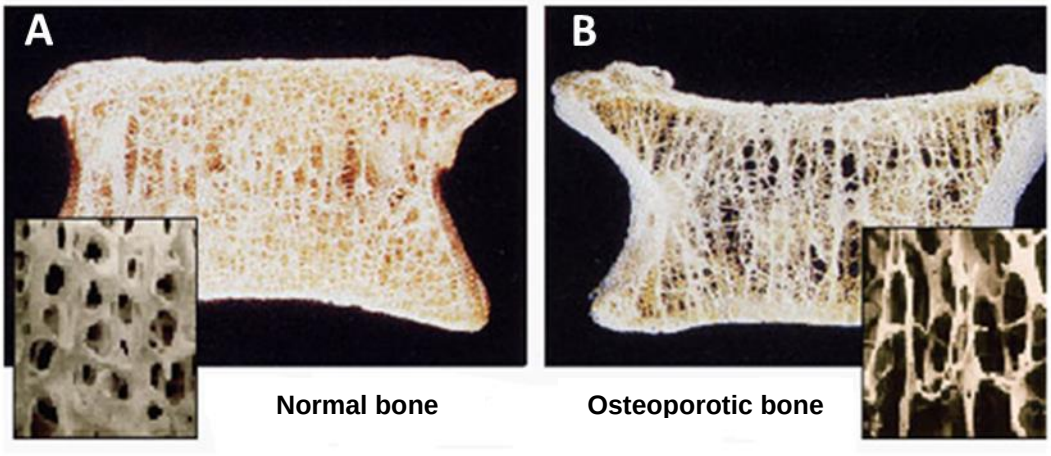

Figure 1.17 Bone microarchitecture of normal and osteoporotic specimen. (A) Healthy vertebra (B) Compressed osteoporotic vertebra with reduced trabecular number, connectivity and density with more trabecular spaces. [Adapted from (Lorentzon and Cummings 2015)]

1.4.3.1 Epidemiology of osteoporosis

Approximately 30% of all postmenopausal women are affected in the UK and 40% of them will go on to develop a fracture (Safaei *et al.* 2007). 1 in 2 women and 1 in 5 men over the age of 50 will suffer a fragility fracture (van Staa *et al.* 2001). Fragility fractures are fractures that result from low-level (or low energy) mechanical forces that would not ordinarily result in fracture (Kanis *et al.* 2001). The World Health Organisation has quantified this as forces equivalent to a fall from standing height or less. It is usually asymptomatic until fragility fracture occurs resulting in substantial pain and severe disability. Fractures of the hip (proximal femur), wrist (distal radius) and spine (vertebra) are most common.

Osteoporosis is a significant public health problem affecting over 9 million people worldwide (Johnell and Kanis 2006) and 3 million people in the UK (National Osteoporosis Society 2015). Every year 500,000 people suffer a fragility fracture (British Orthopaedic Association 2007), including 90,000 hip fractures with a projected rise in the incidence to 101,000 by 2020 (Department of Health (England) 2006). Hip fracture nearly always

requires hospitalisation, is fatal in 20% of cases and leaves 50% permanently disabled (Sernbo and Johnell 1993). Only 30% of patients fully recover. Fragility fractures have a massive impact on healthcare budget, costing the NHS an estimated annual cost of £2 billion (over £5 million per day) in combined hospital and social care for hip fracture alone (Burge *et al.* 2001).

1.4.3.2 Risk factors of osteoporosis

Although osteoporosis can occur at any age, the risk increases significantly with aging and after menopause in women. Osteoporosis can arise from secondary causes (Table 1.5) including glucocorticoid use and chronic diseases such as diabetes mellitus which is of particular relevance to this thesis. Other risk factors for osteoporosis includes premature menopause, amenorrhoea in women or hypogonadism in men, cigarette smoking, dietary factors such as low calcium intake and vitamin D deficiency, low body weight, glucocorticoid therapy, family history of osteoporosis, Asian or Caucasian ethnic origin, and long term immobilisation (Kanis 2002).

1.4.3.3 Diagnosis of osteoporosis

The current clinical diagnosis of osteoporosis is based on densitometry cut-offs proposed by the World Health Organisation (WHO) and modified by the International Osteoporosis Foundation (WHO Study Group 1994, Kanis and Gluer 2000) as shown in Table 1.3. Because bone density values follow a normal Gaussian distribution, BMD values can be expressed in relation to a reference population in standard deviation (SD) units. When the reference population is that of a young healthy adult, the BMD values are expressed as T-scores.

Table 1.3 WHO/IOF Definition of osteoporosis in adults

Definition of Osteoporosis in Adults WHO and International Osteoporosis Foundation Diagnostic Criteria	
Category	**BMD T-score**
Normal	> -1.0
Osteopenia	Between -1.0 and -2.5
Osteoporosis	≤ -2.5
Severe osteoporosis	≤ -2.5 with one or more fragility fracture

Although there is set diagnostic criteria for the diagnosis of osteoporosis, the assessment of fracture risk which is of greater clinical interest is much less straight forward. DXA-derived measures of BMD have been an important determinant of fracture risk with an increase in the relative risk of fracture by approximately 2-fold for every 1 SD decrease in bone mineral density, depending on skeletal sites (Marshall *et al.* 1996). However, BMD alone has a very low sensitivity in predicting the likelihood of fractures as considerable overlap in BMD values was seen in patients with and without fragility fractures (Siris *et al.* 2001, Schuit *et al.* 2004). Furthermore, therapeutic interventions for osteoporosis demonstrated reduction in the risk of fractures with minimal change in BMD (Cummings *et al.* 1996). Kanis described the use of BMD alone to predict fracture risk is akin to the reckless use of blood pressure alone in predicting the risk of stroke, where there is not a clear discriminatory cut off. With this in mind, Kanis and McCloskey founded the Fracture Risk Assessment Tool (FRAX) to evaluate the 10-year probability of hip and other major osteoporotic fractures (Kanis *et al.* 2008). This tool integrates clinical risk factors such as age, gender, previous fracture, glucocorticoid use, and BMD at femoral neck to give the fracture risk estimates. In FRAX, T1D and T2D has been recognised as a secondary cause of osteoporosis which increases the fracture probability independent of BMD (Giangregorio *et al.* 2012).

1.4.4 Osteoporosis in Children

1.4.4.1 Definition of osteoporosis

The 2013 International Society for Clinical Densitometry provided a position statement for the definition of osteoporosis in children which is clinically useful and enabled scientifically valid comparison between studies, as summarised in Table 1.4 (Bishop *et al.* 2014).

Table 1.4 ISCD Definition of osteoporosis in children

Definition of Osteoporosis in Children: ISCD 2013 Position Statement
(1) The presence of one or more vertebral compression (crush) fracture, ***or,*** (2) The presence of a clinically significant fracture ***and*** a BMD Z-score ≤ -2.0 A clinically significant fracture is: (a) two or more long bone fractures by age 10 years (b) three or more long bone fractures by age 19years BMC/BMD Z-score > -2.0 does not preclude the possibility of skeletal fragility and increased fracture risk. The term osteopenia should be avoided.

This position statement emphasises that the diagnosis of osteoporosis in children in not based on densitometry alone and highlights the importance of establishing a detailed fracture history. In addition, vertebral fractures in children are themselves diagnostic of osteoporosis. It also recognises that children with bone fragility can have recurrent fractures despite normal bone mineral density values.

1.4.4.2 Causes of Secondary Osteoporosis

The aetiology of primary osteoporosis, where primary bone disorders result in recurrent fractures is out with the context on this thesis. Secondary osteoporosis is increasingly recognised in children with chronic diseases and is caused by the underlying disease or its treatment (Table 1.5) (Korula *et al.* 2015).

Table 1.5 Causes of secondary osteoporosis

Causes of secondary osteoporosis	
Category	**Aetiological causes**
Reduced mobility	Prolonged immobilisation, cerebral palsy, Duchenne muscular dystrophy (DMD), spinal cord injury and Rett syndrome
Pubertal delay	Chronic illness, primary hypogonadism and induction by drugs
Chronic illnesses	*Haematological:* leukaemia, childhood cancers, thalassaemia and post- bone marrow transplant *Renal:* chronic renal failure and post-renal transplant *Gastrointestinal:* inflammatory bowel disease, coeliac disease, and chronic liver disease *Rheumatological:* systemic lupus erythematosus (SLE) and juvenile idiopathic arthritis (JIA) *Others:* anorexia nervosa, cystic fibrosis, severe burns and HIV
Endocrine causes	Hypogonadism, diabetes mellitus, hyperthyroidism, hyperprolactinaemia, and metabolic bone disease of prematurity
Drug-induced	Glucocorticoids, methotrexate, GnRH analogues, cyclosporin, anticonvulsants, heparin and radiotherapy
Inborn errors of metabolism	Glycogen storage disorder, lysinuric protein intolerance, galactosaemia, Gaucher disease, homocystinuria and Menke's disease

1.4.4.2.1 Reduced mobility

Normal bone development is dependent on mechanical loading and bone-muscle interaction which increase bone formation and bone mineral accrual (Hind and Burrows 2007). Reduced ambulation in children with cerebral palsy and DMD predisposes them to osteoporosis and lower limb fractures. (McDonald *et al.* 2002, Mergler *et al.* 2009). Vertebral fractures have also been found in up to 40% of children with DMD (McDonald *et al.* 2002). Studies have also found greater trabecular vBMD, tibial cortical thickness and tibial muscle cross-sectional area Z-scores in children with partial spinal cord injury who can stand compared to those who are bed bound (Biggin *et al.* 2013).

1.4.4.2.2 Pubertal delay

As described in section 1.4.1, sex steroids play a significant role in bone mineral accrual and longitudinal bone growth, hence the resultant growth spurt in puberty. Pubertal delay negatively affects skeletal development and increases long term fracture risk. The Bone Mineral Density in Childhood Study cohort demonstrated that age of onset of puberty was a strong negative predictor of DXA bone mineral density at skeletal maturity in both genders, independent of the BMD at the beginning of puberty and the length of puberty (Gilsanz *et al.* 2011). Hogler et al showed that pubertal induction halted the reduction in BMD which was seen in pre-pubertal children (Hogler *et al.* 2004).

1.4.4.2.3 Drug-induced

Many medications used to treat chronic illnesses in children predispose them to iatrogenic secondary osteoporosis. Glucocorticoid-induced osteoporosis is very well recognised with an increased risk of fracture in children with a history of frequent oral corticosteroid use [adjusted OR of 1.32 (95% CI, 1.03-1.69)] and a doubling of humeral fracture risk in those who receive four or more courses of oral corticosteroids in a year (van Staa *et al.* 2003). Impairment of bone health is through a direct effect on bone turnover with increase in bone resorption followed by a decrease in bone formation, and indirect influence on muscle and calcium homeostasis (Buckley and Humphrey 2018). In adults, studies have shown the greatest negative effect on trabecular bone in the spine with concomitant vertebral fractures being most common (De Vries *et al.* 2007). This is reversible with fracture rate reported to normalise one year after glucocorticoid discontinuation (Korula *et al.* 2015).

1.4.4.2.4 Chronic inflammatory conditions

A wide variety of chronic inflammatory diseases can result in secondary osteoporosis summarised beautifully in the review by Makitie (Makitie 2013). This occurs not only through the increased inflammatory milieu which is toxic to the bones but also often multifactorial from reduced mobility, pubertal delay, poor nutrition and drug-induced bone loss. Diabetes mellitus, in particular T1D, is one of the disorders where systemic and local inflammatory responses have been demonstrated from the onset of the disease with detrimental effects on bone turnover and resultant skeletal fragility as discussed in more details in section 1.5.3.5.

1.4.5 Fractures in Healthy Children

Fractures in healthy children can be common. In the UK, approximately one third of children are reported to suffer a fracture before the age of 17 years, with a fracture incidence of 3% in boys and 1.5% in girls at their peak ages (Cooper *et al.* 2004) (Figure 1.18A), although other studies have reported differently (Jones *et al.* 2002, Mills and Simpson 2013). These differences could reflect the variation with the geographical area studied.

The fracture incidence varied with age and gender; increasing through childhood, with a steady rise in each 5-year age group, starting at approximately 1% risk in the under 5s, 2% in the 5-9 year olds, 3% in the 10-14 year olds and 4% in the 15-19 years old. Boys consistently had higher fracture incidence than girls, with a widening gap in the teenage years, peaking at 5% in the older teenage boys. (Figure 1.18B) (Mills and Simpson 2013). Across the literature, there is generally an agreement in the peak age of fracture incidence around 14 years old for boys and 11 years old for girls (Jones *et al.* 2002, Cooper *et al.* 2004), with slightly later ages for the Scottish cohort (Mills and Simpson 2013).

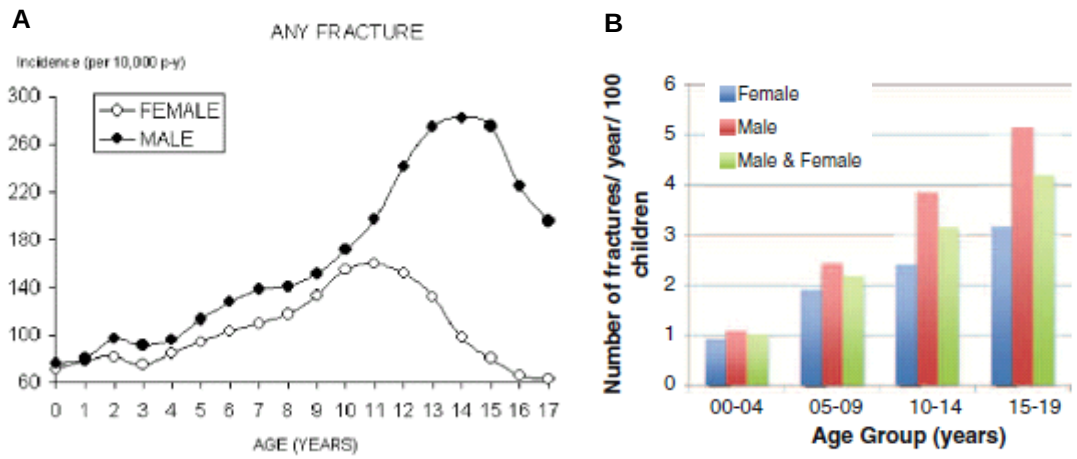

Figure 1.18 Fracture incidence at any site in childhood and adolescence. In England and Wales from 1988-1998 (B) In Scotland from 2005-2010. [Adapted from (Cooper *et al.* 2004) and (Mills and Simpson 2013)]

Seasonal differences with peak in fractures during the summer and a much lower rate during the winter have been noted (Cooper *et al.* 2004). Evidence on socioeconomic status on the incidence of childhood fractures was conflicting. The study in Glasgow using neighbourhood-type analysis demonstrated higher fracture incidence in those living in deprived areas compared to those in more affluent areas (175.3/10,000 vs 140.1/10,000) (Stark *et al.* 2002) whilst the study in South Wales using Townsend scores found no association (Lyons *et al.* 2000). In a large prospective cohort study of over 1400 children

aged 6-17 from the US, children of white Caucasian origin have been found to have substantially higher fracture risk compared to children of black African origin (Wren *et al.* 2012).

A population-based study in Finland has shown a significantly decreased incidence of fractures in the last two decades, following a rise between the 1960s and 1980s (Mayranpaa *et al.* 2010), possibly due to the implementation of injury prevention measures over the years. Studies in Finland and Europe have found a changing pattern in the skeletal sites of childhood fractures with increase in forearm fractures (Oskam *et al.* 1998, Mayranpaa *et al.* 2010) and decrease in femoral (Bridgman and Wilson 2004) and tibial (Emami *et al.* 1996) shaft fractures. Upper limb factures are more common in healthy children, accounting for 65% of all the fractures compared to 7-28% of lower limb fractures (Lyons *et al.* 2000, Wren *et al.* 2012). The most common skeletal site is distal radius (25-43%), followed by fingers and carpal bones (Landin 1983, Moustaki *et al.* 2001). Vertebral fractures are uncommon, with one study reporting the incidence of traumatic fractures of 66 per million (Puisto *et al.* 2010) although asymptomatic vertebral fractures have been identified in fracture-prone children (Mayranpaa *et al.* 2010), which should prompt further investigations into underlying skeletal fragility. Pelvic fracture is the least common in children (Cooper *et al.* 2004).

The risk of further fractures is doubled in children who have had a fracture, especially those in early childhood (Landin 1983, Wren *et al.* 2012). Up to 3% of children experience further fractures in their childhood (Cooper *et al.* 2004).

1.5 Type 1 Diabetes Mellitus (T1D)

1.5.1 Background

Type 1 diabetes (T1D) is a disorder characterised by severe insulin deficiency due to an autoimmune destruction of the pancreatic β cells in genetically predisposed individuals. The disorder affects 300,000 people in the UK, of which 35,000 are children. The incidence of T1D is 1:4000, with peak age at diagnosis between 9-14 years old. It is the second most common chronic disorder in childhood (Gale 2002), although it can occur at any age.

1.5.2 Complications of T1D

T1D is associated with well-known long term microvascular and macrovascular complications. The microvascular complications include retinopathy, nephropathy and neuropathy which lead to visual impairment, renal failure and loss of sensation in the feet with muscle weakness respectively. Macrovascular diseases, similar to that seen in Type 2 diabetes, such as coronary heart disease, peripheral vascular disease and stroke also affect adults with Type 1 diabetes. Although clinically evident diabetes-related vascular complications are rare in childhood and adolescence, early functional and structural abnormalities may be present a few years after diagnosis.

Landmark papers from the Diabetes Control and Complications Trial (DCCT), Epidemiology of Diabetes Interventions and Complications (EDIC) and large randomised controlled trials categorically demonstrated that glycaemic control is the single most important predictor of complications (Nathan *et al.* 1993, Fullerton *et al.* 2014, Lagani *et al.* 2015, Nordwall *et al.* 2015). DCCT was a multicentre, randomised controlled trial involving 1441 patients with Type 1 Diabetes conducted in North America from 1983-1993 whereby patients were randomised to two treatment arms of intensive and conventional treatment (Nathan *et al.* 1993). The intensive therapy group had average HbA1c of 7% whilst the conventional group had HbA1c of 9%. The trial results showed conclusively that intensive therapy reduced the risk of retinopathy and other microvascular complications by 35-76% in the primary prevention (no retinopathy at baseline) and secondary intervention cohorts. Results from the EDIC follow-up study showed that early intensive therapy reduced albuminuria and long term risk of developing clinically significant kidney dysfunction by 50% (de Boer *et al.* 2011) Compared to the age-matched general population, people with T1D have 10-fold increased risk of cardiovascular death (Dorman *et al.* 1984, Krolewski *et al.* 1987) with 57% reduction in the risk of macrovascular complications including non-fatal

heart attack, stroke or death from cardiovascular diseases with intensive glycaemic control (The Diabetes Control and Complications Trial (DCCT) Research Group 1995).

Apart from glycaemic control, the other main driver for the development of microvascular complications is the duration of diabetes. Longer duration of diabetes has been associated with increased risk of renal complications, including microalbuminuria, proteinuria and end-stage renal disease (ESRD) (Elley *et al.* 2013, Lagani *et al.* 2015) and retinopathy (Lachin *et al.* 2008). Nordwall et al showed increasing cumulative incidence of retinopathy with longer diabetes duration, although the role of glycaemic control was difficult to be apportioned (Nordwall *et al.* 2015). Despite this, total glycaemic exposure (HbA1c and duration of diabetes) only explained 11% of the variation in retinopathy risk (Lachin *et al.* 2008) with other factors including environmental and genetic factors, explaining the remaining 89% of the variation independent of HbA1c.

Diabetic end-organ damage are rare before puberty, and the onset of puberty accelerates the microvascular complications, in particular nephropathy (Andersen *et al.* 1983, Krolewski *et al.* 1985). Lawson et al postulated that the physiological changes of increased renal volume and the accompanying macroalbuminuria during puberty may contribute to this (Lawson *et al.* 1996). Children with diabetes appear to go through puberty at the same time as their peers (Thorn *et al.* 2005, Ostman *et al.* 2008) although some studies have shown evidence of delayed menstruation (Kjaer *et al.* 1992, Lombardo *et al.* 2009, Deltsidou 2010). Indeed, the mechanism by which puberty contributes to the development of microvascular complication remains largely unclear. Women with diabetic retinopathy and nephropathy were found to undergo later menarche (Harjutsalo *et al.* 2016) and earlier menopause (Sjoberg *et al.* 2011), further providing evidence to support the effect of sex hormones on the risk of microvascular complications.

Other specific risk factors such as hypertension and adverse cholesterol profile have been associated with retinopathy and diabetic kidney disease (Hovind *et al.* 2004, Gheith *et al.* 2016) as well as macrovascular complications (Diabetes Control and Complications Trial/ Epidemiology of Diabetes and Complications Research Group 2016). A recent large cohort study (27,195 T1D patients) demonstrated that younger age at onset of T1D was not only associated with increased macrovascular complications but also all-cause mortality as shown in Figure 1.19 (Rawshani *et al.* 2018).

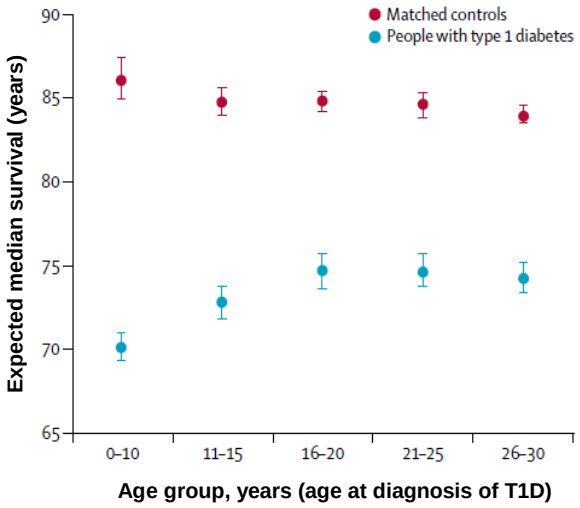

Figure 1.19 Life years lost in relation to age at onset T1D. Loss of life years was estimated by use of separate Cox regression analyses fitted to individuals with T1D and their matched controls within each age group. Conditional medial survival was estimated from the upper limit of each age interval. Life-years lost because of diabetes were calculated as the difference in the expected median survival between people with T1D and controls. [Adapted from (Rawshani *et al.* 2018)]

Interestingly, complications are less likely to occur individually. Recent evidence has highlighted that micro- and macrovascular complications tend to co-occur (Bjerg *et al.* 2018, Sauder *et al.* 2019) with co-occurrence of T1D complications in 6% of adolescents and children, more than would be expected by chance alone (Sauder *et al.* 2019). Specifically, retinopathy with diabetic kidney disease, retinopathy with arterial stiffness, and arterial stiffness with cardiovascular autonomic neuropathy, co-exist most frequently in the ascending order (Sauder *et al.* 2019). Longer duration of diabetes, poor glycaemic control, non-Hispanic white and lower socioeconomic status were identified as predisposing risk factors. The presence of two complications increases the risk of developing another complication. (Bjerg *et al.* 2018).

In the last decade or so, diabetes mellitus has also been implicated with rarer known complications such as hearing impairment (Bainbridge *et al.* 2008, Malucelli *et al.* 2012, Schade *et al.* 2018) and skeletal fragility. The latter may be manifested as reduced bone mass, abnormal bone microarchitecture, increased bone marrow adiposity or fragility fractures, as detailed in the rest of this thesis.

1.5.3 Pathogenesis of altered bone metabolism

1.5.3.1 Hyperglycaemia

Hyperglycaemia contributes to diabetic osteopathy through a variety of effects on the bone cells. Acute hyperglycaemia causes direct glucose toxicity to osteoblast (Cunha *et al.* 2014)

affecting osteoblast numbers and function; suppresses genes involved in osteoblast maturation through osmotic and non-osmotic pathways (Zayzafoon *et al.* 2000, Botolin and McCabe 2006); and affects matrix mineralisation (Balint *et al.* 2001, Cunha *et al.* 2014). Chronic hyperglycaemia impairs osteoblast maturation from 1,25(OH)2D3-induced osteocalcin secretion by down regulation of vitamin D receptor (Inaba *et al.* 1995); and promotes osteoblast apoptosis through glucose autoxidation hydrogen peroxide-induced oxidative stress (Wolff *et al.* 1991, Fatokun *et al.* 2006). Hyperglycaemia-induced acidosis might also enhance bone resorption (Frassetto and Sebastian 2012). Emerging evidence suggests that hyperglycaemia may also alter the differentiation of the MSCs promoting adipogenesis instead of osteogenesis (Keats and Khan 2012). Hyperglycaemia diverts the MSC differentiation signalling pathways toward adipogenesis at the expense of osteogenesis. This effect is achieved via ERK-1/-2-activated P13K/Akt-regulated pathway in mouse MSCs (Chuang *et al.* 2007), and via suppression of HO-1 expression (Barbagallo *et al.* 2010) and Wnt/protein kinase C non-canonical pathway in human MSCs (Keats and Khan 2012), evidenced by increased PPARγ expression in high glucose stimuli and reduction of osteocalcin levels. Indeed, mice with spontaneously and pharmacologically induced diabetes with bone loss have shown increased marrow adiposity, determined by histology and by mRNA markers of adipogenesis (PPARγ and aP2) (Botolin and McCabe 2007).Wang et al. demonstrated that hyperglycemia can also promote adipogenesis through synthesis of hyaluronan matrix which promotes an inflammatory response culminating in demineralisation of trabecular bone (Wang *et al.* 2014).

In addition, hyperglycemia leads to increased non-enzymatic protein glycation and excessive formation of these modified proteins called advanced glycosylation end-products (AGEs). AGEs appear to be the common biochemical entity accumulating in individuals with long term diabetic complications. They are seen in various sites such as vascular tissues, kidneys and bones (Bucala and Vlassara 1995, Yamamoto *et al.* 2001, Bohlender *et al.* 2005). AGEs exert their biological effects by engaging the receptor for AGEs (RAGEs), a multiligand receptor involved in immune and inflammatory responses (Schmidt *et al.* 1999, Chavakis *et al.* 2003). Consequently, AGEs, largely via RAGE, cause oxidative stress contributing to cellular dysfunction and ultimately damage target organs leading to complications such as atherosclerosis (Cipollone *et al*. 2003, Wendt *et al.* 2006) and nephropathy (Tanji *et al*. 2000, Wendt *et al*. 2003).

The accumulation of AGEs increases formation of collagen cross-links which results in increased stiffness of the collagen network in the cortical bone. This results in more brittle

bones that are less able to deform before fracturing. Accumulation of pentosidine, a well-characterised AGE, is negatively correlated to trabecular bone volume and structural strength (Schwartz *et al.* 2009, Silva *et al.* 2009). Bones of diabetic rats with higher content of pentosidine correlated negatively with BMD and bone strength (Tomasek *et al.* 1994, Saito *et al.* 2006). The pentosidine content in cortical and trabecular bones of people with femoral neck fracture is higher compared to post-mortem controls (Saito *et al.* 2006). Urinary and serum pentosidine is also increased in diabetic patients with vertebral fractures (Yamamoto *et al.* 2001, Schwartz *et al.* 2009). Iliac crest biopsies showed a significantly higher level of pentosidine in the trabecular bone of fracturing T1D patients compared to non-fracturing T1D and healthy controls (Farlay *et al.* 2016). In addition to affecting bone physical properties, AGEs also have direct effects on bone cells. Elevated AGEs can inhibit osteoblast proliferation and differentiation (Kume *et al.* 2005), function (Sanguineti *et al.* 2008), synthesis of type 1 collagen (Katayama *et al.* 1996) and osteoblast mineralisation (Ogawa *et al.* 2007). Okazaki et al. demonstrated that the inhibition of osteoblastic differentiation by AGEs can occur independently of hyperglycaemia (Okazaki *et al.* 2012). It is also associated with reduced osteocalcin mRNA expression as seen in rodents with diabetes (Tomasek *et al.* 1994). Furthermore, AGEs can also cause osteoblast death by provoking inflammation and generation of reactive oxygen species (ROS) which in turn lead to cell apoptosis as a result of oxidative stress (Coe *et al.* 2011b, Weinberg *et al.* 2014). The influence of AGEs on osteoclasts showed inconsistent effects with some evidence of increased (Miyata *et al.* 1997), as well as decreased (Valcourt *et al.* 2007) bone resorption.

Not only does hyperglycaemia and AGEs suppress osteoblastic differentiation and mineralisation, the expression of RAGE is also enhanced (Ogawa *et al.* 2007). More importantly, the AGE-RAGE interaction has been shown to affect bone quality with increased risk of vertebral fractures independent of BMD in T2D patients (Yamamoto *et al.* 2009).

1.5.3.2 Insulin, IGF-1 and other growth factors

Insulin has been shown to have an anabolic effect on bones that is distinct from the effect of its analogue IGF-1. This effect is mediated either indirectly through insulin regulation of renal 1alpha-hydroxylase activity and serum vitamin D levels in response to PTH (Hough *et al.* 1982, Ikeda *et al.* 1987), or directly on bone cells through specific insulin receptors (IRs) in osteoblasts. IRs are present on osteoblasts and its expression varies with differentiation status of the osteoblast (Levy *et al.* 1986, Thomas *et al.* 1996b). *In vitro* studies on primary

osteoblasts and clonal osteoblast cell lines show insulin promotes glucose uptake (Hahn *et al.* 1988), alkaline phosphatase activity, collagen synthesis (Canalis 1983, Pun 1989) and osteoblast proliferation (Wergedal and Baylink 1984) of these cells. Maor et al. demonstrated reduced IRs in the skeletal growth centres of mice with streptozotocin (STZ)-induced diabetes and these were reversed with insulin therapy (Maor and Karnieli 1999). Evidence for a direct link between insulin action and bone formation *in vivo* can be observed in IR knock out mice which show altered bone formation (Ferron *et al.* 2010), abnormal trabecular microarchitecture (Fulzele *et al.* 2010) and reduced bone strength (Thrailkill *et al.* 2014). Insulin positively regulates bone formation by stimulating osteocalcin production. Observational studies in people with T1D and T2D, with insulin deficiency and resistance respectively, demonstrate reduced osteocalcin levels compared with controls (Diaz-Lopez *et al.* 2013, Gower *et al.* 2013). Furthermore, there is a positive correlation between insulin dose and BMD (Weinstock *et al.* 1989, Fukunaga *et al.* 1997). The dichotomy of lower BMD in T1D with insulinopenia and higher BMD in T2D with clinical hyperinsulinemia further implicates a causal anabolic effect of insulin on bone.

The direct effect on bone may also be mediated through the IGF-1 pathway. IGF-binding protein (IGFBP) serves as a carrier protein for IGF-1. Insulin inhibits IGFBP-1 and IGFBP-4 expression in osteoblasts. Lack of insulin in T1D leads to an increase in these IGF-binding proteins hence reducing the availability of unbound IGF-1 for anabolic effects on bone (Conover *et al.* 1996). In addition to insulin deficiency, T1D individuals and animal models demonstrate dysregulation of a variety of endocrine factors including reduced amylin and IGF-1 (Rosen 2004, Hofbauer *et al.* 2007). Amylin is another osteotropic factor that is co-secreted by pancreatic beta-cells and absent in T1D (Horcajada-Molteni *et al.* 2001). Amylin-deficient mice displayed low bone mass with increased number of osteoclasts (Dacquin *et al.* 2004) and that treatment with amylin in diabetic rat result in increased BMD and bone strength (Horcajada-Molteni *et al.* 2001). Similarly, diabetic animals with low blood IGF-1 and knock-out mice for its receptor displayed diminished bone formation (Bouxsein *et al.* 2002, Zhang *et al.* 2002). Furthermore, serum IGF-1 level was shown to be an independent predictor of vertebral fractures in postmenopausal women with T2D (Kanazawa *et al.* 2011).

1.5.3.3 Calcium, Vitamin D and calciotropic hormones

It is well known that calcium homeostasis plays a major role in regulating bone metabolism, Therefore, imbalance in systemic factors which are capable of regulating calcium balance

have been found to influence diabetic bone loss (Zhang *et al.* 2011). Studies in diabetic animal models suggested reduced levels of calcium, phosphate and PTH (McCabe *et al.* 2011), with lower 1,25-dihydroxyvitamin D3 (Verhaeghe *et al.* 1990, McCabe *et al.* 2011) and vitamin-D binding proteins (Verhaeghe *et al.* 1990). Many studies have also shown vitamin D deficiency in T1D and T2D individuals albeit normal calcium, phosphate and low normal PTH (Frazer *et al.* 1981, Hampson *et al.* 1998). The effect of diabetes mellitus on calcium metabolism is complex, but essentially it is associated with a negative calcium balance hallmark by both bone and renal loss (Schwartz 2003). Children with T1D have been shown to have markedly reduced 1,25-dihydroxyvitamin–D but raised 24,25-dihydroxyvitamin-D, and this was associated with a decrease in cortical bone mass (Frazer *et al.* 1981). This could be explained by the altered vitamin D metabolic enzyme expressions and decreased expression of renal calcium transporter found in STZ-induced diabetic mice although these mice have reduced pQCT measured trabecular BMD and histologically poorer trabecular, instead of cortical, bone microstructure (Zhang *et al.* 2011). In support of this, treatment with calcitriol in STZ-induced rats demonstrated recovery of BMD (Del Pino-Montes *et al.* 2004). In terms of PTH, several *in vivo* and *in vitro* studies indicate that an imbalance in PTH was associated with bone loss and increased fracture risk (Wang *et al.* 2005, Motyl *et al.* 2012). PTH encourages bone formation and turnover by increasing the expression of osteocalcin, IGF-1, IGFBP-3, β-fibroblast growth factors (FGF), matrix metallopeptidases (MMP)-1 and MMP-13 in rat osteoblasts *in vitro* (Schmid *et al.* 1994), as well as MMP-13 in mice *in vivo* (Porte *et al.* 1999). Moreover, treatment with PTH to T1D and T2D mice demonstrated reversal of trabecular bone parameters through its anabolic effects on osteoblast differentiation and maturation (Motyl *et al.* 2012, Hamann *et al.* 2014). PTH-treatment was also associated with reduced TUNEL-staining of osteoblast suggesting its antiapoptotic effect on osteoblasts. It has been suggested that PTH promotes repair of DNA damage by increasing proliferating cell nuclear antigen (PCNA) and forkhead box protein O3a (FoxO3a) (Schnoke *et al.* 2009), hence prolonging osteoblast survival. Intermittent PTH treatment reversed bone loss to baseline in mice compared to only partial reversal in continuous PTH-treatment, although this effect may be due to underlying differences between the T1D and T2D mouse models (Motyl *et al.* 2012, Hamann *et al.* 2014). Similarly, treatment with PTH-related protein, which is produced at high levels by differentiating osteoblasts, also reverses trabecular bone loss in STZ-induced diabetic mice suggesting its modulatory effect on osteoblast function and role in diabetic osteopenia (Lozano *et al.* 2009).

1.5.3.4 Marrow adiposity and adipokines

There is a growing body of evidence that suggests that the bone-fat connection plays an important role in the pathophysiology of bone loss. Osteoblasts and adipocytes share a common precursor, both derived from the pluripotent MSCs located in the bone marrow suggesting a mutually exclusive and reciprocal lineage selection of one or the other. The main lineage-specific transcription factor which controls adipogenesis is PPARγ (Rosen and MacDougald 2006). In mice, there is evidence of increased PPARγ expression and an increase in visible adipocytes in tibia of T1D mouse models (Botolin *et al.* 2005) and increase in bone marrow adiposity in both spontaneously and STZ-induced T1D mice compared to controls (Botolin and McCabe 2007, Lozano *et al.* 2009, Motyl *et al.* 2011). Rzonca et al. demonstrated *in vivo* that rosiglitazone (PPARγ agonist) administration results in significant bone loss (Rzonca *et al.* 2004) whilst Cock et al. demonstrated that congenitally PPARγ deficient mice had increased BMD and bone trabecular microarchitecture parameter including BV/TV and trabecular thickness (Cock *et al.* 2004). However, Botolin and McCabe found that inhibition of PPARγ by administration of an antagonist to insulin deficient T1D mice prevented bone marrow adiposity but not bone loss (Botolin and McCabe 2007). This inability in preventing bone loss in T1D mice suggested that bone marrow adiposity may only be partially responsible for diabetic bone loss. Bone marrow adiposity can also have direct effects on osteoblasts as demonstrated by several co-culture studies in mouse and human cells (Maurin *et al.* 2000, Elbaz *et al.* 2010, Coe *et al.* 2011a). The presence of adipocytes inhibits osteoblast proliferation (Maurin *et al.* 2000) through the lipotoxic effect of free fatty acid in the bone marrow microenvironment [81]. There have been limited studies looking at marrow fat content in diabetes individuals to date with paucity in those with T1D. Most clinical studies of bone marrow adiposity in T2D women have shown no difference in marrow fat content between cases and controls, although T2D women consistently had lower unsaturated lipids (Baum *et al.* 2012, Patsch *et al.* 2013b, Kim *et al.* 2017). Sheu et al demonstrated higher BMF content in men with T2D, although this became insignificant after excluding two individuals on thiazolidinediones (PPARγ agonists) (Sheu *et al.* 2017, Yu *et al.* 2017). However, a new study published has now demonstrated that the bone marrow in adults with T2D have increased fat accumulation compared to controls (Ferland-McCollough *et al.* 2018), with diabetes itself causing the preferential differentiation of the bone marrow stem cells into adipocytes. Importantly, a positive correlation between HbA1c and marrow fat content has been shown suggesting that BMA may influence or be influenced by glucose metabolism and glycaemic control (Baum *et al.* 2012).

In addition to releasing large amounts of free fatty acid, adipocytes in the bone marrow also secrete cytokines including leptin, adiponectin, monocyte chemoattractant protein-1 (MCP-1) and TNFα, the last of which will be discussed in the next section. Leptin is an adipokine which has a complex regulatory role on bone metabolism, with an indirect inhibitory effect on osteoclastogenesis and a direct stimulatory effect on osteoblastogenesis through a central (hypothalamic) and peripheral pathway (Steppan *et al.* 2000, Reseland *et al.* 2001, Cornish *et al.* 2002). Despite being an adipokine, *in vitro* studies indicate that leptin promotes an osteoblast rather than adipocyte lineage (Reseland *et al.* 2001, Cornish *et al.* 2002). In contrast to T1D patients who demonstrate increased (Luna *et al.* 1999) or slightly decreased leptin level (Karaguzel *et al.* 2006), leptin levels were found to be significantly suppressed in T1D mice, its absence results in reducing bone mass with increasing marrow adiposity (Steppan *et al.* 2000). T2D is typically associated with obesity, which has been associated with higher leptin level and higher BMD. Vasilkova et al., however, demonstrated that leptin has an independent positive correlation to BMD, irrespective of BMI (Vasilkova *et al.* 2011). In addition, interventional studies in mice have demonstrated that leptin administration reduces bone marrow adiposity and increases bone mass (Hamrick *et al.* 2005, Martin *et al.* 2005). However, similar to their work on PPARγ antagonist, Motyl and McCabe concluded that leptin administration to T1D mice modify and prevent marrow adiposity but did not prevent diabetic bone loss (Motyl and McCabe 2009).

Adiponectin (APN), the most abundant adipokine secreted exclusively by adipocytes, regulates energy homeostasis and exerts well-characterized insulin sensitizing properties. The insulin-sensitising effect of OC is known be due to the upregulation of APN gene in adipocytes (Lee *et al.* 2007) but there is some suggestion that in humans the link between OC and APN may be gender specific (Buday *et al.* 2013). APN seems to have an anabolic effect on osteoblasts and an inhibitory effect on osteoclasts *in vitro* (Williams *et al.* 2009). The peripheral and central effects of APN on bone metabolism are beginning to be explored but are still not clearly understood. APN-knockout (APN-KO) mice fed a normal diet exhibit decreased trabecular structure and mineralisation and increased bone marrow adiposity whilst central administration of APN into the brain ventricles decreased osteoclast numbers and increased osteoblastogenic marker expression and trabecular bone mass, in both APN-KO and WT mice (Wu *et al.* 2014). Clinically, serum APN levels have been shown to be positively associated with BMD at the distal radius in Japanese individuals with T2D, although the evidence linking adiponectin to bone mass is conflicting with some studies showing an inverse relationship (Lenchik *et al.* 2003, Tamura *et al.* 2007, Napoli *et al.* 2010).

1.5.3.5 Chronic inflammation

The pathogenesis of both T1D and T2D are associated with activation of the immune system, especially so in T1D which involves an autoimmune destruction of pancreatic β-cells whilst T2D involves a more chronic low-grade inflammatory process (Bending *et al.* 2012, Esser *et al.* 2014). Several experimental studies using T1D mice model indicate that systemic and local inflammatory cytokines are increased at the onset of diabetes with rapid suppression of osteoblast markers and increase in adipocyte markers, indicating that bone inflammation may be another contributing factor to the diabetic bone pathology (Motyl *et al.* 2009, Coe *et al.* 2011a, Roszer 2011). Serum cytokine levels (TNFα, IFNγ, IL-1Rα and lymphotoxin-β) and corresponding bone cytokine mRNA expression were increased from as early as 5 days after induction of diabetes in mouse models (Botolin and McCabe 2007, Motyl *et al.* 2009) with decrease in osteocalcin mRNA expression in bone RNA extracts, and it remains suppressed at 40 days postinduction of diabetes in the mouse models. These inflammatory cytokines can either directly suppress osteoblast differentiation (Gilbert *et al.* 2000), promote osteoblast death directly (Coe *et al.* 2011a) or indirectly by contributing to elevation of ROS causing osteoblast apoptosis from oxidative stress (Hamada *et al.* 2009, Coe *et al.* 2011b), and activate osteoclastogenesis (Glantschnig *et al.* 2003). Coe et al. also found that TNFα in the bone marrow microenvironment directly mediates osteoblast death with increase in expression of proapoptotic factors and osteoblast TUNEL staining, further contributing to T1D bone loss (Coe *et al.* 2011a). Inhibition of the cytokines with TNFα neutralizing antibodies prevented osteoblast apoptosis (Coe *et al.* 2011a) but transgenic mice with IFNγ KO proceeded to have diabetic bone pathology (Motyl *et al.* 2009), supporting the idea that diabetic inflammatory bone loss involves an interplay of more than one cytokine and/or a combination of other factors. Apart from proinflammatory cytokines, abnormal hyaluronan production in bones of diabetic rodents also induced monocyte and macrophage infiltration into the bone collagen matrix, promoting adipogenesis at the expense of osteogenesis (Wang *et al.* 2014). The concept of T2D as an inflammatory disease is relatively new with increased fat depots in T2D implicated as the source for more proinflammatory cytokines and adipokines (Esser *et al.* 2014). The cytokine MCP-1, secreted by mature adipocytes in the bone marrow, acts in a paracrine manner, further promoting MSC differentiation into adipocytes (Ferland-McCollough *et al.* 2018). However, a large prospective population study (EPIC) in Germany found that systemic inflammatory markers are independent predictors for the development of T2D, independent of degree of insulin resistance and obesity (Spranger *et al.* 2003).

1.5.3.6 Vasculopathy

Similar to other diabetic microvascular complications of retinopathy, nephropathy and neuropathy, bone microangiopathy has been insinuated as another possible mechanism for diabetic bone loss. In hypoxic condition (2% oxygen), the bone marrow shifts toward adipogenic lineage by enhancing expression of genes associated with adipogenic/lipogenic phenotype (C/EBPβ, PPARγ2, and aP2) and by suppressing expression of genes associated with osteoblast differentiation (AP) (Irwin *et al.* 2007). Oikawa et al. found that the cumulative vascular density was reduced by threefold in bone marrow of STZ-induced diabetic mice compared to control, along with reduction in blood flow (Oikawa *et al.* 2010). In addition, there is also evidence of reduction in bone marrow volume and bone marrow remodeling with cell depletion mainly affecting the osteoblastic niche secondary to hypoperfusion and oxidative stress (Oikawa *et al.* 2010). Correspondingly, boosting the antioxidative pentose phosphate pathway with benfotiamine supplementation prevented microangiopathy and hypoperfusion in the bone marrow with reduction in cell apoptosis, providing further compelling evidence for vasculopathy in diabetic bone pathology. Regenerating mouse tibia has reduction in blood vessels with lower expression of vascular endothelial growth factor (VEGF), a signalling protein which regulates angiogenesis, and its receptor (Lozano *et al.* 2009). Clinically, histomorphometric evaluation of iliac crest bone biopsy in 118 diabetic patients revealed evidence of diabetic bone microangiopathy in 82% with significant osteopenia and reduction in the sinusoidal capillaries (Burkhardt *et al.* 1981).

1.5.3.7 Anti-diabetic medications

Different classes of anti-diabetic medication, such as thiazolidinediones (TZDs), metformin and glycogen-like peptide 1 (GLP-1) inhibitors have been reported to have varying effects on bone.

1.5.3.7.1 Insulin

Although insulin is considered to have an anabolic effect on bones, individuals with T1D on higher insulin dose have been shown to have lower BMD (Leger *et al.* 2006, Eller-Vainicher *et al.* 2011) whilst individuals with T2D on higher insulin dose have been shown to have increased risk of falls from hypoglycaemic attacks resulting in fractures (Monami *et al.* 2008, Johnston *et al.* 2012). The positive correlation between daily insulin dose and HbA1c (Hofbauer *et al.* 2007) may help explain the negative correlation between daily insulin dose with BMD, reflecting possibly an issue with compliance or possibly the presence of a more

severe disease (more inflammatory processes) in T1D (Leger *et al.* 2006). Findings from the HABC study showed that T2D insulin-treated patients with HbA1c ≤ 6% had an increased risk of falls (Schwartz *et al.* 2008). This finding should be interpreted with caution as T2D patients on insulin usually had longer duration of diabetes and other concurrent microvascular complications such as retinopathy and neuropathy which predispose to falls. Nephropathy with impaired renal function also has a linear correlation to falls (Schwartz *et al.* 2008), possibly as impaired renal function may interfere with vitamin D metabolism resulting in reduced muscle strength.

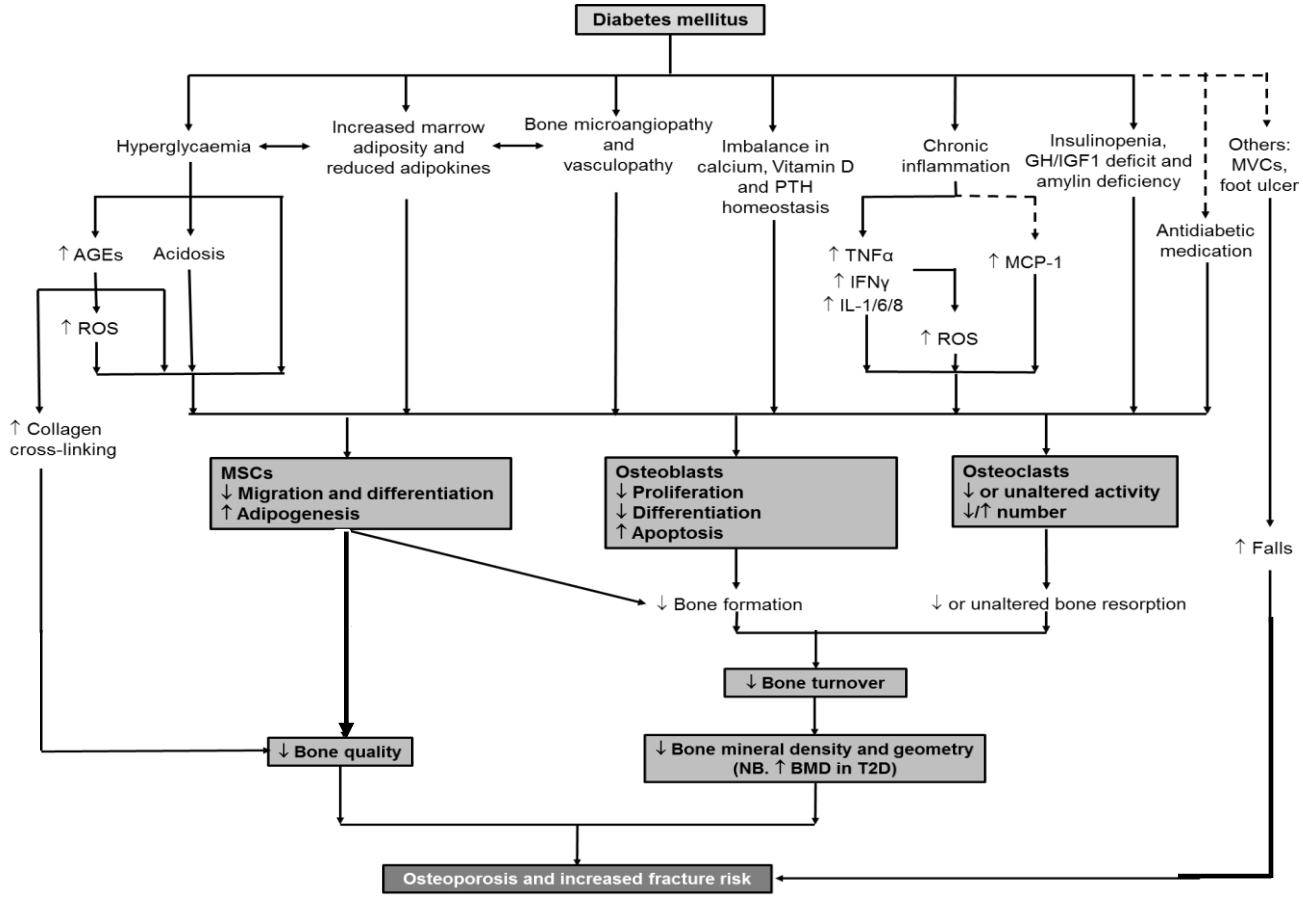

Figure 1.20 Pathophysiological mechanisms of diabetic bone disease. Type 1 (T1D) and Type 2 Diabetes (T2D) mellitus affect bone turnover, bone mineral density and bone quality through a complex interplay of hyperglycaemia, insulinopenia, GH/IGF-1 deficit, chronic inflammation and vasculopathy to name a few, ultimately leading to osteoporosis and increased fracture risk. IGF-1 insulin growth factor-1, PTH parathyroid hormone, MVCs microvascular complications, AGEs advanced glycation end products, ROS reactive oxygen species, TNFα tumour necrosis factor-alpha, IFNγ interferon-gamma, IL(1,6,8); interleukin-(1,6,8), MCP-1 monocyte chemoattractant protein-1, MSCs mesenchymal stem cells, BMD bone mineral density. Solid lines represent pathways affecting both T1D and T2D, with broken lines specific to T2D only.

1.5.3.7.2 Thiazolidinediones

TZDs such as pioglitazone and rosiglitazone have been shown to increase adipocyte differentiation and decreased osteoblast differentiation through activation of PPARγ activity (Rzonca *et al.* 2004, Ali *et al.* 2005, Schwartz 2008). Consistent with these preclinical observations, a comprehensive meta-analyses of 10 randomised controlled-trials (total 13,715 participants) and 2 observational (total 31,679 participants) studies, clearly indicated an increased risk of fractures (OR 2.23, 95% CI 1.65-3.01) with TZD (both pioglitazone and rosiglitazone) use, particularly in women (Loke *et al.* 2009). A more recent meta-analysis, including 22 randomised controlled-trials (total 24,544 participants) further confirmed this gender difference in fracture risk (OR 1.94, 95% 1.6-2.35 in women vs OR 1.02, 95% CI 0.83-1.27 in men), which is independent of age and duration of TZD exposure (Zhu *et al.* 2014). Use of this medication should therefore be avoided in women.

1.5.3.7.3 Metformin

Metformin is the standard first line pharmacologic treatment for T2D. It exerts a direct osteogenic effect *in vitro* by stimulating proliferation and differentiation of osteoblasts (Cortizo *et al.* 2006, Gao *et al.* 2008, Kanazawa *et al.* 2008, Ma *et al.* 2010a, Jang *et al.* 2011) through preventing AGE-induced deleterious effects in osteoblastic cells (Schurman *et al.* 2008) and various other signalling pathways including the PI3K/Akt pathway (Ma *et al.* 2010b), ERK-1/2 (Cortizo *et al.* 2006) and AMPK activation (Kanazawa *et al.* 2008, Jang *et al.* 2011). Zhen et al. also demonstrated an indirect effect of metformin on osteoblast survival through reduction of intracellular ROS (Zhen *et al.* 2010). In addition to its osteoblastogenic potency *in vitro*, metformin can further prevent bone loss by inhibiting osteoclastic differentiation (Mai *et al.* 2011). However, ovariectomized rodents treated with metformin demonstrated inconsistent radiological findings of no change in bone microarchitecture (Jeyabalan *et al.* 2013) to increased BMD (Mai *et al.* 2011). In clinical studies however, metformin has been shown to have a neutral (Monami *et al.* 2008, Colhoun *et al.* 2012, Napoli *et al.* 2014) or positive (Vestergaard *et al.* 2005, Zinman *et al.* 2010) effect on bone metabolism. One of the larger observational studies (total 498,617 participants) reported that metformin was associated with a decreased risk of any fractures (HR 0.81; 95 % CI, 0.70–0.93) (Vestergaard *et al.* 2005). The only randomised trial, ADOPT (total 4351 participants, 1840 women) designed to compare metformin with rosiglitazone and glyburide found that the cumulative incidence of fracture is 1.2 per 100 patient years for metformin and glyburide but up to 9.3 per 100 in women for rosiglitazone (Kahn *et al.* 2006). To date, only one study has investigated the role of metformin in young patients. In the

Treatment Options for type 2 Diabetes in Adolescents and Youth (TODAY) clinical trial, 699 patients aged 10–17 years with T2D were divided into three different treatment groups: metformin plus rosiglitazone; metformin alone; metformin plus lifestyle. BMD and BMC increased in all groups, but increased less in metformin plus rosiglitazone compared with the other two groups after 24 months (0.06 g/cm2 in metformin plus rosiglitazone vs 0.076 g/cm2 in metformin plus lifestyle; p=0.0041) (Today Study Group 2013).

1.5.3.7.4 Sulphonylureas

Sulphonylureas such as glimepiride and glyburide are anti-hyperglycaemic drugs which cause increased secretion of insulin by binding to the K_{ATP}-channel on the cell membrane of pancreatic beta cell. Consequently, these agents have been reported to cause increased risk of hypoglycaemia (Monami *et al.* 2008) and increased fracture risk. Similar to metformin, sulfonylureas have been reported to have either neutral (Melton *et al.* 2008, Monami *et al.* 2008) or a reduction in risk of fractures in patients treated with these agents (Vestergaard *et al.* 2005, Zinman *et al.* 2010). The ADOPT RCT showed comparable cumulative incidence of fractures to metformin of 1.2 per 100 patient years, with 5 year cumulative incidence of fractures (95 % CI) of 5.7 % (3.9–7.6) (Kahn *et al.* 2006). A large population-based case–control study in Denmark (total 124,655 cases with 3:1 age-and -gender matched controls of 373,962) found that treatment with sulfonylureas was associated with a significant decrease in the risk of hip fracture (HR 0.74, 0.58–0.93) versus patients with T2D without treatment (Vestergaard *et al.* 2005). Given the high rate of hypoglycaemia with sulphonylureas, this group of antidiabetic drug should be used with caution in those at higher risks of fragility fractures.

1.5.3.7.5 Incretin-based therapies

Incretins are a group of gastrointestinal hormones which act to lower blood glucose levels by inhibiting glucagon release. It also reduces gastric emptying and can help to increase the secretion of insulin from pancreatic beta cells. The two main groups are the glucagon-like peptide-1 (GLP-1) and dipeptidyl peptidase-4 (DPP-4) inhibitor, the latter is an enzyme which inactivates GLP-1 (Drucker and Nauck 2006). Three meta-analyses have looked at the fracture incidence with GLP-1and DPP-4 inhibitors showing contradicting and favourable effects respectively on bone. GLP-1 liraglutide has been associated with reduced fracture risk (OR 0.38, 95% CI 0.17-0.87) whilst exenatide was correlated with increased fracture risk (OR 2.09, 95% CI 1.03-4.21) (Su *et al.* 2015). Although a meta analyses of DPP-4 inhibitors have shown a reduction in fracture risk (OR 0.60, 95% CI 0.37-0.99)

(Monami *et al.* 2011), more recent studies have demonstrated varying results with sitagliptin reported to have anabolic effects on the bone (Hegazy 2015) but not with saxagliptin in the SAVOR-TIMI trial (Mosenzon *et al.* 2015).

1.5.3.7.6 Sodium/glucose co-transporter 2 (SGLT-2)

SGLT-2 such as dapagliflozin and canagliflozin are a new generation of antidiabetic drugs which work to reduce hyperglycaemia by inhibiting renal reabsorption of glucose from the proximal tubules (DeFronzo *et al.* 2012, Ljunggren *et al.* 2012, Bolinder *et al.* 2014). Dapagliflozin and empagliflozin seem to have a neutral effect on bone metabolism, with no significant changes in bone turnover or BMD parameters (Ljunggren *et al.* 2012). Concerns have been raised for canagliflozin, which might cause bone loss at the hip (Bilezikian *et al.* 2016, Watts *et al.* 2016) and increase the risk of hip fractures (Watts *et al.* 2016).

1.5.4 Clinical evidence of fractures

1.5.4.1 Type 1 Diabetes (T1D)

Adults with T1D have been shown to have a significantly higher risk of hip fractures, of eight- to 18-folds compared to the general population (Miao *et al.* 2005, Ahmed *et al.* 2006). Two large meta-analyses published following that confirmed the increased hip fracture risk of 6.9- and 6.3-folds respectively compared to individuals without T1D (Janghorbani *et al.* 2007, Vestergaard 2007). In a large observational study in Scotland (total of 21,033 individuals with T1D) a consistently increased but lower relative risk of hip fracture, of 3.2 in men and 3.5 in women, was reported (Hothersall *et al.* 2014). A more recent meta-analysis (total 27,300 individuals with T1D) further validated this lower relative fracture risk of over three-folds in all fractures, and not just hip alone (Shah *et al.* 2015). Fractures at the spine, although less marked (OR 2.5, 95% CI 1.3-4.6), are also moderately increased in the T1D population (Vestergaard *et al.* 2005). Zhukouskaya et al reported a significantly higher risk of morphometric vertebral fractures, assessed by VFA, in young adults with T1D (24% vs 6% in healthy controls) with a meta-analysis reporting a pooled relative risk of 2.88 (95% CI 1.71-4.82) in individuals with T1D (Zhukouskaya *et al.* 2013, Shah *et al.* 2015).

Another most disconcerting finding is that the increased risk of fracture extends across all ages, affecting even young adults and children with T1D, with widening discrepancy in the risks from age 40 years. (Hothersall *et al.* 2014, Weber *et al.* 2015). Studies have shown an almost linear association between duration of disease (T1D) and fracture risk (Nicodemus *et al.* 2001, Miao *et al.* 2005), although this was contradicted by others (Ahmed *et al.* 2006).

There is an intriguing proposal of a bimodal relationship with the highest incidence of fracture occurring in the first 2.5 years of diagnosis and again beyond 5 years of diabetes being diagnosed (Vestergaard *et al.* 2005). Most studies, but not all (Neumann *et al.* 2011), have found no association between glycaemic control, as measured by HbA1c, with risk of fracture. Many studies have invariably reported an association between fracture risk and the presence of all types of diabetic complications (Miao *et al.* 2005), and more specifically retinopathy (Ivers *et al.* 2001, Weber *et al.* 2015), nephropathy (Miao *et al.* 2005), neuropathy (Miao *et al.* 2005, Weber *et al.* 2015) and cerebrovascular disease (Strotmeyer *et al.* 2005).

Lower extremity fractures (hip/femur, lower leg/ankle and foot) were more common than upper extremity/vertebral fractures in those with T1D (31.1% vs 25.1% in males, 39.3% vs 32% in females; $p<0.001$) (Weber *et al.* 2015).

1.5.4.2 Type 2 Diabetes (T2D)

T2D has also been associated with increased risk of fractures. The Study of Osteoporotic Fractures (SOF) cohort found that women with T2D have an increased risk of hip and proximal humeral fractures (RR 1.82, 95% CI 1.24-2.69 and RR 1.94, 95% CI 1.24-3.02) compared to the non-diabetic population (Schwartz *et al.* 2001). A meta-analysis of eight prospective studies for the hips and three studies for the wrists in adults with T2D concluded that the relative risk of hip and wrist fractures were 1.4 and 1.2, respectively with no increase in vertebral fracture risk (RR 0.93, 95% CI 0.63-1.37) (Vestergaard 2007). Another meta-analysis published in the same year of 16 epidemiologic studies, of which 4 investigated vertebral fractures, substantiated the neutral vertebral fracture risk but found a slightly higher relative risk of hip fracture of 1.8. This relative risk rose to 2.7 (95% CI 1.7-4.4) when the analysis was restricted to four cohort studies with >10 years of follow-up (Janghorbani *et al.* 2007). In fact, a history of T2D was shown to be the single most important and independent predictor of low-energy subtrochanteric and diaphyseal femoral fractures (Napoli *et al.* 2013). Subsequent to the meta-analysis, more studies have suggested than T2D may also be associated with higher vertebral fracture risks with up to 23% of vertebral fractures reported in post-menopausal women (Ardawi *et al.* 2013). A Japanese cohort study (total participants 996, 1 case:3 controls) further elucidated a gender preponderance with men (OR 4.7, 95% CI 2.19-10.20) more likely to have vertebral fractures than women (OR 1.9 (95% CI 1.11-3.12) (Yamamoto *et al.* 2009, Viegas *et al.* 2011). Fractures of the wrists (de *et al.* 2005) and

foot (Schwartz *et al.* 2001, Bonds *et al.* 2006) also seemed to be more prevalent in individuals with T2D than the general population.

Duration of T2D, glycaemic control, anti-diabetic medications, propensity to fall and T2D-related complications were observed as possible predicting factors for the increased fracture risk in these studies. Cross-sectional studies have indicated that those with increased fractures are older (Nicodemus *et al.* 2001, Janghorbani *et al.* 2007, Yamamoto *et al.* 2008) and have a longer duration of T2D (Yamamoto *et al.* 2008, Viegas *et al.* 2011). The incidence was also higher in those treated with insulin (Janghorbani *et al.* 2007, Melton *et al.* 2008). In T2D, falls are common (Schwartz *et al.* 2001, Schwartz 2008) and the risk of falling may be higher in those with poor balance, arthritis, cardiovascular disease, depression, poor vision and use of medications for sleeplessness or anxiety (Schwartz *et al.* 2001). It is unclear whether this increased risk of fall is also associated with more fractures. The presence of microvascular complications have also been associated with increased risk of fractures, in particular neuropathy (Melton *et al.* 2008) and retinopathy (Viegas *et al.* 2011).

1.5.5 Bone turnover studies

1.5.5.1 T1D

T1D is associated with a low bone turnover state with dissociation between bone formation and bone resorption (Starup-Linde 2013). Both pharmacologically-induced and spontaneously diabetic NOD mice with chronic disease have impaired bone formation and resorption, with concomitant histomorphometric data (Hough *et al.* 1981, Hough *et al.* 1983). In humans, the marker of bone formation, osteocalcin has been found to be low in both adults and children with T1D (Bouillon *et al.* 1995). A recent large meta-analysis further substantiated this with significantly lower osteocalcin -1.51 (-2.76, -0.26) ng/ml) in individuals with diabetes compared to non-diabetes controls. Subgroup analysis demonstrated specifically that the osteocalcin level was depressed in T1D, but not in T2D (Starup-Linde *et al.* 2014). Glycaemic control, as measured by HbA1c was found to be negatively correlated to the osteocalcin levels (Adami 2009, Maggio *et al.* 2010). The level of another bone formation marker, bone alkaline phosphatase (BAP) has been found to be more variable with studies showing a suppressed level (Lumachi *et al.* 2009) and a meta-analysis showing an increased BAP compared to controls (Masse *et al.* 2010, Starup-Linde *et al.* 2014). This imbalance of bone formation markers (increased BAP, decreased osteocalcin) may reflect an impairment of osteoblast differentiation and maturation as BAP is expressed early in the development of osteoblast whilst osteocalcin is released from the

mature osteoblast. Studies on the markers of bone resorption were conflicting with either normal (Alexopoulou *et al.* 2006) or reduced (Campos Pastor *et al.* 2000, Maggio *et al.* 2010, Abdalrahaman *et al.* 2015) circulating levels in individuals with T1D. Pooled data from the meta-analysis concluded that bone resorption is depressed with reduced CTX at -0.14 (-0.22,-0.05) ng/ml in individual with diabetes mellitus, but no sub-analyses by diabetes type was available to distinguish whether bone resorption differed between T1D and T2D. The low bone turnover state appears to be present from the onset of T1D in childhood with normalisation after 3 months (Pater *et al.* 2010), which may be a function of concurrent improvement in the HbA1c with insulin treatment, as adults with T1D continued to have lower osteocalcin, BAP and CTX compared to controls as detailed above. Bone histomorphometry data in T1D is scarce. One study in two patients with T1D showed markedly depressed bone formation compared to non-diabetics (Krakauer *et al.* 1995) but a larger case-control study of 18 T1D patients showed no difference in bone metabolism between the groups (Armas *et al.* 2012). Further sub-analyses of the T1D patients demonstrated a significantly depressed bone formation in the small group who had fractures compared to those without fractures (Armas *et al.* 2012). The incorporation of bone turnover markers into the FRAX model has not explained the increased fracture risk in diabetes patients compared to healthy controls (Bhattoa *et al.* 2013) so at present, bone turnover markers are of limited use in fracture prediction. Heterogeneity between all the studies such as the differences in patient characteristics (age, ethnicity, disease duration, glucose control) and the discrepancies in timing of serum collection and assay variations may have influenced the results.

Sclerostin, produced almost exclusively by osteocytes, is an inhibitor of the canonical Wnt/β-catenin signalling pathway involved in bone formation, thus playing an essential role in osteoblast differentiation and bone turnover (Baron and Kneissel 2013). In animal models, overexpression of *SOST* gene causes osteopenia and limb defects (Loots *et al.* 2005, Baron and Kneissel 2013), while lack of *SOST* causes 3–4 times more bone mass, consistent with human phenotypes in a condition called sclerosteosis (Collette *et al.* 2012). Many studies have found that sclerostin levels were higher in patients with T1D (Catalano *et al.* 2014, Neumann *et al.* 2014) compared to controls, with gender predilection for higher levels in females than males (Catalano *et al.* 2014). The duration of diabetes has also been shown to positively correlate with higher sclerostin levels, further impairing bone health and increasing fracture risk. T1D mice subjected to sclerostin-neutralising antibody treatment demonstrated reversal in the osteopenia, reduced bone marrow adipogenesis and improved fracture outcome (Yee *et al.* 2016). Intriguingly however, sclerostin levels have been shown

to be inversely associated with fracture in T1D patients (Starup-Linde *et al.* 2016). T1D patients with the highest tertile of sclerostin had an 81% decreased risk of fracture compared with the lowest tertile which is counterintuitive and remains unexplained. The reproducibility of this study or further mechanistic explanation has yet to be seen.

1.5.5.2 T2D

Similar to T1D, individuals with T2D are reported to have suppressed bone turnover. Bone formation is consistently lower in people with T2D, as evidenced by lower serum osteocalcin, BAP and procollagen type 1 N-terminal propeptide (P1NP) levels (Dobnig *et al.* 2006, Gennari *et al.* 2012) with suppressed bone resorption as demonstrated by lower CTX levels compared to healthy controls (Dobnig *et al.* 2006, Gennari *et al.* 2012, Reyes-Garcia *et al.* 2013). A large meta-analysis, however, did not show a significant difference (p=0.06) in osteocalcin in T2D individuals compared to healthy controls (Starup-Linde *et al.* 2014) and did not analyse CTX by subtype of diabetes hence it remains unclear whether bone resorption is affected in T2D. In accordance with the former, bone histomorphometry demonstrated reduced histologic measures of mineralising surface and bone formation rate (Manavalan *et al.* 2012). Serum PTH tends to be lower (Dobnig *et al.* 2006, Garcia-Martin *et al.* 2012, Reyes-Garcia *et al.* 2013) in T2D. The relative (moderate or subclinical) hypoparathyroidism in diabetes patients, with normal calcium and phosphate levels, could contribute to the low bone turnover state as the levels of osteocalcin and CTX have been shown to correlate with PTH levels (Yamamoto *et al.* 2012, Reyes-Garcia *et al.* 2013).

Increased sclerostin levels have been found in patients with T2D compared to healthy controls (Garcia-Martin *et al.* 2012, Gaudio *et al.* 2012, van Lierop *et al.* 2012). The elevated sclerostin levels were associated with osteoporotic fractures (Ardawi *et al.* 2012, Heilmeier *et al.* 2015) in postmenopausal women and also importantly, an increased risk of vertebral fractures (Ardawi *et al.* 2012) in T2D patients of both genders independently of BMD.

1.5.6 Bone imaging studies

1.5.6.1 T1D

Imaging studies have provided the wealth of evidence linking diabetes mellitus, both T1D and T2D, with impaired bone health. The effects of T1D on bone health may be manifested as aberrant bone mass (Gunczler *et al.* 1998, Heap *et al.* 2004, Saha *et al.* 2009b) and abnormal bone microarchitecture (Abdalrahaman *et al.* 2015), predisposing ultimately to the clinically significant increased risk of fractures (Vestergaard 2007, Hothersall *et al.* 2014) in this population.

1.5.6.1.1 Bone mineral density (BMD)

Almost universally, using the more sensitive modern dual energy X-ray absorptiometry (DXA) scanners, studies have shown reduced BMD in adults (Campos Pastor *et al.* 2000, Strotmeyer *et al.* 2005, Rakic *et al.* 2006, Mastrandrea *et al.* 2008, Eller-Vainicher *et al.* 2011) and children (Gunczler *et al.* 1998, Valerio *et al.* 2002, Leger *et al.* 2006, K. Heilman *et al.* 2009) with T1D at either lumbar spine (LS), femoral neck (FN) or total body (TB), bar a few exceptions (Lunt *et al.* 1998, Pascual *et al.* 1998, Ingberg *et al.* 2004, Bridges *et al.* 2005). All major studies reporting on bone densitometry in children with T1D have been summarised in Table 1.6. The studies which showed no difference in BMD between diabetic and non-diabetic population were methodically suboptimal, in not adjusting for group differences in BMI (Lunt *et al.* 1998) as BMI is a very important determinant of BMD or taking into account size correction for DXA interpretation in children (Pascual *et al.* 1998). The reduction in BMD varied markedly from 8-67%, with a reported pooled estimated LS BMD Z-score of -0.22 ± 0.01 and FN BMD Z-score -0.37 ± 0.16 (both $p<0.05$) in a meta-analysis comparing individuals with T1D and without (Vestergaard 2007). Lower BMD was associated with the presence of microvascular complications although further meta-regression showed that neither duration of disease nor glycaemic control, as measured by HbA1c, was associated with BMD (Vestergaard 2007). Several studies have demonstrated a reduction in BMD from the onset of T1D diagnosis (Gunczler *et al.* 2001, Lopez-Ibarra *et al.* 2001) suggesting a predisposing variant rather than chronic metabolic consequences of the disease on bones.

Table 1.6 Bone densitometry studies in children with T1D, based on dual-energy x-ray absorptiometry (DXA) and peripheral quantitative computed tomography (pQCT).

Author, year	n (F/M)	Age (yrs)†	Disease duration (yrs)†	Modality	Site	Bone density findings	Additional findings of bone-related parameters/ Other comments
(Lettgen *et al.* 1995)	21	NA	NA	pQCT	NA	↓Trabecular and cortical vBMD ↓TB BMD	Trabecular vBMD inversely associated with disease duration. TB BMD inversely correlated with HbA1c
(Gunczler *et al.* 1998)	26 (11/15)	12.1±3.1	4.3±2.9	DXA	TB,LS,FN	↓LS BMD	DXA interpretation not size-corrected. No association with disease duration or HbA1c.
(Pascual *et al.* 1998)	55 (29/26)	M 9.7±4.3 F 11.2±3.8	1-13.8	DXA	LS, Radius	↔ LS BMD	DXA interpretation not size-corrected. No relationship to HbA1c or disease duration. Adjusted for age and sex.
(Gunczler *et al.* 2001)	23 (16/7)	9.5±2.2	0.5±0.1	DXA	TB,LS,FN	↓LS BMD	Matched to age and height. All prepubertal and newly diagnosed T1D.
(Heap *et al.* 2004)	55 (25/35)	M 14.6±1.7 F 14.7±1.9	5.8±4.3	pQCT DXA	Tibia TB,LS,FN	↓Trabecular and cortical vBMD ↓TB and FN BMD	BMD adjusted for LBM. Trabecular vBMD and TB BMD inversely associated withn HbA1c.
(Moyer-Mileur *et al.* 2004)	42 (16/26)	M 16.0±1.7 F 15.1±1.8	4.2±3.1	pQCT DXA	Tibia TB,LS,FN	↓Cortical vBMD , ↓TB and LS BMD	BMD adjusted for LBM and LBM-for-height. Lower annual gain of tibia cortical bone and TB BMD; inverse association to HbA1c.
(Leger *et al.* 2006)	127 (54/73)	12.9 (10.2-15.2)	5.6(4.6-8.8)	DXA	TB,LS	↓ TB vBMD	Adjusted for LBM and LBM-for-height. Girls have lower LS and TB BMC than boys. Lower IGF1 in T1D, but no correlation to HbA1c or disease duration.
(Bechtold *et al.* 2006)	88 (42/46)	11.7±3.0	5.6±3.7	pQCT DXA	Radius	↔ Trabecular and cortical vBMD ↓ Cortical BMD, ↔TB BMD.	Early age at T1D diagnosis associated with reduced total, cortical and muscle CSA. No difference with HbA1c or disease duration. NB: Higher weight and BMI in T1D cohort.
(Bechtold *et al.* 2007)	41 (20/21)	15.4±2.3	9.8±2.8	pQCT	Radius	↔ Cortical vBMD	Normalisation of total, cortical and muscle CSA. Reduced trabecular vBMD but no comment to reference population. NB: Higher weight and BMI in T1D cohort.
(Brandao *et al.* 2007)	44 (22/22)	8.8±4.4	6.6±3.9	DXA	LS (L1-L4)	↔ LS BMD	66% prepubertal. Negative association of disease duration and HbA1c with BMD only in girls.
(Mastrandrea *et al.* 2008)	37 (37/0)	16.2±1.8	NA	DXA	TB,LS,FN	↔ all BMD.	Adjusted for age, BMI and OC use. Trend of lower TB BMD in T1D. No correlation to HbA1c or disease duration.

Author, year	n (F/M)	Age (yrs)†	Disease duration (yrs)†	Modality	Site	Bone density findings	Additional findings of bone-related parameters/ Other comments
(Moyer-Mileur *et al.* 2008)	11 (11/0)	12.9±1.0	5.9±3.7	pQCT DXA	Tibia TB,LS,FN	↓Cortical vBMD ↓TB,FN BMD and LS BMAD	Adjusted for height for age, BMC to BA. Lower IGF-1 noted in poorer HbA1c and younger age at diagnosis. Cortical thickness positively assoc with age at diagnosis.
(Kaire Heilman *et al.* 2009)	30 (11/19)	4.7-18.6	5.4±3.4	DXA	LS, TB	↓TB BMC and LS vBMD	Adjusted for age, height and BMI. Only present in boys. Inverse association to urinary markers of oxidative stress, plasma ICAM-1 levels and HbA1c.
(Saha *et al.* 2009a)	48 (26/22)	12-17.8	6.8 (1-13.5)	pQCT DXA	Radius/ Tibia LS, FN	↔ Trabecular/ cortical vBMD ↓FN BMC	Adjusted for age, weight and height. Smaller cortical areas at radius and tibia. Boys affected more than girls.
(Inge Roggen *et al.* 2013)	56 (23/33)	M 17.9 (17.2–24.8) F 18.1 (17.8-22.9)	M 10.6±3.9 F 10.0±2.7	pQCT	Radius	↔ Trabecular vBMD,	Smaller CSA in T1D, esp males. In girls, the CSA SDS correlated negatively with the BMI SDS and positively with the height SDS. No correlation to HbA1c.
(Loureiro *et al.* 2014)	75 (29,46)	12 (6-20)	5.0±3.5	DXA	LS (L1-L4)	↓ LS BMD	Inverse association to HbA1c.Adjusted for age, height, weight, puberty.
(de Souza *et al.* 2016)	86 (46,40)	12.3±4.2	5.6±4.3	DXA	LS (L1-L4)	↓ LS BMD	Adjusted for age and sex. No association to HbA1c but inverse association with disease duration. Lower IGF1 mRNA expression between cases and controls.
(Tsentidis *et al.* 2016) (Tsentidis *et al.* 2017)	40 (22/18)	13.0±3.5	5.2±3.3	DXA	TB, LS	↓ TB and LS BMD	Adjusted for age and sex. No difference in sclerostin levels between cases and controls. Higher DKK-1 in T1D; inverse association with LS BMD..
(Sav *et al.* 2017)	50 (24,26)	11.6±2.2	6.0±2.7	DXA	LS (L2-L4)	↔ LS BMD	Adjusted for age and sex but not size corrected. Higher urinary Pyr and DPyr.
(Maratova *et al.* 2018)	95 (36/59)	16.2±1.2	7.8±4.8	pQCT	Tibia	↓ Trabecular vBMD	↓ cortical thickness but ↑ cortical vBMD. No association with HbA1c.Reduced bone strength. Reduced muscle power; inversely associated with disease duration.

BMC: bone mineral content, BMD: Bone mineral density, vBMD volumetric BMD, TB total body, LS lumbar spine, FN femoral neck, BMI body mass index; CSA cross sectional area; GH/IGF-1:growth hormone/ insulin-like growth factor-I; mRNA messenger ribonucleic acid, DKK Dipkoff-1, Pyr pyridinoline, DPyr deoxypyridinoline.†(median/range *or* means± SD

1.5.6.1.2 Bone size and microarchitecture

The most crucial finding from the meta-analysis by Vestergaard et al. is that the marginal reduction in BMD in individuals with T1D, as assessed by DXA, only generated an expected relative fracture risk of 1.09 at the spine and 1.42 at the hip, which is significantly less than the 3-7-fold increased risk seen clinically as detailed in section 1.5.4.1. This, and the overlap in the BMD values of subjects with and without osteoporotic fracture (Schuit *et al.* 2004), highlighted that bone fragility in not only dependent on bone mineral mass but also alterations in bone macro- and microstructure. Historically, the only technique to assess bone microarchitecture required bone biopsy but the advance in imaging techniques have opened up many non-invasive options.

High resolution(HR)-pQCT studies have documented smaller cross sectional radial and tibial bone area in T1D compared to controls (Heap *et al.* 2004, Bechtold *et al.* 2006, Saha *et al.* 2009b, Roggen *et al.* 2013), especially during childhood (Saha *et al.* 2009b) with normalisation before entering adulthood (Bechtold *et al.* 2007). In addition, HR-pQCT has enabled the distinction between the bone compartments demonstrating not only reduction in trabecular/cortical volumetric BMD in distal radius or tibia of individuals with T1D (Forst *et al.* 1995, Lettgen *et al.* 1995, Heap *et al.* 2004, Bechtold *et al.* 2006, Danielson *et al.* 2009, Saha *et al.* 2009b), but also lower cortical thickness with resultant decrease in estimated bone strength calculated using finite element analysis, which is a computerised numerical method to study such simulation. (Shanbhogue *et al.* 2015). These alterations had also been shown to be associated with glycaemic control and the presence of other microvascular diseases (Heap *et al.* 2004, Shanbhogue *et al.* 2015). T1D patients with microvascular complications were found to have lower trabecular thickness (radius $p<0.01$), greater trabecular separation (radius $p<0.01$, tibia $p<0.01$) and network inhomogeneity (radius $p<0.01$, tibia $p<0.01$) in comparison to T1D patients without microvascular complications (Shanbhogue *et al.* 2015). There was no difference noted in the cortical porosity between T1D, even in those with microvascular complications, compared to healthy controls (Shanbhogue *et al.* 2015).

Magnetic resonance imaging (MRI) confirmed trabecular deficits with reduced trabecular bone volume and trabecular number with greater trabecular separation in young adults with T1D and further implicated the presence of microvascular complications, in particular retinopathy, with diabetic osteopathy (Abdalrahaman *et al.* 2015). Furthermore, using magnetic resonance spectroscopy (MRS), Granke et al found that the fracture toughness of

bone was negatively associated with pentosidine levels (Granke *et al.* 2015), a well-known AGE found in diabetic patients.

Interestingly, bone histomorphometry and micro-CT of the biopsied specimens showed a reduction in trabecular bone volume, trabecular thickness and trabecular number with greater trabecular separation in T1D adults compared to healthy age and gender matched controls, with even more exaggerated aberrations in these parameters in the diabetics who have fractured, although these did not reach statistical significance (Armas *et al.* 2012). This could be due to the small sample size of the study (n=18 in each arm), but more importantly the selection bias of a cohort of T1D patients with very good glycaemic control [median HbA1c 6.8% (6.3-8.3), or 51mmol/mol].

1.5.6.1.3 Bone marrow adiposity

Given the association between marrow adiposity and morphometric vertebral fractures (Schwartz *et al.* 2013), the study of diabetic osteopathy and fracture risk will not be comprehensive without assessing the bone marrow compartment as well. There are only two studies to date looking at marrow adiposity in individuals with T1D, which demonstrated higher vertebral bone marrow fat in cases compared to healthy controls, although both were not statistically significant most likely due to the small sample sizes (Abdalrahaman *et al.* 2015, Abdalrahaman *et al.* 2017). However, Abdalrahaman et al. demonstrated good correlation between glycaemic control and % fat fraction in individuals with T1D; those who had poorer glycaemic control had significantly higher vertebral bone marrow fat. In addition, the same group also showed that bone marrow adiposity also correlated significantly with total body and lumbar spine BMD.

1.5.6.2 Bone imaging studies in T2D

Contrary to T1D, adults with T2D have been found to have increased BMD, in the range of 5-10% above an age-matched non-diabetic population (Bonds *et al.* 2006), with a reported pooled estimated LS BMD Z-score of 0.41 ± 0.01 and FN BMD Z-score 0.27 ± 0.01 (Vestergaard 2007). A more recent meta-analysis substantiated this increased BMD ranging from 25-50% higher compared to non-diabetic controls at the hip and spine but not the forearm (Ma *et al.* 2012). Meta-regression from both meta-analyses showed that body mass index (BMI) was a major determinant for BMD. One meta-analysis found longer duration of disease to be associated with reduced BMD at the hip but not spine (Vestergaard 2007) with no association with glycaemic control, contradicted by the later meta-analyses which

showed a rather counterintuitive positive correlation between HbA1c and BMD levels (Ma *et al.* 2012). The authors proclaimed considerable heterogeneity which may have influenced the associations found, stemming from large variation in types of study design, diagnostic definitions and individual characteristics including ethnicity. Importantly, BMD remains a significant predictor of fracture risk in T2D, that is independent of diabetes mellitus itself (Leslie *et al.* 2013).

Interestingly, HR-pQCT showed that individuals with T2D have lower cortical vBMD and higher cortical porosity in distal radius compared with controls (Burghardt *et al.* 2010, Farr *et al.* 2014b). Trabecular vBMD was 10% higher in T2D patients with significantly increased trabecular thickness in the tibia compared to the non-diabetics (Burghardt *et al.* 2010). This suggests that in T2D the cortical bone compartment may be more affected and the higher trabecular mineralisation could account for the higher BMD seen in this population as assessed by DXA. However, two other studies did not find any cortical deficits in patients with T2D compared to non-diabetics except in the subgroup with microvascular complications (Shanbhogue *et al.* 2016) and in those with T2D who fractured (Patsch *et al.* 2013a). MRI further confirmed increased cortical porosity in T2D patients (Pritchard *et al.* 2012, Pritchard *et al.* 2013) with no difference in bone marrow adiposity between cases and controls (Baum *et al.* 2012, Patsch *et al.* 2013b, Kim *et al.* 2017). HbA1c was positively correlated with vertebral bone marrow adiposity (Baum *et al.* 2012).

In summary, the available data suggests that T1D and T2D may have differential effects on the structural quality of bone although data are still scarce and somewhat controversial. There are limitations such as small sample sizes, different techniques to measure and interpret data and inadequate adjustment of confounders such as age, disease duration and metabolic status which may have affected the findings.

1.6 Approaches to investigating bone health

There are a wide variety of methods for assessing bone properties. Non-invasive methods such as qualitative ultrasounds (QUS), dual energy X-ray absorptiometry (DXA), computed tomography (CT) and magnetic resonance imaging (MRI) are more commonly used, although the more invasive methods of bone turnover studies and histomorphometry can provide more functional information.

1.6.1 Bone quantitative ultrasound (QUS)

Quantitative ultrasound is a very attractive technique for the evaluation of skeletal status in a large population such as diagnosis of osteoporosis, as it is low cost, highly portable and free from radiation exposure (Gluer 1997). It is highly suitable for screening and follow-up in children as it is painless, fast to execute and completely free of contraindications which is ideal for compliance in the paediatric population (Baroncelli *et al.* 2001, McDevitt and Ahmed 2007). The velocity and degree of penetration of the sound waves provides two important measures in QUS; speed of sound (SOS, m/s) and broadband attenuation (BUA, dB/MHz). These measures do not directly measure bone mass, but provide information on apparent bone density, trabecular structure and bone elasticity (Gluer *et al.* 1994). The major limitation of this technique, however, is reproducibility with inferior precision compared to DXA bone densitometry (Naessen *et al.* 1995, Gluer 1997) as it is highly technician dependent and restricted to use only in superficial peripheral bones such as phalanges, metacarpals and calcaneus (Naessen *et al.* 1995, Baroncelli *et al.* 2001).

1.6.2 Dual X-ray Absorptiometry (DXA)

DXA has been available for clinical use since 1987 and is by far the most widely used technique for measuring bone density in clinical trials and epidemiological studies. This is done through the projection of two x-ray beams of different peak voltage over the bone area of interest which allows the soft tissue component to be subtracted generating the bone density values. It is a well standardised and easy to use technique with high precision (maximum acceptable precision error, 2-2.5%) and low radiation dose (0.5-35 µSv). Importantly, DXA BMD correlates well with biochemically determined bone strength (Ammann and Rizzoli 2003) and fracture risk with approximately 1.6 fold increase for every SD decrement in BMD irrespective of gender (Johnell *et al.* 2005, Cummings *et al.* 2006, Rivadeneira *et al.* 2007). DXA, however, has some pertinent disadvantages: Firstly, it is a 2-dimensional measurement which gives *areal* BMD (g/cm^2) rather than true volumetric

BMD (g/cm^3). This is particularly crucial in growing children, when DXA will overestimate fracture risk in a child with smaller size who will have lower areal BMD than a normal sized-individuals. Secondly, it does not distinguish between cortical and trabecular bone, hence provides limited information on bone quality; the reason why DXA BMD only explains approximately 70% of bone strength. In addition, DXA has limitations in measuring BMD in obese patients, older patients with bony degenerative changes or vascular calcifications (Tothill *et al.* 1997, Diederichs *et al.* 2011).

1.6.3 Quantitative computed tomography (QCT)

More advanced radiological modalities have enabled the assessment of bone macro- and microarchitecture using high resolution micro-computed tomography (μQCT), synchrotron radiation computed tomography (SRCT), peripheral quantitative computed tomography (pQCT) and magnetic resonance imaging (MRI).

QCT is a three-dimensional non-projection imaging technique of assessing bone. The main advantages of QCT over DXA are that it provides (a) true volumetric BMD (mg hydroxyapatite /cm^3), which is independent of body size hence better prediction of fragility fracture risks (Yu *et al.* 1995, Bergot *et al.* 2001) and (b) information on bone architecture distinguishing between cortical and trabecular bones (Black *et al.* 2003). As multidetector CT (MDQCT) can specifically detect changes in the more metabolically active trabecular bone, it is a more sensitive discriminator of BMD changes than DXA (Heuck *et al.* 1989, Graeff *et al.* 2007). The incorporation of finite element analysis (FEA) modelling into non-invasive bone further improved QCT estimation of bone strength and stiffness, differentiating the degree of cortical versus trabecular loss providing insight into the pathophysiology of vertebral fractures with aging (Christiansen *et al.* 2011). The major limitations of QCT is the high radiation exposure (60-2900 μSv) (Table 1.7), rendering it unsuitable for the paediatric population or any longitudinal studies limiting its current use to *ex-vivo* or pre-exisiting *in vivo* cohort studies only. Specifically in relation to microarchitecture, MDQCT scanners are restricted by the spatial resolution of 250-300 μm, which is larger than the thickness of a trabecula 50-200 μm (Issever *et al.* 2010).

High resolution peripheral QCT (HR-pQCT) confers better spatial resolution (~120 μm) and a smaller effective radiation dose (<3 μSV). With improved spatial resolution, the trabecular spacing (400-800 μm) and trabecular thickness can be more accurately assessed (Boutroy *et al.* 2005), although the latter is still subjected to a degree of partial volume averaging. In

addition, pQCT can also give information on bone geometry and muscle cross sectional area, enabling the study of the interaction between muscle and bone systems (Schoenau *et al.* 2000, Rauch *et al.* 2001, Bajaj *et al.* 2015). The main limitations of HR-pQCT are that it requires a dedicated scanner and is limited to studying the peripheral skeleton such as radius and tibia. This is however particularly useful for examining cortical bone changes in metabolic bone disorders as the distal radius contains more cortical bone than the vertebral body. As HR-pQCT scanners have high-resolution, these examinations require a longer scanning time (3-10mins) than QCT (in seconds) and are more prone to motion artifacts, especially in children.

Table 1.7 Radiation dose exposure based on different X-ray based imaging techniques

Test	Effective Dose (μSv)	Equivalent Period of Background Radiation*
Chest X-ray (single anterior posterior)	20	3 days
DXA (hip and spine)	3	<1 day
2D QCT spine, scout image and 3 slices of 10mm thickness	60	1 week
3D multidetector QCT spine, L1-L2, pitch 1	1500	6 months
3D multidetector QCT hip, pitch 1	2900	1 year
HR-pQCT	<3	< 1 day
Roundtrip transcontinental airplane flight	*60*	*1 week*

*Based on the calculation of natural background radiation at sea level of 3000 μSv per year (rounded up to the nearest day). DXA dual absorptiometry, QCT quantitative CT, HR-pQCT high resolution peripheral quantitative CT, 2D two-dimensional, 3D three-dimensional

[Modified from (Damilakis *et al.* 2010)]

1.6.4 Magnetic resonance imaging (MRI)

MRI is emerging as a more comprehensive tool in the assessment of bone health given its capability of quantifying *all* the various bone compartments including bone macro- and microarchitecture without the burden of ionising radiation. This lends itself well for repeatability in longitudinal studies, especially in the paediatric population. It can directly acquire images in any plane de novo and has the potential to derive functional information to better understand patho-mechanisms of impaired bone health. From a set of contiguous image slices the 3-dimensional structure of bone can be reconstructed and measures of the cortical and trabecular bone microarchitecture can be obtained, including topology (eg, plate vs rod character of the trabeculae) of the latter (Wehrli 2007). The spatial resolution achievable is 200-300 μm, making it impossible to delineate individual trabeculae. This

inferiority to HR-pQCT however, is definitely outweighed by the ability of MRI to image more proximal and larger joints such as proximal tibia and femur; commonly implicated in fragility fractures. With the addition of FEA as described above, the mechanical properties of bone such as stiffness, elasticity and predicted strength can be assessed (Wehrli 2007, Magland *et al.* 2012). Bone mineral density can also be measured which strongly correlates to the BMD obtained from QCT (Hong *et al.* 2000, Ho *et al.* 2013).

The current main attraction of MRI is its ability to evaluate the bone marrow compartment, specifically looking at the bone marrow fat content with or without spectroscopy (Li *et al.* 2011, Bandirali *et al.* 2015). There has been a growing interest in the effects of bone marrow adiposity on bone health because of the shared stem cell lineage between osteoblasts and adipocytes (Paccou *et al.* 2019). Importantly, vertebral bone marrow adiposity has been shown to be an independent predictor of fracture in osteoporotic women (Wehrli *et al.* 2000). Furthermore, MRI is also the only modality available for imaging bone matrix, the collagenous non-mineralised component of bone onto which the mineralised component of bone is deposited (Cao *et al.* 2008, Cao *et al.* 2010, Wu *et al.* 2010). Its major drawbacks include the high cost, longer scanning time (20-30mins) and specific contraindications.

1.6.5 Bone histomorphometry

Bone biopsy can provide both qualitative and quantitative information on bone tissue, the latter referred to as bone histomorphometry. It is the only available method to study bone cell function within the *in vivo* structural content to understand the patho-mechanisms of metabolic bone diseases. Standard histomorphometric analyses measure structural parameters, static bone formation and resorption parameters, and dynamic formation parameters, as summarised in Table 1.7 (Rauch 2009). The bone specimens should be horizontal, full thickness biopsy sample of uncrushed bone containing two cortices separated by a trabecular component. This can be theoretically from any sites although transiliac samples are most commonly used, due to limited reference data for other sites in children (Glorieux *et al.* 2000, Rauch 2003). This technique is also of particular importance for paediatric use as the histomorphometric results are not directly influenced by the growth process (Parfitt *et al.* 2000). The major drawbacks of histomorphometry are the invasive procedure with prior bone labelling, labour intensive process and need for special equipment and expertise (Rauch 2009).

Remodelling activity is indeed elevated in young children, decreases until the age of 8 or 9 years, and increases again during puberty. After the age of puberty, remodelling activity declines into the much lower adult range (Parfitt *et al.* 2000).

Table 1.8 Commonly used bone histomorphometric parameters

Structural parameters	• Core width (mm) • Cortical width (µm) • Bone volume/tissue volume (%) • Trabecular thickness (µm) • Trabecular number (mm^{-1})
Static formation parameters	• Osteoid thickness (µm) • Osteoid surface/bone surface (%) • Osteoid volume/bone volume (%) • Osteoblast surface/bone surface (%) • Wall thickness (µm)
Dynamic formation parameters	• Mineralising surface/bone surface (%) • Mineral apposition rate (%) • Mineralisation lag time (days) • Bone formation rate/bone surface
Static resorption parameters	• Eroded surface/bone surface (%) • Osteoclast surface/bone surface (%)

[Modified from **(Rauch 2009)**]

1.6.6 MicroRNAs

In addition to biochemical markers of bone turnover, recent studies have found a crucial role for miRNAs in bone development and homeostasis (Kim and Lim 2014). MicroRNAs (miRNAs) are small non-coding RNAs that regulate gene expression at a post-transcriptional level, either by suppressing translation or inducing mRNA degradation (Rodriguez *et al.* 2004). They are important regulators and modulators of cell differentiation, proliferation and apoptosis as a single miRNA can target up to 100 distinct mRNAs, hence controlling the expression of entire gene networks (Baek *et al.* 2008). Dysregulation of miRNA have been associated with osteoporosis and shown to be discriminative of fragility fractures (Li *et al.* 2009, Seeliger *et al.* 2014). Heilmeier et al. discovered specific miRNAs involved in osteogenesis, adipogenesis, or both and demonstrated that these circulating miRNAs in combination were able to differentiate the fracture status in post-menopausal osteoporosis and T2D women (Heilmeier *et al.* 2016).

1.7 Metformin

Metformin is a biguanide class of drug, well known as the most frequently prescribed first line anti-diabetic medication for Type 2 diabetes (T2D) (Nathan *et al.* 2009). It maintains glucose homeostasis by supressing liver glucose production and increase peripheral glucose uptake (Bailey and Turner 1996). Metformin is considered an insulin-sensitizer as it lowers glycaemic levels without increasing insulin secretion (Garber and Samson 2004). In addition, metformin has also been shown to have cardiovascular benefits including improvement in lipid profile, improved endothelial dysfunction with lower intravascular thrombotic risk. However, despite being around for over 50 years, the precise mechanism of action of metformin remains unclear.

1.7.1 Metformin action in the liver

Several studies have shown that metformin can act via activation of the enzymes tyrosine kinase (Dominguez *et al.* 1996) and AMP-activated protein kinase (AMPK) (Zhou *et al.* 2001, Musi *et al.* 2002). AMPK activation phosphorylates the enzymes involved in several hepatic biosynthetic pathways such as acetyl-CoA carboxylase, hydroxymethylglutaryl-CoA reductase, glycogen synthase and endothelial nitric oxide synthase, which results in a decrease in glucose production, cholesterol and triglyceride synthesis from the liver (Zhou *et al.* 2001). This has been the widely accepted mechanism of action until genetic loss of function experiments with AMPK deficient hepatocytes (Foretz *et al.* 2010) challenged it. Since then, studies have put forward different mechanisms of action by which metformin suppresses gluconeogenesis in hepatocytes through inhibition of (i) the mitochondrial respiratory chain complex I (El-Mir *et al.* 2000) and (ii) a specific mitochondrial enzyme glycerophosphate dehydrogenase (mGPD) (Madiraju *et al.* 2014), which consequently decrease hepatic glucose output. Miller et al also discovered another novel action of metformin in glucose homeostasis by blocking glucagon-dependent glucose output from hepatocytes by reducing production of cyclic AMP and protein kinase A activity (Miller *et al.* 2013).

1.7.2 AMPK

AMPK has been a widely studied subject in the last two decades owing to its importance as a master sensor of cellular energy status. It is a heterotrimeric serine/threonine kinase comprising of α catalytic and regulatory β and γ subunits (Hardie *et al.* 1998). The α catalytic subunit contains the conventional serine/threonine protein kinase domain as well as the

autoinhibitory sequences, the β subunit contains a glycogen-binding domain and a tethering domain for α and γ subunits, while the γ subunit contains four cystathionine-β-synthase sequence repeats, which are responsible for the binding of regulatory nucleotides (McBride and Hardie 2009, Oakhill *et al.* 2009). Mammals express two α (α1, α2), two β (β1, β2) and three γ subunits (γ1, γ2, γ3) in 12 possible combinations of AMPK heterotrimer in a tissue specific manner, allowing for different subcellular localisation and regulation (Hardie 2007). The predominant isoforms in most cells are α1, β1 and γ1, although hepatocytes significantly expresses α2 (Woods *et al.* 1996), whereas skeletal and cardiac muscles also express α2, β2, γ2 and γ3 (Stapleton *et al.* 1996, Thornton *et al.* 1998, Cheung *et al.* 2000). The degree of AMP-dependence is highly reliant on the α and γ subunits, with stimulation varying from only 50% for the α1γ3 complexes to more than 5-fold for the α2γ2 combination (Cheung *et al.* 2000). Also the α2 complexes are enriched within the nucleus whilst α1 complexes are largely cytoplasmic (Salt *et al.* 1998, Turnley *et al.* 1999). As the name suggests, AMPK is activated when AMP binds to the regulatory γ subunit, which promotes phosphorylation of Thr-172 by the upstream kinases (*e.g.* LKB1, CAMKKβ) within the α catalytic subunit and protects Thr-172 from dephosphorylation by protein phosphatases (Shaw *et al.* 2004, Hawley *et al.* 2005).

In mammals, AMPK is functionally important as a regulator of cellular energy homeostasis, akin to a thermostat for temperature. Increase in cellular AMP to ATP ratio, a signal of cellular energy compromise, will activate AMPK to switch on energy-generating (catabolic) pathways and switch off energy-consuming (anabolic) pathways that are not essential for short term cell survival in order to restore the AMP/ATP ratio (Kahn *et al.* 2005, Hardie 2007). AMPK is switched on by cellular stresses that either interfere with ATP production (*e.g.* hypoxia, glucose deprivation or ischaemia) (Kudo *et al.* 1995, Marsin *et al.* 2000) or by stresses that increase ATP consumption (*e.g.* muscle contraction and exercise) (Winder and Hardie 1996, Fujii *et al.* 2000). Specifically, in pancreatic β-cells low glucose activates AMPK in the same range of concentrations over which it inhibits insulin release (Salt *et al.* 1998). The AMPK activation by exercise is dependent on both the duration and the intensity of the exercise (Rasmussen and Winder 1997, Stephens *et al.* 2002). It is also activated by hormones that act via Gq-coupled receptors, and by leptin and adiponectin. Hence, AMPK is able to regulate many metabolic pathways in peripheral tissues by phosphorylating different metabolic enzymes involved in lipid (Hardie and Pan 2002), glucose and glycogen metabolisms.

Pharmacologically, several chemical compounds are known AMPK activators, such as 5-aminoimidazole-4-carboxamide riboside (AICAR) and metformin. AICAR is taken up into cells and converted to monophosphorylated nucleotide 5-aminoimidazole-4-carboxamide-1-D-ribofuranosyl-5'-monophosphate (ZMP), which mimics all the activating effects of AMP on the AMPK system without disturbing the cellular levels of AMP, ADP or ATP (Corton *et al.* 1995). Metformin has also been found to activate AMPK (Zhou *et al.* 2001) by a mechanism that involves phosphorylation of the upstream kinase but interestingly, with no alteration in cellular AMP:ATP ratio (Fryer *et al.* 2002, Hawley *et al.* 2002). There are not many AMPK inhibitors. Compound C (also called dorsomorphin) is the only available cell-permeable AMPK inhibitor, which has been shown to rescue the proliferative actions of AICAR and metformin (Isakovic *et al.* 2007). It is however, a non-selective (low specificity) AMPK inhibitor as it has also been found to inhibit BMP (Yu *et al.* 2008) and several other kinases (Vogt *et al.* 2011).

1.7.3 The role of AMPK and metformin in bones

In the last decade, there have been novel findings that AMPK signalling pathway plays a role in bone physiology. On the cellular level, AMPK subunit isoforms are expressed in bones. The α1 subunit is the most dominant isoform in primary osteoblasts, osteoblastic cell lines, osteoclasts and bone tissue (Kim *et al.* 2008, Kasai *et al.* 2009, Quinn *et al.* 2010, Shah *et al.* 2010), in contrast to the very low α2 subunit expressions. Both β1 and β2 subunits are equally expressed, whilst the γ1 is the preferential γ form with minimal/non-existent γ2 and γ3 expressions.

Many *in vitro* and *in vivo* studies have shown a positive effect of AMPK activation on bone cell activities. AMPK activation by AICAR and metformin on mouse pre-osteoblasts MC3T3-E1 showed a dose-dependent increase in cell proliferation, type 1 collagen production, alkaline phosphatase activity and mineral deposition (Cortizo *et al.* 2006, Kanazawa *et al.* 2007). Similarly, AMPK activation in rat primary osteoblasts with AICAR and metformin demonstrated increases in cell proliferation (Zhen *et al.* 2010), AP activity (Shah *et al.* 2010, Zhen *et al.* 2010), increase in mineralisation of bone matrix and bone nodule formation (Utting *et al.* 2006, Shah *et al.* 2010, Zhen *et al.* 2010),with similar dose-dependency. The role of AMPK activation in bone formation is further reinforced when co-treatment of pre-osteoblast with AICAR and compound C demonstrated suppression of the stimulatory effect of AICAR on bone formation (Shah *et al.* 2010). Molinuevo et al. demonstrated that metformin also has positive osteogenic effect on *in vitro* and *in vivo* rat

bone marrow progenitor cells, mediated through AMPK activation (Molinuevo *et al.* 2010). This study also suggested for the first time that metformin may have some effect on suppressing adipogenesis. There are however studies with contradictory findings of decreased AMPK activity during osteoblast differentiation (Kasai *et al.* 2009, Chen *et al.* 2017, Chava *et al.* 2018).

Through AMPK signalling pathway, adiponectin was demonstrated to suppress bone resorption by inhibiting TNFα-induced osteoclastogenesis (Yamaguchi *et al.* 2008). AMPK activation via metformin also stimulated OPG and inhibited RANKL mRNA and protein expression in osteoblasts, reducing osteoclast differentiation and activity (Mai *et al.* 2011).

The most compelling evidence for the role of AMPK signalling in bone mass regulation came from genetic studies. Mice with deletion of AMPKα2 subunit demonstrated no change in tibial bone mass, in line with the low expression of α2 subunit in bone. In contrast, AMPKα1 knock-out (KO) mice showed both significant cortical and trabecular bone deficits on imaging, with 40% less trabecular volume, 30% less trabecular number and 12% reduction in trabecular thickness and compromised cortical indexes (Shah *et al.* 2010) compared to wild-type (WT) mice. Similarly with AMPKβ1 or β2 KO mice, trabecular bone density and mass were reduced although no differences were noted in osteoblast and osteoclast numbers (Quinn *et al.* 2010), suggesting a more significant impact of AMPK activation on bone cell activities than numbers alone.

The complex signalling pathways involved in the commitment and differentiation of MSC towards adipocytes or osteocytes have been eluded to in section 1.3.2.3., but the mechanisms linking AMPK activation to bone cell differentiation and bone mass however remain poorly understood. Studies have shown a possible cross talk with Wnt/β-catenin signalling in the regulation of osteoblast differentiation (Zhao *et al.* 2011) where activation of AMPK by AICAR/metformin promoted β-catenin transcription (Zhao *et al.* 2011) and marked increase in Runx2 expression with no effects on PPARγ (Molinuevo *et al.* 2010). The involvement of melavonate pathway for both osteoblast and osteoclast differentiation (Kanazawa *et al.* 2009) has also been shown. Further studies to investigate the differentiation of MSCs and better define the underlying molecular mechanisms involved would be needed, in particular the link between AMPK and PPARγ.

1.8 Aims of the thesis

This thesis was designed to understand the effects of T1D on the bone health of children with the condition, given the current knowledge of diabetic osteopathy in adults.

The primary hypothesis is that:

1. Children with T1D have deficit in bone microarchitecture, as determined by high resolution MRI, compared to children without T1D

The secondary hypotheses included:

1. Children with T1D have increased bone marrow adiposity, as determined by magnetic resonance spectroscopy, compared to children without T1D

2. Poorer diabetes control, as measured by HbA1c, is positively correlated to bone microarchitecture deficit and increase in bone marrow adiposity

3. Metformin can promote osteogenesis and prevent adipogenesis by acting on mesenchymal stem cells.

By studying the problem at a cellular and clinical level, the intention is to be able to better define the problem, if any, in children and suggest a mechanistically sound therapeutic approach.

The principle aims of the thesis are to:

1. Determine if bone health is impaired in children with T1D

2. Study the bone microarchitecture and bone marrow adiposity of children with T1D

3. Identify the mechanisms of action of metformin, and its potential use as a bone therapeutic agent

2 Methodology

2.1 Introduction

This chapter details the methodology adopted for the multi-modality assessment of bone health in the clinical study in Chapter 4 of this thesis. The modalities involved are MRI of the right knee, MRS of the lumbar spine, DXA scan of total body, hip and lumbar spine, and the biochemical assays of bone markers of turnover. Information on the image acquisition and analysis protocols are provided for all imaging studies. Additionally, the methodology used in the laboratory studies in Chapter 5 of this thesis is also described.

Clinical studies: Imaging and Biochemistry

2.2 MRI

2.2.1 Principles of MRI

The early concept of MRI scanning first appeared in medical use in the late 1960s when Raymond Damadian discovered that malignant tissue had different nuclear magnetic resonance (NMR) parameters to normal tissue. The ability to tissue characterise using a magnetic scanner allowed him to produce the image of a rat tumour in 1974 (Damadian and Cope 1974) before pioneering the first super conducting magnetic scanner in the late 1970s to produce the first image of the human body (Goldsmith *et al.* 1977). In its most basic, an MRI scanner comprises a couch for the patient to lie on, a large magnet, a radiofrequency (RF) coil to transmit and receive the RF waves and a processor which converts the received RF signals into an MRI image.

Fundamentally, MRI is based on the intrinsic magnetic properties of atomic nuclei. All atomic nuclei consist of protons and neutrons which spin about its own axis. In nuclei with an even number of protons and neutrons, half spin in one direction and the other half in the opposite direction resulting in no net spin. Nuclei with an *odd* number of protons (positively charged) and neutrons, such as ^{1}H, ^{13}C, ^{19}F, ^{23}Na, ^{31}P, however, have a net spin (motion), making them important in MRI as they produce a small magnetic field (Westbrook *et al.* 2011, Brown *et al.* 2014).

Hydrogen nuclei are ideal in clinical MRI as they are the most abundant element in the human body present within water (H_2O) and fat (CH3 etc.) and their solitary protons give them the largest relative magnetic moment. MRI uses a strong external magnetic field (B_0) to align these magnetic moments in the tissues of the body. In the absence of an applied magnetic field, the magnetic moments of these hydrogen nuclei are randomly orientated (Figure 2.1A). When placed in a strong magnetic field, two things happen to the hydrogen nuclei:

1. They **align** with the magnetic field, in one of two ways: parallel or anti-parallel (Figure 2.1B). The factors affecting the direction of alignment are determined by the strength of the external magnetic field (in unit Tesla) and the thermal energy of the nuclei. Hydrogen nuclei which do not possess enough energy to oppose the magnetic field known as the low-energy nuclei align parallel to the magnetic field, whilst the high-energy nuclei with sufficient energy to oppose the magnetic field align anti-parallel. There are always fewer higher energy nuclei than low-energy nuclei, resulting in a small excess lined up parallel to B_0 constituting the **net magnetisation vector** (NMV) (Figure 2.1B). The magnitude of NMV is larger at higher field strengths as fewer nuclei possess enough energy to oppose the magnetic field hence more align parallel to B0, resulting in improved signal.

2. They rotate or **"precess"** around the axis of the magnetic spin at a special frequency called the **Larmor frequency**, which is dependent on the strength of the external magnetic field.

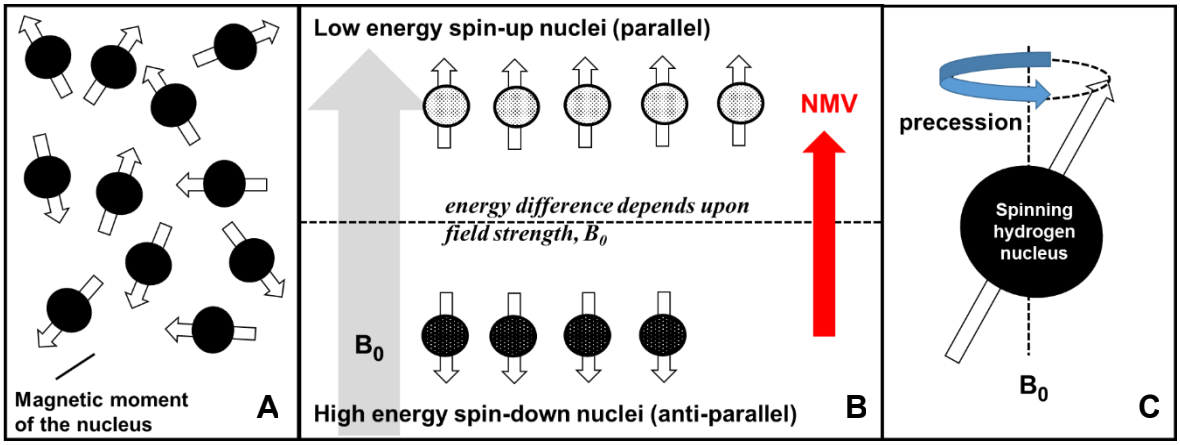

Figure 2.1 Motions in the atoms (hydrogen nuclei in clinical MRI). The magnetic moments of the spinning hydrogen nuclei are normally randomly aligned as shown in A. When an external magnetic field is applied (B_0), the magnetic moments of the hydrogen nuclei will do one of two things: i) *Align* parallel, or anti-parallel to B_0 depending on the strength of B_0 applied, as shown in B. Hydrogen nuclei which absorb enough energy to oppose the magnetic field will lie anti-parallel to B_0. There are usually more low energy than high energy nuclei resulting in a net magnetic moments, also known as net magnetisation vector (NMV) marked in red arrow. ii) *Precess* around B_0 (marked with blue arrow). The application of B0 accords the already spinning hydrogen nucleus an additional spin along the precessional path as shown in C. [Adapted from (Westbrook *et al.* 2011)]

The next pre-requisite to obtain an MRI image is a radiofrequency (RF) pulse which is where the resonance comes from in the name magnetic resonance imaging. When a RF pulse with a frequency matching exactly the precessional frequency of the MR active nuclei is delivered in a perpendicular direction to B0, the nucleus gains energy from the RF pulse and resonates. The application of a RF pulse that causes resonance is termed excitation, which results in the net magnetisation (NMV) moving out of alignment from B0, lying at an angle to it (flip angle) (Figure 2.2). The magnitude of the flip depends on the amplitude and duration of the RF pulse. The flip angle is usually 90 degrees, resulting in the NMV deviating from the longitudinal plane into the transverse plane (Figure 2.2).

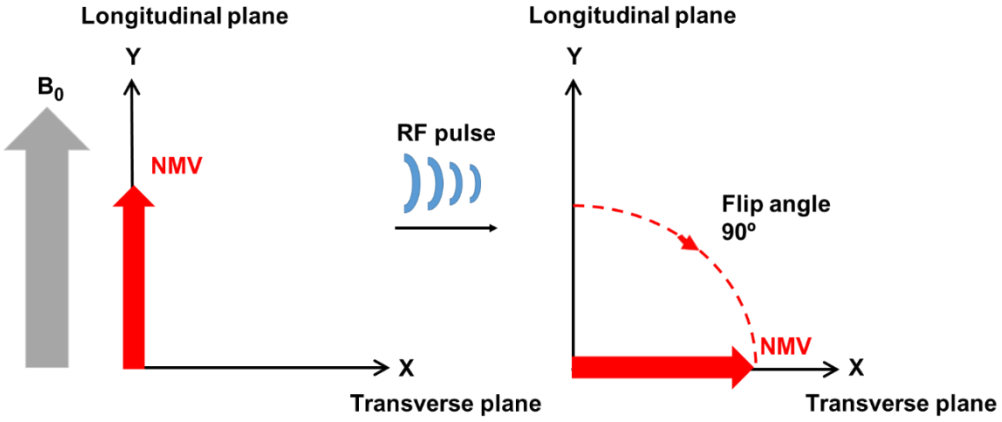

Figure 2.2 Excitation phase. Transfer of net magnetisation vector (NVM) from the longitudinal plane (Y) to the transverse plane (X) when RF pulse is applied during the excitation phase.

When the RF pulse is switched off, the hydrogen nuclei give up the absorbed energy and the NMV returns, or 'relaxes' back to the longitudinal plane (B0). The relaxation process can be divided into 2 parts called T1 and T2 relaxation, which are two independent processes which occur simultaneously (Blink 2004). T1 relaxation, also known as the spin-lattice relaxation, describes the recovery of the longitudinal magnetisation when the nuclei lose their energy to the surrounding environment (lattice). T2 relaxation, also known as the spin-spin relaxation, describes the decay of transverse magnetisation due to the magnetic fields of the neighbouring nuclei interacting with each other (Figure 2.3).

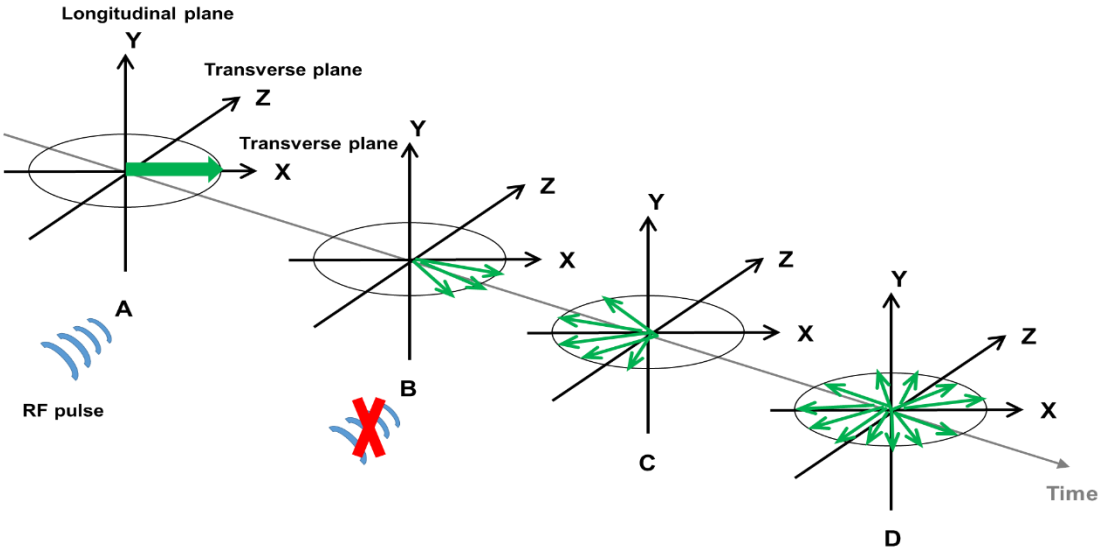

Figure 2.3 T2 relaxation (or spin-spin relaxation) phase. A) Immediately after the 90° RF pulse, the net magnetisation vector all lie in the transverse plane, X, with *all* hydrogen nuclei vectors rotating in the X-Z plane around the Y-axis. The vectors are *in-phase* as they all point in the same direction. B) Once the RF pulse is switched off, T2 relaxation begins with decay of the transverse magnetisation as the magnetic fields of each hydrogen nuclei affect one another. The nuclei will start to rotate at different speeds and so the vectors no longer all point in the same direction. This is called 'dephasing'. C) Over time, T2 decay progresses and more dephasing happens until there is no phase coherence left, ie. not one vector is pointing in the same direction anymore as seen in D [Adapted from (Blink 2004)].

The time taken for T1 and T2 relaxation to occur varies between tissues, and so at a given time *t*, the signal intensity available to create the MRI image will be different for each tissue (Figure 2.4). T1 relaxation time is the time it takes 63% of the longitudinal magnetisation to recover in the tissue, whilst T2 relaxation time is the time it takes for 63% of the transverse magnetisation to be lost, *i.e.* 37% remain (Figure 2.4A and Figure 2.4B, respectively). Fat has a short T1 and T2 time, respectively, due to its inherent low energy state and large lipid molecules which are closely packed together (Figure 2.4C and Figure 2.4D). Water, on the other hand, has a high inherent energy so does not easily give up energy into its lattice from the hydrogen nuclei so the T1 time is long (Figure 2.4C). The T2 time of water is also long,

compared to fat and muscle, as the molecules are spaced apart and hence spin-spin interaction is less likely to occur (Figure 2.4D).

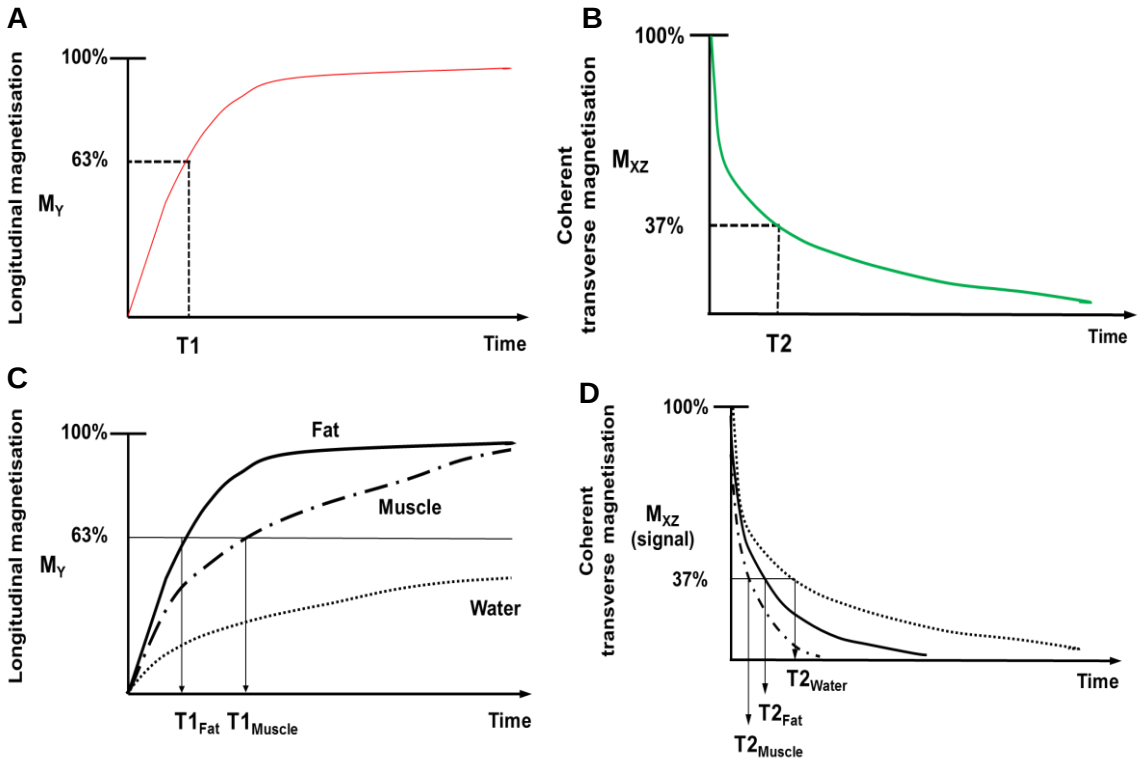

Figure 2.4 T_1 and T_2 relaxation times and their respective curves for different tissues. A)T1 relaxation time is the time taken for 63% of the longitudinal magnetisation (M_Y) to recover whilst B) T2 relaxation time is the time taken for 63% of the coherent transverse magnetisation to be lost (ie 37% remaining) T1 and T2 times vary for the different tissues with the T1 times for fat, muscle and fluid shown in C) whilst the T2 times shown in D) [Adapted from (Ridgway 2010, Westbrook *et al.* 2011)]

The magnitude and timings of the RF pulses constitutes a pulse sequence. Figure 2.5 shows a typical MRI pulse sequence, specifically a gradient echo pulse sequence (http://www.revisemri.com/questions/pulse_sequences/se_ge_differences.). The **repetition time (TR)** is the time between two RF pulses which determines the amount of longitudinal relaxation (T1) that is allowed to occur before the next excitation. **The echo time (TE)** is the time from the application of the RF pulse to the peak of the signal induced in the coil which determines the amount of decay of transverse magnetisation (T2 relaxation) prior to the signal being read. The signal which is the energy shed by the nuclei during the relaxation processes are retrieved by a receiver coil (some transmit coil can also act as receiver). In order to orientate the signals received into a coherent 3-dimensional image, a field of view (FOV) is placed over the body part to be imaged and this is 'divided' into volume element, also known as voxels. Three gradient wire coils are placed within the magnet to create additional graduated magnetic fields which are activated at different times to encode the

signals: slice-encoded axially head-to-toe (G_s), phase-encoded anterior-posteriorly (G_p) and frequency-encoded to determine left-right (G_f) (Figure 2.5) into an image (Blink 2004).

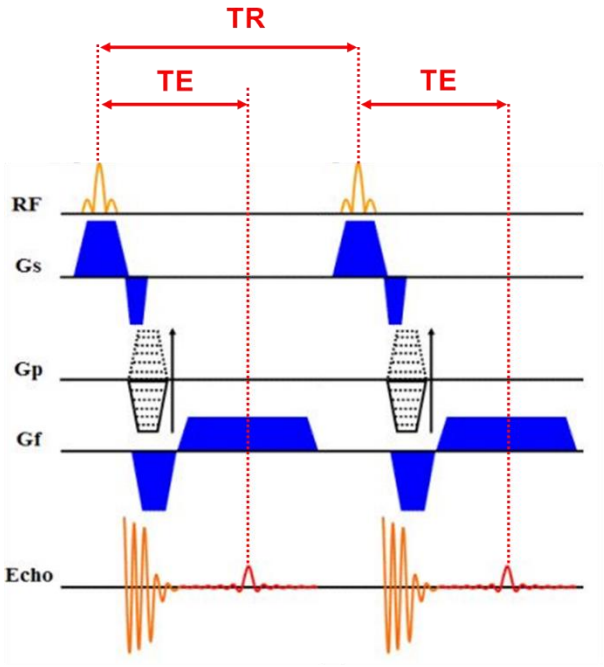

Figure 2.5 Example of an MRI pulse sequence diagram. The RF pulses are shown on the top line, and the magnetic field gradients are shown on the lines marked Gs, Gp, and Gf, where the subscripts refer to the slice, frequency and phase directions. The important timing parameters shown in the pulse sequence diagram are the repetition time (TR) and the echo time (TE). TR is the time between subsequent applications of the pulse sequence, and TE is the time between the application of the first RF pulse and the measurement of the signal in the transverse plane [Adapted from (http://www.revisemri.com/questions/pulse_sequences/se_ge_differences.)].

Manipulation of the pulse sequence parameters together with the magnetic field gradients used forms the basis of contrast generation in MRI scanning. The factors that affect image contrast in diagnostic imaging are usually divided into intrinsic or extrinsic parameters, the former of which cannot be changed as they are inherent to the biological tissues (eg T1 and T2 times). Extrinsic parameters are those that can be altered such as the pulse sequence parameters (eg TR, TE, flip angle etc) which can be optimised by varying the acquisition parameters. T1-weighted imaging have short TR, characterised by bright fat and dark water. T2-weighted imaging have long TE and is characterised by bright water and dark fat. Other tissues will have an intensity of somewhere in between in either.

An optimal image quality, is dependent not only on good image contrasts but also on several other factors, including:

- signal-to-noise (SNR) ratio
- spatial resolution, and
- scan time.

The signal-to-noise ratio and spatial resolution are both dependent on voxel volume which itself is controlled by: 1) slice thickness, 2) image matrix and 3) field of view (FOV). Care needs to be exercised as one trades off the other. Increasing slice thickness will increase voxel volume resulting in enhanced SNR but this will compromise spatial resolution. Larger voxel makes it harder to resolve small structures well as the individual signal intensities are averaged together resulting in a ***partial volume effect***. Scan time should be as short as possible to reduce movement artefacts which inevitably degrades image quality.

Conventionally, MRI is seen as the imaging modality for soft tissues but technical advances in the last 10-15 years have significantly improved the utility of magnetic resonance in the musculoskeletal system with high resolution MRI and specialised pulse sequence development (Young and Bydder 2003). Escalation from 1.5T to 3.0T static magnetic field strength has improved the signal-to-noise ratio with better image quality, as with innovation in the array of detector coils available. The development of high resolution MRI has also markedly facilitated imaging of solid structures, especially bone, where RF with rapid switch from excitation of spins to detection of signals allow high signal levels to be obtained with short T2 (Gatehouse and Bydder 2003). An example MRI image of the tibia is shown in Figure 2.6, which illustrates the differences in signal intensities between bone, bone marrow, muscle and subcutaneous fat. The signal intensities of bone and fatty marrow are very different, which makes MRI ideal for imaging trabecular structure.

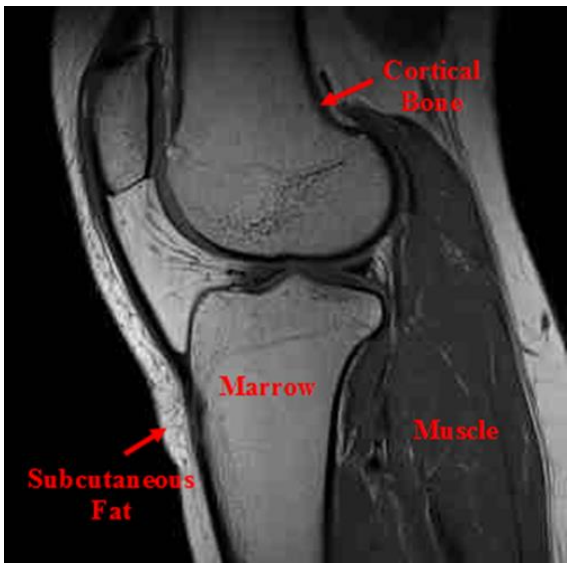

Figure 2.6 Sagittal image of MRI tibia. The difference in signal intensities between bone, bone marrow, muscle and subcutaneous fat is demonstrated.

2.2.2 Proximal Tibia Imaging

Imaging was performed on a 3 Tesla (T) Siemens MAGNETOM Prisma MRI scanner (Siemens, Erlangen, Germany) using a transmit/receive (Tx/Rx) extremity coil for the knee. The MR images were then pre-processed, coded and analysed using MATLAB (Mathworks Inc, San Mateo, CA, USA) software.

2.2.2.1 Acquisition

The participants were positioned supine with legs extended throughout the scan. Ear plugs were provided for noise minimisation and comfort. MRI images of the proximal tibia were acquired using an extremity coil positioned over the right knee. The knee was further immobilised with additional paddings placed within the coil itself. Three localiser scans were initially performed in the sagittal, coronal and axial planes to identify the region of interest (ROI) using a T1-weighted spin-echo sequence (Figure 2.7A-C). Twenty axial micro-MRI images (0.4mm thickness) of the metaphysis were collected, with the first slice positioned immediately distal to the epiphyseal growth plate, and subsequent slices positioned distal to that. The TrueFISP (true fast imaging with steady state precession) pulse sequence with the parameters shown in

Table 2.1, was used to provide a 3D volumetric data set of isotropic resolution in the axial plane (Figure 2.7D). The in-plane spatial resolution achievable at 200µm can resolve larger trabeculae (usually 78-200µm), while the lower spatial resolution in the slice direction at 400µm will contribute significantly to the partial volume effect.

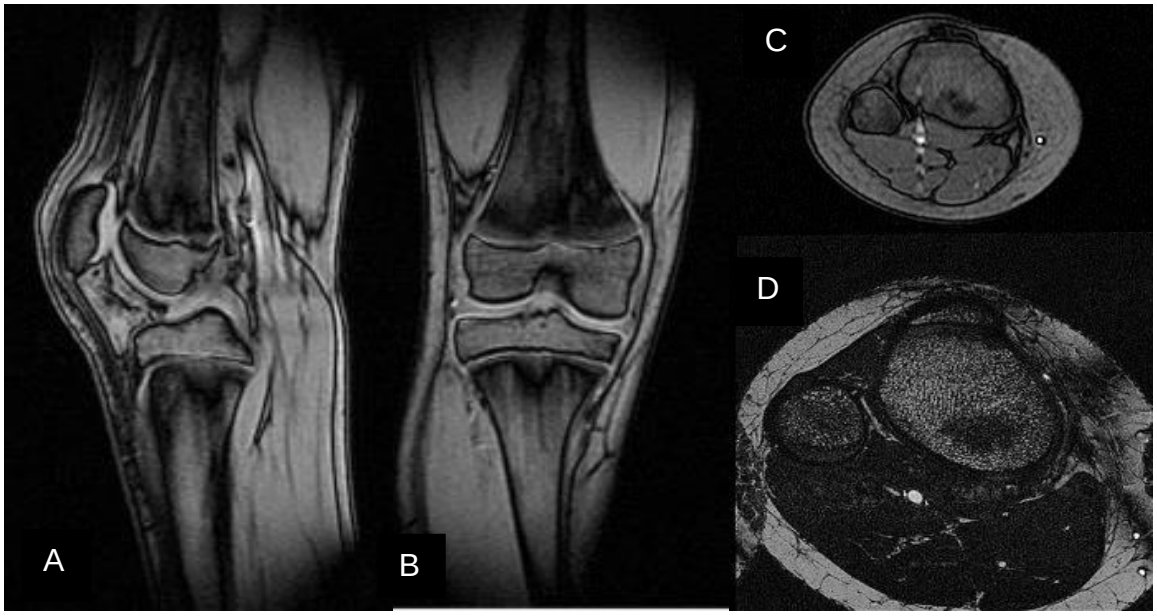

Figure 2.7 Image acquisition of proximal tibia MRI. Initial localiser scans in sagittal (A), coronal (B) and axial (C) views and a representative slice of the axial images obtained (D).

Table 2.1 TrueFISP Pulse sequence parameters for imaging of the proximal tibia

Parameter	Value
Resolution (mm^3)	0.2 x 0.2 x 0.4 (slice thickness)
Echo time [TE] (ms)	4.69
Repetition time [TR] (ms)	10.83
Flip angle (^{o})	60
Number of averages	15
Field of View (mm^2)	100 x 100
Matrix size	448 x 448
Number of slices	20
Bandwidth (Hz/pixel)	189
Scan time (mins)	10

2.2.2.2 Image Pre-Processing

Prior to analysis, images were imported into and pre-processed in MATLAB to improve the image quality and enable better quantification.

a) Sharpening Filter

A sharpening filter was applied to the trabecular bone image to increase the contrast along the edges where the different colours meet, resulting in a sharper image. The 'unsharp

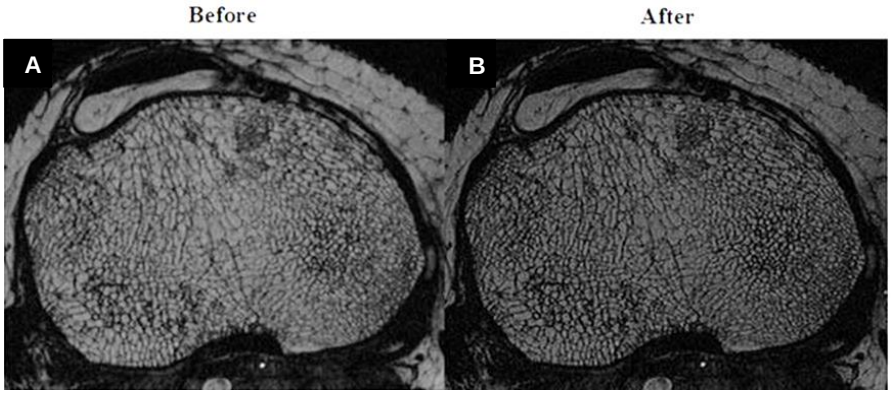

Figure 2.8 MRI axial image before (A) and after (B) application of sharpening filter.

masking' technique in the analysis software sharpened the image by subtracting a blurred (unsharp) version of the image from the original one. The use of a sharpening filter, however, does not compensate for movement artefact. An example of an image before and after the use of a sharpening filter is shown in Figure 2.8

b) Low-pass filter

A low-pass filter was then applied to correct for bone marrow inhomogeneity in paediatric images, due to the physiological conversion of yellow to red marrow in children (see Chapter 1, section 1.2.4). This step is crucial as without which the darker regions of the marrow can be wrongly assigned as bone by the analysis software in the binarisation stage (see section 2.2.2.3a) which will affect the quantitative results. Figure 2.9 shows an image before and after correction for bone marrow inhomogeneity, and the corresponding binarised images.

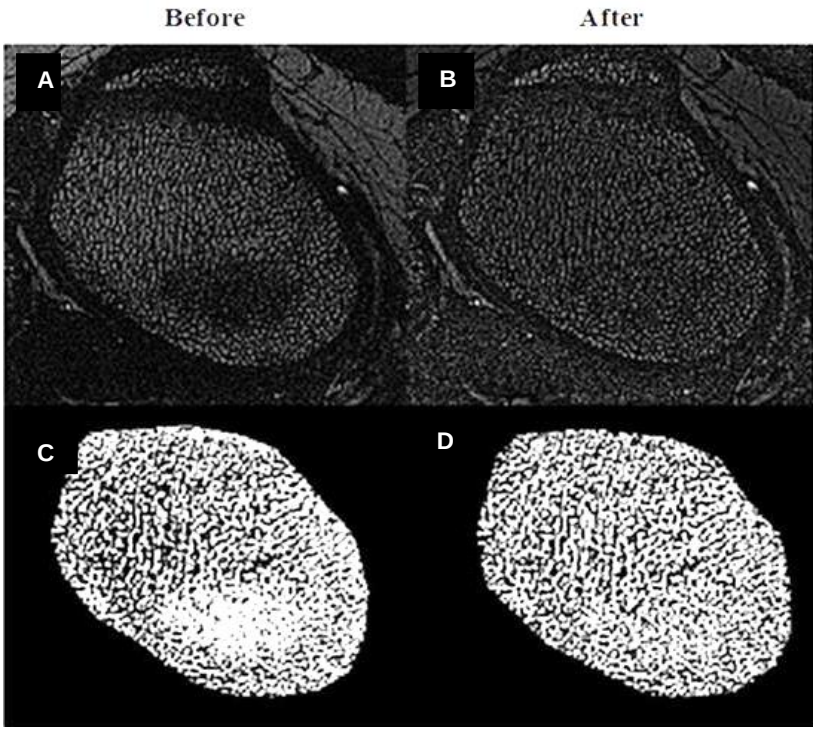

Figure 2.9 Paediatric MRI image before (A) and after (B) application of a low-pass filter to correct for bone marrow inhomogeneity, and the corresponding binarised images (C and D). Binarisation is where the image is being assigned to either 'bone' or 'marrow' before quantification.

2.2.2.3 Image Analysis

After filtering, the images were coded and analysed using MATLAB based on a method previously described by Majumdar et al., to give measures for apparent bone volume to total volume ratio (appBV/TV), apparent trabecular number (appTbN), apparent trabecular thickness (appTbTh) and apparent trabecular separation (appTbSp) (Majumdar *et al.* 1997). Validation of the software was performed using a custom-made phantom as described previously, with high intra-operator, inter-operator and inter-scan repeatability (McComb *et al.* 2014b).

Five image slices (Slice 9, 10, 11, 12 and 13 out of the 20 slices) per participant were analysed and the mean taken, based on a separate study carried out by our group to determine the feasibility of partial image analysis in yielding a representative estimate of trabecular bone microarchitecture by high-resolution MRI (detailed in Chapter 3).

a) Image Segmentation/Binarisation

In the filtered MRI images, bone appeared dark (low signal intensity) while fatty marrow was bright (high signal intensity) (Figure 2.10B). Using a graphics cursor, the region of interest (ROI) in each axial slice was manually drawn along the trabecular-cortical boundary

to ensure the analysed ROI consisted only of the trabecular bone and bone marrow (Figure 2.10C). Once defined, the ROI was displayed in *reverse grey scale* for ease of visualisation, where trabecular bone has a high signal intensity as the cortical rim whilst bone marrow has a low intensity. Muscle tissue has an intermediate signal intensity.

The image was then thresholded and binarised, where by each pixel was assigned as either 'bone' or 'marrow' (binarisation) using a standardised method of image thresholding (Figure 2.10D) (Majumdar *et al.* 1995, Majumdar *et al.* 1997). A histogram of the signal intensities in the ROI was plotted and the mean signal intensity (I_{ROI}) of the ROI was obtained Figure 2.10E). Due to the thickness of the image slices exceeding the dimension of trabecular bone, each pixel in the image may not correspond to only one kind of tissue i.e., either bone or marrow but may contain a mixture of the two tissues in varying degree (partial volume effect). Consequently, the histogram of the signal intensities, did not have two individual peaks but a single peak and an asymmetric tail for the lower signal intensities. The intensity of the trabecular bone (I_{Bone}) was obtained based on that of the thick cortical rim. The peak of the histogram represents the most frequently occurring pixel intensity value in the ROI.

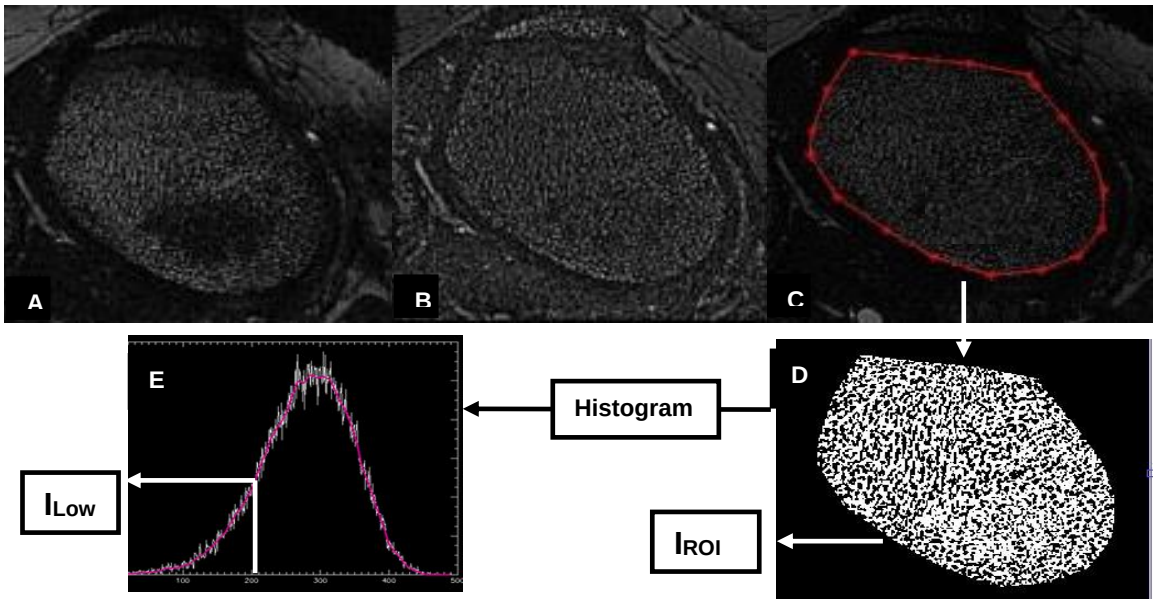

Figure 2.10 Sequence of image analysis for a representative MRI axial image. Raw image acquired (A), filtered to correct marrow inhomogeneity (B), region of interest (ROI) manually drawn in red and then image binarised (D) resulting in a histogram depicting all the signal intensities in the ROI. I_{ROI} is the mean signal intesity of the region of interest and I_{Low} is the signal intensity of bone marrow, also known as I_{Marrow}.

This peak intensity, since it is the mixture of the two phases, should have a value that is lower than the high intensity trabecular intensity, I_{Marrow}, was set at the lower signal intensity at which the histogram reached half its peak value (Figure 2.11). This is an empirical level and was adopted for the purpose of standardisation as it is very difficult to identify a trabecular space which contains solely bone marrow. Applying these intensity thresholds and taking into the spatial resolution of the slice thickness, the image is then binarised using a clustering method of similarity measures known as fuzzy c-mean clustering (Folkesson *et al.* 2010).

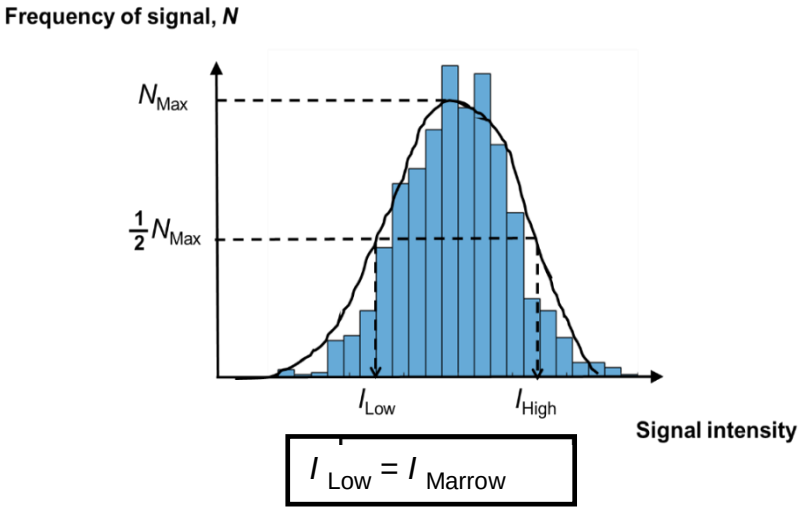

Figure 2.11 Assignment of marrow intensity (I_{Marrow}), which is set at the lower intensity where the histogram reached half its peak value. This is an empirical method for standardisation due to difficulty in identifying a trabecular space with solely bone marrow.

Calculation of Apparent Trabecular Bone Volume/Total Volume (appBV/TV)

Based on the values from the histogram, the appBV/TV (i.e. the number of bone pixels/total number of pixels) can be calculated from the following equation (Majumdar *et al.* 1997):

$$I_{ROI} = (appBV/TV)I_{bone} + (1 - appBV/TV)I_{marrow}$$

$$\Rightarrow appBV/TV = \frac{I_{ROI} - I_{marrow}}{I_{bone} - I_{marrow}}$$

Equation 1

The intensity value at which the fractional trabecular bone content in the ROI corresponded to the calculated appBV/TV was selected as the threshold, and the image was binarised into a bone and a marrow phase.

b) Image quantification of trabecular structure

Standard stereological method was extended to quantify the trabecular structures in the binarised image (Majumdar *et al.* 1995). A grid of parallel lines, each one pixel thick and separated by 10 pixels, was used as a mask, so that only the sections of the image which lie along the lines were considered and the rest of the image was set to zero. For each line in turn, a starting value corresponding to the value of the first pixel in the line was established. Each pixel along the line is then examined in turn, and the number of times that a change from bone to marrow (1 to 0) or marrow to bone (0 to 1) occurs was counted, and defined as $P_L(\theta)$. The number of pixels which correspond to bone, P_P are also counted.

Based on these, the mean intercept length (MIL) was calculated from the following equation (Majumdar *et al.* 1995, Majumdar *et al.* 1997):

$$MIL(\theta) = 2 \cdot \frac{P_P}{P_L(\theta)}$$

Equation 2

Calculation of Apparent Trabecular Thickness (appTbTh)

The MIL is calculated for all angles between 0° and 360° in steps of 10°. The apparent trabecular thickness (in mm) is then calculated using the following equation (Majumdar *et al.* 1996):

$$appTbTh(mm) = 0 \cdot 5 * mean\left(MIL(\theta)_{\vartheta=0,360}\right) * R$$

Equation 3

where *R* is the pixel resolution in mm.

Calculation of Apparent Trabecular Number (appTbN)

Apparent trabecular number (in mm^{-1}) is calculated using the following equation (Majumdar *et al.* 1996):

$$appTbN\left(mm^{-1}\right) = \frac{appBV/TV}{appTbTh}$$

Equation 4

Calculation of Apparent Trabecular Spacing (appTbSp)

Apparent trabecular spacing (in mm) is calculated using the following equation (Majumdar *et al.* 1996):

$$appTbSp(mm) = \frac{1}{appTbN} - appTbTh$$

Equation 5

2.3 MRS

2.3.1 Principles of MRS

Magnetic resonance spectroscopy (MRS) can be used in conjunction with MRI for non-invasive *in vivo* quantification of a certain metabolite of interest. Instead of producing an image, ^{1}H MRS measures the abundance of hydrogen (1H) in the different elements (including water and fat) within the tissue to produce a spectra of signal intensity versus chemical shift. Based on the Larmor equation similar in MRI, the resonant frequency of a hydrogen nucleus is determined by the strength of the external magnetic field. However, the shielding effect of the orbiting electron cloud around the hydrogen nuclei, causes a chemical shift, expressed in unit parts per million (ppm), which results in identical nuclei resonating at different frequencies within the tissue (Westbrook *et al.* 2011). This generates well resolved signal peaks which enable the different metabolites to be distinguished (Figure 2.12).

Radiofrequency (RF) coils are used to transmit the RF magnetic induction field (B_1) and to detect the resulting signal using a transmit/receive coil or a separate dedicated receiver coil. Using a point-resolve spatially localised spectroscopy pulse sequence (PRESS), a spectrum of the different metabolites present can be obtained from a single well-defined spatial volume (single voxel spectroscopy) (Jansen *et al.* 2006). The spectrum displays the metabolites as separate peaks due to the difference in their resonance frequency with their characteristic line widths,

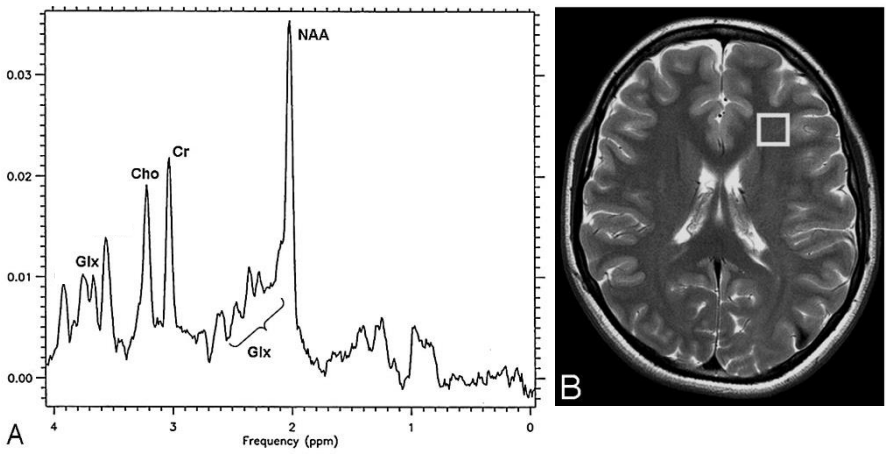

Figure 2.12 ^{1}H-MR spectroscopy of a normal brain. ^{1}H spectra of a normal brain (A) with the volume of interest (marked with a square) placed in the white matter of the left frontal cortex as seen in the corresponding T2-weighted MR image (B) The spectra exhibit the various different metabolites present including *N*-acetylaspartate (NAA). total choline (Cho), glutamate plus glutamine (Glx) and Creatine (Cr). [Adapted from (Ricci *et al.* 2007)]

line shapes, phase and area. Quantification of the concentration of the metabolite of interest can be done by accurately calculating the area under the peak. Figure 2.12 demonstrates the MR image and spectra of the metabolites in the brain, which is the organ where this technique is most widely used clinically.

2.3.2 Lumbar spine imaging

Imaging was performed on a 3 Tesla (T) Siemens MAGNETOM Prisma MRI scanner (Siemens, Erlangen, Germany) using a transmit/receive (Tx/Rx) extremity coil for the knee. The MR images were then pre-processed, coded and analysed using MATLAB (Mathworks Inc, San Mateo, CA, USA) software.

2.3.2.1 Acquisition

Both MRI and MRS imaging were performed on the same 3T-MRI scanner during a single scanning session for each participant. Once the knee coil was removed, the participant was positioned further into the MRI scanner to image the lumbar spine at the level of L3. Ideally, measurement of marrow adiposity would be done at the same site as the measurements for the trabecular bone microarchitecture in the lower limb but this is technically impossible. Localiser and T2 scans (sagittal and axial) were performed to allow positioning of the voxel within the vertebral body of L3 (Figure 2.13A). A Point-REsolved Spectroscopy Sequence (PRESS), as summarised in Table 2.2, with no water suppression and a short echo time (TE) was used to enable detection of lipids.

Table 2.2 PRESS Pulse sequence parameters for imaging of the lumbar spine (L3)

Parameter	Value
Resolution (mm^3)	20 x 20 x 20
TE (ms)	30
TR (ms)	2000
Flip angle (°)	90
Number of averages	80
Bandwidth (Hz/pixel)	1200
Scan time (mins)	2.5

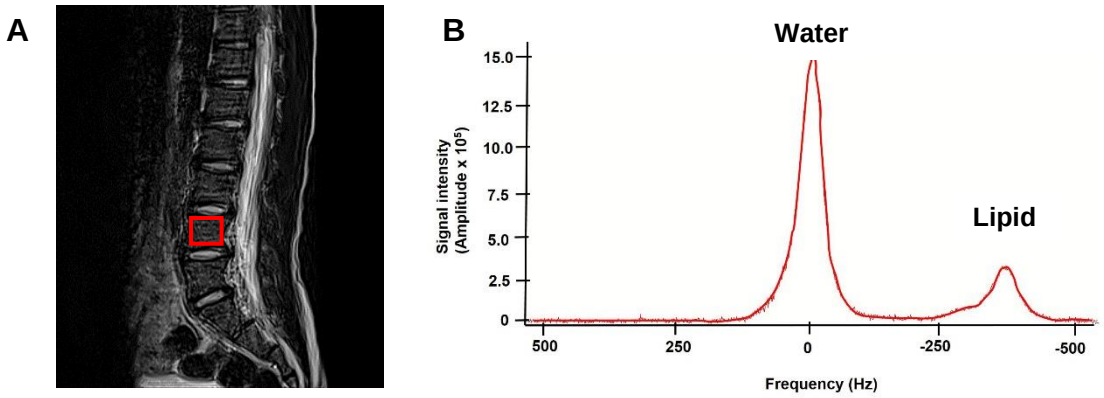

Figure 2.13 ^{1}H Spectroscopy of lumbar spine. (A) Representative MR image of the lumbar spine with the region of interest (marked with a red square) placed in L3 and (B) its corresponding ^{1}H spectra of water and lipid peaks respectively.

2.3.2.2 Image Analysis

MRS analysis was performed using the Java-based magnetic resonance user interface (jMRUI) software package to obtain measures for the calculation of percentage fat fraction (%FF) within the bone marrow (Vanhamme *et al.* 1997, Naressi *et al.* 2001). The resulting spectrum shows peaks corresponding to water and fat as shown in Figure 2.13B. A best-fit Gaussian model was applied to the acquired spectra, and the area under the resulting water peak (I_{Water}) and lipid peak (I_{Lipid}) were measured to work out the lipid-to-water ratio (LWR).

$$LWR = \frac{I_{\text{Lipid}}}{I_{\text{Water}}}$$

The percentage fat fraction (FF) was then calculated, as a measure of bone marrow adiposity, using the following equation (Schellinger *et al.* 2004):

$$\%FF = \left(\frac{LWR}{LWR+1} \right) \times 100$$

2.4 Dual Energy X-ray Absorptiometry (DXA)

2.4.1 Principles of DXA

Conventional X-ray images are insensitive to bone density changes with at least 30% of bone mineral losses required before they may be visually detected. This has led to the development of, initially single and now dual energy, radiographic absorptiometry devices specifically designed to quantitate bone density. DXA scanners usually consist of a couch for the patient, an x-ray source underneath which moves together with a mobile radiation detector arm placed directly above. The patient is placed on the couch in the path of the radiation beam from the source, and the radiation detector is then scanned back and forth over the measurement site. Fundamentally. DXA is reliant on the difference in the attenuation of the dual x-ray beams (high energy and low energy) when they pass through soft tissue and bone. Both bone and soft tissue will attenuate the dual beams as they pass through the body, with the low energy attenuated more than the high energy beam, but the difference is much greater in bone (Faulkner 2001). The attenuation values of the soft tissues and that of bone at the respective high and low energies are used to compute the mass of the bone (or BMC, g) at each *point* in the X-ray beam based on the following equations:

$$I^L = I_0^L\,[\exp - (\mu_b^L\, m_b + \mu_t^L\, m_t)]$$

$$I^H = I_0^H\,[\exp - (\mu_b^H\, m_b + \mu_t^H\, m_t)]$$

$$m_b = \frac{(\mu_s^L/\mu_s^H)\log(I^H/I_0^H) - \log(I^L/I_0^L)}{\mu_b^L - \mu_b^H\,(\mu_s^L/\mu_s^H)}$$

Equation 6

where: I_0 = incident radiation intensity

I = transmitted radiation intensity

μ = mass attenuation value for the attenuating material (cm^2/g)

m = mass of the attenuating material (g)

and subscripts b and t refer to bone and tissue, respectively, while L and H for high and low energies, respectively. The computer then evaluates the bone area in the coronal plane of the area scanned and the BMD (measured in g/cm^2) is determined as the total bone mass (BMC, measured in g) divided by the bone area (BA, measured in cm^2).

$$\text{BMD } (g/cm^2) = \frac{\text{BMC } (g)}{\text{BA } (cm^2)}$$

Equation 7

Since the densitometry is a projectional technique providing a two-dimensional image of the bone being measured, the BMD derived is therefore the mass of the bone tissue per unit *area*, not per unit *volume*. It is therefore often referred to as *areal* BMD (aBMD) to emphasize that it is not a true volumetric density. Additionally, as the dual beam allows for the delineation of soft tissue versus bone, DXA can also be used to assess body composition (fat mass, lean body mass, and percentage body fat), on both total body (TB) and regional basis (Korkusuz 2015).

The clinical utility of DXA falls into three broad categories:

1. confirmation of low bone mass by comparison with normative data

2. assessment of fracture risk

3. monitoring skeletal change in response to therapy or due to aging

DXA can measure effectively any skeletal site, but its clinical use in the assessment of fracture risk has been commonly concentrated on the lumbar spine, hip (femoral neck and total hip) and total body. For BMD measurements to be clinically useful, they need to be compared to established normative data and expressed in two standard deviations (SD) of BMD, categorised as T-score and Z-score. The T-score compares the patient's BMD to the young-adult reference population of the same gender and has been adopted as the WHO diagnostic classification of osteoporosis. It is, however, restricted to postmenopausal women and men age 50 and older, and not applicable for children and young people. On another hand, the Z-score is applicable for children, premenopausal women and men younger than 50 years, as it is compared to the BMD of an age-, sex-, and ethnicity-matched reference population. Its measurement of -2.0 or lower is indicative of significantly decreased bone density for chronological age (Cosman *et al.* 2014).

Care must be exercised to avoid erroneous BMD measurements. Most of these pitfalls can be broadly categorised into technical and interpretation errors (Peh 2014). Over time, the scanner system can be expected to drift due to hardware deterioration such as X-ray tube aging, environmental changes and other factors resulting in technical errors. Daily scanning of the calibration standard supplied with the system needs to be carried out to ensure accurate BMD measurements (Faulkner 2001, Peh 2014). The scanner can self-adjust to bring it back into the original calibration if a small drift is detected, without the need for technical assistance. Periodically, scanning of a quality control phantom (simulated bone material encased in plastic designed to mimic soft tissues) is also carried out to monitor for scanner stability as well as allowing for cross-calibration between different scanners if necessary. The positioning of patient and the placement of ROIs, both crucial for proper image acquisition, can be technically difficult due to patient cooperation and under developed skeletal landmarks in younger children (Lenchik *et al.* 1998).

The greatest challenge in paediatric densitometry, however, is in the interpretation of DXA measurements. This is much more complex in young growing patients, necessitating a validated adjustment method to take into account the altered growth, stages of puberty and the effects of chronic disease on bone size. The revised ISCD Official Position in 2013 recommended that in children with short stature or growth delay, spine BMC and aBMD results should be adjusted using either bone mineral apparent density (BMAD) or the height Z-score (Crabtree *et al.* 2014). TBLH BMC and aBMD, on the other hand, should be adjusted using the height Z-score. When considering adjustments of DXA measurements for bone size, height, LBM, skeletal age, or pubertal stage in growing children, it is relevant to consider the goal of the exercise as there is no single adjustment ideal for all. Crucially, size adjustment techniques have been shown to improve the DXA predictive ability for fracture (Crabtree *et al.* 2013). The paucity of large representative normative databases can add to dilemma in interpretation as many manufacturer reference databases are often small in numbers and not representative of the individual population being studied (Crabtree *et al.* 2014). A well-trained and experienced DXA technologist is required to avoid most of the errors in acquisition and analysis.

2.4.2 Whole Body Imaging

All imaging were performed systematically by one practitioner (SS) using a Lunar Prodigy densitometer (GE Medical Systems, Wisconsin, USA) to assess the bone and body composition parameters and analysed using the Encore software (Version 13.0). Following height and weight measurements, the participants were positioned supine on the scanner couch and the mobile X-ray source moved from in a cranio-caudal manner to obtain whole body (TB) and lumbar spine (LS) measurements. Total scan time was 10-15mins per participant. Bone parameters obtained include bone mineral content (BMC) [g], bone area (BA) [cm^2] and mean areal bone mineral density (BMD) [g/cm2]. Body composition parameters obtained include whole body lean mass (LM) [g] and fat mass (FM) [g].

2.4.2.1 Analysis

As outlined in previous studies, the predicted and percentage predicted bone area (ppBA) for age and sex were calculated based on our reference data (Warner *et al.* 1998, Ahmed *et al.* 2004). This allowed for a comparison of the actual bone mineral content (BMC) of the individual participant with the predicted BMC of a subject of the same sex and bone area from which the percentage predicted BMC (ppBMC), expressed as an SDS (BMC SDS) could be calculated. The coefficient of variation (%CV) calculated on repeated DXA measurement of a phantom was <1% of BMC and <2.5% *in vivo*. Body composition parameters were adjusted for height to minimise the size-related effects of DXA.

2.5 Biochemical assessment

2.5.1 Blood sampling

Non-fasting blood samples were obtained from all participants in the morning to avoid any bias from diurnal variation. Serum markers for bone formation (bone alkaline phosphatase [BAP], octeoclacin [OC]), bone resorption (C terminal telopeptide of Type I collagen [CTX]), adiposity (pre-adipocyte factor-1 [PREF-1]), growth hormone axis (IGF-1, IGF-BP-3, the acid labile subunit [ALS]), sclerostin and other regulator markers of bone turnover (PTH, AP, 25-Hydroxy-vitamin D [25OHD]) were measured.

2.5.2 Biochemical assays

All samples of whole blood were centrifuged on the same day to obtain the serum, which was aliquoted and stored at -80^{0}C until the assays were run. The samples were analysed in duplicate concurrently and samples from each patient were analysed in a single run to minimise analytical variation. Osteocalcin (OC), bone-specific alkaline phosphatase (BAP), C terminal telopeptide of Type I collagen (CTX) were analysed by ELISA (Immunodiagnostic systems, Boldon, UK). The intra-assay variation for OC, BAP and CTX was 1.4%, 9.6% and 3.1%, respectively. Plasma IGF-1 and its binding proteins, IGFBP-3, and the acid labile subunit (ALS) were analysed by ELISA (Mediagnost GmbH, Reutlingen, Germany). Intra-assay variabilities were 16.0%, 2.9%, and 10.9%, respectively. Sclerostin (SOST) was also analysed by ELISA (TECO, Pathway Diagnostics, Surrey, UK) with intra-assay variation of 14.1%. Parathyroid hormone (PTH) and alkaline phosphatase (AP) were measured using chemiluminescent microparticle immunoassay (Abbott Diagnostics, IL, USA). Intra-assay variations were <6.3% and <8.0% respectively. 25-hydroxy-Vitamin D was measured by liquid chromatography-tandem mass spectroscopy (LC-MS/MS) based on our in-house previously published method, with intra-assay variation of <10% (Knox *et al.* 2009). Reference data for the respective assays were obtained from the literature to calculate the age- and gender-specific SDS values (Rauchenzauner *et al.* 2007, Ertl *et al.* 2014).

Laboratory-based experiments: Material and Methods

2.6 Cell culture

2.6.1 Principle of cell culture: proliferation and differentiation

Cell culture is a technique whereby prokaryotic, eukaryotic or plant cells are grown under controlled condition. Most commonly it refers to the culturing of cells derived from animals or humans. Harrison was thought to be the father of cell culture as he successfully cultivated frog neuroblasts in a lymph clot *in vitro* for several weeks in 1907 (Harrison *et al.* 1907). There are several milestones in the development of cell culture technology, the first being the discovery of trypsin in the 1950s which enabled the removal of intact adherent cells allowing cell subcultures (Dulbecco 1952) Trypsinisation also facilitated the generation of a single cell suspension, further advancing single cell cloning. Secondly, the introduction of antibiotic use in cell culture inhibited the growth of contaminant, which facilitated long-term cell line propagation (Cruickshank and Lowbury 1952). The third major milestone was the use of chemically defined culture media to maintain the cells at an appropriate stage of maturation to retain their proliferative capacity instead of favouring differentiation, and vice versa. (Eagle 1955). This led ultimately to serum-free media (Ham 1965) which can facilitate the selective growth of a particular type of cell, eg. Dulbecco's Modified Eagle's Medium (DMEM) for embryonic mouse cells (Dulbecco and Freeman 1959). Crucially, all these are carried out *in vitro* in an aseptic environment, working within a hood with particulate air filter with principals of laminar flow, and key sterile manipulation techniques.

Primary culture is the cultivation of surgically or enzymatically removed cells from an organism, in a suitable culture environment (Freshney 2005). These cells can be passaged to create further subcultures, also called cell lines. Subcultures provide the opportunity to expand a cell population, apply further selective pressure with a selective medium and achieve a higher growth fraction and also the generation of replicate cultures for characterisation, preservation by freezing or experimentation. Briefly, subculture involves the dissociation of the cells from one another and the substrate to be reseeded at a reduced concentration into a flask to generate a secondary culture and tertiary culture and so on. Each time a cell is subcultured, it will proliferate and multiply back to previous density by going through the growth cycle: *lag* period of no growth to recover from trypsinisation and cytoskeleton reconstruction enabling them to re-enter cell cycle, *log* phase of exponential growth and *plateau* or stationary phase. Some cells readily differentiate once in plateau phase, others exit the cell cycle into G_0 but retaining viability. Reduced proliferation in the

stationary phase is due partly to exhaustion of growth factors in the medium as well as contact inhibition from cells when they are in high density.

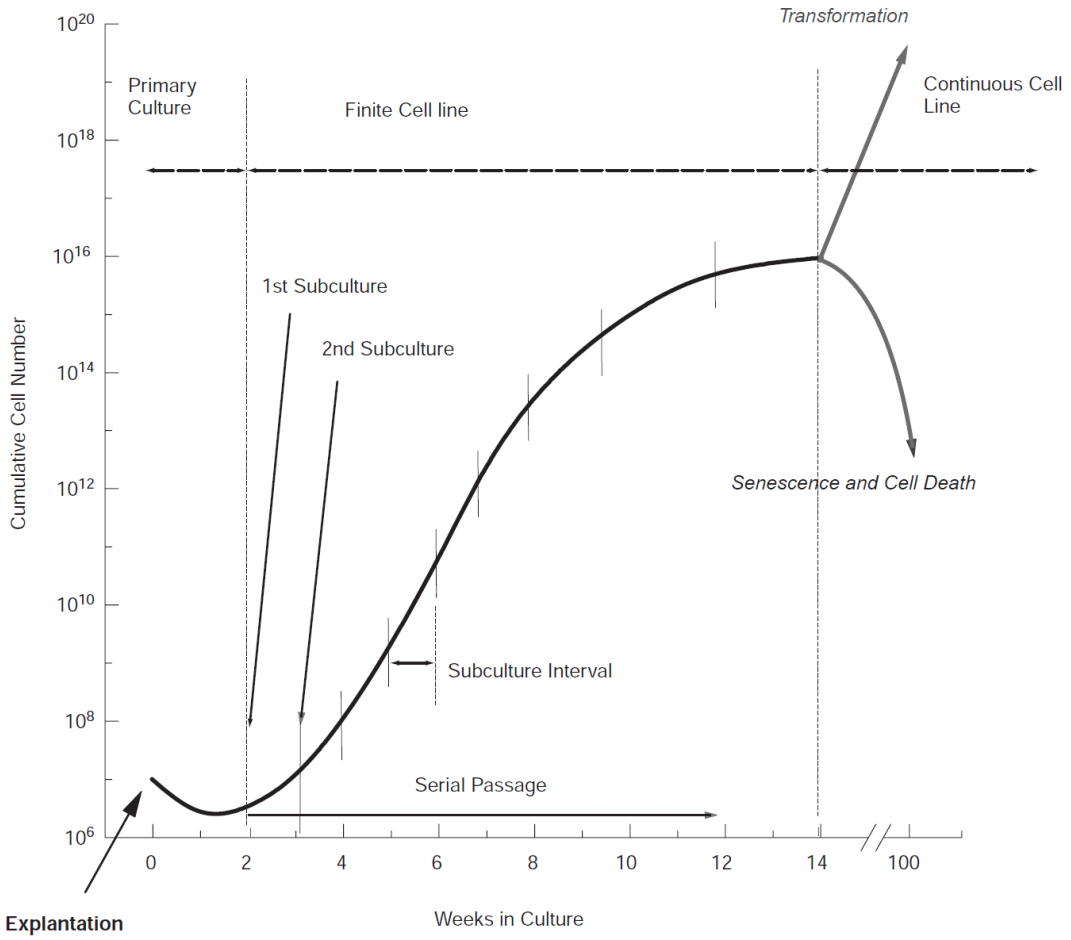

Figure 2.14 Evolution of a Cell Line. The vertical (Y) axis represents total cell growth (assuming no reduction at passage) for a hypothetical cell culture. Total cell number (cell yield) is represented on this axis on a log scale, and the time in culture is shown on the X-axis on a linear scale. Although a continuous cell line is depicted arising at 14 weeks, with different cells it could arise at any time. Likewise, senescence may occur at any time, but for human diploid fibroblasts it is most likely to occur between 30 and 60 cell doubling time. [Adapted from (Hayflick and Moorhead 1961)]

Cell proliferation is regulated by signals from the environment, either contact-mediated or molecular-signalling (Freshney 2005). Low cell density is conducive for cell proliferation giving them room for spreading, which permits entry into cell cycle in the presence of mitogenic growth factors. Most cell lines have limited life span becoming senescent after several passages. With subsequent passages, cells also lose their ability to differentiate. Cell differentiation is the process where a cell changes from one cell type to another, usually into a more specialised cell type. The condition required for differentiation, however, is often antagonistic to that of proliferation. Cell differentiation favours a high cell density where there is enhanced cell-cell and cell-matrix interaction together with the presence of various specific differentiation factors (Freshney 2005). Based on these, it is often necessary in cell

culture to define two sets of culture conditions – one to optimise cell proliferation and one to optimise cell differentiation.

2.6.2 Cell Culture experiments

AMPK α1/α2 knockout mouse embryonic fibroblasts (MEFs), C3H10T1/2 mouse mesenchymal stem cells (Clone 9; ATCC CCL-226) and 3T3-L1 preadipocytes were maintained in DMEM (41965-039, Sigma-Aldrich Ltd, Gillingham, Dorset, UK) containing 10% (v/v) FCS, 2 mM glutamine, 100 U/mL penicillin and 100 µg/ml streptomycin. Differentiation experiments were undertaken at 80-90% confluence. To promote adipogenic differentiation, cells were cultured in the standard media supplemented with either 10 µM pioglitazone alone or in combination with 100 nM insulin, 500 µM 3-isobutyl-1-methylxanthine (IBMX) and 10 µM dexamethasone (IID medium). For osteogenic differentiation, cells were cultured in standard media supplemented with 284 µmol/L ascorbic acid, 10 mM β-glycerophosphate and 10 nM dexamethasone (AGD medium). Differentiation media was changed every 3 days.

2.6.3 Preparation of Cell Extracts

C3H10T1/2 MSCs were harvested and nuclear extracts prepared using the Nuclear Extraction kit from Active Motif, Belgium. Briefly, the media was aspirated and cells were harvested in ice-cold PBS containing phosphatase inhibitors and centrifuged (200 x *g*, for 5 minutes at 4ºC) to obtain a cell pellet. The cell pellet was re-suspended in complete lysis buffer containing 10 mM DTT and phosphatase inhibitor cocktail and then centrifuged (14000 x *g*, for 10 minutes at 4ºC) to obtain nuclear and supernatant fractions.

2.7 Electrophoresis and Immunoblotting

2.7.1 Principles of electrophoresis

Electrophoresis is a technique used for separation of proteins in vertical slab gels to identify/investigate a target protein of interest or to purify proteins for further applications (Sambrook and Russell 2001, Ausubel *et al.* 2003). The separation of proteins is dependent on protein characteristics: surface features, bioproperties, molecular size, and net charge, of which electrophoresis exploits the latter two. Typically, a constant electric field is applied to the electrophoresis chamber (10-20v per cm gel length) loaded with the protein samples, which causes migration of negatively charged molecules through the gel sieve in the

direction of the positively charged anode. Small proteins migrate relatively easier through the gel than larger proteins, hence allowing the separation of protein by molecular size. The separated proteins are then transferred from the gels onto a membrane such as polyvinylidene difluoride (PVDF) or nitrocellulose membranes to allow further staining and quantification.

SDS-PAGE, or sodium dodecyl sulfate-polyacrylamide gel electrophoresis, is a discontinuous one-dimensional electrophoresis system conceived by Ulrich K Laemmli, which is most commonly used to separate proteins with molecular masses between 5 and 250kDa (Laemmli 1970). SDS acts as a surfactant, covering the proteins' intrinsic charges and conferring them very similar charge-to-mass ratios, negating the intrinsic charges of the proteins, allowing for precise protein separation by mass. The SDS-PAGE method is composed of *gel preparation*, *sample preparation*, *electrophoresis*, protein staining or *western blotting*, which is detailed in section 1.7.2. and 1.7.3.

2.7.1.1 Gel preparation

Typically, the separating gels are 14cm x14cm in size, although smaller mini-gels 6cm x 8cm are also often used, with thickness of up to 0.75mm. Mini gels provide faster separation at the expense of lower resolution (Ausubel *et al.* 2003). The separating and stacking gels are cast and hand-poured into special moulds with combs inserted to create little wells for the protein samples (Figure 2.15). The desired percentage of acrylamide in the separating gel depends on the molecular size of the protein being separated, in particular the one of interest. Polymerisation of the polyacrylamide with cross-linking formed from bisacrylamide results in gels of different porosity, crucial for its sieving function. A general rule of thumb, of 5% gels for 60-200kDa and 10% gels for 16-70kDa and 15% gels for 12-45kDa. The composition for making up the separating and stacking gels, with varying amounts of acrylamide and bisacrylamide, are available from most laboratory manuals (Sambrook and Russell 2001), with one example shown in Figure 2.16, although pre-cast gels are available commercially.

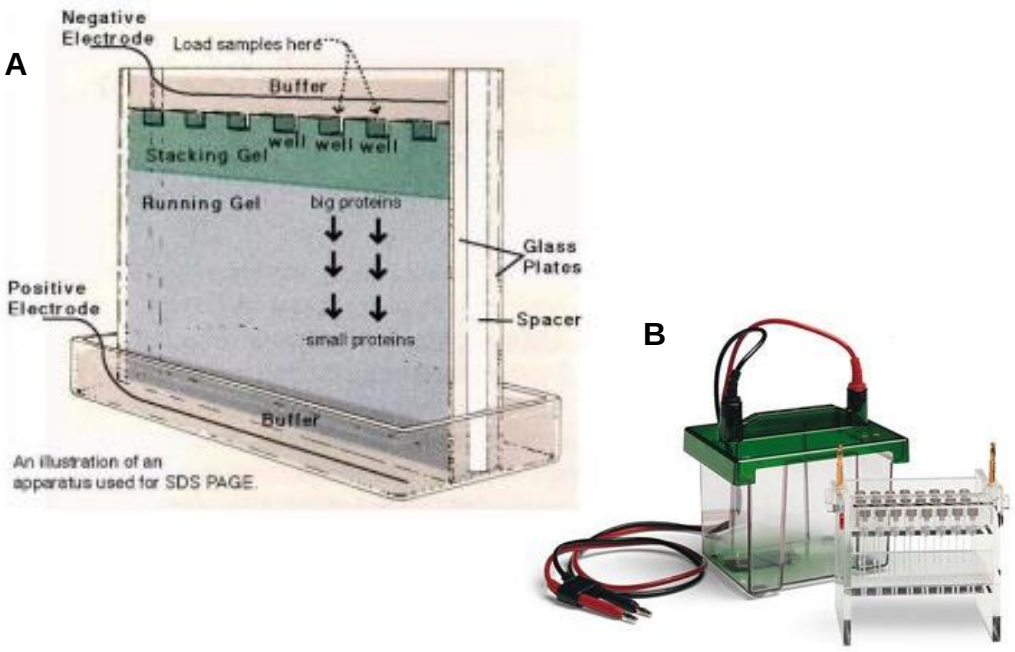

Figure 2.15 SDS-Polyacrylamide Gel Electrophoresis (SDS-PAGE). (A) Schematic representation of an SDS-PAGE set up, with the stacking and running/separating gels, and (B) a Bio-rad model of the apparatus [Images from www.chemistry.gatech.edu and www.biorad.com]

SEPARATING GEL

Stock solution[b]	Final acrylamide concentration in separating gel (%)[c]									
	5	6	7	7.5	8	9	10	12	13	15
30% acrylamide/ 0.8% bisacrylamide	2.50	3.00	3.50	3.75	4.00	4.50	5.00	6.00	6.50	7.50
4× Tris·Cl/SDS, pH 8.8	3.75	3.75	3.75	3.75	3.75	3.75	3.75	3.75	3.75	3.75
H_2O	8.75	8.25	7.75	7.50	7.25	6.75	6.25	5.25	4.75	3.75
10% (w/v) ammonium persulfate[d]	0.05	0.05	0.05	0.05	0.05	0.05	0.05	0.05	0.05	0.05
TEMED	0.01	0.01	0.01	0.01	0.01	0.01	0.01	0.01	0.01	0.01

Figure 2.16 Recipes for polyacrylamide separating gel with volume in mililitres (mls) of each solution needed depending on percentage (%) of gel required. Polymerisation of the polyacrylamide with cross-linking formed from bisacrylamide results in gels of different porosity, crucial for its sieving function [Adapted from (Ausubel *et al.* 2003)]

2.7.1.2 Sample preparation

The protein sample is diluted 1:1 (v/v) with 2x SDS buffer and heated to 95°C for 3-5mins in a sealed microcentrifuge tube. The comb is removed and the wells are carefully filled with the protein samples using pipettes. By convention, the far left lane is filled with a protein-molecular weight standards (or protein marker) mixture.

2.7.1.3 Electrophoresis and protein transfer

Once the protein samples are loaded into the wells, the electrophoresis running chamber is filled with a running buffer solution before an electrical field is passed through the chamber until the bromphenol blue dye in the protein marker lane has reached the bottom of the gel. During this stage, the proteins are separated by their molecular sizes vertically, with larger proteins which travel slower through the gel isolated at the top closest to the loading point, whilst smaller proteins further below in molecular mass order Figure 2.17

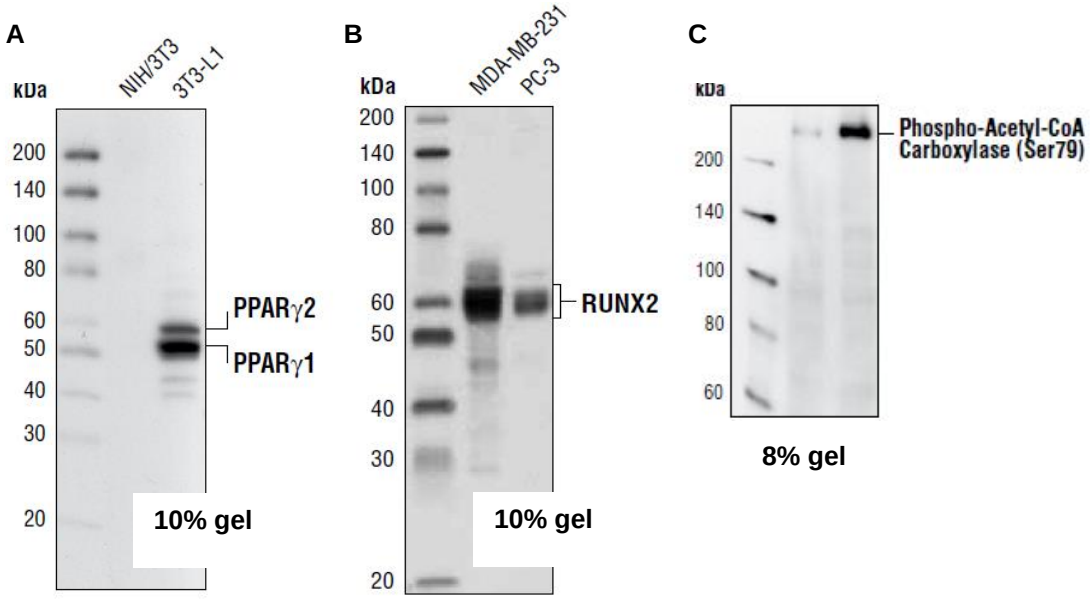

Figure 2.17 Molecular sizes of the protein of interests (A) PPARγ, (B) Runx2 and (C) phospho-ACC dictates the corresponding choice of polyacrylamide gel use. Protein of bigger molecular mass require higher gel porosity to allow better capture ideally in the middle of the separating gel, hence lower polyacrylamide/bisacrylamide content.

Two-dimensional gel electrophoresis separates the proteins in the first dimension by isoelectric focusing and in the second dimension in the presence of SDS, with incredible resolving power.

2.7.2 Principles of immunoblotting

Immunoblotting (also referred to as Western blotting) is a technique used to identify specific antigens or target proteins among unrelated protein species, by employing the function of polyclonal or monoclonal antibodies (Sambrook and Russell 2001, Ausubel *et al.* 2003). It involves identification of the protein of interest using an antigen-antibody (or protein-ligand) specific reactions. Proteins are typically solubilised using sodium dodecyl sulfate (SDS) then separated by electrophoresis, as described in section 2.7.1.

The first step to immunoblotting is to electrophoretically transfer these proteins from the SDS-polyacramide gels onto membranes to allow subsequent quantification. The gel is removed from the electrophoresis running chamber into a new set up (Figure 2.18) containing a transfer buffer solution termed as the electrophoresis transfer chamber in this thesis. For transfer from SDS gels, the membrane must be placed on the side of the gel facing the anode in a very specific 'sandwich' arrangement (Figure 2.18) for an effective horizontal transfer to occur. The choice of membrane, from nitrocellulose to nylon and PVDF membranes is largely dependent on the binding efficiency of the protein of interest to them. Nitrocellulose remains a standard membrane used in immunoblotting, although PVDF membranes have an approximately 6-fold stronger binding affinity which can ensure the proteins are retained more efficiently for subsequent steps (Van Oss *et al.* 1987).

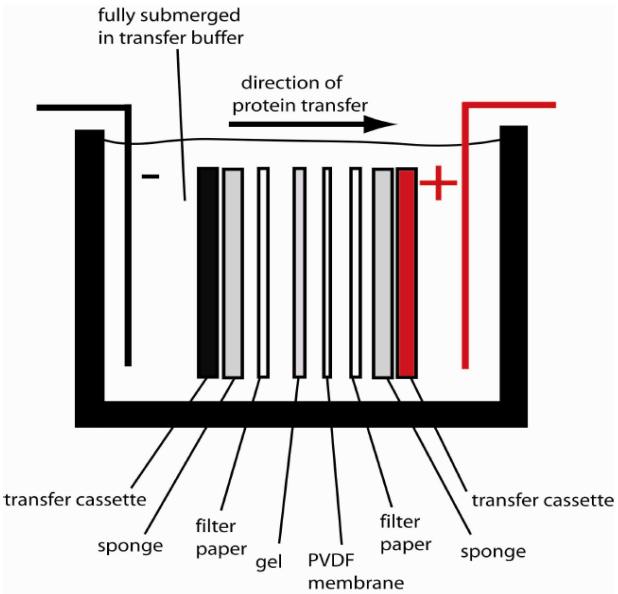

Figure 2.18 Electrophoresis transfer chamber set-up. protein transfer from SDS-polyacrylamide gels onto PVDF/nitrocellulose membranes. Protein transfer from the SDS-polyacrylamide gel onto the PVDF/nitrocellulose membrane occur in the direction of the positive anode, hence the specific 'sandwich' arrangement whereby the membrane must lie on the side of the gel facing the anode. [Images from www.mitosciences.com]

At this stage, removable Ponceau staining can be used to check how well the proteins have transferred across (Muilerman *et al.* 1982). The transferred protein sits on the surface of the membrane, allowing access for reaction with immunodetection reagents. Additional bindings sites are blocked by immersing the membrane in a solution containing protein (*e.g.* milk) or detergent blocking agent solution (*e.g.* TBST). The membrane can then be probed with a primary antibody (usually raised in mouse, rabbit or sheep) to target a specific antigen/protein and then with a secondary antibody (usually raised in donkey) labelled, with either enzymes (*e.g.* horseradish peroxidase, or alkaline phosphatase), or radioisotopes to enable detection and quantification, as shown in Figure 2.19. Conveniently, the membranes can be stripped and re-probed as needed.

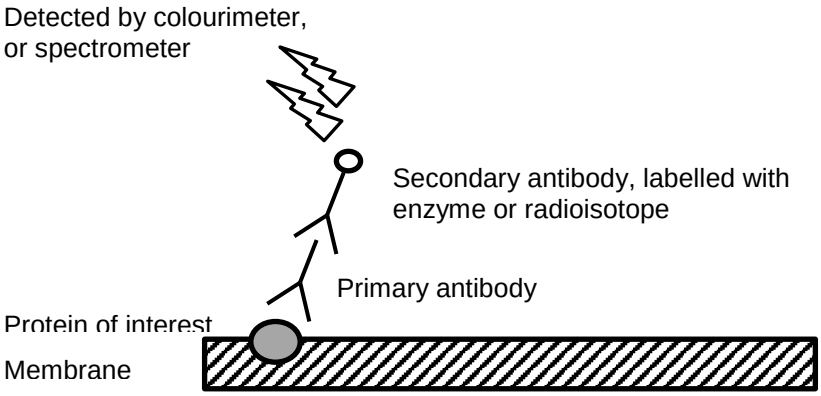

Figure 2.19 Principles of immunoblotting (also known as Western blotting), using antibodies to detect a specific antigen or target protein (in grey filled circle).

Immunoblotting is now widely used in conjunction with two-dimensional polyacrylamide gel electrophoresis, not only for traditional goals, such as the immunoaffinity identification of proteins and analysis of immune responses but also as a genome-proteome interface technique.

2.7.3 Western blotting experiments

Protein samples were separated by SDS-PAGE and then transferred electrophoretically onto nitrocellulose membranes. During electrophoresis, gels were run for 80 mins at 120V and then transferred for 120mins at a constant current of 400mA. Membranes were blocked with 5% (w/v) Marvel milk powder in TBS (20 mM Tris-HCl pH 7.5, 150 mM NaCl) for 1 hour. Membranes were then incubated with primary antibodies overnight at 4^{o}C. Following washes with TBST (TBS supplemented with 0.5% (v/v) Tween-20), membranes were incubated with secondary antibodies for 1 hour at room temperature. Antibodies were diluted to the required concentration in 50% (v/v) Sea Block (Thermo Scientific) and 50% (v/v)

TBST. The primary antibodies used were to peroxisome proliferator-activated receptor gamma (PPARγ; marker for adipogenesis, Cell Signalling Technologies (CST), Danvers, MA), Runt-related transcription factor 2 (Runx2; marker for osteogenesis, CST, Danvers, MA), phosphorylated-ACC (P-ACC (Ser79); marker for AMPK activity, CST, Danvers, MA) and phosphorylated-$p70^{S6K}$ (P-$p70^{S6K}$ (Thr389); upstream regulator of mTOR signalling, CST, Danvers, MA). Antibodies were detected using a LI-COR® Odyssey Infrared Imaging systems and densitometric analysis was carried out using ImageJ software (National Institute of Health, UK) software Version 1.47.

2.8 Oil Red O staining

2.8.1 Principles of Oil Red O staining

Oil red O staining (ORO) is a histological technique used in the visualisation of fat cells and neutral fat (Mehlem *et al.* 2013). Under light microscopy, lipid-laden adipocytes that are stained with ORO appear bright red/orange, leaving the remainder of the cellular constituents non-stained (nuclei can be counterstained). The ORO dye can be made from stock (needs to be protected from UV light) or purchased ready-made. Isopropanol, propylene glycol and triethyl phosphate (TEP) can be used as solvent-carriers for ORO.

2.8.2 Oil Red O staining experiments

C3H10T1/2 cells were incubated with adipogenic IID media in the presence or absence of either 10 µM pioglitazone, 500 µM metformin, 100 µM of the AMPK-activator, A769662, or 10 µM of the $p70^{S6K}$-inhibitor, rapamycin. Following differentiation, media was aspirated and cells were fixed to cell culture plates with 10% (v/v) neutral buffered formalin for 30 minutes. The formalin was then aspirated and staining was carried out with the addition of 0.3% (w/v) ORO in isopropanol:water (60:40) for 5 minutes in room temperature. The ORO was then aspirated and wells washed with distilled water four times. Imaging was carried out using a Zeiss Axiovert 25 microscope with QImaging camera and supporting software.

2.9 Transfection and Luciferase reporter assays

2.9.1 Principles of transient transfection and luciferase reporter assay

Luciferase reporter assay is a bioluminescence technique used to study gene regulation, based on the interaction of the enzyme luciferase, with a luminescent substrate. Common commercially available luciferases are from the firefly *(Photinus pyralis)* and Renilla *(Renilla reniformis)*, which is a sea pansy, both of which have different substrates D-luciferin and coelenterazine respectively (Cormier *et al.* 1975, Allard and Kopish 2008). Using genetic reporters (known as reporter genes), gene expression and cellular events coupled to gene expression can be examined. Typically, a DNA reporter constuct is prepared, where the reporter gene is attached to a regulatory sequence of the gene of interest and cloned into an expression vector (plasmid) that is then transfected into cells. The Renilla luciferase gene is commonly used as an internal control to normalise the values of the experimental reporter genes for variations that could be caused by effectiveness of transfection and sample handling (Shifera and Hardin 2010). It is the control of choice as Renilla is constitutively expressed in transfected cells and its expression is not up- or down-regulated by the experimental factors. More crucially, it does not have any effect on the substrate of firefly luciferase due to its action on an entirely different substrate (Cormier *et al.* 1975, Shifera and Hardin 2010). Once the cells are harvested, the luciferase and Renilla detection agents are added and the DNA of the gene of interest can be quantified. The advantages of bioluminescent reporters include: i) almost instantaneous results, ii) typically no endogenous activity in host cells to interfere with quantification, and iii) exceptional sensitivity, 10- to 1000-fold higher assay sensitivity than fluorescent reporters such as the green fluorescent protein (GFP) which is highly useful in detecting target protein in vanishingly small quantity enveloped within an intricate biological environment (Allard and Kopish 2008).

2.9.2 Transient transfection and luciferase assay experiments

C3H10T1/2 cells were transfected with the indicated plasmids in 6-well plates, with 1.125 μg/well PPRE (PPARγ reporter, purchased from Adgene) and 6xOSE reporter constructs (Runx2 reporter, supplied by Jian Huang, Rush Medical Centre, Chicago, USA) using Lipofectamine 2000 reagent (Invitrogen, Carlsbad, CA) and then treated with metformin, A769662 or rapamycin with and without adipogenic differentiation media. Cells were then harvested 48 hours after transfection and assayed using the Luciferase reporter assay system (Promega, Madison, WI) according to manufacturer's instructions. As a transfection control,

the *Renilla* plasmid 0.125 μg/well was co-transfected in each transfection experiment, and the luciferase activity was normalised to the *Renilla* activity.

2.10 Statistical analyses

2.10.1 Clinical imaging studies

All data were analysed using SPSS for Windows software program, Version 22 (SPSS, Chicago, IL, USA). Group differences were compared by Mann-Whitney test for continuous variables and Chi-square test used for categorical variables. Spearman's rank correlation co-efficient was used to assess the association between variables. Specific sub-analyses were performed and factors significant on univariate analysis were included in a multivariate logistic regression. All continuous data were presented as median (ranges) with $p<0.05$ considered as significant. Further information about the statistical analyses are detailed in the relevant individual chapters.

2.10.2 Laboratory studies

All experiments were performed in triplicate and statistical analysis was performed using Student's t-test or one-way ANOVA in SPSS for Windows software program, Version 22 (SPSS, Chicago, IL, USA). Results are expressed as mean ± standard error (SEM) and differences with $p<0.05$ were considered statistically significant.

3 The Precision of Partial Image Analysis of Trabecular Bone Microarchitecture in High-Resolution Magnetic Resonance Imaging

3.1 Abstract

High-resolution magnetic resonance imaging (HR-MRI) can assess trabecular bone microarchitecture but the number of image slices required for reliable assessment is unclear. The feasibility of partial image analysis was determined on the proximal tibia MRI images of 20 healthy controls (all female; median age 21 years (range 18,35) and 10 cases (3M:7F; median age 19.5 years (range 16,48) with known bone abnormalities including osteogenesis imperfecta and other endocrinopathies. Images were analysed using Matlab to generate the trabecular bone microarchitecture parameters, including apparent trabecular volume to total volume (appBV/TV), trabecular thickness (appTbTh), trabecular number (appTbN) and trabecular separation (appTbSp). The mean values obtained from twenty images (20IM) of the total image set were compared to that for 10 images (10IM), 5 images (5IM) and one image (1IM) from the centre of the total image set using Bland-Altman analysis. Co-efficient of variations (CV) within subjects were compared for the total and partial image set and significance level analysed with Levene's test and Mann-Whitney U-test. The results demonstrated that partial image analyses of 5IM or 10IM were quantitatively as reliable as analysis of the full image set of 20IM, for both cases and controls. The mean intra-subject CV (±SD) for appBV/TV in healthy controls was 2.6±1.1% for 20IM, 3.0±1.5% for 10IM and 3.1±1.5% for 5IM. Cases had higher mean appBV/TV CV (SD) at 3.7±2.1% for 20IM, 4.7±3.0% for 10IM and 4.3±3.1% for 5IM; all $p>0.05$ when compared to that of controls. However, sub-analysis of the 4 cases with osteogenesis imperfecta, a more severe osteopathy, demonstrated even higher mean CV (±SD) at 4.6±2.7% for 20IM, 7.1±3.1% for 10IM and 5.9±3.6%) for 5IM ($p=0.183$, $p<0.005$ and $p=0.157$, respectively). In conclusion, these findings indicate that partial image sets can reliably represent a larger complete set of images when assessing trabecular bone microarchitecture parameters. Given that the time taken to analyse 5 images per participant is half that of analysing 10 images, this Chapter has objectively informed the final analyses in Chapter 4 for using 5 image partial image set analysis.

3.2 Introduction

High-resolution magnetic resonance imaging (HR-MRI) can be used to assess trabecular bone microarchitecture. Each scan, however, generates a high number of image slices which can lead to a laborious and time-consuming analysis process. The minimum number of image slices required to be analysed for a meaningful result is unclear. The main aim of this chapter was to determine the number of images that needed to be analysed to yield representative estimates of the trabecular bone parameters.

3.3 Methods

Retrospective analyses of the MRI images obtained in a previous study cohort of 20 healthy adult controls (all female; median age 21 years (range 18,35) and 10 adult cases (3M:7F; median age 19.5 years (range 16,48) with known childhood-onset bone abnormalities including osteogenesis imperfecta and other endocrinopathies were undertaken (McComb *et al.* 2014b). Each participant had 30 slices of MR images taken of the right proximal tibia, with the first slice placed immediately distal to the growth plate as a point of reference. The first five (slices 1-5) and last five slices (slices 26-30) were not suitable for analysis due to the low signal-to-noise ratio of these images.

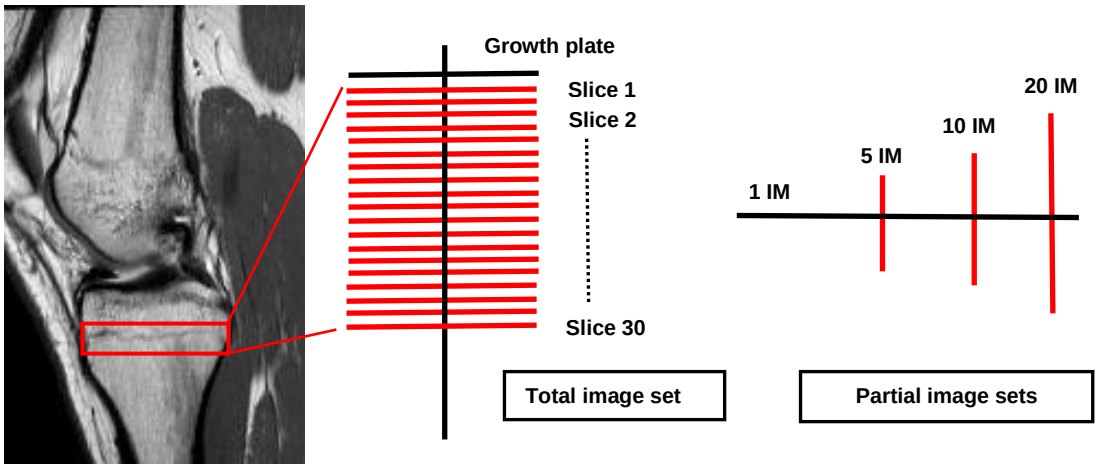

Figure 3.1 Partial image set analysis. Thirty MR image slices were taken per participant from the right proximal tibia, with the first slice placed immediately distal to the growth plate, as shown in the red rectangular box .All 30 slices were analysed per participant and the partial image set involved analysis of slice 16 as the central most slice (1 IM), slices 14-18 (5 IM), slices 11-20 (10 IM) and slices 6-25 (20 IM).

Using MATLAB software, the 20 most central images (20 IM; slices 6-25), which represented the total image set, were analysed to generate the trabecular bone microarchitecture parameters, including apparent trabecular volume to total volume (appBV/TV), trabecular thickness (appTbTh), trabecular number (appTbN) and trabecular separation (appTbSp). The same analyses were conducted for partial image sets of 10 images (10 IM; slices 11-20), 5 images (5 IM; slices 14-18) and one image (1 IM; slice 16) from the centre of the total image set (Figure 3.1). Bland-Altman analysis was used to determine the agreement between the partial image set analysis to that of the total image set. The Shapiro-Wilk test was conducted on the distribution of the differences between the partial and total image sets to confirm normality. Analysis of variance (ANOVA) was used to compare the means between groups and Levene's tests used to assess the significance of the CV within subjects. All the images were analysed by a single investigator (myself) to ensure consistency. There was no blinding carried out in the analysis.

3.4 Results

The mean trabecular bone microarchitecture parameters for 20IM, 10IM, 5IM and 1IM were summarised in Table 3.1. There were no significant differences between trabecular bone microarchitecture parameters from 10IM, 5IM or 1IM vs 20IM (p>0.05).

Table 3.1 Measures of trabecular bone microarchitecture parameters in 20 healthy adults

	20IM*	10IM*	5IM*	1IM*
appBV/TV	0.442 ± 0.024	0.441 ± 0.024	0.442 ± 0.025	0.447 ± 0.027
appTbTh (mm)	0.771 ± 0.049	0.769 ± 0.049	0.764 ± 0.048	0.787 ± 0.051
appTbN	0.576 ± 0.043	0.578 ± 0.043	0.584 ± 0.044	0.569 ± 0.045
appTbSp (mm)	0.979 ± 0.104	0.976 ± 0.105	0.966 ± 0.104	0.981 ± 0.114

appBV/TV = apparent trabecular bone volume/total volume; appTbTh = apparent trabecular thickness; appTbN = apparent trabecular number; appTbSp = apparent trabecular separation; IM = number of images analysed from the total or partial image sets; Values in mean±SD. *Between group comparisons all *p>0.05*

The differences between the total (20IM) and partial image analyses (10IM, 5IM and 1IM) became more apparent when partial image analyses of fewer image slices were used, with more values scattered away from the mean difference, as shown in Figure 3.2 and Figure 3.3. Figure 3.2 demonstrated that partial image set analyses of 10IM, 5IM and 1IM agreed well with the total image set analysis for 20IM in healthy controls, as most of the values laid

between the upper and lower limits of agreement. The differences in appBV/TV values for partial image set of 1IM compared to 20IM, however, were far more dispersed from the mean, with significantly more values lying outwith 95% confidence interval of the mean difference. Similar agreements were found for partial image set analyses in cases with childhood-onset bone abnormalities, as shown in Figure 3.3. Partial image analyses of 10IM, 5IM and 1IM agreed well with total image analysis for 20IM, although most values outwith the 95% confidence interval of the mean difference.

The reproducibility of the image analysis was determined in the cases and controls with the intra-subject CV for apparent bone volume/total volume summarised in Table 3.2. Although the mean CV for appBV/TV were higher in cases than controls, these did not reach statistical significance (all $p>0.05$). Further sub-analysis of only the cases with osteogenesis imperfecta (OI), which is a more severe osteopathy, demonstrated significantly higher mean CV compared to healthy controls ($p<0.05$) for all total and partial image sets.

Table 3.2 Measures of intra-subject coefficient of variation (CV) for apparent bone volume **total volume (appBV/TV)**

	Intra-subject CV for appBV/TV				
Image sets	**Controls**	**Cases (All)**	***p***	**Cases (OI only)**	***p***
	n=20	n=10		n=4	
20IM	2.6 ± 1.1	3.7 ± 2.1	>0.05	4.6 ± 2.7	0.037
10IM	3.0 ± 1.5	4.7 ± 3.0	>0.05	7.1 ± 3.1	0.028
5IM	3.1 ± 1.5	4.3 ± 3.1	>0.05	5.9 ± 3.6	0.017

IM = number of images analysed from the total or partial image sets; Values in mean±SD.

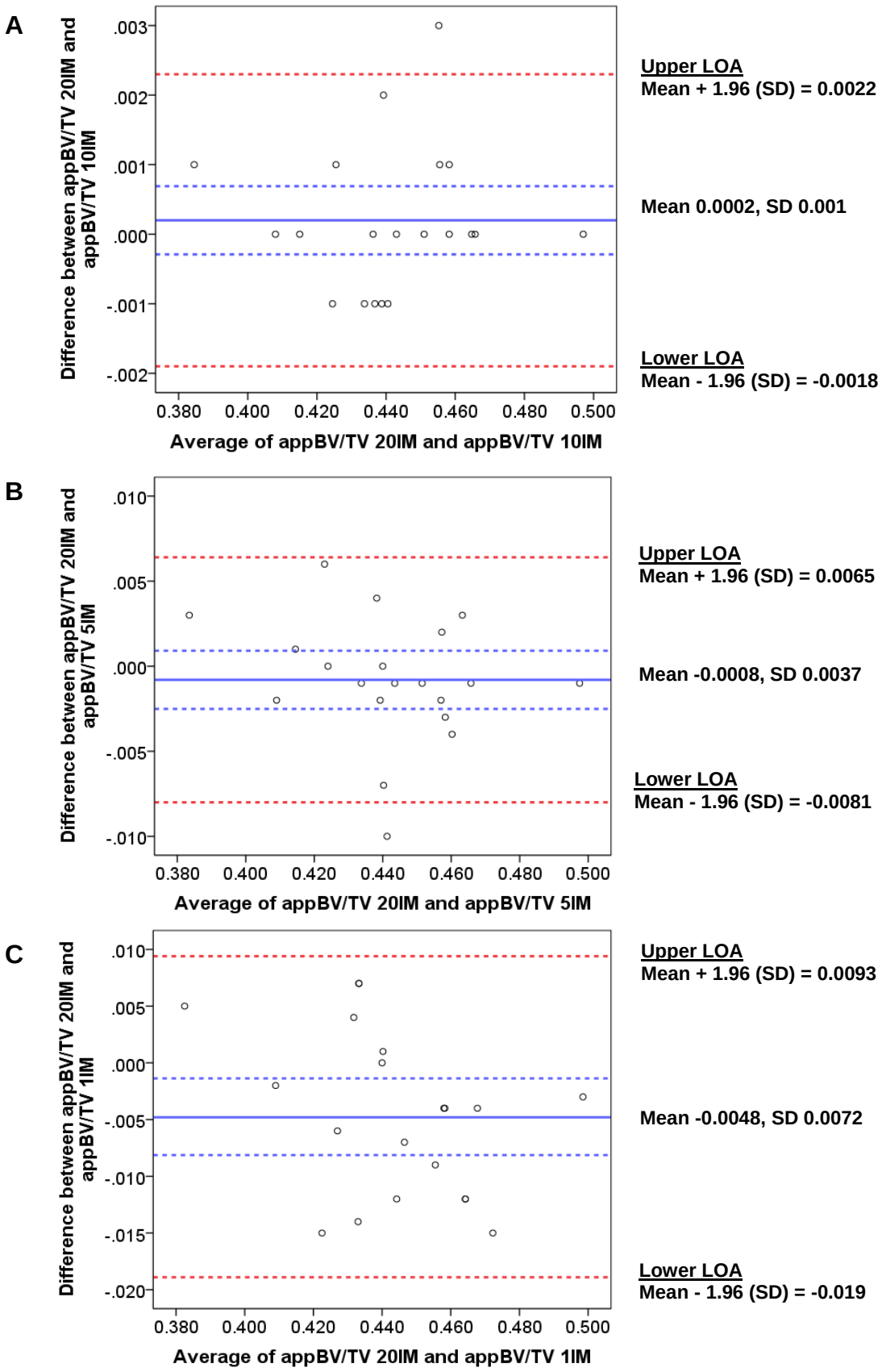

Figure 3.2 The agreement between partial and total image sets estimates of apparent trabecular bone volume/total volume (appBV/TV) in healthy subjects, using Bland-Altman analysis. Partial image sets of (A) 10 images (10IM), (B) 5 images (5IM) and (C) 1 image (1IM), agreed well with the total image set (20IM), although 1IM had most values dispersed outwith the 95% confidence interval of the mean difference. Mean difference marked with solid blue line whilst upper and lower limits of agreement (LOA) marked with dashed red lines. Dashed blue lines indicate the 95% confidence interval of the mean difference.

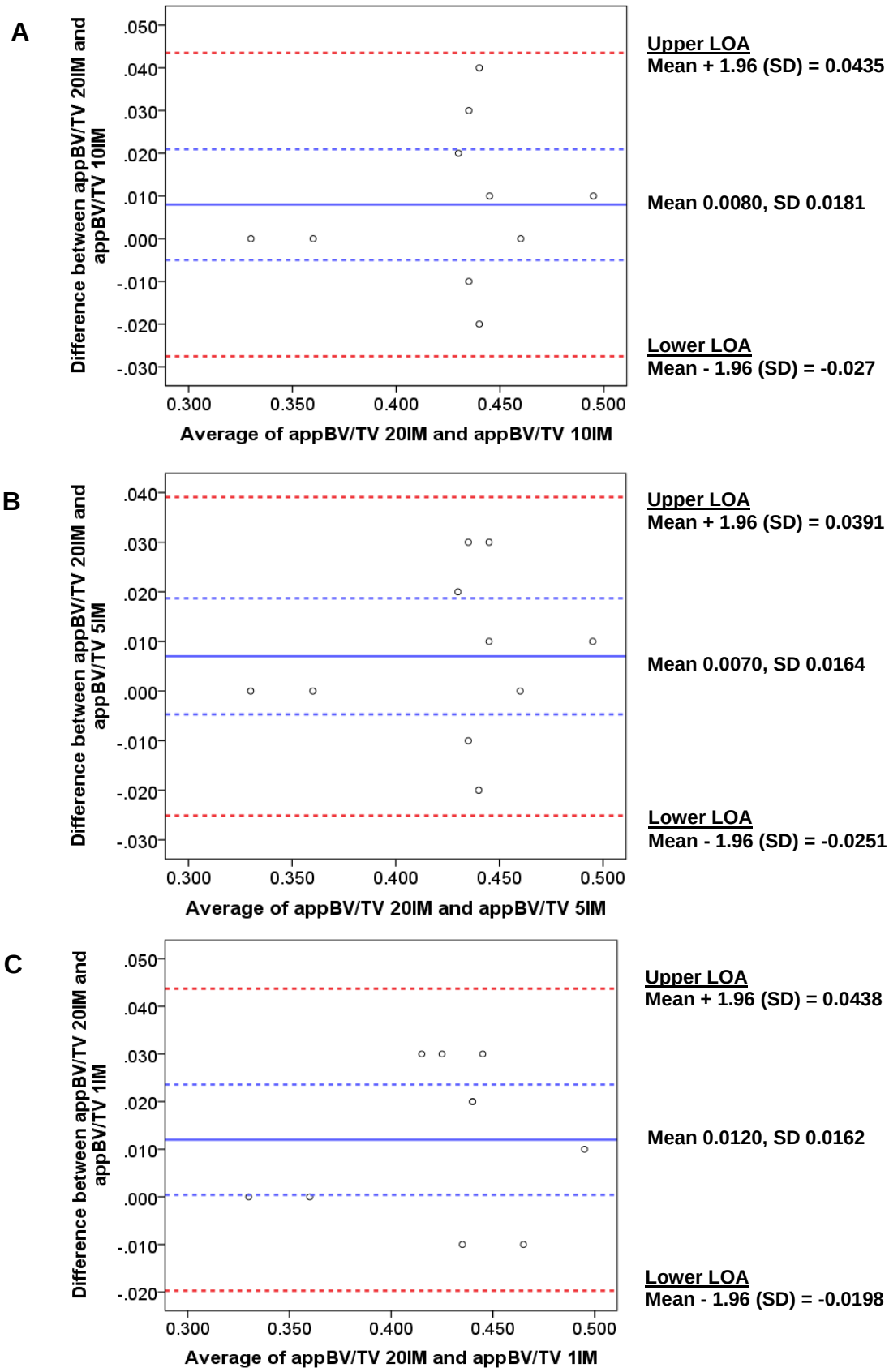

Figure 3.3 The agreement between partial and total image sets estimates of apparent trabecular bone volume/total volume (appBV/TV) in cases with childhood-onset bone abnormalities, using Bland-Altman analysis. Partial image sets of (A) 10 images (10IM), (B) 5 images (5IM) and 1 image (1IM), agreed well with the total image set (20IM), although 1IM had most values dispersed outwith the 95% confidence interval of the mean difference. Mean difference marked with solid blue line whilst upper and lower limits of agreement (LOA) marked with dashed red lines. Dashed blue lines indicate the 95% confidence interval of the mean difference.

3.5 Discussion

Although laborious, this exercise in Chapter 3 has been instrumental in informing the final decision with regards to the minimum number of image slices needed in partial image set analysis to be representative of the total image set. Based on the results, partial image analyses of 10 images, 5 images and even 1 central image only were quantitatively as reliable as analysis of the full image set of 20 images, for both cases and controls. Although remaining within the upper and lower limits of agreement, the values of the differences between 1IM and 20IM were mostly scattered closer to the extremes of the limits with most sitting outwith the 95% confidence interval of the mean difference. This made the partial image analysis of 1IM not ideal.

The principal advantage of using fewer images to assess trabecular bone microarchitecture is a substantial reduction in time for analysis. The time taken to analyse each slice was approximately 1.5 minutes. Therefore, partial image analysis of 5 images vs 20 images reduced the analysis time from approximately 30 minutes to 7.5 minutes per participant. Correspondingly, the analysis time for 10 images were 15 minutes per participant. Given that the partial image analyses for 5 and 10 images corresponded well with the total image analysis of 20 images, it is concluded that partial image analysis of 5 images per participant was the most time-efficient, yet accurate representative of the total image set. The final MRI analyses of Chapter 4 were, therefore conducted with partial image analysis of 5 images per participant as detailed in 2.2.2.3.

The reproducibility of the image analysis method was also studied in this Chapter as the region of interest per image per participant had to be manually drawn each time. Based on the result, the within subject CV compared well for partial and total images analyses. More importantly, the within subject CV between cases and controls were not significantly different. Further sub-analysis of the cases with osteogenesis imperfecta, a more severe osteopathy, demonstrated significantly higher mean CV suggesting that in cases with severe abnormalities of bone health, a larger set of images may need to be analysed to improve precision. This, however, should be interpreted with caution due to the very small sample size (n=4). The very precise nature of bone microarchitecture estimates seen in this Chapter 3, even in individuals who were older, would confidently allow extrapolation for the younger cohort studied in Chapter 4, except for measures of trabecular thickness which was limited by partial volume effect based on the current imaging sequence.

In conclusion, these findings indicate that partial image sets can reliably represent a larger complete set of images when assessing trabecular bone microarchitecture parameters, reducing the overall time taken for image analysis.

4 The Assessment of Bone Health in Children with Established Type 1 Diabetes

4.1 Abstract

To understand the effects of T1D on bone health, 32 affected children at a median (range) age of 13.7 years (10.4, 16.7), were recruited for multimodality assessment of bone health. Serum bone alkaline phosphatase (BAP) and c-terminal telopeptide of type 1 collagen (CTX) as well as DXA total body (TB) and lumbar spine (LS) bone mineral content (BMC) adjusted for bone area were converted to SDS. 3T MRI of the proximal tibia was performed to assess bone volume/total volume (appBV/TV), trabecular number (appTbN) and vertebral bone marrow fat fraction (%) and compared to 26 healthy controls. In T1D, median BAP SDS and CTX SDS were -0.6 (-2.5, +2.1) and -1.1 (-2.5, +0.5) and median TB and LS BMC SDS were -0.1 (-1.1, 0.9) and -0.3 (-1.0, 1.8), respectively. Median appBV/TV in cases and controls was 0.55 (0.47, 0.63) and 0.59 (0.47, 0.63) (p=0.024) and median appTbN was 1.67 (1.56, 1.93) and 1.82 (1.56, 1.99); p=0.004), respectively. The median bone marrow fat fraction in cases and controls was similar at 23% (11, 66) and 20% (8, 61), respectively (p=0.25). Median BAP SDS in T1D cases with HbA1c>75mmol/mol was -0.79 (-2.5, -0.54) compared to 0.5 (-0.64, 2.10) in those with HbA1c<58mmol/mol) (p=0.009). Children who presented in DKA and those treated with insulin via MDI had significantly lower BAP SDS compared to those not in DKA, and those on insulin pump, with p=0.017 and p=0.025 respectively. Fractures were encountered in 10/32 (31%) cases after diagnosis of T1D and in 5/26 (19%) controls (p<0.001). Median HbA1c in those cases with and without fracture was 72mmol/mol (49, 100) and 62mmol/mol (27, 87), respectively (p=0.007) whilst median TB BMC SDS was -0.5 (-1.1, 0.0) and 0.0 (-0.5, +0.9), respectively (p<0.001). There was no significant difference in bone microarchitecture or bone marrow adiposity between these fracture groups. Children with T1D display a low bone turnover state associated with reduced bone mineralisation and poorer bone microarchitecture. Fractures were associated with poorer glycaemic control and bone mineral status.

4.2 Introduction

Adults with T1D have a significantly increased risk of fracture compared to the general population (Vestergaard 2007, Hothersall *et al.* 2014). Indeed, recent studies also confirm that this increased fracture risk affects children and young people with T1D (Weber *et al.* 2015, Vavanikunnel *et al.* 2019). New presentation of T1D peaks between the ages of 9 and 14 years (Scottish Diabetes Survery Monitoring Group NHS Scotland 2014, Health Quality Improvement Partnership and Royal College of Paediatrics and Child Health 2015) and given that childhood and adolescence are important physiological periods for optimal bone development (Baxter-Jones *et al.* 2011), it is possible that these young people with T1D may be especially susceptible to abnormalities of bone health.

Earlier studies suggested that the deficit in bone mass in T1D may be present quite early on, with evidence of osteopenia as early as two years after the diagnosis (McNair *et al.* 1978, Gunczler *et al.* 1998, Gunczler *et al.* 2001). Children with T1D have also been reported to have lower lumbar spine bone mineral density (BMD) within the first few months of diagnosis (Gunczler *et al.* 2001). This reduction worsens in children with disease duration of more than three months but stabilises with no further correlation between longer disease duration and BMD, suggesting that there may be a degree of reversibility in the process. It is unclear whether the duration of the condition or any other clinical parameters of diabetes or its control are associated with adverse skeletal morbidity. As the significantly increased fracture risk is disproportionate to the marginal reduction in bone mineral density in adults with T1D (Vestergaard *et al.* 2007), there is an increasing realisation that a comprehensive assessment of bone requires an assessment of bone microarchitecture as well as bone densitometry (McComb *et al.* 2014b).

Metabolic conditions that may affect bone health, such as diabetes, are also associated with marked alterations in body composition, adiposity and bone marrow adiposity (Baum *et al.* 2012, Patsch *et al.* 2013b, Sheu *et al.* 2017). Glycaemic control in diabetes has been shown to be positively related to lumbar spine marrow adiposity (Baum *et al.* 2012, Yu *et al.* 2017). MRI with its ability to study microarchitecture as well as bone marrow adiposity promises to be a useful imaging modality. Indeed, recent MRI-based studies in young women with childhood-onset T1D revealed a deficit in trabecular bone microarchitecture (Abdalrahaman *et al.* 2015). The current study was performed to better understand the effects of T1D on bone health in children, and specifically to determine whether these MRI-based findings in trabecular bone microarchitecture were present at an earlier age in children with T1D. The

detailed multimodality analysis of bone health performed in these children also provided a mechanistic insight into the effect of diabetes on the developing skeleton.

4.3 Methods

4.3.1 Subjects

Children and adolescents aged between 10-18 years old with T1D for at least three years were recruited from the Paediatric Diabetes Service at the Royal Hospital for Children, Glasgow during the period August 2014 and January 2016. The diagnosis of T1D was based on clinical presentation and ongoing insulin requirement with autoantibody confirmation in uncertain cases. For the MRI-based studies, age and sex-matched children and adolescents without T1D were recruited from general paediatric clinics, siblings of the index cases and children of staff members to provide a reference group. Exclusion criteria included other chronic diseases or medications known to affect bone health and children with metallic implants and pacemakers incompatible with MRI. Children with autoimmune conditions such as hypothyroidism and Coeliac disease were included if they had good compliance with the respective treatments as determined biochemically.

4.3.2 Design

Information on personal health, medication history and lifestyle habits, including dairy intake, use of vitamins or calcium supplementation, cigarette smoking, and a family history of early osteoporosis was collected. History of fractures was also ascertained, and only those radiologically-confirmed (sustained after diagnosis of T1D) were included. Age-appropriate questionaires were used to collect information on level of physical activity (Kowalski *et al.* 1997a, Kowalski *et al.* 1997b). In children with T1D, additional information was also collected on age at diagnosis, severity of initial presentation, disease duration, glycaemic control, as measured by glycosylated haemoglobin (HbA1c) over the last 12 months, and presence of microvascular complications. Glycaemic control was categorised as good (HbA1c <7.5% or <58 mmol/mol), moderate (HbA1c 7.5-9.0% or 58-75mmol/mol) or poor (HbA1c >9.0% or >75mmol/mol) (Rewers *et al.* 2009). Children with T1D had assessments of bone biochemical markers, DXA, MRI and MRS whilst healthy controls only underwent MRI and MRS. The study protocol was approved by the West of Scotland Research Ethics Committee and informed consent was obtained from the study participants.

4.3.3 Anthropometry and puberty staging

All children had height measured using a stadiometer without footwear and weighed barefooted with only light clothing on. Age- and sex-adjusted Z scores for height, weight and BMI were calculated using the LMS method based on UK population reference data (Cole 1990). Puberty assessment was undertaken and categorised according to Tanner stages for girls and boys, with the additional option of self-assessment in those who did not want to be examined (Morris and Udry 1980). For analysis, pubertal status was defined by genital status in male and breast development in female. Based on the assessment, all children were categorised into pre-pubertal (Tanner Stage 1), early puberty (Tanner Stage 2 and 3) and late puberty (Tanner Stage 4 and 5).

4.3.4 Biochemical Markers of Bone Metabolism & GH/IGF-1 Axis

In all 32 cases, non-fasting blood samples were collected in the morning to coincide with clinic visit, centrifuged and the supernatant stored at -80^0C. Details of the specific assays are as described in Chapter 2. Markers of bone formation (bone alkaline phosphatase [BAP], osteocalcin [OC]), bone resorption (C terminal telopeptide of Type I collagen [CTX]), adiposity (pre-adipocyte factor-1 [PREF-1]), growth hormone axis (IGF-1, IGFBP-3, the acid labile subunit [ALS]), sclerostin and other regulator markers of bone turnover (PTH, AP, 25-Hydroxy-vitamin D [25OHD]) were measured.

4.3.5 Dual energy X-ray Absorptiometry (DXA)

Lumbar spine (LS, L2-L4) and total body (TB) measurements were acquired by a Lunar Prodigy densitometer (GE Medical Systems, Waukesha, Wisconsin, USA) and analysed using Encore software (Version 13.0). Details of the image acquisition and analysis are as described in Chapter 2. As outlined in previous studies, reference data were used to calculate a predicted and a percentage predicted bone area (BA) for age and sex (Warner *et al.* 1998, Ahmed *et al.* 2004). The reference data allowed for a comparison of the actual bone mineral content (BMC) of the individual with the predicted BMC of a subject of the same sex and bone area from which the percentage predicted BMC (ppBMC), expressed as an SDS (BMC SDS) could be calculated. The coefficient of variation (%CV) calculated on repeated DXA measurement of a phantom was <1% of BMC and the *in vivo* %CV was <2.5%. DXA was also used to perform thoracolumbar vertebral fracture assessment, as previously described (Kyriakou *et al.* 2016).

4.3.6 Magnetic Resonance Imaging (MRI) Assessment of Microarchitecture

All 32 children with T1D and 26 healthy controls were scanned. Twenty slice images were acquired at the proximal tibia using a 3T Siemens MAGNETOM Prisma MRI scanner (Siemens, Erlangen, Germany) and analysed using MATLAB software (Mathworks Inc, San Mateo, CA, USA) to obtain measures for apparent bone volume ratio (appBV/TV), apparent trabecular number (appTbN), apparent trabecular thickness (appTbTh), and apparent trabecular separation (appTbSp). Details of the image acquisition and analysis are as described in Chapter 2. The repeatability of microMRI is high with an average CV of 1%. The images were of sufficiently good quality to be analysed in 30 of the 32 cases and in all 26 control participants.

4.3.7 Magnetic Resonance Spectroscopy (MRS) Assessment of Bone Marrow Adiposity

All 32 children with T1D and 22 healthy controls were scanned. 1H-MRS was performed using an 18-channel body array (anterior) and a 32-channel spine coil (posterior) to acquire images at the lumbar spine (L3) position. Analysis was performed using the Java-based magnetic resonance user interface (jMRUI) software to calculate the percentage fat fraction (%FF) within the bone marrow as a measure of bone marrow adiposity (Schellinger *et al.* 2004). Details of the image acquisition and analysis are as described in Chapter 2. The repeatability of MRS is also high with an average CV of 2.5%. The images were of sufficiently good quality to be analysed in 29 of 32 children with T1D and 21 of 22 healthy controls.

4.3.8 Sample Size Calculation and Statistical Analyses

The primary hypothesis was that children with T1D would have a lower appBV/TV compared to healthy children. The estimated coefficient of variation (CV) for appBV/TV was less than 5% in our previous work (McComb *et al.* 2014b, Abdalrahaman *et al.* 2015) and based on this a 7.5% difference at $p<0.05$ with a power of 0.8 would require at least 25 subjects in each arm.

Data were analysed using IBM SPSS software (Version 22, SPSS, Chicago, IL, USA) and described as medians (ranges). Group differences between cases and controls were initially compared by Mann-Whitney test for continuous variables and Chi-square test for categorical

variables, and then adjusted for multiple testing using false discovery rates (FDR). Specifically, biochemical markers of bone turnover and DXA parameters were compared against 0, using the above tests depending on the variables. Spearman's rank correlation co-efficient was used to assess the association between variables. Further analysis was performed to compare the characteristics of those children with T1D with a history of fractures with those without fractures. Factors significant on univariate analysis (HbA1c, TB BMC and physical activity score) were included in a multivariate logistic regression for comparison between the fracture and non-fracture groups. All continuous data were presented as median (ranges) with $p<0.05$ considered as significant, unless otherwise specified.

4.4 Results

4.4.1 Clinical characteristics

Thirty-two children with T1D, median (range) age 13.7 years (10.4, 16.7), were recruited (16 boys) (Table 4.1). The median age at diagnosis was 5.9 years (1.3, 10.8) and median duration of disease was 7.2 years (3.1, 12.4). The median average HbA1c in the preceeding 12 months was 8.1% (4.6, 11.3) or 65mmol/mol (27, 100); glycaemic control was good in seven, moderate in 19 and poor in six. Of the 32 children, 3 were pre-pubertal, 17 in early puberty (Tanner stages 2 and 3) and 12 in late puberty (Tanner stages 4 and 5). Ten presented with diabetic ketoacidosis (DKA) at the time of diagnosis. The median insulin dose was 1.0unit/kg/day (0.6, 1.8) with 10 out of 32 on continuous subcutaneous insulin infusion (CSII) via pump. Of the 24 eligible children with T1D, 16 had undergone retinopathy screening and 19 had assessment of microalbuminuria. Mild background retinopathy was present in 3 (19%) and microalbuminuria was absent in all.

4.4.2 Bone Metabolism & GH/IGF-1 Axis

Children with T1D had reduced BAP SDS -0.57 (-2.50, 2.10), with median absolute value 59.2mcg/L (14.4, 118.5) (Table 4.2). Those with poor control had a lower BAP SDS of -0.79 (-2.5, -0.54) compared to 0.50 (-0.64, 2.10) for children with good glycaemic control ($p=0.009$) and -0.62 (-1.62, 1.11) for children with moderate control ($p=0.03$) (Figure 4.1A). Serum osteocalcin did not show any relationship to glycaemic control, age or duration of diagnosis. Although median CTX SDS was also reduced compared to controls ($p<0.001$) (Table 4.2) this did not show the same relationship to glycaemic control as BAP ($p=0.954$) (Figure 4.1C). However, median CTX SDS (r, -0.44, $p=0.012$) and sclerostin were inversely

related to age of diagnosis (*r*, -0.38, *p*=0.038) (Figure 4.1D and Figure 4.1F). Although serum IGF-1 was not significantly lower in children with T1D, the latter had a lower ALS SDS ($p<0.001$) and a higher IGFBP-3 SDS ($p<0.001$) (Table 4.2). Children with T1D who were in DKA at initial presentation had significantly lower BAP SDS than those who were not acidotic ($p<0.017$) (Figure 4.2A). Further hospital admissions with DKA subsequent to the initial presentation, however, did not appear to have an effect on BAP ($p=0.734$) (Figure 4.2B). The T1D children on continuous subcutaneous insulin infusion (CSII; pump therapy), did not only have significantly lower HbA1c ($p=0.005$) and lower daily insulin requirement for weight ($p=0.04$), but also had higher BAP SDS ($p=0.025$) compared to those on MDI (Figure 4.2C-E).

Table 4.1 Clinical characteristics of the whole cohort, with sub-categories of children with T1D based on glycemic control as per HbA1c

	Whole Cohort			T1D Cases Based on Glycemic control (HbA1c)			
	T1D (n=32)	**Control (n=26)**	***p***	**Good (n=6)**	**Moderate (n=20)**	**Poor (n=6)**	***p***
Age (years)	13.7 (10.4,16.7)	13.8 (10.2,17.8)	0.994	12.3 (11.5,16.4)	13.8 (10.7,16.7)	13.1 (10.4,16.4)	0.633
Gender (M/F)	16/16	13/13	0.999	3/3	8/12	6/0	**0.031**
Height SDS	0.3 (-1.5,2.5)	-0.1 (-1.6,2.7)	0.173	0.3 (-0.8,1.3)	0.7 (-1.5,2.5)	0.2 (-1.4,1.2)	0.479
Weight SDS	0.8 (-1.3,3.2)	0.6 (-1.2, 3.1)	0.569	0.2 (-0.4,0.5)	1.0 (-0.4,3.2)	0.5 (-1.3,2.4)	0.119
BMI SDS	0.5 (-0.6,2.9)	1.0 (-1.6,2.7)	0.798	-0.1 (-0.2,0.0)	1.0 (-0.6,2.4)	0.5(-0.6,2.9)	0.084
Tanner stage (Pre/Early/Late) (n)	3/17/12	4/13/9	0.831	1/4/1	2/11/7	0/3/3	0.758
Age at diagnosis (yr)	5.9 (1.3,10.8)			6.3 (4.2,10.3)	5.5 (1.3,10.8)	6.2 (3.7,10.8)	0.810
Disease duration (yr)	7.2 (3.1,12.4)			7.3 (3.1,10.1)	7.3 (3.1,12.3)	6.7 (3.1,9.6)	0.639
HbA1c average in last 12m (%)	8.1 (4.6,11.3)			7.0 (6.6,7.3)	8.1 (7.5,8.9)	10.0 (9.2,11.3)	**<0.001**
HbA1c average in last 12m (mmol/mol)	65 (27,100)			53 (49,56)	65 (58,74)	86 (77,100)	**<0.001**
HbA1c at diagnosis (%)	10.7 (7.3,17.2)[a]			9.5 (7.3,9.9)	11.1 (7.9,17.2)	9.6 (8.8,12.1)	0.069
HbA1c at diagnosis (mmol/mol)	93 (56,164)[a]			80 (56,85)	98 (63,164)	81 (73,109)	0.069
DKA at initial presentation (Y/N) (n=31)	21/10			0/5	7/12[d]	3/3	0.187
Insulin dose (unit/kg/day)	1.0 (0.6,1.8)[b]			0.89 (0.60,1.03)	1.03 (0.73,1.50)	1.6 (1.24,1.81)	**<0.001**
Insulin pump/injections	10/22			6/0	5/15	0/6	**0.001**
25-OH Vitamin D (nmol/L)	48 (18,75)			53 (48,60)	47 (18,70)	51 (39,75)	0.283
Physical activity score	2.4 (1.3,4.1)	2.5 (1.6,4.1)[c]	0.425	2.0 (1.4,3.7)	2.4 (1.6,3.5)	3.0 (1.3,4.1)	0.361
Previous fracture(s)(Y/N)	10/22	5/21	**<0.001**	1/5	5/15	4/2	0.130

Values are presented as median (range). [a] n=25, [b] n=27, [c] n=24, [d] n=19

The median 25-OH vitamin D level was 48nmol/L (18, 75) and PTH 3.6mmol/L (1.5, 6.6) in the children with T1D. There were no intergroup differences in 25-OH vitamin D levels in the children with [47nmol/L (25,70)] and without [49nmol/L (18,75)] DKA at initial presentation (p=0.555) or the children on continuous subcutaneous insulin infusion (CSII; pump therapy) [49nmol/L (37,60)] compared to those on multiple daily injections (MDI) [47nmol/L (18,75)] of insulin (p=0.602).

4.4.3 Bone Densitometry by DXA

Median BMC SDS for TB and LS was marginally but significantly lower than 0 at -0.1 (-1.1, 0.9) and -0.3 (-1.0, 1.8), respectively (Table 4.2). TB and LS BMC SDS did not show any correlation to glycaemic control (p=0.236, p=0.256, respectively), age at diagnosis (p=0.235, p=0.896), or disease duration (p=0.956, p=0.757). TB and LS BMC SDS were also not significantly different whether the children were acidotic or not at initial presentation (p=0.145 and p=0.260 respectively) (Figure 4.3A, B, D-F). TB BMC SDS, however, was inversely related to CTX SDS (r, -0.5, p=0.003) (Figure 4.3C).

4.4.4 Bone microarchitecture by MRI

Comparison of bone microarchitecture variables revealed that appBV/TV and appTbN were significantly lower and appTbSp higher in T1D children than healthy controls (Table 4.2, Figure 4.4A, C-D). Serum ALS showed an inverse association to appBV/TV (r, -0.54, p=0.002), appTbTh (r, -0.42, p=0.02) and appTbSp (r, 0.46, p=0.01) in the T1D children; however, removal of two cases with high values of ALS SDS resulted in an absence of this association except for appBV/TV where an inverse association was still present at r, -0.44 (p=0.02) (Figure 4.5Figure 4.4A). In the T1D cases, there was no association of appBV/TV, appTbN, or app TbSp with HbA1c, age at diagnosis or duration of T1D. The bone microarchitecture parameters were also not significantly different whether the children were acidotic at the time of presentation for appBV/TV, appTbTh, appTbN, or app TbSp with p=0.795, p-0.962, p=0.620, p=0.925 respectively. However, daily insulin dose corrected for weight were positively associated with TbN (r= 0.41, p=0.036) (Figure 4.5B). There was no evidence of an association between any of the bone microarchitecture variables and BMC SDS for TB or LS.

Table 4.2 Biochemical markers, DXA and MRI-based Measures of Bone Microarchitecture and Vertebral Bone Marrow Adiposity

Parameters	T1D (n=32)	Controls (n=26)	*p*
Biochemical markers			
25-OH Vitamin D (nmol/L)	48 (18,75)[a]		
PTH (mmol/L)	3.6 (1.5,6.6)[a]		
Sclerostin (ng/ml)	0.22 (0.01,0.7)		
Osteocalcin (ng/ml)	56.5 (13.9,262.8)		
BAP SDS	-0.57 (-2.50,2.10)		**0.002**[c]
CTX SDS	-1.05 (-2.49,0.51)		**<0.001**[c]
IGF-1 SDS	-0.24 (-3.64,1.48)		0.364[c]
IGFBP3 SDS	1.66 (0.13,3.81)		**<0.001**[c]
ALS SDS	-0.70 (-1.67,0.76)		**<0.001**[c]
DXA			
TB BMC for BA SDS	-0.1 (-1.1,0.9)		**0.018**[c]
LS BMC for BA SDS	-0.3 (-1.0,1.8)		**0.011**[c]
MRI			
appBV/TV	0.55 (0.47,0.63)[a]	0.59 (0.47,0.63)	**0.024**
appTbN (mm^{-1})	1.67 (1.56,1.93)[a]	1.82 (1.56,1.99)	**0.004**
appTbSp (mm)	0.27 (0.21,0.32)[a]	0.24 (0.20,0.33)	**0.001**
appTbTh (mm)	0.32 (0.27,0.39)[a]	0.32 (0.25,0.38)	0.954
Marrow FF (%)	23.1 (11.0,66.0)[b]	20.0 (8.0,61.1)	0.250

Values are presented as median (range). PTH = parathyroid hormone, BAP = bone alkaline phosphatase, CTX = c-terminal telopeptide of collagen 1, IGF = insulin-like growth factor, IGFBP = insulin-like growth factor binding protein, ALS = acid labile subunit, DXA = dual energy xray absorptiometry, TB = total body, LS = lumbar spine, BMC = bone mineral content, BA = bone area, SDS = standard deviation score, MRI = magnetic resonance imaging, appBV/TV = apparent bone volume to total volume, appTbN = apparent trabecular number, appTbSp = apparent trabecular separation, appTbTh = apparent trabecular thickness. FF = fat fraction.

[a] n=30, [b] n=29, [c] compared to 0

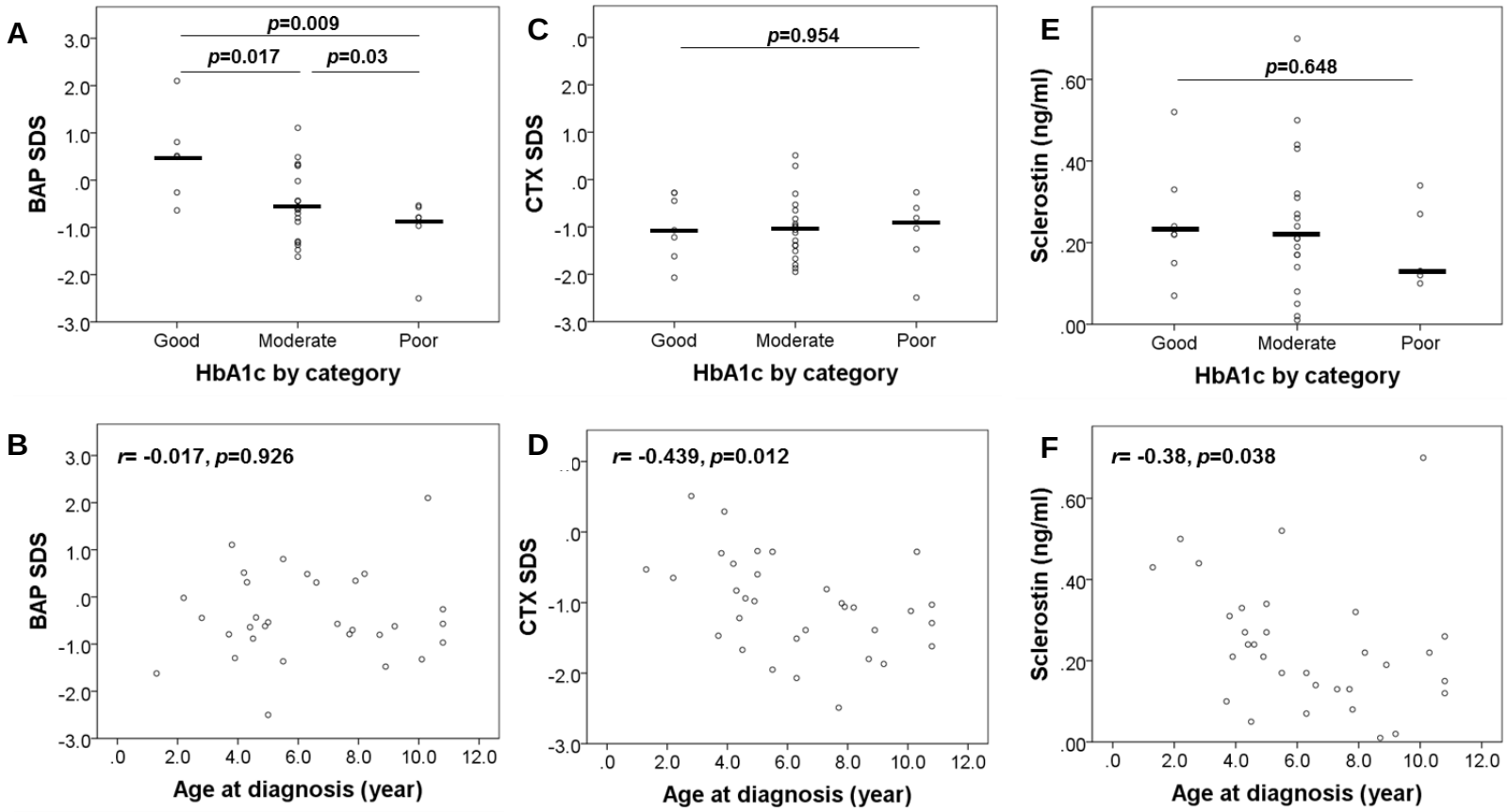

Figure 4.1 The relationships between T1D disease characteristics and markers of bone turnover (as assessed by bone formation marker BAP, bone resorption marker CTX and sclerostin). Children with poor glycaemic control had significantly lower bone formation marker compared to children with moderate and good controls. Children diagnosed younger with T1D had significantly higher bone resorption and sclerostin levels.

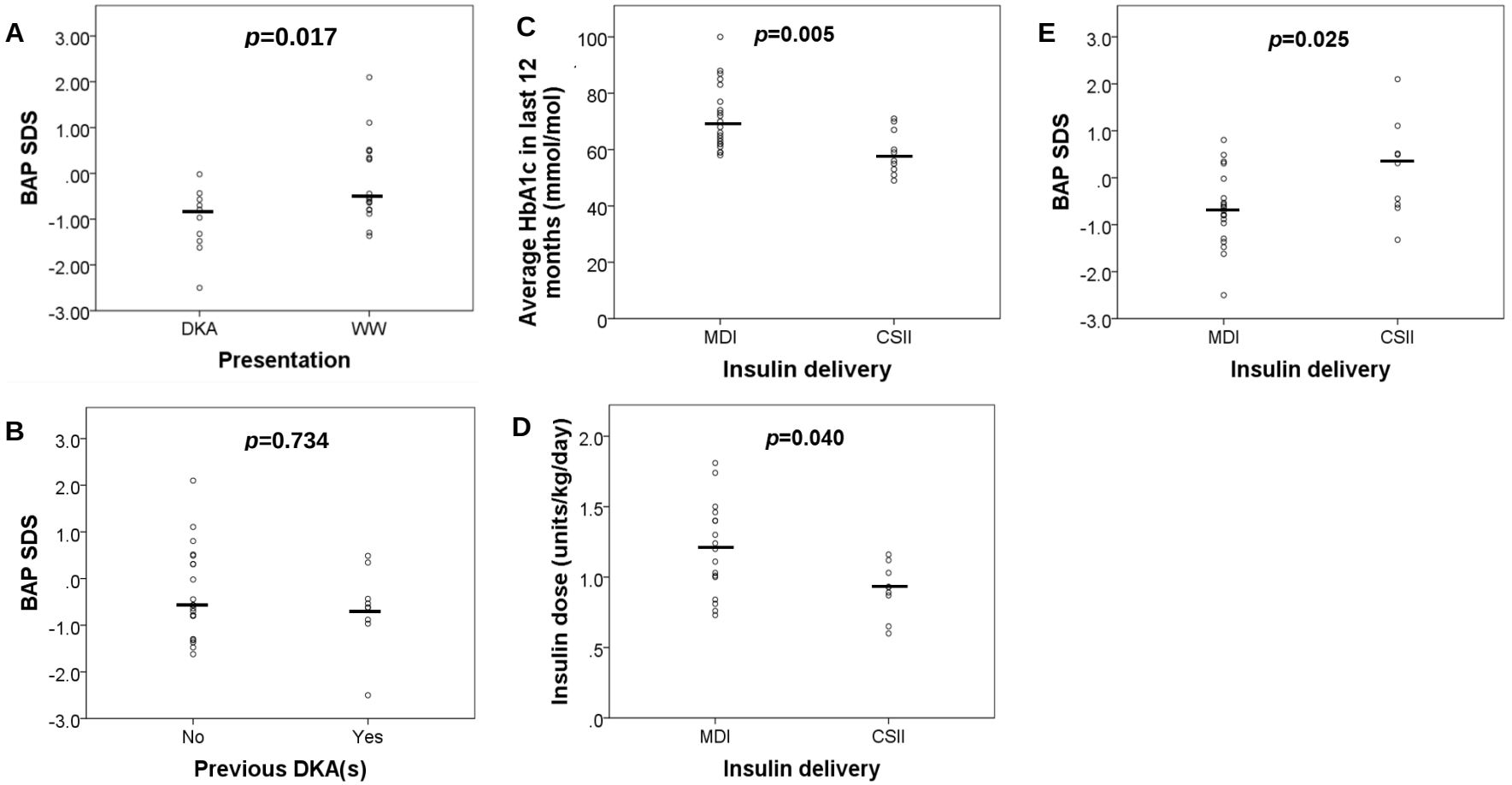

Figure 4.2 The relationships between acidosis (DKA) and methods of insulin delivery (MDI vs CSII) and T1D disease characteristics, bone formation marker (BAP) and bone density (as assessed by DXA). Children with T1D who were acidotic at initial presentation had significantly lower BAP SDS than those who were not acidotic (A). This relationship did not stand with total number of acidotic events requiring hospital attendance (B). Children with insulin delivered by CSII (pump) did not only have lower HbA1c (C) and lower total daily insulin dose (D), but also has higher bone formation marker (E). [DKA=diabetic ketoacidosis, WW- Walking wounded, or non-DKA, MDI=multiple daily injection, CSII (continuous subcutaneous insulin infusion, DXA=dual x-ray absorptiometry, BAP=bone alkaline phosphate

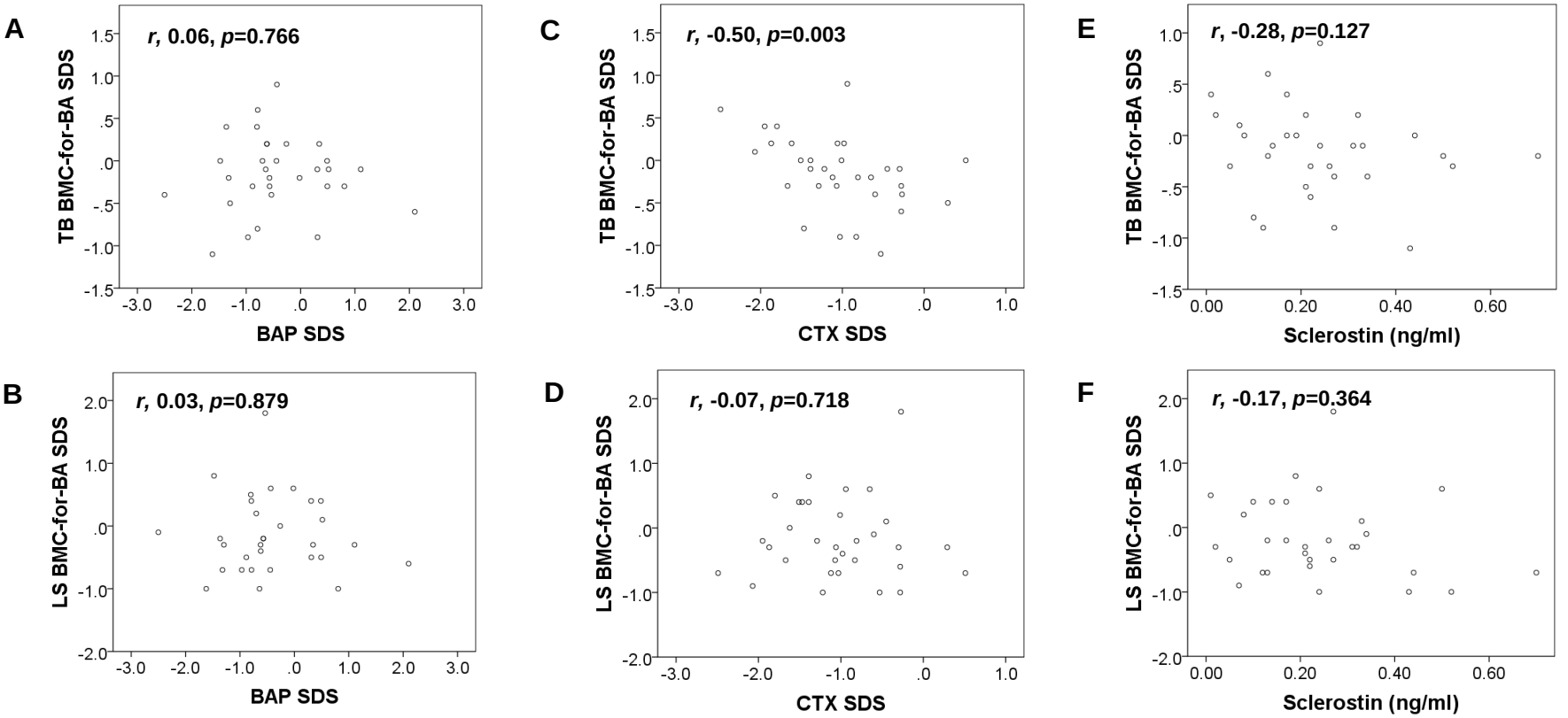

Figure 4.3 The relationships between bone mineral density status (as assessed by DXA) and markers of bone turnover (as assessed by bone formation marker BAP, bone resorption marker CTX and sclerostin) in children with T1D. TB BMC SDS was inversely related to CTX SDS. [BAP bone alkaline phosphatise; CTX c-terminal telopeptide of type 1 collagen]

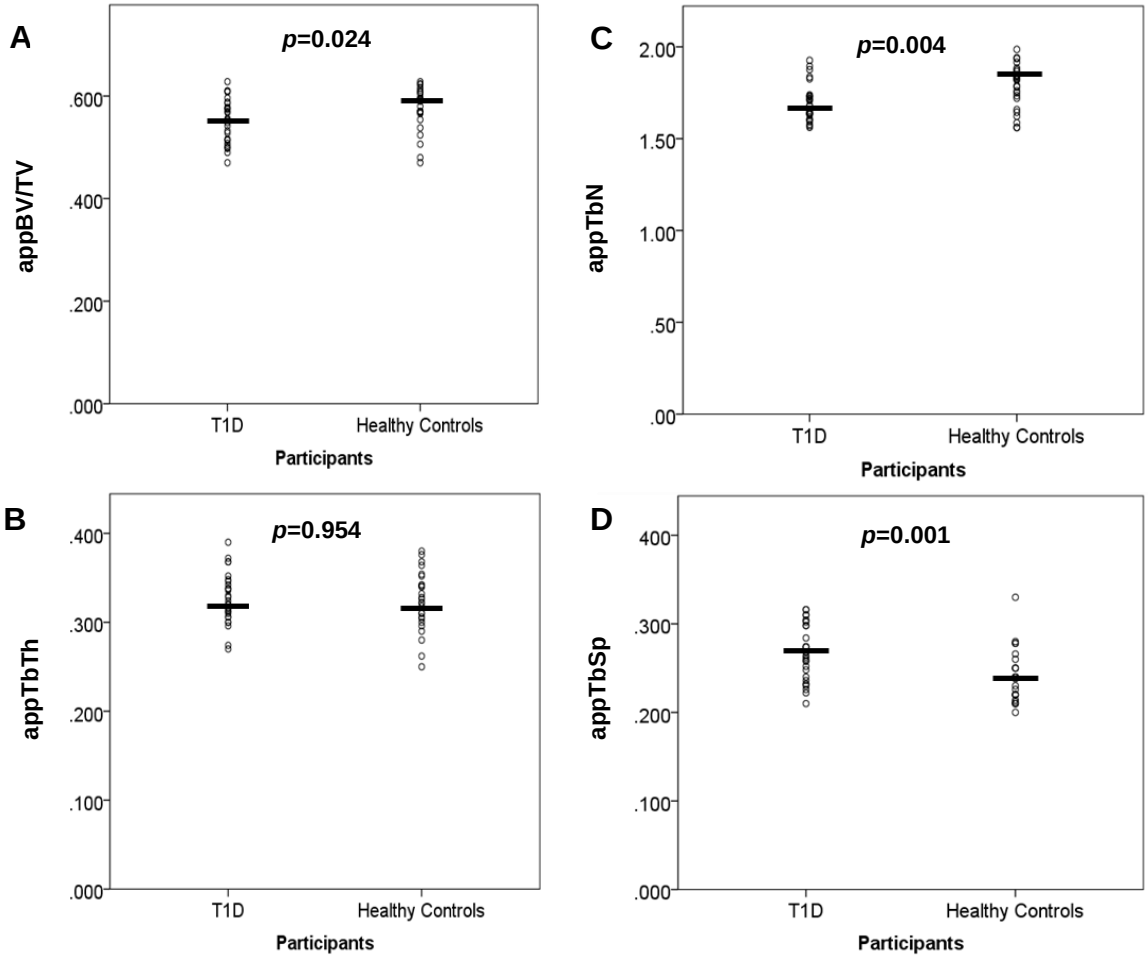

Figure 4.4 Bone microarchitecture parameters comparing children with T1D and healthy controls. Children with T1D have significantly altered bone microarchitecture, including (A) lower bone volume to total volume, (C)lower trabecular number and (D) higher trabecular separation. [appBV/TV=apparent bone volume to total volume, appTbTh=apparent trabecular thickness, appTbN=apparent trabecular number, appTbSp=apparent trabecular separation

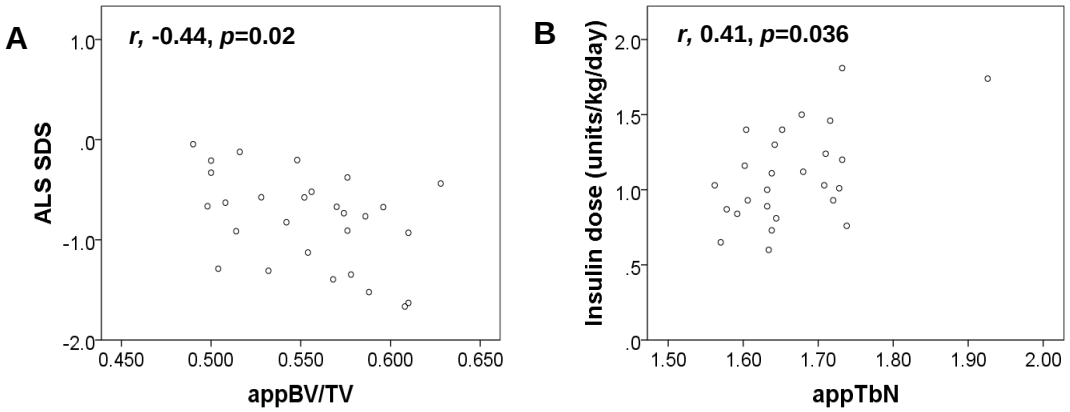

Figure 4.5 The relationships between bone microarchitecture parameters with markers of GH/IGF-1 axis and insulin dose in children with T1D. Serum ALS was inversely associated with appBV/TV whilst insulin dose is positively associated with appTbN. [ALS=acid labile subunit, appBV/TV= apparent bone volume to total volume, appTbN=apparent trabecular number]

4.4.5 Bone Marrow Adiposity by MRI

Median vertebral bone marrow adiposity, expressed as percentage fat fraction (%FF), was higher in cases than controls, but this did not reach statistically significant difference (Table 4.2,Figure 4.6). In the cases, there was no association between %FF and markers of GH/IGF-1 axis or bone turnover, BMC SDS for TB or LS. Combined analysis of the cases and controls showed an inverse association between %FF and appTbN (r, -0.40, p=0.004) and a positive association with appTbSp (r, 0.33, p=0.021) (Figure 4.7).

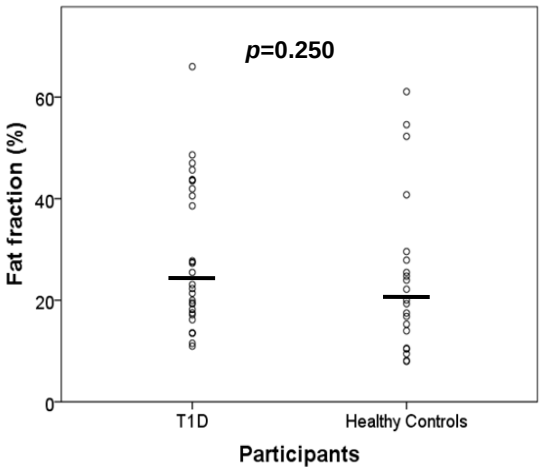

Figure 4.6 Vertebral bone marrow adiposity, expressed in fat fraction % in T1D children and healthy controls. Children with T1D had higher fat fraction compared to healthy controls, although this did not reach statistical significance.

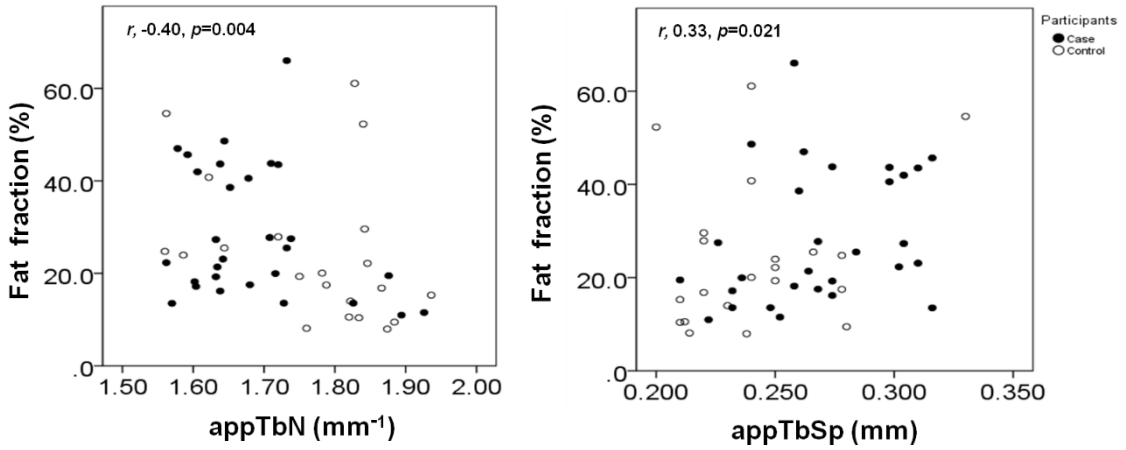

Figure 4.7 The relationships between percentage fat fraction (%FF) and bone microarchitecture parameters in the whole cohort. %FF is inversely associated with trabecular number and positively associated with trabecular separation.

4.4.6 Fracture data

Children with T1D were significantly more likely to fracture compared to healthy controls (p<0.001) (Table 4.1). Of the 32 children with T1D, 10 (31%) had radiologically confirmed fracture following the diagnosis of T1D, as summarised in Table 4.3. Two out of these 10 sustained a lower extremity fracture (lower leg/ankle, or foot), whilst the rest had upper extremity limb fractures (humerus, elbow, forearm, hand). The children with lower extremity fractures were younger when diagnosed with T1D. None of the children had any abnormalities identified on vertebral fracture assessment by DXA.

The clinical characteristics of the fracture and non-fracture group were comparable for age, gender, puberty, anthropometric measurements, insulin doses and delivery systems (Table 4.4). The median age of diagnosis was 4.4 years (1.3, 10.8) in the fracture group and 6.5 years (3.8, 10.8) in the non-fracture group, although this did not reach statistical significance between groups (p=0.077) (Figure 4.8A, Table 4.4). The median duration of disease was 8.6 years (3,1,12.4) in the fracture group and 7.0 years (3.1,10.9) in the non-fracture group (p=0.204). The median HbA1c was higher in the fracture group at 8.7% (6.6, 11.3) or 72mmol/mol (49, 100) compared to the non-fracture group of 7.8% (4.6, 10.1) or 62mmol/mol (27, 87) (p=0.005 and p=0.007 respectively) (Table 4.4, Figure 4.8B).

Table 4.3 Age, distribution, sites of fracture and the events preceeding in the fracture cohort

Age at diagnosis (year)	Sex	Age at fracture (year)	Duration of disease to fracture time (year)	Fracture distribution (UL/LL/Other)	Site of Fracture	Event preceding fracture
1.3	M	12.3	11.0	LL	Left tibia + metatarsals	Hyperextension injury during football
		13.1	11.8	LL	Left calcaneum	Fell off skateboard at low speed
		13.2	11.9	UL	Left 5th proximal phalange	Hyperextension injury during football
2.2	F	4.9	2.7	LL	Right fibula	Fell in park from standing height
		6.1	4.5	UL	Left supracondyle	Fell off motorcycle with protective gear
2.8	M	5.9	3.1	Other	Right clavicle	Fell in park from standing height
3.7	M	6.4	2.7	UL	Left radius and ulnar	Fell on outstretched hand
4.3	M	10.9	6.6	UL	Right radius and ulnar	Fell in school from standing height
4.5	F	7.4	2.9	UL	Right radius	Trip over schoolbag
5.0	M	8.1	3.1	UL	Left supracondyle	Fell onto left side from standing height
7.3	M	10.4	3.1	UL	Left radius	Slipped and fell during football
		12.0	4.7	UL	Left radius	Hyperextension injury during football
10.3	F	11.5	1.2	UL	Left radius	Fell on outstretched hand
10.8	M	11.2	0.4	UL	Left scaphoid	Fell on outstretched hand
		11.8	1.0	UL	Left humeral supracondyle	Fell off bicycle

M = Male, F = Female, UL = upper limb, LL = lower limb

Table 4.4 Clinical characteristics of all children with T1D by sub-categories of fracture and non-fracture

Parameters	No Fracture (n=22)	Fracture (n=10)	*p*
Age (years)	13.5 (10.7,16.7)	13.8 (10.4,16.4)	0.920
Gender (M/F)	9/13	7/3	0.127
Height SDS	0.3 (-1.5,2.5)	0.4 (-1.4,2.1)	0.795
Weight SDS	0.8 (-0.4,2.4)	0.5 (-1.3,3.2)	0.366
BMI SDS	0.6 (-0.6,2.9)	0.5 (-0.6,2.4)	0.411
Tanner stage (Pre/Early/Late) (n)	3/10/9	0/7/3	0.316
Age at diagnosis (yr)	6.5 (3.8,10.8)	4.4 (1.3,10.8)	0.077
Disease duration (yr)	7.0 (3.1,10.9)	8.6 (3.1,12.4)	0.204
HbA1c average in last 12m (%)	7.8 (4.6,10.1)	8.7 (6.6,11.3)	**0.005**
HbA1c average in last 12m (mmol/mol)	62 (27,87)	72 (49,100)	**0.007**
HbA1c at diagnosis (%)	10.8 (7.3,17.2)	10.3 (8.8,13.3)	0.574
HbA1c at diagnosis (mmol/mol)	95 (56,164)	89 (73,122)	0.574
Severity at diagnosis - Not DKA/DKA/unknown (n)	14/7/1	6/4/0	0.740
Insulin dose (unit/kg/day)	1.0 (0.6,1.8)	1.2 (0.8,1.7)	0.264
Insulin pump/injections	7/15	3/7	0.921
TB BMC for BA SDS	0.0 (-0.5,0.9)	-0.5 (-1.1,0.0)	**<0.001**
LS BMC for BA SDS	-0.3 (-1.0,0.8)	-0.5 (-1.0,1.8)	0.617
25-OH Vitamin D (nmol/L)	48 (18,70)	47 (25,75)	0.884
PTH (mmol/L)	3.7 (1.8,6.6)	3.4 (1.5,5.7)	0.475
Sclerostin (ng/ml)	0.21 (0.01,0.70)	0.25 (0.05,0.50)	0.734
Osteocalcin (ng/ml)	44.3 (16.1,204.4)	60.6 (13.9,262.8)	0.190
BAP SDS	-0.62 (-2.50,1.11)	-0.55 (-1.62,2.10)	0.764
CTX SDS	-1.17 (-2.49,0.29)	-0.73 (-1.67,0.51)	**0.047**
IGF-1 SDS	-0.30 (-3.64,1.14)	-0.06 (-2.33,1.48)	0.734
IGFBP-3 SDS	1.78 (0.13,3.81)	1.37 (0.16,3.26)	0.952
ALS SDS	-0.67 (-1.67,0.76)	-0.79 (-1.63,-0.12)	0.434
Physical activity score	2.2 (1.3,3.7)	2.8 (1.7,4.1)	**0.043**
appBV/TV	0.55 (0.47,0.63)	0.54 (0.50,0.61)	0.571
appTbN (mm^{-1})	1.71 (1.56,1.93)	1.64 (1.57,1.84)	0.512
appTbSp (mm)	0.26 (0.21,0.32)	0.27 (0.23,0.32)	0.389
appTbTh (mm)	0.32 (0.27,0.39)	0.32 (0.27,0.37)	0.587
%FF	26.4 (13.5,66)	20.0 (11.0,45.7)	0.451

Values are presented as median (range). PTH = parathyroid hormone, BAP = bone alkaline phosphatase, CTX = c-terminal telopeptide of collagen 1, IGF = insulin-like growth factor, IGFBP = insulin-like growth factor binding protein, ALS = acid labile subunit, DXA = dual energy xray absorptiometry, TB = total body, LS = lumbar spine, BMC = bone mineral content, BA = bone area, SDS = standard deviation score, MRI = magnetic resonance imaging, appBV/TV = apparent bone volume to total volume, appTbN = apparent trabecular number, appTbSp = apparent trabecular separation, appTbTh = apparent trabecular thickness. FF = fat fraction.

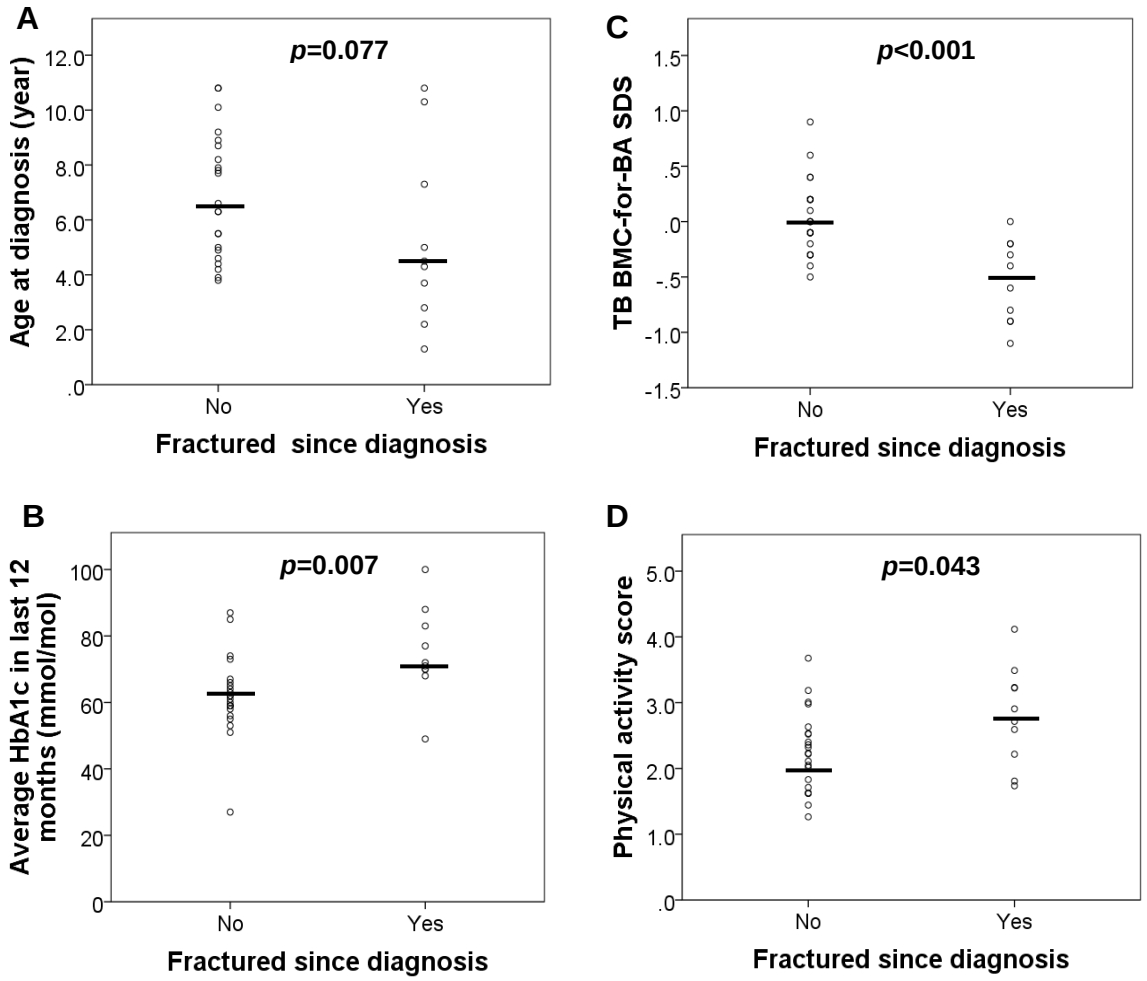

Figure 4.8 Sub-analysis of children with T1D depending on fracture status. Children with T1D who fractured had poorer glycaemic control (with higher HbA1c) and lower TB BMC-for-BA SDS than those without fractures. The physical activity score was higher in the fracture cohort.

The children with a history of fracture had lower TB BMC SDS (p<0.001) with a median of -0.5 (-1.1, 0.0) (Figure 4.8C), but similar LS BMC SDS (p=0.617) (Table 4.4). Both groups had similar BAP SDS, IGF-1 SDS and CTX SDS (Table 4.4). The median physical activity score (1=least, 5=most active) for the fracture group was 2.8 (1.7, 4.1) and 2.2 (1.3, 3.7) in the non-fracture group (p=0.043) (Figure 4.8D). There was no significant difference in bone microarchitecture or bone marrow adiposity between these fracture groups (Table 4.4). On multivariate analysis, taking into account HbA1c, TB BMC, and physical activity score, the only significant variable was TB BMC (adjusted OR 0.002, 95% CI 0.0 - 0.765, p=0.04).

4.5 Discussion

This is the first study to look in detail and specifically at the association between T1D disease characteristics, bone microarchitecture and marrow adiposity by MRI and fracture incidence in children. The group of children studied had an overall diabetes control which was better than expected for adolescents (Cameron and Wherrett 2015) but similar to that described recently in a population based study of skeletal morbidity in young people with T1D (Weber *et al.* 2015). In addition, contrary to other studies of bone health in children and adolescents with T1D (Parthasarathy *et al.* 2016), the current cohort were well nourished and were also vitamin D sufficient.

Previous studies on bone turnover status of children and adolescents with T1D have produced variable results (Valerio *et al.* 2002, Hamed *et al.* 2011, Tsentidis *et al.* 2016). Given that these markers vary markedly in growing children, the values for the two commonly studied markers of bone formation and bone resorption, BAP and CTX, were adjusted for age and sex in the current study. The existence of a low bone turnover state, characterised by low circulating levels of both BAP and CTX, is important to highlight in a group of well-controlled children with T1D. This biochemical picture has also been described in young adults with T1D (Starup-Linde *et al.* 2014, Abdalrahaman *et al.* 2015). Whilst, it is possible that this low bone turnover state may also be a reflection of functional growth hormone resistance which may exist in people with diabetes (Baroncelli *et al.* 2000), circulating IGF-1 was not particularly low in the current cohort. Given that there was a clear inverse association between bone formation and glycaemia and between bone resorption and the age at diagnosis of diabetes, it is possible that the mechanisms that influence bone turnover in T1D are mediated through several pathways including those that may be dependent on chronic hyperglycaemia or insulinopenia (Abdalrahman *et al.* 2015). For instance, the inverse association between circulating sclerostin and age at diagnosis further supports the notion of a sclerostin-mediated signalling pathway inhibition of bone turnover (Gennari *et al.* 2012).

Marked reduction in diabetes complications have been reported in T1D adolescents with a shift towards a more physiologic insulin replacement using continuous subcutaneous insulin infusion (CSII) via pump (Downie *et al.* 2011). The higher levels of BAP in T1D children on CSII compared to those on multiple daily injections (MDI) suggests that this form of replacement may indeed be advantageous for bone health preservation. However, given that this group also had a lower HbA1c could suggest a degree of selection bias. The lower levels

of BAP in children who presented in DKA at initial diagnosis is very interesting and suggests the possibility of an additional programming effect of acidosis or sustained hyperglycaemia prior to initial presentation on skeletal development. Given that the effects of acidosis on bone homeostasis may be independent of calciotropic hormones (Topaloglu *et al.* 2005) and it is possible that acidosis may have an effect on mesenchymal stem cell differentiation (Guntur *et al.* 2018), a long lasting effect on bone health that may result from the initial acidotic insult deserves further exploration. Alternatively, as DKA at T1D presentation is more likely to occur in younger children, the lower BAP may be an indication of a more aggressive autoimmune process leading to more marked insulin deficiency or shorter honeymoon period.

In the current study, children with T1D had marginally lower bone mineral density when corrected for size and this is consistent with previous studies demonstrating that children and adolescents with T1D have lower bone mineral density status (Leger *et al.* 2006, Saha *et al.* 2009b, Loureiro *et al.* 2014). Although bone microarchitecture studies have been performed in T1D and some have reported deficits (Maratova *et al.* 2018, Samelson *et al.* 2019) the current study is the first study in children with T1D that has shown a deficit in MRI-based assessment of trabecular bone microarchitecture, a finding which is similar to what has been described before in young women with T1D (Abdalrahaman *et al.* 2015). It is interesting to note that that the two studies (Maratova *et al.* 2018, Samelson *et al.* 2019) that have shown a deficit and the one (I. Roggen *et al.* 2013) which did not show a deficit examined the tibia and radius, respectively and the possibility of a selective effect on a weight bearing site needs further exploration in adequately powered studies.

The inverse association of bone microarchitecture parameters with bone marrow adiposity in children confirms our previous reports of this finding in young women (Abdalrahaman *et al.* 2017) and not only does this further reinforce the hypothesis that the observed skeletal deficit in T1D may have its origins in a shift of mesenchymal stem cell differentiation towards adipogenesis rather than osteogenesis but it also highlights the unique benefit of MRI based assessment for providing mechanistic insight when studying bone health. Furthermore, the positive association between insulin dose and trabecular number substantiates the anabolic effect of insulin on bone (Thomas *et al.* 1996a, Fulzele *et al.* 2010). The lack of an association between bone microarchitecture parameters and DXA-based measures of bone density has also been previously noted in young women with T1D (Abdalrahaman *et al.* 2017) and highlights the point that bone microarchitecture assessment provides additional information on bone health that cannot be obtained from bone

densitometry. Recent histomorphometric and microCT based studies of trabecular bone microarchitecture have shown an inverse association with HbA1c (de Waard *et al.* 2018, Karim *et al.* 2018) but this was not observed in the current study or our previous study in young women (McComb *et al.* 2014a) and perhaps these studies were not sufficiently powered to investigate this association. An association between the deficits in trabecular features and fractures was also not observed and this may also require a larger cohort as well as a study of cortical parameters, as described recently in adults (Samelson *et al.* 2019). In the previous study performed in young women with T1D, we had reported that bone microarchitectural deficits were more likely in those who had retinopathy (Abdalrahaman *et al.* 2015). However, given the low prevalence of microvascular complications in children (Sauder *et al.* 2019), the current study was not sufficiently powered to investigate this finding in this age group.

Approximately a third of the current cohort of children with T1D had suffered a radiologically confirmed fracture before the median age of 13.8 years. Fracture rates in children with T1D have rarely been reported but the current rate of fractures was higher than previously reported in children and young people with T1D (Cameron and Wherrett 2015, Parthasarathy *et al.* 2016, Sauder *et al.* 2019) and the control group. In the UK, approximately one third of children are reported to suffer a fracture before the age of 17 years, with a fracture incidence of 3% in boys and 1.5% in girls at their peak (Cooper *et al.* 2004). Therefore, it is possible that the control group had a relatively lower incidence of fractures. In hindsight, one of the limitations of the study is the lack of data on the rate of fracture in the children before diagnosis of T1D, as this could exclude the remote possibility that by chance the T1D subgroup had individuals with increased bone fragility unrelated to the diabetes.

There were some notable differences between the groups of children with T1D who suffered a fracture compared to those who had not suffered a fracture. Children who fractured had lower total body bone mineral density and poorer glycaemic control compared to the non-fracture group. Abnormalities in cortical bone mineral density with reduced muscle cross-sectional area have been previously reported in T1D and are consistent with an anabolic bone deficit (Bechtold *et al.* 2006). This is further supported by our finding of significantly lower total body, but not lumbar, bone mineral density in T1D children with fracture. Given that bone microarchitecture at the proximal tibia was not significantly different between the fracture and the non-fracture group, this reinforces the need to study cortical bone architecture in more detail in this condition. Although the combination of lower bone mineral

density, poorer glycaemic control and an increased risk of fractures could have been explained by reduced physical activity (Goulding 2007), this confounder was discarded as both groups had comparable levels of physical activity.

In summary, children and adolescents with relatively well controlled T1D are more likely to have a history of fractures and show deficits in trabecular bone microarchitecture, BMD and bone formation. Although, the association of these markers of bone health to clinical markers of T1D and its management require further exploration through prospective clinical trials, we would recommend that assessment of bone health should become routine in all therapeutic trials in the field of diabetes.

5 The Effects of Anti-Diabetic Drugs on Mesenchymal Stem Cell Differentiation and the Molecular Mechanism of Metformin on Adipogenesis Suppression

5.1 Abstract

It is possible that people with diabetes mellitus (DM) have altered mesenchymal stem cell (MSC) differentiation in the bone marrow, leading to a shift in the balance of differentiation away from bone formation (osteogenesis) in favour of fat cell development (adipogenesis) and a predisposition to fragility fractures. Different classes of antidiabetic drugs have been shown to affect bone health differently, with negative effects from thiazolidinediones whilst metformin is associated with clinical reduction in fracture risk. The effects of metformin on the differentiation of mouse C3H10T1/2 mesenchymal stem cells into fat and bone cells were investigated, with particular interest in the reciprocity of the bone-fat balance. The underlying molecular signalling involved, specifically in the adipogenesis effect of metformin, was also studied, focussing on the AMPK signalling given that metformin in a known AMP-activated protein kinase (AMPK) activator. Metformin was found to exert reciprocal control over the osteogenic transcription factor Runx2, and the adipogenic transcription factor, PPARγ with increase in Runx2 transcriptional activities, independently on Runx2 protein expression and suppression of PPARγ - suggesting a bone protective mechanism through promotion of osteogenesis and suppression of adipogenesis. The suppression of adipogenesis by metformin appeared to be independent of AMPK activation but rather through the suppression of the mTOR/$p70^{S6K}$ signalling pathway. Basal AMPK and mTOR/$p70^{S6K}$ activity did appear to be required for adipogenesis, as demonstrated by the use of the AMPK inhibitor, compound C. It appears, therefore, that basal AMPK activity is required for adipogenesis and that metformin can inhibit adipogenesis through AMPK-dependent or -independent mechanisms, depending on the cellular context.

5.2 Introduction

Adults with Type 1 Diabetes (T1D) and Type 2 Diabetes (T2D) have a significantly increased risk of fractures compared to the general population (Vestergaard 2007, Hothersall *et al.* 2014). Studies have shown that different classes of antidiabetic drug used in T2D have different effects on the bone. Thiazolidinediones (TZDs), such as pioglitazone and rosiglitazone, have been irrefutably shown to increase fracture risk (Schwartz *et al.* 2006, Kahn *et al.* 2008, Loke *et al.* 2009) whilst the effects of metformin remain inconclusive. Several large population-based case control studies have associated metformin with a reduction in fracture risk (Vestergaard *et al.* 2005, Melton *et al.* 2008, Borges *et al.* 2011) although others did not show any convincing benefit (Kahn *et al.* 2008). It would be conveniently advantageous if metformin, which is also low cost and safe, confers a bone protective role as it is increasingly used in T1D to improve insulin resistance with a modest effect on glycaemic control (Vella *et al.* 2010).

There is a growing body of evidence supporting the bone-fat balance and its important role in the pathophysiology of bone loss. Osteoblasts and adipocytes share a common precursor, both derived from the pluripotent MSCs located in the bone marrow, suggesting a mutually exclusive and reciprocal lineage selection of one or the other (Figure 5.1).

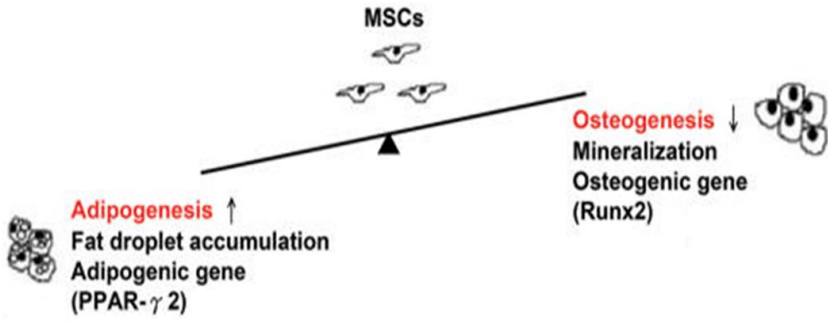

Figure 5.1. Bone-fat balance. Osteogenesis and adipogenesis are proposed to be mutually exclusive given that osteoblasts and adipocytes originate from the common progenitor mesenchymal stem cells. PPARy2 is the key regulator of adipogenesis whilst Runx2 activation determines osteogenesis [Adapted from (Yang *et al.* 2008)].

The differentiation of MSCs are dependent on two main lineage-specific transcription factors, namely runt-related transcription factor 2 (Runx2) for osteogenesis and the peroxisome proliferator-activated receptor γ (PPARγ) for adipogenesis. By reason that TZDs are agonists of the PPAR family of nuclear transcription factors, particularly the PPARγ isoform (Yki-Jarvinen 2004), their use is detrimental to bone (negative skeletal consequences) as it activates PPARγ and promotes adipogenesis at the expense of

osteogenesis (Rzonca *et al.* 2004). This is evident is both mice (Botolin *et al.* 2005) and men (Schwartz *et al.* 2006, Grey *et al.* 2007).

On the contrary, the mechanism of action of metformin on skeletal health is less clear. Metformin is a known AMP-activated protein kinase (AMPK) activator as detailed in section 1.7. Mice with deleted AMPK subunits demonstrated a reduction in bone volume and trabecular number supporting the role of AMPK in bones (Shah *et al.* 2010). AMPK functions to inhibit ATP consuming pathways and at the same time activate catabolic pathways to re-establish cellular energy homeostasis. Osteoblast differentiation has been proposed to be dependent on the cellular energy sensor AMP-activated protein kinase (AMPK), as the expression of various osteogenic genes has been shown to be inhibited by compound C, a chemical inhibitor of AMPK, and a dominant negative form of AMPK (Banerjee *et al.* 1997).

Indeed, metformin was found to have direct osteogenic effect *in vitro* by stimulating proliferation and differentiation of osteoblasts, through various signalling pathways including the PI3K/Akt pathway (Ma *et al.* 2010b), ERK-1,2 (Cortizo *et al.* 2006) and AMPK activation (Kanazawa *et al.* 2008, Jang *et al.* 2011). Based on the bone-fat balance theory, the main aims of the current study are to: (i) determine the effects of metformin on mesenchymal stem cell differentiation in particular its effects on adipogenesis, to examine the suggested bone-fat reciprocity and (ii) understand the underlying molecular mechanisms involved, in particular the role of the AMPK signalling pathway in these processes.

5.3 Materials and Methods

5.3.1 Cell culture and induction of differentiation

Commercially available C3H10T1/2 mouse mesenchymal stem cells (Clone 9; ATCC CCL-226) were chosen as they do not undergo spontaneous differentiation under normal culture conditions and show a more homogenous colony-forming rates during cell expansion as compared to human cell lines, as detailed in section 1.3.3. The C3H10T1/2 cells were maintained in DMEM (41965-039, Sigma-Aldrich Ltd, Gillingham, Dorset, UK) containing 10% (v/v) foetal calf serum (FCS), 2 mM glutamine, 100 U/mL penicillin and 100 µg/ml streptomycin. Cells were kept to 80-90% sub-confluence before further subculture and plating.

At confluence, cells in plates were treated for 5 days with specific differentiation media and treatments for 5 days. To promote adipogenic differentiation, cells were cultured in the standard media supplemented with either 10 μM pioglitazone (PIO) alone or in combination with 100 nM insulin, 500 μM 3-isobutyl-1-methylxanthine (IBMX) and 10 μM dexamethasone (IID medium). Insulin is widely used to induce proliferation and differentiation of pre-adipocytes, as it mimics insulin-like growth factor-1 at high concentration and activates the mitogen-activated protein kinase pathways. IBMX is a competitive, nonselective phosphodiesterase inhibitor, which together with dexamethasone, promotes transcriptional activation of PPARγ through protein kinase A signalling. They also induce C/EBPδ and C/EBPβ which are both transcriptions factors for growth and differentiation. For osteogenic differentiation, cells were cultured in standard media supplemented with 284 μmol/L ascorbic acid, 10 mM β-glycerophosphate and 10 nM dexamethasone (AGD medium). The culture media was changed every 3 days. Cells were also incubated with 10% FCS alone, as negative control for differentiation. The specific treatments included 500 μM metformin, 100 μM of the AMPK-activator (A769662), or 10 μM of the $p70^{S6K}$-inhibitor (rapamycin), as used previously (Molinuevo *et al*. 2010, Moreno *et al.* 2008, Yarwood *et al*. 1999). Cells were also incubated with 10% FCS alone, as negative control for differentiation.

5.3.2 Preparation of cell extracts

C3H10T1/2 MSCs were harvested and nuclear extracts prepared using the Nuclear Extraction kit from Active Motif, Belgium. Briefly, the media was aspirated and cells were harvested in ice-cold PBS containing phosphatase inhibitors and centrifuged (200 x *g*, for 5 minutes at 4ºC) to obtain a cell pellet. The cell pellet was re-suspended in complete lysis buffer containing 10 mM DTT and phosphatase inhibitor cocktail and then centrifuged (14000 x *g*, for 10 minutes at 4ºC) to obtain nuclear and supernatant fractions. Protein concentration of the nuclear fraction was calculated by bicinchoninic acid assay (BCA) (Smith *et al*. 1985) using prepared BCA kit reagents from Thermo Fisher before loading of samples for electrophoresis.

5.3.3 Western blotting

Protein samples were separated by SDS-PAGE and then transferred electrophoretically onto nitrocellulose membranes. Membranes were blocked with 5% (w/v) Marvel milk powder in TBS (20 mM Tris-HCl pH 7.5, 150 mM NaCl) for 1 hour. Membranes were then incubated with primary antibodies overnight at 4ºC. Following washes with TBST (TBS supplemented

with 0.5% (v/v) Tween-20), membranes were incubated with secondary antibodies for 1 hour at room temperature. Antibodies were diluted to the required concentration in 50% (v/v) Sea Block (Thermo Scientific) and 50% (v/v) TBST. The primary antibodies used were to peroxisome proliferator-activated receptor gamma (PPARγ; marker for adipogenesis, Cell Signalling Technologies (CST), Danvers, MA; dilution 1:1000), Runt-related transcription factor 2 (Runx2; marker for osteogenesis, CST, Danvers, MA; dilution 1:1000), phosphorylated-ACC (P-ACC (Ser79); marker for AMPK activity, CST, Danvers, MA; dilution 1:1000) and phosphorylated-$p70^{S6K}$ (P-$p70^{S6K}$ (Thr389); upstream regulator of mTOR signalling, CST, Danvers, MA; dilution 1:1000). Antibodies were detected using a LI-COR® Odyssey Infrared Imaging systems and densitometric analysis was carried out using ImageJ software (NIH, UK) software Version 1.47.

5.3.4 Oil Red O staining

After 5 days of cell differentiation and treatment (as described in section 5.3.1), the media was aspirated and cells were fixed to cell culture plates with 10% (v/v) neutral buffered formalin for 30 minutes. The formalin was then aspirated and staining was carried out with the addition of 0.3% (w/v) Oil Red O (ORO) in isopropanol:water (60:40) for 5 minutes in room temperature. The ORO was then aspirated and wells washed with distilled water four times. Imaging was carried out using a Zeiss Axiovert 25 microscope with QImaging camera and supporting software.

5.3.5 Transient transfection and luciferase assay

C3H10T1/2 cells were transfected with the indicated plasmids in 6-well plates, with 1.125 μg/well PPRE (PPARγ reporter, purchased from Adgene) and 6xOSE reporter constructs (Runx2 reporter, supplied by Jian Huang, Rush Medical Centre, Chicago, USA) using Lipofectamine 2000 reagent (Invitrogen, Carlsbad, CA) and then treated with metformin, A769662 or rapamycin with and without adipogenic differentiation media. Cells were then harvested 48 hours after transfection and assayed using the Luciferase reporter assay system (Promega, Madison, WI) according to manufacturer's instructions. As a transfection control, the *Renilla* plasmid 0.125 μg/well was co-transfected in each transfection experiment, and the luciferase activity was normalised to the *Renilla* activity.

5.3.6 Statistical analysis

All experiments were performed in triplicate and statistical analysis was performed using Student's t-test or one-way ANOVA. Results are expressed as mean ± standard error (SEM) and differences with $p<0.05$ were considered statistically significant.

5.4 Results

5.4.1 Effects of antidiabetic drugs pioglitazone and metformin on murine MSC (C3H10T1/2) differentiation

In confluent C3H10T1/2 MSCs cells (Figure 5.2A and Figure 5.2B), IID-containing medium promoted lipid accumulation (Figure 5.2C), an effect that was further enhanced by co-treatment of cells with PIO (Figure 5.2D) as seen on Oil red O staining. In addition, treatment of cells with either metformin or A769662 suppressed adipogenesis promoted by IID alone (Figure 5.2E and Figure 5.2G, respectively) or by a combination of IID plus PIO (Figure 5.2F and Figure 5.2G). Metformin was a more effective inhibitor of lipid accumulation and less so with A769662, possibly as A769662 is only a selective activator of AMPK β1-containing complexes.

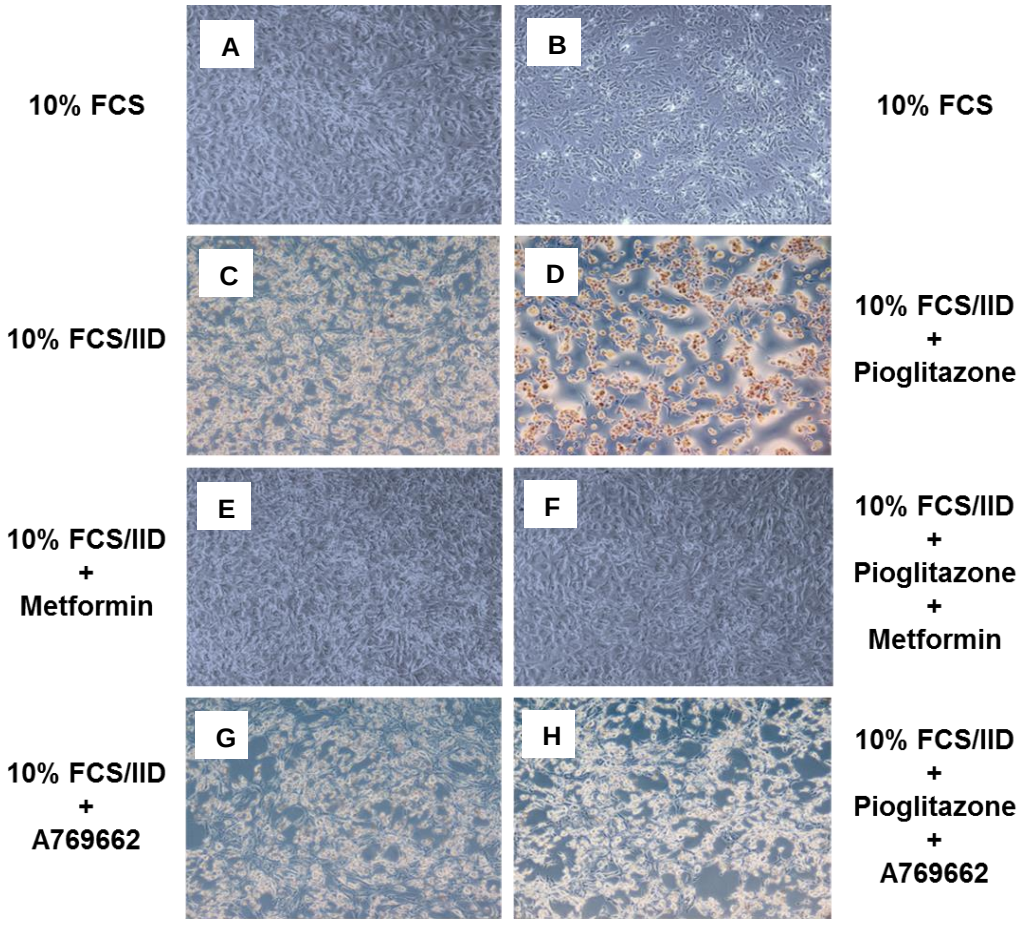

Figure 5.2 Effects of pioglitazone and metformin on lipid accumulation in C3H10T1/2 MSCs. Confluent C3H10T1/2 MSCs (A and B) were induced to differentiate by addition 10% foetal calf serum (FCS) in the presence or absence of adipogenic IID medium (insulin, isobutylmethylxanthine (IBMX) and dexamethasone and/or 10 μM pioglitazone (PIO), 500 μM metformin or 100 μM A769662. After 5 days cells were fixed with formalin and stained with Oil Red O to detect neutral lipid accumulation (red). IID and pioglitazone promoted lipid accumulation (C and D) whilst metformin and the AMPK-activator, A769662, suppress adipogenesis (E-H). Representative micrographs from an experiment carried out on three separate occasions with similar results are shown.

The western blot experiments demonstrated that treatment with IID or PIO induced a significant increase in the two PPARγ splice variants, PPARγ1 and PPARγ2 (Figure 5.3A and Figure 5.3B), which correlated with a significant increase in PPARγ transcriptional activity, as determined by luciferase assay (Figure 5.4A). In agreement with the ORO experiments in Figure 5.2, treatment of cells with either metformin or A769662 effectively suppressed IID- and PIO-stimulated increases in PPARγ protein levels (Figure 5.3A and Figure 5.3B), as well as IID- and PIO-stimulated PPARγ activity (Figure 5.4A).

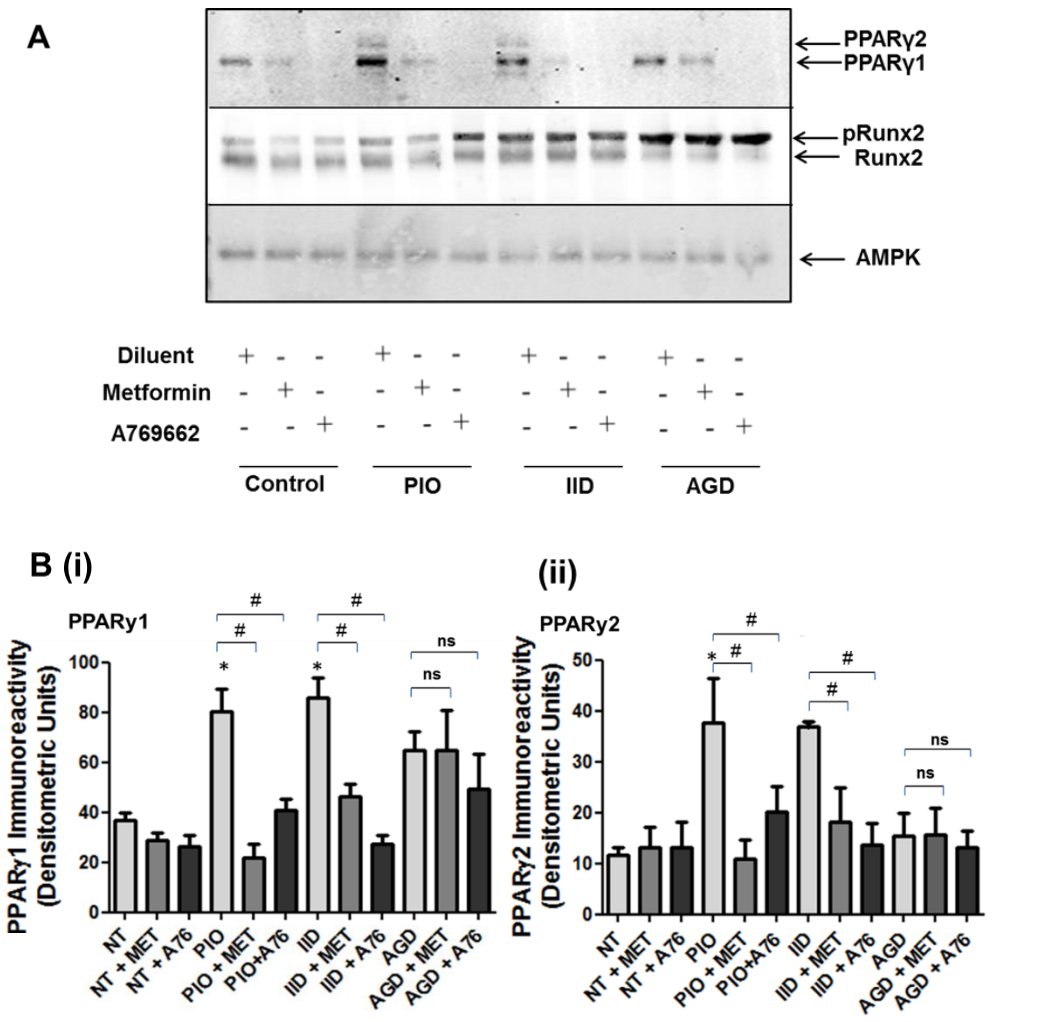

Figure 5.3 Effects of Pioglitazone, Metformin and the AMPK-activator, A769662, on early markers of differentiation in C3H10T1/2 cells. (A) Confluent CH3H10T1/2 cells were stimulated for 5 days with 10 µM pioglitazone (PIO) or an adipogenic (IID) or osteogenic (AGD) cocktail, in the presence or absence of 500 µM metformin or 100 µM A769662. Cell extracts were then prepared and immunoblotted with antibodies to PPARγ, Runx2 and AMPK. The phosphorylation-dependent electrophoretic mobility shift of Runx2 induced by AGD treatment is indicated (pRunx2). Representative immunoblots from an experiment carried out on three separate occasions with similar results are shown. (B) Densitometric analysis of PPARγ1 (i) and PPARγ2 (ii) levels are shown as means±SEM. Significant increases (*, p<0.05) relative to control, and significant decreases relative to PIO-stimulated cells (#, p<0.05), are indicated (n=3). Non-significant changes are also indicated (ns)

Treatment of cells with AGD did not significantly affect PPARγ protein levels (Figure 5.3A and Figure 5.3B) or activity (Figure 5.4B). AGD treatment alone did promote a noticeable phosphorylation band-shift of Runx2 protein compared to control (Figure 5.3A). Neither metformin nor A76 affected the protein expression level or Runx2 (Figure 5.3A). However, treatment with either metformin or A769662 significantly increased Runx2 transcriptional activity in C3H10T1/2 cells (Figure 5.4B), which did not correlate with an increase in AGD-promoted phospho-Runx2 levels, as determined by band-shift (Figure 5.3A).

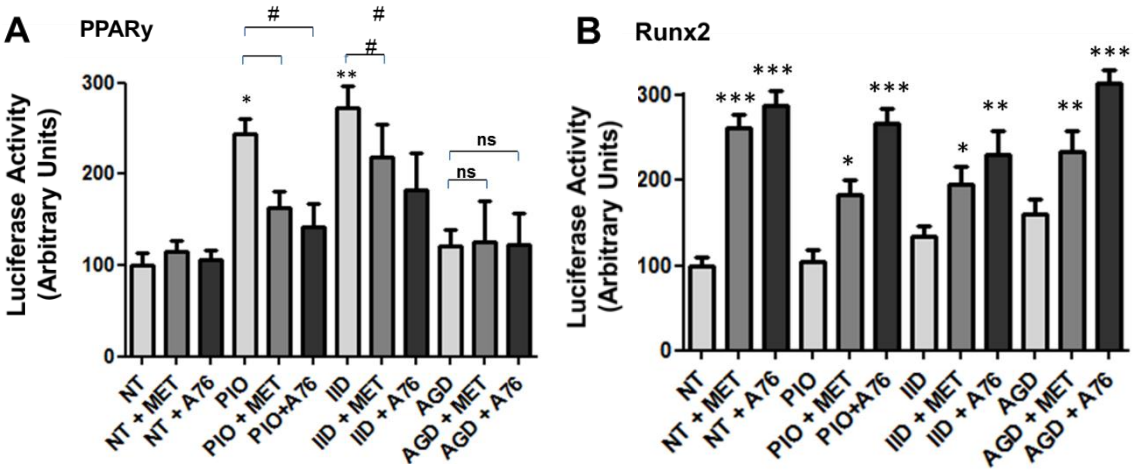

Figure 5.4 Luciferase reporter assays to determine activity of the transcription factors PPARγ and Runx2. (A) Confluent C3H10T1/2 cells were transfected with a PPARγ and Runx2 luciferase gene reporter constructs, together with control *Renilla* luciferase vector, and then stimulated for two days with 500 µM metformin or 100 µM A769662, in the presence or absence of 10 µM pioglitazone (PIO), adipogenic medium (IID) or osteogenic medium (AGD). Cell extracts were then prepared and luciferase activities were measured using a dual luciferase reporter assay. PIO and IID significantly induced, whilst metformin and A76 significantly suppressed PPARγ activity Metformin and A76 promoted Runx2 activity in control, adipogenic and osteogenic media (B). Luciferase activities from three separate experiments are shown as means±SEM. Significant increases in luciferase activity are indicated; *, $p<0.05$, **, $p<0.01$ and ***, $p<0.001$, as are significant decreases in activity, #, $p<0.05$ (n=3). Non significance is indicated (ns).

5.4.2 Molecular mechanisms involved in the action of metformin on adipogenesis

Based on metformin being a known AMPK activator, its ability to activate AMPK was examined by measuring the phosphorylation of a known AMPK substrate, Ser 79 of acetyl coenzyme carboxylase (ACC), using phospho-specific antibodies. A769662 provoked a robust and rapid phosphorylation of ACC, which was maintained for up to 48 hours, but metformin did not induce a significant phosphorylation of ACC, even after 48 hours stimulation (Figure 5.5).

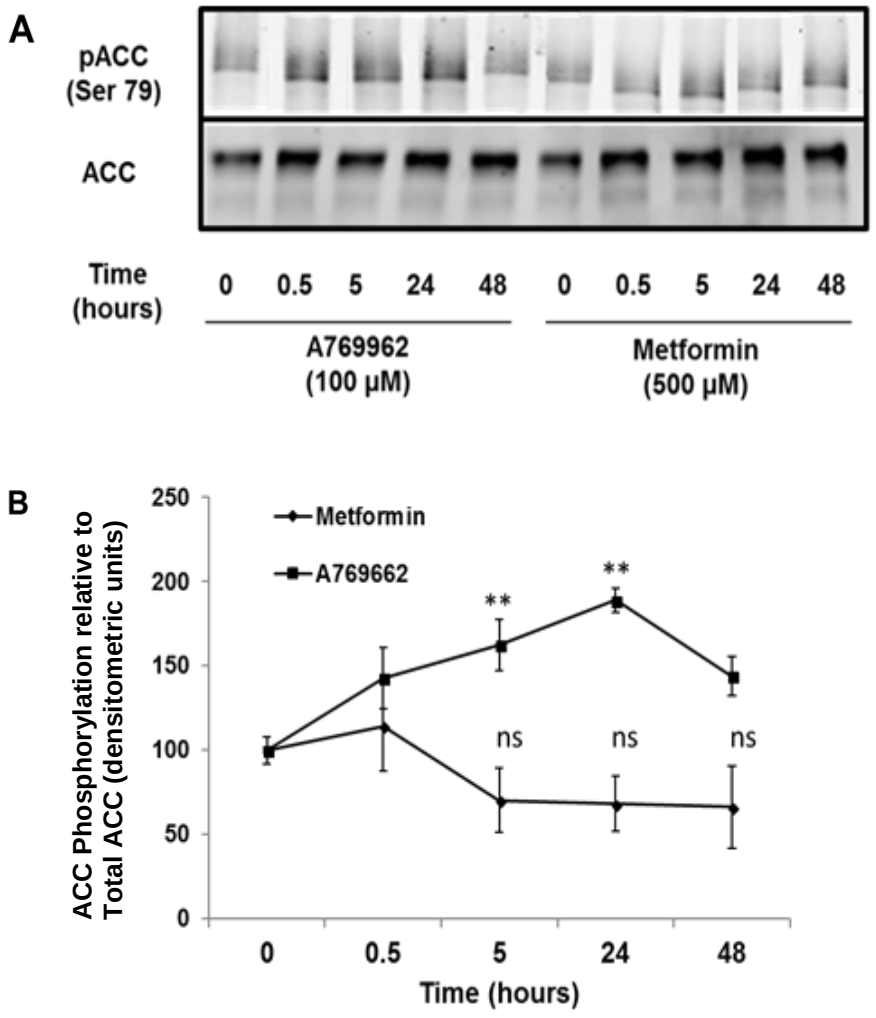

Figure 5.5 The AMPK activator, A769662, but not metformin activates AMPK in C3H10T1/2 cells. (A) Confluent C3H10T1/2 cells were stimulated for the indicated times with 100 µM A769662 or 500 µM metformin. Cell extracts were then prepared and immunoblotted with antibodies towards the phosphorylated form of the AMPK substrate, ACC, or total ACC. (B) Densitometric values were obtained from immunoblots from three separate experiments and are shown as means±SEM in the line graph. Significant increases in pACC are indicated; **, p<0.01 (n=3). Non significance is also indicated (ns).

Treatment of the differentiating cells with rapamycin, a known mTOR/p70^{S6K} inhibitor, dramatically inhibited lipid accumulation associated with adipogenesis, as determined by ORO staining (Figure 5.6A). Rapamycin also suppressed PPARγ activity, as determined by gene reporter assays, indicating that the mTOR/p70^{S6K} pathway is required for adipogenesis of C3H10T1/2 cells (Figure 5.6B).

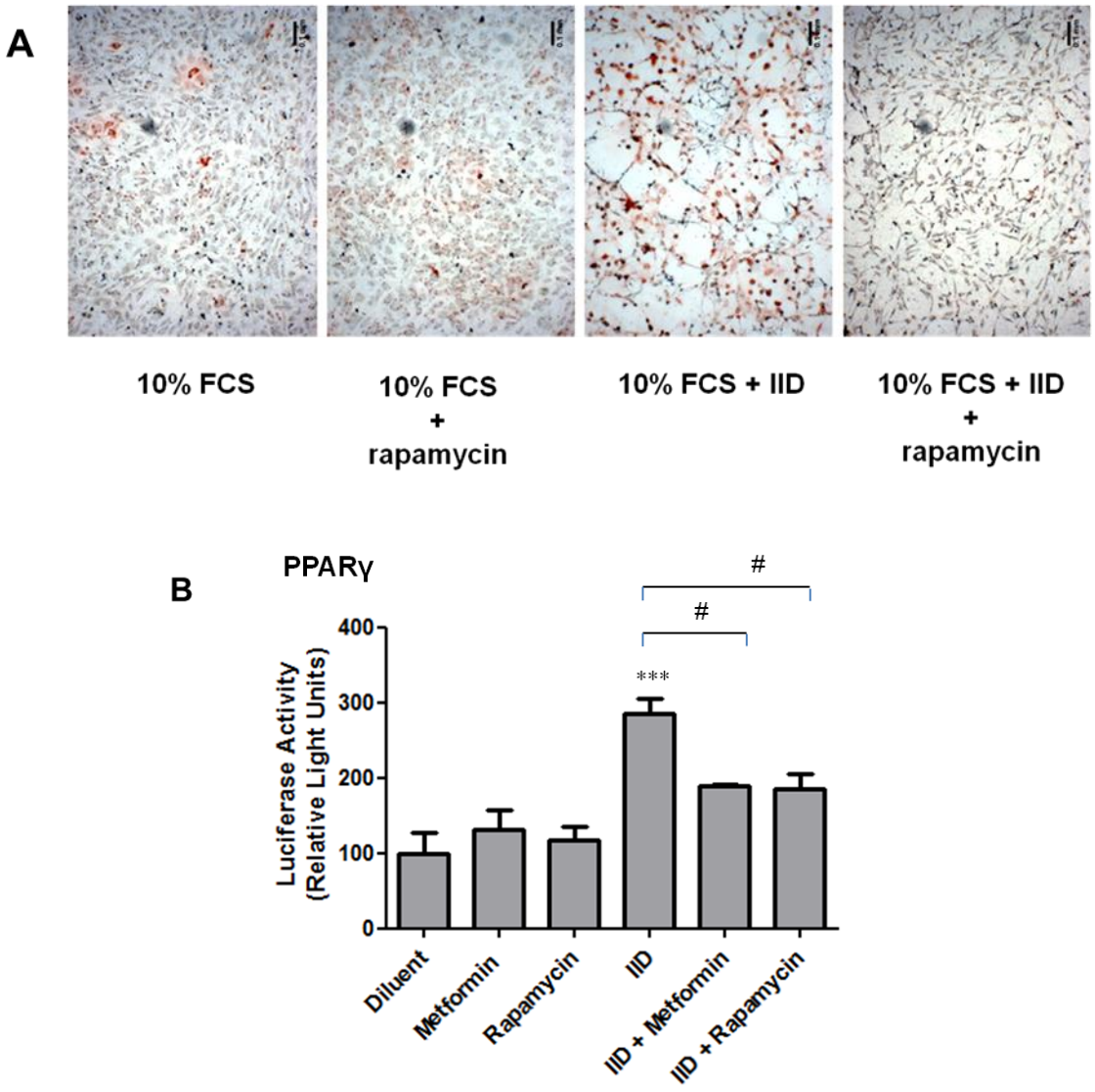

Figure 5.6 The mTOR inhibitor, rapamycin, suppresses adipogenesis of C3H10T1/2 cells. (A) Confluent CH3H10T1/2 cells were induced to differentiate by addition of 10% foetal calf serum (FCS) supplemented with adipogenic cocktail (IID), in the presence or absence of the mTOR inhibitor, 10 μM rapamycin. After 5 days cells were fixed with formalin and stained with Oil Red O to detect neutral lipid accumulation. Representative micrographs from an experiment carried out on three separate occasions with similar results are shown. (B) Confluent C3H10T1/2 cells were transfected with PPARγ luciferase gene reporter construct, together with control *Renilla* luciferase vector and then stimulated for two days with 500 μM metformin or 10 μM rapamycin, in the presence or absence of IID. Cell extracts were then prepared and luciferase activity was measured using a dual luciferase reporter assay. Luciferase activities from three separate experiments are shown as means±SEM. Significant increases in PPARγ activity are indicated ***, $p<0.001$, as are significant decreases in PPARγ activity, #, $p<0.05$, relative to IID-stimulated cells (n=3).

Rapamycin treatment had no significant effect on phospho-ACC levels (Figure 5.7A and Figure 5.7B), but significantly inhibited phosphorylation of $p70^{S6K}$ on Thr 389 (Figure 5.7C and Figure 5.7D). Both metformin and A769662 also inhibited $p70^{S6K}$ phosphorylation (Figure 5.7C and Figure 5.7D).

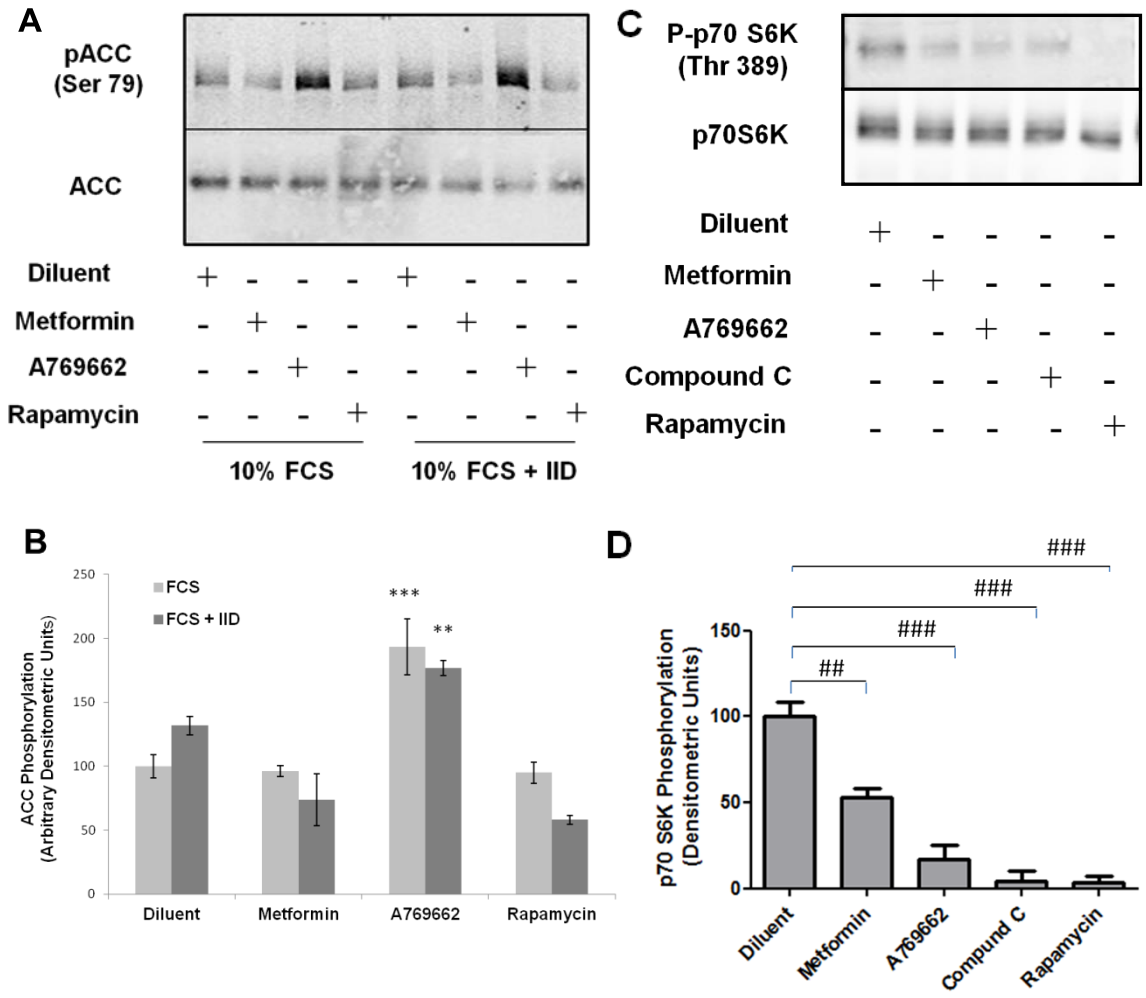

Figure 5.7 The effects of rapamycin on AMPK and $p70^{S6K}$ activities in C3H10T1/2 cells. (A) Confluent CH3H10T1/2 cells were stimulated for 5 days with IID, in the presence or absence of 500 µM metformin, 100 µM A769662 or 10 µM rapamycin. Cell extracts were then prepared and immunoblotted with antibodies to phosphorylated ACC (Ser 79). Representative immunoblots from an experiment carried out on three separate occasions with similar results are shown. (B) Densitometric values from 3 separate experiments are shown in the *lower panel* as means±SEM. Significant increases relative to control are indicated, **, p<0.01 and ***, p<0.001 (n=3). (C) Confluent CH310T1/2 cells were stimulated for 5 days with IID, in the presence or absence of 500 µM metformin, 100 µM A769662, 10 µM compound C or 10 µM rapamycin. Cell extracts were then prepared and immunoblotted with antibodies to phosphorylated $p70^{S6K}$ and total $p70^{S6K}$. Representative immunoblots from an experiment carried out on three separate occasions with similar results are shown. (D) Densitometric analysis of mean ± SEM $p70^{S6K}$ phosphorylation from 3 separate experiments are shown. Significant increases (*, p<0.05) relative to control, and significant decreases relative to IID-stimulated cells (##, p<0.01 and ###, p<0.001), are indicated (n=3).

Compound C, a known AMPK inhibitor, significantly inhibited both basal $p70^{S6K}$ (Thr 389; Figure 5.7B) and ACC (Ser 79; Figure 5.8A and Figure 5.8B) phosphorylation, suggesting that AMPK is linked to the activation of mTOR/$p70^{S6K}$ signalling in these cells. In addition, 10 μM compound C inhibited adipogenesis of C3H10T1/2 cells treated with IID (Figure 5.8C).

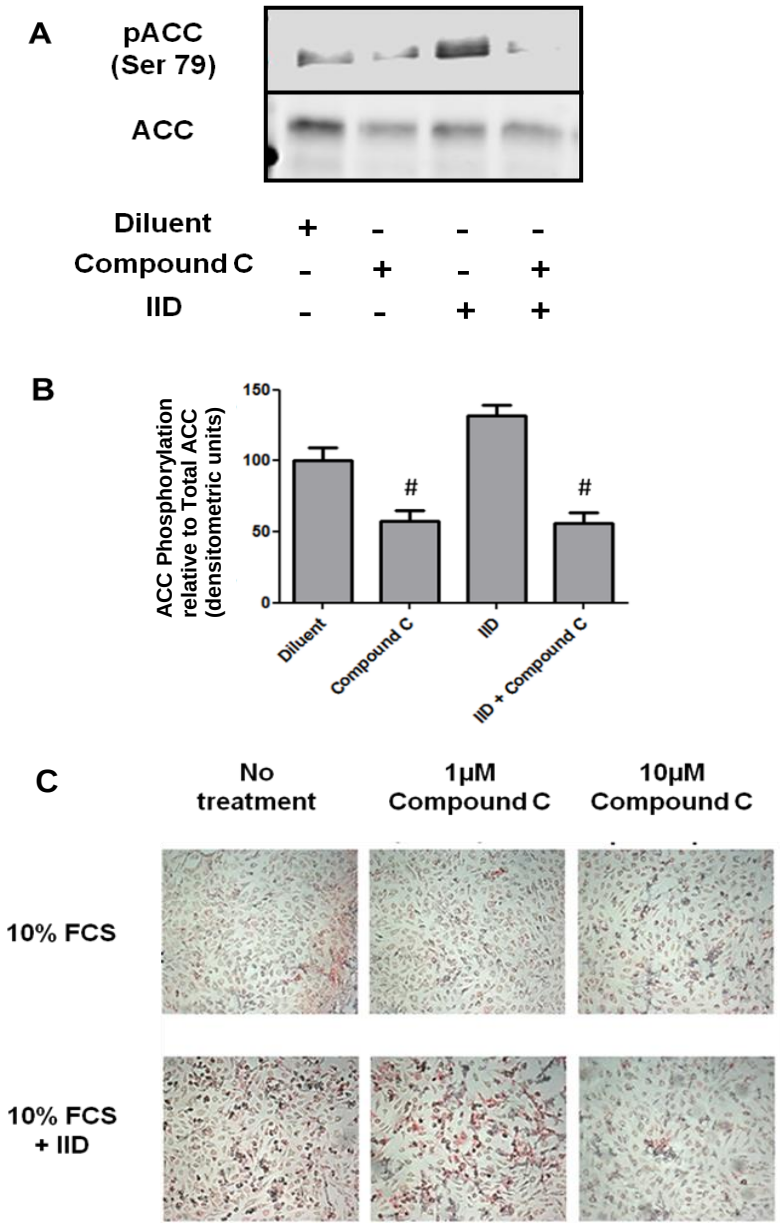

Figure 5.8 Compound C inhibits adipogenesis of C3H10T1/2 cells. (A) Confluent CH3H10T1/2 cells were stimulated for 5 days with IID, in the presence or absence of the AMPK inhibitor, 10 μM compound C. Cell extracts were then prepared and immunoblotted with antibodies to phosphorylated ACC (Ser 79). Representative immunoblots from an experiment carried out on three separate occasions with similar results are shown. (B) Densitometric values from 3 separate experiments are shown as means±SEM. Significant decreases relative to control are indicated, #, p<0.05.(C) Confluent CH3H10T1/2 cells were treated with 10% foetal calf serum (FCS) supplemented with adipogenic cocktail (IID), in the presence or absence of the indicated concentrations of compound C. After 5 days cells were fixed with formalin and stained with Oil Red O to detect neutral lipid accumulation. Representative micrographs from an experiment carried out on three separate occasions with similar results are shown.

5.5 Discussion

In this study, the different effects of antidiabetic drugs on murine C3H10T1/2 mesenchymal stem cell differentiation was established. Pioglitazone, which is a thiazolidinedione, promoted adipogenesis with increased PPARγ protein expression, PPARγ transcriptional activity and increased lipid droplet accumulation. Metformin on the other hand, inhibited adipogenesis with suppression of PPARγ protein expression, PPARγ transcriptional activity and reduced lipid droplet formation. Metformin also promoted osteogenesis with increased Runx2 transcriptional activity, unaided by osteogenic-linked increases in Runx2 phosphorylation. In addition, the novel finding of an AMPK-independent action of metformin on the inhibition of adipogenesis further adds to the current literature in this area.

It has been previously reported that metformin induced osteoblastic differentiation and matrix mineralisation in MC3T3-E1 pre-osteoblasts via activation of the AMPK signalling pathway (Cortizo *et al.* 2006, Kanazawa *et al.* 2007, Jang *et al.* 2011). Metformin also promoted osteogenesis in rat primary osteoblasts (Shah *et al.* 2010, Zhen *et al.* 2010), rat bone marrow progenitor cells (Molinuevo *et al.* 2010) and more recently in human MSCs (Wang *et al.* 2018). Jang et al found that metformin-induced AMPK activation increased the level of Runx2 mRNA and protein expression (Jang *et al.* 2011), which increased alkaline phosphatase activity and mineralisation in mesenchymal cells and osteoblast cells *in vitro* (Ducy *et al.* 1997, Harada *et al.* 1999). This contrasted with our finding as metformin promoted Runx2 transcriptional activity with no effect on Runx2 protein expression, which may be due to cell specific differences. Discrepancies between protein expression and enzymatic activity have been previously described highlighting the drawbacks of merely interpreting protein, or even mRNA expressions, to target outcomes (Anderson and Seilhamer 1997, Miyamoto *et al.* 2001). The examination of enzymatic activity is key considering the complex regulatory mechanisms for gene expression that occur both at post-transcriptional and post-translational levels. A recent breakthrough study provided a plausible explanation, suggesting that because the transcription factors for osteogenesis are already at high basal activity in undifferentiated MSCs, they are therefore only modestly regulated at the mRNA level as opposed to the transcription factors for adipogenesis which are more likely to be transcriptionally regulated being barely active in MSCs (Rauch *et al.* 2019).

Similar to Molineuvo et al, the current study demonstrated that metformin suppressed adipogenesis with reduced lipid droplet accumulation on Oil red O staining (Molinuevo *et*

al. 2010), and proceeded to demonstrate the reciprocal effects of metformin on the adipogenic transcription factor PPARγ and osteogenic transcription factor Runx2. Given that increases in PPARγ activity during the early stages of adipogenesis are necessary and sufficient to promote terminal fat cell development (Rosen and Spiegelman 2000), it appears that the ability of metformin and A769662 to inhibit adipogenesis is linked to their ability to suppress PPARγ protein expression. Moreover, given that the PPARγ luciferase reporter assays were carried out after only two days of differentiation, it appears that the adipogenic suppressive actions of metformin and A769662 occur at a very early stage of the differentiation process in favour of Runx2 activity promotion.

Metformin exerted these effects on the transcription factors similarly to A769662, which is a known potent, reversible AMPK activator suggesting the role of AMPK activation in mesenchymal stem cell differentiation. Both metformin and A769662 have been reported to activate AMPK in a variety of cell types (Zhou *et al.* 2001, Cool *et al.* 2006). Previous studies have validated the role of AMPK activation in osteogenesis, with the use of metformin and 5-aminoimidazole-4-carboxamide riboside (AICAR), the latter which is another pharmacological activator of AMPK (see section 1.7.2). In human adipose-derived and bone marrow MSCs, AMPK activation was also crucial (Kim *et al.* 2012, Lee *et al.* 2014) in osteogenesis with pharmacological induced AMPK inhibition and AMPKα1 knock-out mice demonstrating reduced bone matrix mineralisation, alkaline phosphatase (AP) activity, Runx2 and osteocalcin protein expression (Kim *et al.* 2012). AMPK knock-out mice have also been shown to have reduced trabecular bone mass and cortical indexes. Paradoxically, studies have also shown that osteoblast differentiation is functionally associated with decreased AMPK activity (Kasai *et al.* 2009).

The role of AMPK activation in adipogenesis, however, is less well understood. AMPK activation with AICAR has been shown to inhibit the conversion of pre-adipocytes to fat cells (Habinowski and Witters 2001, Lee *et al.* 2011). Paradoxically, however, the widely used AMPK inhibitor, compound C, has also been reported to inhibit adipogenesis of preadipocyte cell lines (Nam *et al.* 2008). Previous work has shown that AMPK activation suppresses adipogenesis in favour of osteogenesis in adipocyte-derived human MSCs (hMSCs) and bone marrow-derived MSCs (Kim *et al.* 2012, Lee *et al.* 2014). Chava *et al.* in a recently published study have demonstrated that RUNX2 was in fact a novel substrate for AMPK, with metformin-induced AMPK activation preventing RUNX2 ubiquination in osteogenesis over adipogenesis (Chava *et al.* 2018). Given the inhibitory effects of these two compounds on early and late markers of adipogenesis in C3H10T1/2 MSCs, it was rather

intriguing to find that metformin did not inhibit adipogenesis through AMPK activation. The use of rapamycin to study the mTOR/p70^{S6K} signalling pathway became apparent following recent work showing the interaction between PPARγ and the mTOR/p70^{S6K} (Sun *et al.* 2013). Moreover, metformin has been shown to inhibit the activation of the p70^{S6K} pathway independently of AMPK (Vazquez-Martin *et al.* 2009) in tumour cells and p70^{S6K} has been shown to be required for the growth hormone-dependent adipose conversion of 3T3-F442A preadipocytes (Yarwood *et al.* 1999). In the present study, rapamycin specifically inhibited phosphorylation of p70^{S6K} on Thr 389, which is the mTOR phosphorylation site critical for kinase function (Saitoh *et al.* 2002), with no significant effect of phospho-ACC levels highly indicative of an AMPK-independent action.

This, however, does not rule out a role for AMPK in the control of p70^{S6K} activation. In fact, it has been reported that AMPK inhibits mTOR/p70^{S6K} signalling, which is thought to underlie the actions of metformin in a range of cellular contexts (Dowling *et al.* 2011, Viollet *et al.* 2012). The suppression of adipogenesis with Compound C, which is an AMPK inhibitor, may suggest that AMPK is linked to the activation of mTOR/p70^{S6K} signalling in these cells, although Compound C itself is a very non-selective AMPK inhibitor (Yu *et al.* 2008, Vogt *et al.* 2011). There may be a basal level of AMPK activity that is necessary for supporting adipose conversion of these cells, and this could be examined further with the use of AMPK knock out models. A recent study published has also demonstrated an intriguing dose dependency effect of metformin on adipogenesis (Chen *et al.* 2018).

The AMPK-independent action of metformin on the inhibition of adipogenesis reported here may be due to *cell type-specific* effects during the differentiation process. For example, most of the studies demonstrating an AMPK-dependent action of metformin have been conducted in more differentiated cell lines, such as pre-osteoblasts (Cortizo *et al.* 2006, Kanazawa *et al.* 2008, Jang *et al.* 2011), pre-adipocytes (Moreno-Navarrete *et al.* 2011, Lee *et al.* 2012), myoblasts (Longnus *et al.* 2005, Fulco *et al.* 2008, Kobashigawa *et al.* 2014) and neuronal mouse cell lines (Bang *et al.* 2014), instead of the more primitive progenitor cells as investigated here.

In addition, the AMPK-independent action noted may also be due to *cell stage-specific* effects during the commitment and differentiation process. Pantovic et al. (Pantovic *et al.* 2013) have demonstrated that there is a coordinated time-dependent activation of different signalling pathways during the osteogenic differentiation of hMSCs, which is AMPK-dependent in the early stages of differentiation followed by late stage activation of the

Akt/mTOR signalling pathway. Given the results presented here, it could be argued that similar mechanisms might regulate adipogenesis in murine MSCs. We found an overall requirement for basal levels of AMPK activity for adipogenesis in C3H10T1/2 cells but the ability of metformin to control the commitment of MSCs to differentiate into either osteoblasts or adipocytes is governed at an early stage through the inhibition of mTOR/$p70^{S6K}$ signalling.

Overall, my work suggests that metformin as an anti-diabetic agent has a promising bone protective function given its positive role in osteogenesis and negative effect on adipogenesis in mesenchymal stem cell differentiation. It is worth noting the supraphysiological dose of metformin used may limit its translation to clinical studies although other biguanides such as phenformin which is much more effective at lower doses is currently being used in clinical trials. It exerts multiple effects to inhibit adipogenesis in different cell types. Therefore, the overriding view that metformin exerts its effects on adipogenesis simply by promoting AMPK activation may therefore need some revision, especially as the role of AMPK itself appears to be complex. In conclusion, further investigation into how metformin suppresses signalling through the mTOR/$p70^{S6K}$ pathway may enable the discovery of new therapeutic intervention strategies to prevent unwanted bone marrow adipogenesis associated with diseases, such as diabetes mellitus, where bone health is impaired**.**

6 Final Discussion and Future Directions

6.1 Final discussion

Diabetic osteopathy as a complication of diabetes mellitus has undoubtedly gained increasing awareness amongst clinicians and researchers in the last two decades. The programme of research described in this thesis was borne out of an appetite to understand if skeletal fragility affects the paediatric population with Type 1 diabetes (T1D) and the contribution of bone microarchitecture and the intriguing bone-fat balance hypothesis to diabetic osteopathy.

Using novel technique of high-resolution MRI (3T) to image bones in children with T1D, the findings in this thesis add to the current body of evidence in this field, with original results that address the knowledge gap. Findings from Chapter 4 showed that children with T1D demonstrated deficit in bone microarchitecture compared to their healthy age- and gender-matched peers, novel to the current knowledge base. Across all the paediatric age group, children with T1D have lower trabecular bone volume fraction, which was the primary hypothesis of the study. The deleterious effect of T1D on trabecular bone microarchitecture has been shown, not only in mouse models of T1D using microCT (Nyman *et al.* 2011), but also in adults with T1D from pQCT studies (Shanbhogue *et al.* 2015). Abdalrahaman et al. performed the first MRI-based assessment of bone microarchitecture in young adults with T1D which concluded similarly of trabecular deficits (Abdalrahaman *et al.* 2015), but this was contradicted by histomorphometry findings (Armas *et al.* 2012). Armas et al. showed no abnormalities in trabecular bone on histomorphometry and microCT specimens in a small cohort of adults with T1D, although the study may not be sufficiently powered to detect the differences with a small sample size of 18 cases (Armas *et al.* 2012). In addition, the study in Chapter 4 found that the trabecular deficits were present early, within 10 years from T1D diagnosis. Comparatively, decrease in trabecular bone volume fraction was noted by 10 weeks of T1D diagnosis in mouse models (Nyman *et al.* 2011), which is equivalent to 20 human years, supporting the need to intervene early for bone health optimisation.

Intuitively, chronic hyperglycaemia and insulin deficiency have been implicated in the pathogenicity of diabetic osteopathy, along with the complex interplay of GH/IGF-1 pathway inactivity, increased marrow adiposity, chronic inflammation and vasculopathy as detailed in section 1.5.3. The study in Chapter 4 contributed to an improved understanding

of the possible mechanisms for diabetic bone loss. Chronic hyperglycaemia, as reflected by high HbA1c, was significantly associated with reduced bone formation. This is in line with experimental and animal models of type 1 diabetes (T1D) (Rico *et al.* 1989, Verhaeghe *et al.* 1990), and consistent with clinical studies reporting a reduction in biochemical markers of bone formation (Gunczler *et al.* 1998, Pater *et al.* 2010, Starup-Linde *et al.* 2014).

The other novel finding in Chapter 4 was the effect of acidosis at initial T1D presentation on lower bone formation marker suggesting the additional programming effect of either sustained hyperglycaemia, or acidosis on skeletal development. Acidosis has been shown to affect bone homeostasis (Topaloglu *et al.* 2005) and may also have an effect on mesenchymal stem cell differentiation (Guntur *et al.* 2018). In addition to reduced bone formation, children with T1D also have reduced bone resorption as described in section 1.5.5.1, further confirming the low bone turnover seen in T1D (Campos Pastor *et al.* 2000, Moyer-Mileur *et al.* 2008, Starup-Linde *et al.* 2014, Shanbhogue *et al.* 2015). This may reflect functional growth hormone resistance as outlined in section 1.5.3.2, although the study found no difference in circulating IGF-1 levels in T1D compared to healthy controls. However, the inverse association between serum ALS and the apparent trabecular bone volume fraction found in this study highlighted a role for the GH/IGF-1 pathway in diabetic osteopathy, which the study was not specifically powered to look for. Bone turnover markers have been known to correlate with bone deficit and predicted fragility fractures (Szulc and Delmas 2008) with IGF-1 reported as a fracture predictor in post-menopausal women with T2D independent of BMD. Further studies with larger sample size are needed to evaluate the validity of IGF-1 as an independent fracture predictor for T1D and to better understand the contribution of the GH/IGF-1 pathway in this condition.

Vasculopathy has been strongly implicated in the pathogenesis of diabetic bone loss as detailed in section 1.5.3.6., with the direct effect of bone microangiopathy and the reduction of blood flow on mesenchymal stem cell differentiation. The independent association of microvascular complications with reduced BMD and increased fracture risk in T1D is well established (Ivers *et al.* 2001, Miao *et al.* 2005, Vestergaard 2007, Weber *et al.* 2015). In addition, clinical studies have demonstrated that the presence of associated microvascular complications, such as retinopathy and nephropathy, are significantly associated with adverse cortical and trabecular bone microarchitecture in individuals with T1D, rather than having T1D on its own (Abdalrahaman *et al.* 2015, Shanbhogue *et al.* 2015). The study in Chapter 4 looked at this association and found no difference in the bone microarchitecture

in the T1D children with and without microvascular complications, primarily limited by the very small number of children who have developed retinopathy or nephropathy by this point.

The other possible explanations for bone deficit in T1D include sclerostin-mediated inhibition of bone formation, as detailed in section 1.5.5.1. Sclerostin, produced almost exclusively by osteocytes, is an inhibitor of the canonical Wnt/β-catenin signalling pathway involved in bone formation, thus playing an essential role in osteoblast differentiation and bone turnover (Baron and Kneissel 2013). Many studies have found higher sclerostin levels in T1D individuals (Catalano *et al.* 2014, Neumann *et al.* 2014), with overexpression of sclerostin causing osteopenia in mouse models (Baron and Kneissel 2013). Although sclerostin was measured in children with T1D in the study in Chapter 4, the interpretation of this was limited by not measuring the levels in the healthy controls and the paucity of normative data for sclerostin in this age range. An inverse relationship was found between sclerostin and the age of T1D diagnosis. Children who were younger at T1D diagnosis had higher sclerostin levels, as well as higher bone resorption, which may adversely affect their bone health. Manifestation of T1D at an early age has been shown to negatively impact bone development (Bechtold *et al.* 2006). This may suggest a predisposing variant, the so-called 'more aggressive' T1D lending to poorer long-term outcomes, rather than chronic metabolic consequences of the disease, or duration of disease on the bones. The duration of diabetes has, however, been shown to positively correlate with higher sclerostin levels, potentially impairing bone health and increasing fracture risk (Catalano *et al.* 2014). The study in Chapter 4 did not find any association between sclerostin levels and bone microarchitecture. Interestingly, sclerostin levels have been shown to be inversely associated with fracture in T1D individuals, in that, those with the highest tertile of sclerostin having a markedly reduced (by 81%) risk of fracture compared with those in the lowest tertile (Starup-Linde *et al.* 2016). This is counterintuitive and remains unexplained. The reproducibility of that study or further mechanistic explanation has yet to be seen.

Ultimately, the most important consequence of diabetic bone loss is fractures with a significant cost to the individual and health economy as a whole, not to mention early onset osteoporosis which also impacts on quality of life. The stimulation for this thesis was the lack of understanding of whether skeletal fragility affects the paediatric population with Type 1 diabetes (T1D), especially given the fact that childhood and adolescents are the peak ages for both the: 1) diagnosis of T1D and the 2) attainment of peak bone mass. Since this work began in 2014, Weber et al. demonstrated in 2015 in a large population-based study that the increased risk of fractures in T1D did not only affect adults, but began in childhood

and extended across the life span (Weber *et al.* 2015). The clinical study in Chapter 4 confirmed this finding that children with T1D have higher incident fractures compared to their healthy age- and gender-matched peers. Children who fractured had poorer glycaemic control, although HbA1c were not associated with any of the trabecular bone parameters suggesting a complex link between glycaemic control, bone formation and bone microarchitecture. More recent studies, however, have shown an inverse association between trabecular bone microarchitecture and HbA1c in individuals with T2D (de Waard *et al.* 2018, Karim *et al.* 2018) although this relationship was not found in young adults with T1D (Abdalrahaman *et al.* 2015). The absence of a relationship between the bone parameters and HbA1c also beckons the need to explore other markers of glycation such as pentosidine. Indeed, Granke et al found that the fracture toughness of bone were negatively associated with pentosidine levels (Granke *et al.* 2015), a well-known advanced glycation end (AGE) product found in diabetic patients, which may marry better the link between hyperglycaemia, bone microstructure and fractures. Children who fractured also had lower total body BMD. Given that fractures were associated with total body BMD but not lumbar spine BMD, and an association between the deficits in trabecular bone microarchitecture and fractures was not observed, there may be a need to investigate cortical parameters to better understand bone health in T1D as previously done in adults with T1D (Lettgen *et al.* 1995). A larger cohort study is warranted for more detailed investigations of T1D characteristics and its association with bone microarchitecture in individuals with T1D.

This is the first study to demonstrate a deficit in MRI-based trabecular deficit in children with T1D, contributing not only new findings to the current knowledge base but also evidence of the feasibility of using this non-invasive technique in children in clinical studies. As discussed in section 1.5.6.1.1, although evidence have universally shown reduction in BMD in adults and children with T1D, there is a considerable overlap in BMD values in patients with and without fragility fractures. Specifically, the work in this thesis showed reduction in BMD in T1D children who fractured but did not discover any evidence of an association between bone microarchitecture variables and DXA-derived bone mineral density, for reasons as described in the previous paragraph. MRI-based assessment is free from ionising radiation, as compared to DXA, rendering it superior especially for repeated measurements in prospective clinical trials to further explore the association of clinical markers of T1D, 3D-volumetric density and the different compartments of bone, including trabecular and cortical bones, especially in children.

Additionally, MRI provides the unique imaging modality to study bone marrow adiposity, given that the bone marrow is home to pluripotent mesenchymal stem cells capable of differentiating into osteoblasts and adipocytes. The bone-fat hypothesis suggested thatadipogenesis in the marrow occurs at the expense osteogenesis, which has been shown *in vitro* in mouse and human cells and *in vivo* in mouse models but not in clinical trials in T2D, as detailed in section 1.5.3.4. The study in Chapter 4 supported this mechanism through the negative association of trabecular number with marrow fat fraction, and a corresponding positive association of trabecular separation with marrow fat fraction, when the whole cohort with and without T1D was analysed. This is the first study to demonstrate an association of marrow adiposity and MRI-based bone microarchitecture. Previous studies have shown a similar inverse association between marrow adiposity with pQCT-based trabecular and cortical parameters in obesity (Bredella *et al.* 2012) and DXA-based BMDs in a healthy population (Shen *et al.* 2012a, Shen *et al.* 2012b). However, similar to the only study to date looking at BMA in T1D, this study found a non-significant increase in BMA in individuals with T1D compared to controls. Additionally, there were no association between BMA and glycaemic control, markers of GH/IGF-1 axis, bone turnover markers, or BMD. Poor glycaemic control has been shown to be associated with increased bone marrow adiposity in T2D (Baum *et al.* 2012), where hyperglycaemia diverts the differentiation of mesenchymal stem cells towards adipogenesis (Wang *et al.* 2014). A recent study published, however, demonstrated that adipocytes readily accumulated in the bone marrow of individuals with T2D compared than controls (Ferland-McCollough *et al.* 2018). Unfortunately, our study was limited in its exploration of the bone marrow adiposity by the cross-sectional design and its small sample size, which was not powered to study these associations. With an increasing direct link between BMA with bone strength (Karampinos *et al.* 2015) and BMA with fracture risk (Patsch *et al.* 2013b), it would be critical to explore the role of marrow adiposity in future larger prospective cohort studying diabetic osteopathy.

The ability of metformin on a molecular level to manipulate the differentiation of mesenchymal stem cell (MSC) differentiation may be key to the clinical findings of reduced fracture risk in T2D individuals on this medication. The work in this thesis in Chapter 5 studied the effects of metformin on commercially available murine MSCs and found that metformin promoted osteogenesis with reciprocal suppression of adipogenesis, further affirming the bone-fat balance. This is similar to the findings of Molineuvo et al. demonstrating a positive osteogenic effect of metformin on rat bone marrow progenitor cells, with partial suppression of adipogenesis (Molinuevo *et al.* 2010). More importantly, a recent study had demonstrated that metformin also promotes osteogenesis in human bone-marrow

derived MSCs (Wang *et al.* 2018). Although bone-marrow derived human MSCs can be commercially purchased, these are expensive. Primary human MSCs are less readily available, and can be harvested from bone marrow, periosteum, adipose tissue, amniotic fluid and fetal tissues. Adipose tissue MSCs are seen as most easily available from liposuction procedures or bariatric surgery. However, despite the fact that these can be phenotypically similar, they display heterogeneity in differentiation potential compared to bone-marrow derived MSCs (Pittenger *et al.* 1999, Anker *et al.* 2003), hence are not readily interchangeable. Moreover, the challenge remains in identifying factors that promote specific osteogenic and adipogenic commitment of humans MSCs, which is different from that of mouse MSCs (Marie and Fromigue 2006). Primary human MSCs also take longer to grow and achieve confluency for induction of differentiation, taking approximately 4 times longer than the choice of C3H10T1/2 murine MSCs at each subculture (Charbord *et al.* 2011). Interestingly, metformin appeared to have a negative angiogenic potential on human mesenchymal stem cells, which may potentially negate its positive skeletal effects (Montazersaheb *et al.* 2018).

The effect of metformin on adipogenesis in MSCs has been less well studied (Molinuevo *et al.* 2010, Shin *et al.* 2013). Molineuvo et al found that metformin promoted early markers of adipogenesis with lipid droplet accumulation on ORO but no PPARγ expression (Molinuevo *et al.* 2010). Data from the experiments in Chapter 5 demonstrated that metformin inhibited adipogenesis through suppression of adipogenic transcription factor PPARγ expression level and transcriptional activity, through AMPK-dependent and independent signalling pathways. The AMPK independent signalling pathway of metformin on adipogenesis, through suppression of mTOR/p70s6K is novel and adds to the current body of literature with new targets for therapeutic potentials. In osteogenesis, however, metformin has been extensively shown to act through AMPK activation. Previous studies in 3T3-L1 pre-adipocytes demonstrated that metformin behaved in a biphasic manner with dose dependency in adipogenic differentiation (Chen *et al.* 2018). Lower concentrations of metformin (1.25-2.5mM) induced adipogenesis, mediated in an AMPK-independent manner, while higher concentrations of metformin (5-10mM) inhibited adipogenesis via AMPK activation (Chen *et al.* 2018). The experiments in Chapter 5 were primarily a proof of concept study which demonstrated the positive osteogenic and negative adipogenic effects of metformin at 10mM. This poses translational difficulty due to that being a supraphysiological dose of metformin in human, which is 100 folds the current therapeutic dose of 1g twice daily in the treatment of T2D.

Metformin is not infrequently used in T1D to improve insulin sensitivity and reduce insulin dose requirement with marginal effects on glycaemic control (Vella *et al.* 2010). A recent randomised controlled trial has shown the additional cardiovascular benefits of metformin in reducing atherosclerosis progression, LDL-cholesterol and weight in adults with T1D (Petrie *et al.* 2017). With the increasing use of metformin in T1D, it would be conveniently advantageous given that metformin confers a bone protective role on a molecular level. To date, no studies have been published specifically studying the benefits of metformin on bone health. A prospective cohort study is warranted given the therapeutic potentials of metformin, a cheap and safe drug, in addressing the skeletal fragility in T1D.

6.2 Future directions

This thesis has opened up some intriguing avenues for further research, based on some of the limitations of the studies identified as well as new findings from the work. From the limitations of the current work, studies with larger sample sizes are needed to better understand the associations of the clinical characteristics of T1D, such as HbA1c, age at diagnosis, duration of disease and the presence of other microvascular complications, with bone microarchitecture and fractures. It would not be unreasonable to suggest that all intervention studies in diabetes should include some assessment of bone health amongst the secondary outcomes that are assessed.

In my opinion, future interventions to manage and prevent diabetic osteopathy lie in understanding the underlying principles of diabetes induced bone loss. The lack of an overt link between glycaemic control, surrogated by HbA1c, and bone microarchitecture and marrow adiposity highlighted the need to look at other ways chronic hyperglycaemia could detriment bone. As mentioned, it would be worth exploring the relationship of other glycation products such as pentosidine, a well-known advanced glycation end-product in diabetes, particularly as this has been linked to the structural integrity of bone (Granke *et al.* 2015). In the last decade, glycaemic variability has also become the new subject of contention in interpreting the glycaemic control of individuals with diabetes. Highly variable glucose levels have been implicated as an independent risk factor for developing diabetes-related microvascular complications (Brownlee and Hirsch 2006). It has also been associated with macrovascular complications, with worse cardiovascular outcomes in both T1D (Jun *et al.* 2019) and T2D (Benalia *et al.* 2019). With similar HbA1c, individuals with diabetes could have very different glycaemic variability, depending on the extent of their blood glucose excursions. Therefore, understanding the contribution of advanced-glycation end protein and glycaemic variability on the bone microarchitecture may improve the understanding of the effects of hyperglycaemia on skeletal fragility in diabetes, with potential therapeutic implications.

Given that the trabecular bone microarchitecture at the proximal tibia was not significantly different between the fracture and the non-fracture group, this suggests a need to examine the cortical bone architecture in more detail in this condition. Further investigations of cortical bone parameters by using MRI could add mechanistic insights into the pathophysiology of diabetic bone loss in particular looking at its relationship to bone marrow adiposity as well. In addition to exploring different bone compartments, imaging a different

skeletal site such as the hip may be more informative, given that hip fractures are the most common fragility fracture affecting adults with T1D. Future studies should focus on pulse sequences for MR image acquisition from the neck of femur, with thicker cortical bone ideal for better characterisation in this condition. Furthermore, the feasibility of 7T-MR imaging at the hip has been demonstrated with promising results (Chang *et al.* 2014).

With metformin being a promising therapeutic option for bone protection in diabetes mellitus, a prospective longitudinal clinical trial with defined musculoskeletal outcomes should be explored to demonstrate efficacy, determine optimum dose, and possibility a minimum duration of exposure necessary for clinical benefit. This is especially pertinent as bone microarchitecture abnormalities are already observed in the paediatric age group and metformin is not licensed for use in children under 10 years of age. The adult REMOVAL (Reducing with MetfOrmin Vascular Adverse Lesions) cohort (Petrie *et al.* 2017), which was randomised to 3 years of metformin treatment would provide an ideal starting platform to study the effects of metformin of the bone microarchitecture of individuals with T1D, with the limitation of absent baseline imaging prior to treatment. By incorporating dynamic contrast enhanced (DCE) MRI (Tofts 1997, Radjenovic *et al.* 2008), the effect of metformin on bone marrow vascularity could also be studied given the potential unwanted anti-angiogenic potential of this drug (Montazersaheb *et al.* 2018).

List of References

Abdalrahaman, N., McComb, C., Foster, J. E., Lindsay, R. S., Drummond, R., McKay, G. A., Perry, C. G. and Ahmed, S. F. (2017) 'The relationship between adiposity, bone density and microarchitecture is maintained in young women irrespective of diabetes status', *Clin Endocrinol (Oxf)*, 87(4), 327-335.

Abdalrahaman, N., McComb, C., Foster, J. E., McLean, J., Lindsay, R. S., McClure, J., McMillan, M., Drummond, R., Gordon, D., McKay, G. A., Shaikh, M. G., Perry, C. G. and Ahmed, S. F. (2015) 'Deficits in Trabecular Bone Microarchitecture in Young Women With Type 1 Diabetes Mellitus', *J Bone Miner Res*, 30(8), 1386-93.

Abdalrahman, N., Chen, S. C., Wang, J. R. and Ahmed, S. F. (2015) 'An update on diabetes related skeletal fragility', *Expert Review of Endocrinology & Metabolism*, 10(2), 193-210.

Adami, S. (2009) 'Bone health in diabetes: considerations for clinical management', *Curr Med Res Opin*, 25(5), 1057-72.

Ahmed, L. A., Joakimsen, R. M., Berntsen, G. K., Fonnebo, V. and Schirmer, H. (2006) 'Diabetes mellitus and the risk of non-vertebral fractures: the Tromso study', *Osteoporos Int*, 17(4), 495-500.

Ahmed, S. F., Horrocks, I. A., Patterson, T., Zaidi, S., Ling, S. C., McGrogan, P. and Weaver, L. T. (2004) 'Bone Mineral Assessment by Dual Energy X-ray Absorptiometry in Children With Inflammatory Bowel Disease: Evaluation by Age or Bone Area', *Journal of Pediatric Gastroenterology and Nutrition*, 38, 276-281.

Ahmed, S. F., Horrocks, I. A., Patterson, T., Zaidi, S., Ling, S. C., McGrogan, P. and Weaver, L. T. (2004) 'Bone mineral assessment by dual energy X-ray absorptiometry in children with inflammatory bowel disease: evaluation by age or bone area', *J Pediatr Gastroenterol Nutr*, 38(3), 276-80.

Alexopoulou, O., Jamart, J., Devogelaer, J. P., Brichard, S., de Nayer, P. and Buysschaert, M. (2006) 'Bone density and markers of bone remodeling in type 1 male diabetic patients', *Diabetes Metab*, 32(5 Pt 1), 453-8.

Ali, A. A., Weinstein, R. S., Stewart, S. A., Parfitt, A. M., Manolagas, S. C. and Jilka, R. L. (2005) 'Rosiglitazone causes bone loss in mice by suppressing osteoblast differentiation and bone formation', *Endocrinology*, 146(3), 1226-35.

Allard, S. and Kopish, K. (2008) 'Luciferase reporter assays:powerful, adaptable tools for cell biology research', *Cell Notes*, 21, 23-26.

Ammann, P. and Rizzoli, R. (2003) 'Bone strength and its determinants', *Osteoporos Int*, 14 Suppl 3, S13-8.

Andersen, A. R., Christiansen, J. S., Andersen, J. K., Kreiner, S. and Deckert, T. (1983) 'Diabetic nephropathy in Type 1 (insulin-dependent) diabetes: an epidemiological study', *Diabetologia*, 25(6), 496-501.

Anderson, L. and Seilhamer, J. (1997) 'A comparison of selected mRNA and protein abundances in human liver', *Electrophoresis*, 18(3-4), 533-7.

Anker, P. S. I., Noort, W. A., Scherjon, S. A., Kleuburg-van der Keur, C., Kruisselbrink, A. B., van Bezoolien, R. L., Beekhuizen, W., Willemze, R., Kanhai, H. H. H. and Fibbe, W. E. (2003) 'Mesenchymal stem cells in human second-trimester bone marrow, liver, lung, and spleen exhibit a similar immunophenotype but a heterogeneous multilineage differentiation potential', *Haematologica*, 88(8), 845-852.

Ardawi, M. S., Akhbar, D. H., Alshaikh, A., Ahmed, M. M., Qari, M. H., Rouzi, A. A., Ali, A. Y., Abdulrafee, A. A. and Saeda, M. Y. (2013) 'Increased serum sclerostin and decreased

serum IGF-1 are associated with vertebral fractures among postmenopausal women with type-2 diabetes', *Bone*, 56(2), 355-62.

Ardawi, M. S., Rouzi, A. A., Al-Sibiani, S. A., Al-Senani, N. S., Qari, M. H. and Mousa, S. A. (2012) 'High serum sclerostin predicts the occurrence of osteoporotic fractures in postmenopausal women: the Center of Excellence for Osteoporosis Research Study', *J Bone Miner Res*, 27(12), 2592-602.

Arlot, M. E., Sornay-Rendu, E., Garnero, P., Vey-Marty, B. and Delmas, P. D. (1997) 'Apparent pre- and postmenopausal bone loss evaluated by DXA at different skeletal sites in women: the OFELY cohort', *J Bone Miner Res*, 12(4), 683-90.

Armas, L. A., Akhter, M. P., Drincic, A. and Recker, R. R. (2012) 'Trabecular bone histomorphometry in humans with Type 1 Diabetes Mellitus', *Bone*, 50(1), 91-6.

Ausubel, F., Brent, R., Kingston, R., Moore, D., Seidman, J., Smith, J. and Struhl, K. (2003) *Current Protocols in Molecular Biology*, Wiley & Sons.

Baek, D., Villen, J., Shin, C., Camargo, F. D., Gygi, S. P. and Bartel, D. P. (2008) 'The impact of microRNAs on protein output', *Nature*, 455(7209), 64-71.

Bailey, C. J. and Turner, R. C. (1996) 'Metformin', *N Engl J Med*, 334(9), 574-9.

Bailey, D. A., McKay, H. A., Mirwald, R. L., Crocker, P. R. and Faulkner, R. A. (1999) 'A six-year longitudinal study of the relationship of physical activity to bone mineral accrual in growing children: the university of Saskatchewan bone mineral accrual study', *J Bone Miner Res*, 14(10), 1672-9.

Bainbridge, K. E., Hoffman, H. J. and Cowie, C. C. (2008) 'Diabetes and hearing impairment in the United States: audiometric evidence from the National Health and Nutrition Examination Survey, 1999 to 2004', *Ann Intern Med*, 149(1), 1-10.

Bajaj, D., Allerton, B. M., Kirby, J. T., Miller, F., Rowe, D. A., Pohlig, R. T. and Modlesky, C. M. (2015) 'Muscle volume is related to trabecular and cortical bone architecture in typically developing children', *Bone*, 81, 217-227.

Balint, E., Szabo, P., Marshall, C. F. and Sprague, S. M. (2001) 'Glucose-induced inhibition of in vitro bone mineralization', *Bone*, 28(1), 21-8.

Bandirali, M., Di Leo, G., Papini, G. D., Messina, C., Sconfienza, L. M., Ulivieri, F. M. and Sardanelli, F. (2015) 'A new diagnostic score to detect osteoporosis in patients undergoing lumbar spine MRI', *Eur Radiol*, 25(10), 2951-9.

Banerjee, C., McCabe, L. R., Choi, J. Y., Hiebert, S. W., Stein, J. L., Stein, G. S. and Lian, J. B. (1997) 'Runt homology domain proteins in osteoblast differentiation: AML3/CBFA1 is a major component of a bone-specific complex', *Journal of Cellular Biochemistry*, 66(1), 1-8.

Bang, S., Chen, Y., Ahima, R. S. and Kim, S. F. (2014) 'Convergence of IPMK and LKB1-AMPK signaling pathways on metformin action', *Mol Endocrinol*, 28(7), 1186-93.

Barbagallo, I., Vanella, A., Peterson, S. J., Kim, D. H., Tibullo, D., Giallongo, C., Vanella, L., Parrinello, N., Palumbo, G. A., Di Raimondo, F., Abraham, N. G. and Asprinio, D. (2010) 'Overexpression of heme oxygenase-1 increases human osteoblast stem cell differentiation', *J Bone Miner Metab*, 28(3), 276-88.

Baron, R. and Kneissel, M. (2013) 'WNT signaling in bone homeostasis and disease: from human mutations to treatments', *Nature Medicine*, 19(2), 179-92.

Baroncelli, G. I., Bertelloni, S., Ceccarelli, C., Cupelli, D. and Saggese, G. (2000) 'Dynamics of bone turnover in children with GH deficiency treated with GH until final height', *Eur J Endocrinol*, 142(6), 549-56.

Baroncelli, G. I., Federico, G., Bertelloni, S., de Terlizzi, F., Cadossi, R. and Saggese, G. (2001) 'Bone quality assessment by quantitative ultrasound of proximal phalanxes of the hand in healthy subjects aged 3--21 years', *Pediatr Res*, 49(5), 713-8.

Baum, T., Yap, S. P., Karampinos, D. C., Nardo, L., Kuo, D., Burghardt, A. J., Masharani, U. B., Schwartz, A. V., Li, X. J. and Link, T. M. (2012) 'Does vertebral bone marrow fat content correlate with abdominal adipose tissue, lumbar spine bone mineral density, and blood biomarkers in women with type 2 diabetes mellitus?', *Journal of Magnetic Resonance Imaging*, 35(1), 117-124.

Baxter-Jones, A. D., Faulkner, R. A., Forwood, M. R., Mirwald, R. L. and Bailey, D. A. (2011) 'Bone mineral accrual from 8 to 30 years of age: an estimation of peak bone mass', *J Bone Miner Res*, 26(8), 1729-39.

Baxter-Jones, A. D., Kontulainen, S. A., Faulkner, R. A. and Bailey, D. A. (2008) 'A longitudinal study of the relationship of physical activity to bone mineral accrual from adolescence to young adulthood', *Bone*, 43(6), 1101-7.

Baxter-Jones, A. D., Mirwald, R. L., McKay, H. A. and Bailey, D. A. (2003) 'A longitudinal analysis of sex differences in bone mineral accrual in healthy 8-19-year-old boys and girls', *Ann Hum Biol*, 30(2), 160-75.

Bechtold, S., Dirlenbach, I., Raile, K., Noelle, V., Bonfig, W. and Schwarz, H. P. (2006) 'Early manifestation of type 1 diabetes in children is a risk factor for changed bone geometry: data using peripheral quantitative computed tomography', *Pediatrics*, 118(3), e627-34.

Bechtold, S., Putzker, S., Bonfig, W., Fuchs, O., Dirlenbach, I. and Schwarz, H. P. (2007) 'Bone size normalizes with age in children and adolescents with type 1 diabetes', *Diabetes Care*, 30(8), 2046-50.

Bellido T, P. L., Bruzzaniti A (2014) 'Bone cells' in MR, B. D. a. A., ed., *Basic and Applied Bone Biology*Academic Press, 37-38.

Benalia, M., Zeller, M., Mouhat, B., Guenancia, C., Yameogo, V., Greco, C., Yao, H., Maza, M., Verges, B. and Cottin, Y. (2019) 'Glycaemic variability is associated with severity of coronary artery disease in patients with poorly controlled type 2 diabetes and acute myocardial infarction', *Diabetes Metab*.

Bending, D., Zaccone, P. and Cooke, A. (2012) 'Inflammation and type one diabetes', *Int Immunol*, 24(6), 339-46.

Beresford, J. N., Bennett, J. H., Devlin, C., Leboy, P. S. and Owen, M. E. (1992) 'Evidence for an Inverse Relationship between the Differentiation of Adipocytic and Osteogenic Cells in Rat Marrow Stromal Cell-Cultures', *Journal of Cell Science*, 102, 341-351.

Bergot, C., Laval-Jeantet, A. M., Hutchinson, K., Dautraix, I., Caulin, F. and Genant, H. K. (2001) 'A comparison of spinal quantitative computed tomography with dual energy X-ray absorptiometry in European women with vertebral and nonvertebral fractures', *Calcif Tissue Int*, 68(2), 74-82.

Berry, R. and Rodeheffer, M. S. (2013) 'Characterization of the adipocyte cellular lineage in vivo', *Nature Cell Biology*, 15(3), 302-308.

Bhattoa, H. P., Onyeka, U., Kalina, E., Balogh, A., Paragh, G., Antal-Szalmas, P. and Kaplar, M. (2013) 'Bone metabolism and the 10-year probability of hip fracture and a major osteoporotic fracture using the country-specific FRAX algorithm in men over 50 years of age with type 2 diabetes mellitus: a case-control study', *Clin Rheumatol*, 32(8), 1161-7.

Bianco, P., Riminucci, M., Gronthos, S. and Robey, P. G. (2001) 'Bone marrow stromal stem cells: nature, biology, and potential applications', *Stem Cells*, 19(3), 180-92.

Biggin, A., Briody, J. N., Ramjan, K. A., Middleton, A., Waugh, M. C. and Munns, C. F. (2013) 'Evaluation of bone mineral density and morphology using pQCT in children after spinal cord injury', *Dev Neurorehabil*, 16(6), 391-7.

Biggs, J. R., Peterson, L. F., Zhang, Y., Kraft, A. S. and Zhang, D. E. (2006) 'AML1/RUNX1 phosphorylation by cyclin-dependent kinases regulates the degradation of AML1/RUNX1 by the anaphase-promoting complex', *Mol Cell Biol*, 26(20), 7420-9.

Bilezikian, J. P., Watts, N. B., Usiskin, K., Polidori, D., Fung, A., Sullivan, D. and Rosenthal, N. (2016) 'Evaluation of Bone Mineral Density and Bone Biomarkers in Patients With Type 2 Diabetes Treated With Canagliflozin', *J Clin Endocrinol Metab*, 101(1), 44-51.

Bishop, N., Arundel, P., Clark, E., Dimitri, P., Farr, J., Jones, G., Makitie, O., Munns, C. F., Shaw, N. and International Society of Clinical, D. (2014) 'Fracture prediction and the definition of osteoporosis in children and adolescents: the ISCD 2013 Pediatric Official Positions', *J Clin Densitom*, 17(2), 275-80.

Bjerg, L., Hulman, A., Charles, M., Jorgensen, M. E. and Witte, D. R. (2018) 'Clustering of microvascular complications in Type 1 diabetes mellitus', *J Diabetes Complications*, 32(4), 393-399.

Black, D. M., Greenspan, S. L., Ensrud, K. E., Palermo, L., McGowan, J. A., Lang, T. F., Garnero, P., Bouxsein, M. L., Bilezikian, J. P., Rosen, C. J. and Pa, T. H. S. I. (2003) 'The effects of parathyroid hormone and alendronate alone or in combination in postmenopausal osteoporosis', *N Engl J Med*, 349(13), 1207-15.

Blink, E. (2004) *Basic MRI: Physics* [online], available: http://mri-physics.net/bin/mri-physics-en-rev1.3.pdf.

Blumsohn, A., Hannon, R. A., Wrate, R., Barton, J., al-Dehaimi, A. W., Colwell, A. and Eastell, R. (1994) 'Biochemical markers of bone turnover in girls during puberty', *Clin Endocrinol (Oxf)*, 40(5), 663-70.

Bohlender, J. M., Franke, S., Stein, G. and Wolf, G. (2005) 'Advanced glycation end products and the kidney', *American Journal of Physiology-Renal Physiology*, 289(4), F645-F659.

Bolinder, J., Ljunggren, O., Johansson, L., Wilding, J., Langkilde, A. M., Sjostrom, C. D., Sugg, J. and Parikh, S. (2014) 'Dapagliflozin maintains glycaemic control while reducing weight and body fat mass over 2 years in patients with type 2 diabetes mellitus inadequately controlled on metformin', *Diabetes Obes Metab*, 16(2), 159-69.

Bonds, D. E., Larson, J. C., Schwartz, A. V., Strotmeyer, E. S., Robbins, J., Rodriguez, B. L., Johnson, K. C. and Margolis, K. L. (2006) 'Risk of fracture in women with type 2 diabetes: the Women's Health Initiative Observational Study', *J Clin Endocrinol Metab*, 91(9), 3404-10.

Bonewald, L. F. and Mundy, G. R. (1990) 'Role of transforming growth factor-beta in bone remodeling', *Clin Orthop Relat Res*, (250), 261-76.

Borges, J. L., Bilezikian, J. P., Jones-Leone, A. R., Acusta, A. P., Ambery, P. D., Nino, A. J., Grosse, M., Fitzpatrick, L. A. and Cobitz, A. R. (2011) 'A randomized, parallel group, double-blind, multicentre study comparing the efficacy and safety of Avandamet (rosiglitazone/metformin) and metformin on long-term glycaemic control and bone mineral density after 80 weeks of treatment in drug-naive type 2 diabetes mellitus patients', *Diabetes Obes Metab*, 13(11), 1036-46.

Botolin, S., Faugere, M. C., Malluche, H., Orth, M., Meyer, R. and McCabe, L. R. (2005) 'Increased bone adiposity and peroxisomal proliferator-activated receptor-gamma 2 expression in type I diabetic mice', *Endocrinology*, 146(8), 3622-3631.

Botolin, S. and McCabe, L. R. (2006) 'Chronic hyperglycemia modulates osteoblast gene expression through osmotic and non-osmotic pathways', *Journal of Cellular Biochemistry*, 99(2), 411-24.

Botolin, S. and McCabe, L. R. (2007) 'Bone loss and increased bone adiposity in spontaneous and pharmacologically induced diabetic mice', *Endocrinology*, 148(1), 198-205.

Bouillon, R., Bex, M., Van Herck, E., Laureys, J., Dooms, L., Lesaffre, E. and Ravussin, E. (1995) 'Influence of age, sex, and insulin on osteoblast function: osteoblast dysfunction in diabetes mellitus', *J Clin Endocrinol Metab*, 80(4), 1194-202.

Boutroy, S., Bouxsein, M. L., Munoz, F. and Delmas, P. D. (2005) 'In vivo assessment of trabecular bone microarchitecture by high-resolution peripheral quantitative computed tomography', *J Clin Endocrinol Metab*, 90(12), 6508-15.

Bouxsein, M. L., Rosen, C. J., Turner, C. H., Ackert, C. L., Shultz, K. L., Donahue, L. R., Churchill, G., Adamo, M. L., Powell, D. R., Turner, R. T., Muller, R. and Beamer, W. G. (2002) 'Generation of a new congenic mouse strain to test the relationships among serum insulin-like growth factor I, bone mineral density, and skeletal morphology in vivo', *J Bone Miner Res*, 17(4), 570-9.

Brandao, F. R., Vicente, E. J., Daltro, C. H., Sacramento, M., Moreira, A. and Adan, L. (2007) 'Bone metabolism is linked to disease duration and metabolic control in type 1 diabetes mellitus', *Diabetes Res Clin Pract*, 78(3), 334-9.

Bredella, M. A., Lin, E., Gerweck, A. V., Landa, M. G., Thomas, B. J., Torriani, M., Bouxsein, M. L. and Miller, K. K. (2012) 'Determinants of bone microarchitecture and mechanical properties in obese men', *J Clin Endocrinol Metab*, 97(11), 4115-22.

Bridges, M. J., Moochhala, S. H., Barbour, J. and Kelly, C. A. (2005) 'Influence of diabetes on peripheral bone mineral density in men: a controlled study', *Acta Diabetol*, 42(2), 82-6.

Bridgman, S. and Wilson, R. (2004) 'Epidemiology of femoral fractures in children in the West Midlands region of England 1991 to 2001', *J Bone Joint Surg Br*, 86(8), 1152-7.

British Orthopaedic Association (2007) *The Care of Patients with Fragility Fractures*.

Brown, R., Cheng, N., Haacke, M., MR, T. and Venkatesan, R. (2014) *Magnetic resonance imaging: physical principles and sequence design*, 2nd ed., Wiley-Blackwell.

Brownlee, M. and Hirsch, I. B. (2006) 'Glycemic variability: a hemoglobin A1c-independent risk factor for diabetic complications', *JAMA*, 295(14), 1707-8.

Bucala, R. and Vlassara, H. (1995) 'Advanced glycosylation end products in diabetic renal and vascular disease', *American Journal of Kidney Diseases*, 26(6), 875-88.

Buckley, L. and Humphrey, M. B. (2018) 'Glucocorticoid-Induced Osteoporosis', *N Engl J Med*, 379(26), 2547-2556.

Buday, B., Pach, F. P., Literati-Nagy, B., Vitai, M., Vecsei, Z. and Koranyi, L. (2013) 'Serum osteocalcin is associated with improved metabolic state via adiponectin in females versus testosterone in males. Gender specific nature of the bone-energy homeostasis axis', *Bone*, 57(1), 98-104.

Burge, R., Worley, D., Johansen, A., Bhattacharyya, S. and Bose, U. (2001) 'The cost of osteoporotic fractures in the UK: projections for 2000–2020', *Journal of Medical Economics*, 4, 51-62.

Burghardt, A. J., Issever, A. S., Schwartz, A. V., Davis, K. A., Masharani, U., Majumdar, S. and Link, T. M. (2010) 'High-resolution peripheral quantitative computed tomographic imaging of cortical and trabecular bone microarchitecture in patients with type 2 diabetes mellitus', *J Clin Endocrinol Metab*, 95(11), 5045-55.

Burkhardt, R., Moser, W., Bartl, R. and Mahl, G. (1981) 'Is diabetic osteoporosis due to microangiopathy?', *Lancet*, 1(8224), 844.

Burr, D. and Akkus, O. (2014) 'Bone morphology and organization' in Burr, D. A., M., ed., *Basic and Applied Bone Biology*Academic Press, 3-25.

Calvo, M. S., Eyre, D. R. and Gundberg, C. M. (1996) 'Molecular basis and clinical application of biological markers of bone turnover', *Endocr Rev*, 17(4), 333-68.

Camacho, P. M., Petak, S. M., Binkley, N., Clarke, B. L., Harris, S. T., Hurley, D. L., Kleerekoper, M., Lewiecki, E. M., Miller, P. D., Narula, H. S., Pessah-Pollack, R., Tangpricha, V., Wimalawansa, S. J. and Watts, N. B. (2016) 'American Association of Clinical Endocrinologists and American College of Endocrinology Clinical Practice Guidelines for the Diagnosis and Treatment of Postmenopausal Osteoporosis - 2016', *Endocr Pract*, 22(Suppl 4), 1-42.

Cameron, F. J. and Wherrett, D. K. (2015) 'Care of diabetes in children and adolescents: controversies, changes, and consensus', *Lancet*, 385(9982), 2096-106.

Campos Pastor, M. M., Lopez-Ibarra, P. J., Escobar-Jimenez, F., Serrano Pardo, M. D. and Garcia-Cervigon, A. G. (2000) 'Intensive insulin therapy and bone mineral density in type 1 diabetes mellitus: a prospective study', *Osteoporos Int*, 11(5), 455-9.

Canalis, E. (1983) 'Effect of hormones and growth factors on alkaline phosphatase activity and collagen synthesis in cultured rat calvariae', *Metabolism-Clinical and Experimental*, 32(1), 14-20.

Cao, H., Ackerman, J. L., Hrovat, M. I., Graham, L., Glimcher, M. J. and Wu, Y. (2008) 'Quantitative bone matrix density measurement by water- and fat-suppressed proton projection MRI (WASPI) with polymer calibration phantoms', *Magn Reson Med*, 60(6), 1433-43.

Cao, H., Nazarian, A., Ackerman, J. L., Snyder, B. D., Rosenberg, A. E., Nazarian, R. M., Hrovat, M. I., Dai, G., Mintzopoulos, D. and Wu, Y. (2010) 'Quantitative (31)P NMR spectroscopy and (1)H MRI measurements of bone mineral and matrix density differentiate metabolic bone diseases in rat models', *Bone*, 46(6), 1582-90.

Capulli, M., Paone, R. and Rucci, N. (2014) 'Osteoblast and osteocyte: games without frontiers', *Arch Biochem Biophys*, 561, 3-12.

Catalano, A., Pintaudi, B., Morabito, N., Di Vieste, G., Giunta, L., Bruno, M. L., Cucinotta, D., Lasco, A. and Di Benedetto, A. (2014) 'Gender differences in sclerostin and clinical characteristics in type 1 diabetes mellitus', *Eur J Endocrinol*, 171(3), 293-300.

Chamberlain, G., Fox, J., Ashton, B. and Middleton, J. (2007) 'Concise review: Mesenchymal stem cells: Their phenotype, differentiation capacity, immunological features, and potential for homing', *Stem Cells*, 25(11), 2739-2749.

Chang, G., Deniz, C. M., Honig, S., Egol, K., Regatte, R. R., Zhu, Y., Sodickson, D. K. and Brown, R. (2014) 'MRI of the hip at 7T: feasibility of bone microarchitecture, high-resolution cartilage, and clinical imaging', *Journal of Magnetic Resonance Imaging*, 39(6), 1384-93.

Chang, G., Honig, S., Liu, Y., Chen, C., Chu, K. K., Rajapakse, C. S., Egol, K., Xia, D., Saha, P. K. and Regatte, R. R. (2015) '7 Tesla MRI of bone microarchitecture discriminates between women without and with fragility fractures who do not differ by bone mineral density', *J Bone Miner Metab*, 33(3), 285-93.

Charbord, P., Livne, E., Gross, G., Haupl, T., Neves, N. M., Marie, P., Bianco, P. and Jorgensen, C. (2011) 'Human bone marrow mesenchymal stem cells: a systematic reappraisal via the genostem experience', *Stem Cell Rev*, 7(1), 32-42.

Chava, S., Chennakesavulu, S., Gayatri, B. M. and Reddy, A. B. M. (2018) 'A novel phosphorylation by AMP-activated kinase regulates RUNX2 from ubiquitination in osteogenesis over adipogenesis', *Cell Death Dis*, 9(7), 754.

Chavakis, T., Bierhaus, A., Al-Fakhri, N., Schneider, D., Witte, S., Linn, T., Nagashima, M., Morser, J., Arnold, B., Preissner, K.T., Nawroth, P.P. (2003), 'The pattern recognition receptor (RAGE) is a counterreceptor for leukocyte integrins: a novel pathway for inflammatory cell recruitment', *J Exp Med,* 198,1507–1515.

Chen, D., Ji, X., Harris, M. A., Feng, J. Q., Karsenty, G., Celeste, A. J., Rosen, V., Mundy, G. R. and Harris, S. E. (1998) 'Differential roles for bone morphogenetic protein (BMP) receptor

type IB and IA in differentiation and specification of mesenchymal precursor cells to osteoblast and adipocyte lineages', *J Cell Biol*, 142(1), 295-305.

Chen, D., Wang, Y., Wu, K. and Wang, X. (2018) 'Dual Effects of Metformin on Adipogenic Differentiation of 3T3-L1 Preadipocyte in AMPK-Dependent and Independent Manners', *Int J Mol Sci*, 19(6).

Chen, J. and Long, F. (2013) 'beta-catenin promotes bone formation and suppresses bone resorption in postnatal growing mice', *J Bone Miner Res*, 28(5), 1160-9.

Chen, S. C., Brooks, R., Houskeeper, J., Bremner, S. K., Dunlop, J., Viollet, B., Logan, P. J., Salt, I. P., Ahmed, S. F. and Yarwood, S. J. (2017) 'Metformin suppresses adipogenesis through both AMP-activated protein kinase (AMPK)-dependent and AMPK-independent mechanisms', *Mol Cell Endocrinol*, 440, 57-68.

Cheng, X. G., Lowet, G., Boonen, S., Nicholson, P. H., Brys, P., Nijs, J. and Dequeker, J. (1997) 'Assessment of the strength of proximal femur in vitro: relationship to femoral bone mineral density and femoral geometry', *Bone*, 20(3), 213-8.

Cheung, P. C., Salt, I. P., Davies, S. P., Hardie, D. G. and Carling, D. (2000) 'Characterization of AMP-activated protein kinase gamma-subunit isoforms and their role in AMP binding', *Biochem J*, 346 Pt 3, 659-69.

Christiansen, B. A., Kopperdahl, D. L., Kiel, D. P., Keaveny, T. M. and Bouxsein, M. L. (2011) 'Mechanical contributions of the cortical and trabecular compartments contribute to differences in age-related changes in vertebral body strength in men and women assessed by QCT-based finite element analysis', *J Bone Miner Res*, 26(5), 974-83.

Chuang, C. C., Yang, R. S., Tsai, K. S., Ho, F. M. and Liu, S. H. (2007) 'Hyperglycemia enhances adipogenic induction of lipid accumulation: involvement of extracellular signal-regulated protein kinase 1/2, phosphoinositide 3-kinase/Akt, and peroxisome proliferator-activated receptor gamma signaling', *Endocrinology*, 148(9), 4267-75.

Ciarelli, T. E., Fyhrie, D. P., Schaffler, M. B. and Goldstein, S. A. (2000) 'Variations in three-dimensional cancellous bone architecture of the proximal femur in female hip fractures and in controls', *J Bone Miner Res*, 15(1), 32-40.

Cibula, D., Skrenkova, J., Hill, M., Stepan, J.J. 'Low-dose estrogen combined oral contraceptives may negatively influence physiological bone mineral density acquisition during adolescence', *Eur J Endocrinol*, 166,1003-1011

Cipollone, F., Iezzi, A., Fazia, M., Zucchelli, M., Pini, B., Cuccurullo, C., De Cesare, D., De Blasis, G., Muraro, R., Bei, R., Chiarelli, F., Schmidt, A.M., Cuccurullo, F., Mezzetti, A. (2003) 'The receptor RAGE as a progression factor amplifying arachidonate-dependent inflammatory and proteolytic response in human atherosclerotic plaques: role of glycemic control', *Circulation*, 108,1070–1077

Clarke, B. (2008) 'Normal bone anatomy and physiology', *Clin J Am Soc Nephrol*, 3 Suppl 3, S131-9.

Cock, T. A., Back, J., Elefteriou, F., Karsenty, G., Kastner, P., Chan, S. and Auwerx, J. (2004) 'Enhanced bone formation in lipodystrophic PPARgamma(hyp/hyp) mice relocates haematopoiesis to the spleen', *EMBO Rep*, 5(10), 1007-12.

Coe, L. M., Irwin, R., Lippner, D. and McCabe, L. R. (2011a) 'The bone marrow microenvironment contributes to type I diabetes induced osteoblast death', *J Cell Physiol*, 226(2), 477-83.

Coe, L. M., Lippner, D., Perez, G. I. and McCabe, L. R. (2011b) 'Caspase-2 deficiency protects mice from diabetes-induced marrow adiposity', *Journal of Cellular Biochemistry*, 112(9), 2403-11.

Cole, T. J. (1990) 'The LMS method for constructing normalized growth standards', *Eur J Clin Nutr*, 44(1), 45-60.

Colhoun, H. M., Livingstone, S. J., Looker, H. C., Morris, A. D., Wild, S. H., Lindsay, R. S., Reed, C., Donnan, P. T., Guthrie, B., Leese, G. P., McKnight, J., Pearson, D. W., Pearson, E., Petrie, J. R., Philip, S., Sattar, N., Sullivan, F. M., McKeigue, P. and Scottish Diabetes Research Network Epidemiology, G. (2012) 'Hospitalised hip fracture risk with rosiglitazone and pioglitazone use compared with other glucose-lowering drugs', *Diabetologia*, 55(11), 2929-37.

Collette, N. M., Genetos, D. C., Economides, A. N., Xie, L., Shahnazari, M., Yao, W., Lane, N. E., Harland, R. M. and Loots, G. G. (2012) 'Targeted deletion of Sost distal enhancer increases bone formation and bone mass', *Proc Natl Acad Sci U S A*, 109(35), 14092-7.

Conover, C. A., Lee, P. D., Riggs, B. L. and Powell, D. R. (1996) 'Insulin-like growth factor-binding protein-1 expression in cultured human bone cells: regulation by insulin and glucocorticoid', *Endocrinology*, 137(8), 3295-301.

Cool, B., Zinker, B., Chiou, W., Kifle, L., Cao, N., Perham, M., Dickinson, R., Adler, A., Gagne, G., Iyengar, R., Zhao, G., Marsh, K., Kym, P., Jung, P., Camp, H. S. and Frevert, E. (2006) 'Identification and characterization of a small molecule AMPK activator that treats key components of type 2 diabetes and the metabolic syndrome', *Cell Metabolism*, 3(6), 403-416.

Cooper, C., Dennison, E. M., Leufkens, H. G., Bishop, N. and van Staa, T. P. (2004) 'Epidemiology of childhood fractures in Britain: a study using the general practice research database', *J Bone Miner Res*, 19(12), 1976-81.

Cormier, M. J., Lee, J. and Wampler, J. E. (1975) 'Bioluminescence: recent advances', *Annu Rev Biochem*, 44, 255-72.

Cornish, J., Callon, K. E., Bava, U., Lin, C., Naot, D., Hill, B. L., Grey, A. B., Broom, N., Myers, D. E., Nicholson, G. C. and Reid, I. R. (2002) 'Leptin directly regulates bone cell function in vitro and reduces bone fragility in vivo', *J Endocrinol*, 175(2), 405-15.

Cortizo, A. M., Sedlinsky, C., McCarthy, A. D., Blanco, A. and Schurman, L. (2006) 'Osteogenic actions of the anti-diabetic drug metformin on osteoblasts in culture', *Eur J Pharmacol*, 536(1-2), 38-46.

Corton, J. M., Gillespie, J. G., Hawley, S. A. and Hardie, D. G. (1995) '5-aminoimidazole-4-carboxamide ribonucleoside. A specific method for activating AMP-activated protein kinase in intact cells?', *Eur J Biochem*, 229(2), 558-65.

Cosman, F., de Beur, S. J., LeBoff, M. S., Lewiecki, E. M., Tanner, B., Randall, S., Lindsay, R. and National Osteoporosis, F. (2014) 'Clinician's Guide to Prevention and Treatment of Osteoporosis', *Osteoporos Int*, 25(10), 2359-81.

Crabtree, N., Hogler, W., Cooper, M. and Shaw, N. (2013) 'Diagnostic evaluation of bone densitometric size adjustment techniques in children with and without low trauma fractures', *Osteoporosis International*, 24, 2015-2024.

Crabtree, N. J., Arabi, A., Bachrach, L. K., Fewtrell, M., El-Hajj Fuleihan, G., Kecskemethy, H. H., Jaworski, M., Gordon, C. M. and International Society for Clinical, D. (2014) 'Dual-energy X-ray absorptiometry interpretation and reporting in children and adolescents: the revised 2013 ISCD Pediatric Official Positions', *J Clin Densitom*, 17(2), 225-42.

Crofton, P. M., Evans, N., Taylor, M. R. and Holland, C. V. (2002) 'Serum CrossLaps: pediatric reference intervals from birth to 19 years of age', *Clin Chem*, 48(4), 671-3.

Cromer, B.A., Stager, M., Bonny, A., Lazebnik, R., Rome, E., Ziegler, J. Debanne, S.M. (2004) 'Depot medroxyprogesterone acetate, oral contraceptives and bone mineral density in a cohort of adolescent girls', *J Adolesc Health*, 35(6),434-41

Cruickshank, C. N. and Lowbury, E. J. (1952) 'Effect of antibiotics on tissue cultures of human skin', *Br Med J*, 2(4793), 1070-2.

Cummings, S., Black, D. and Vogt, T. (1996) 'Changes in BMD substantially underestimate the anti-fracture effects of alendronate and other antiresorptive drugs', *J Bone Miner Res*, 11, S102.

Cummings, S. R., Cawthon, P. M., Ensrud, K. E., Cauley, J. A., Fink, H. A., Orwoll, E. S., Osteoporotic Fractures in Men Research, G. and Study of Osteoporotic Fractures Research, G. (2006) 'BMD and risk of hip and nonvertebral fractures in older men: a prospective study and comparison with older women', *J Bone Miner Res*, 21(10), 1550-6.

Cunha, J. S., Ferreira, V. M., Maquigussa, E., Naves, M. A. and Boim, M. A. (2014) 'Effects of high glucose and high insulin concentrations on osteoblast function in vitro', *Cell Tissue Res*, 358(1), 249-56.

D'Alimonte, I., Lannutti, A., Pipino, C., Di Tomo, P., Pierdomenico, L., Cianci, E., Antonucci, I., Marchisio, M., Romano, M., Stuppia, L., Caciagli, F., Pandolfi, A. and Ciccarelli, R. (2013) 'Wnt signaling behaves as a "master regulator" in the osteogenic and adipogenic commitment of human amniotic fluid mesenchymal stem cells', *Stem Cell Rev*, 9(5), 642-54.

Dacquin, R., Davey, R. A., Laplace, C., Levasseur, R., Morris, H. A., Goldring, S. R., Gebre-Medhin, S., Galson, D. L., Zajac, J. D. and Karsenty, G. (2004) 'Amylin inhibits bone resorption while the calcitonin receptor controls bone formation in vivo', *J Cell Biol*, 164(4), 509-14.

Damadian, R. and Cope, F. W. (1974) 'Nmr in Cancer .5. Electronic Diagnosis of Cancer by Potassium (K-39) Nuclear Magnetic-Resonance - Spin Signatures and Tau-1 Beat Patterns', *Physiological Chemistry and Physics*, 6(4), 309-322.

Damilakis, J., Adams, J. E., Guglielmi, G. and Link, T. M. (2010) 'Radiation exposure in X-ray-based imaging techniques used in osteoporosis', *Eur Radiol*, 20(11), 2707-14.

Danielson, K. K., Elliott, M. E., LeCaire, T., Binkley, N. and Palta, M. (2009) 'Poor glycemic control is associated with low BMD detected in premenopausal women with type 1 diabetes', *Osteoporos Int*, 20(6), 923-33.

Davis, R. L., Weintraub, H. and Lassar, A. B. (1987) 'Expression of a Single Transfected Cdna Converts Fibroblasts to Myoblasts', *Cell*, 51(6), 987-1000.

Day, T. F., Guo, X., Garrett-Beal, L. and Yang, Y. (2005) 'Wnt/beta-catenin signaling in mesenchymal progenitors controls osteoblast and chondrocyte differentiation during vertebrate skeletogenesis', *Dev Cell*, 8(5), 739-50.

de Boer, I. H., Sun, W., Cleary, P. A., Lachin, J. M., Molitch, M. E., Steffes, M. W., Zinman, B. and on behalf of the DCCT EDIC Research Group (2011) 'Intensive diabetes therapy and glomerular filtration rate in type 1 diabetes', *N Engl J Med*, 365(25), 2366-76.

de, L., II, van der Klift, M., de Laet, C. E., van Daele, P. L., Hofman, A. and Pols, H. A. (2005) 'Bone mineral density and fracture risk in type-2 diabetes mellitus: the Rotterdam Study', *Osteoporos Int*, 16(12), 1713-20.

de Souza, K. S., Ururahy, M. A., da Costa Oliveira, Y. M., Loureiro, M. B., da Silva, H. P., Bortolin, R. H., Melo Dos Santos, F., Luchessi, A. D., Neto, J. J., Arrais, R. F., Hirata, R. D., das Gracas Almeida, M., Hirata, M. H. and de Rezende, A. A. (2016) 'Low bone mineral density in patients with type 1 diabetes: association with reduced expression of IGF1, IGF1R and TGF B 1 in peripheral blood mononuclear cells', *Diabetes Metab Res Rev*, 32(6), 589-95.

De Vries, F., Bracke, M., Leufkens, H. G., Lammers, J. W., Cooper, C. and Van Staa, T. P. (2007) 'Fracture risk with intermittent high-dose oral glucocorticoid therapy', *Arthritis Rheum*, 56(1), 208-14.

de Waard, E. A. C., de Jong, J. J. A., Koster, A., Savelberg, H., van Geel, T. A., Houben, A., Schram, M. T., Dagnelie, P. C., van der Kallen, C. J., Sep, S. J. S., Stehouwer, C. D. A., Schaper, N. C., Berendschot, T., Schouten, J., Geusens, P. and van den Bergh, J. P. W. (2018) 'The association between diabetes status, HbA1c, diabetes duration, microvascular

disease, and bone quality of the distal radius and tibia as measured with high-resolution peripheral quantitative computed tomography-The Maastricht Study', *Osteoporos Int*.

DeFronzo, R. A., Davidson, J. A. and Del Prato, S. (2012) 'The role of the kidneys in glucose homeostasis: a new path towards normalizing glycaemia', *Diabetes Obes Metab*, 14(1), 5-14.

Del Pino-Montes, J., Benito, G. E., Fernandez-Salazar, M. P., Covenas, R., Calvo, J. J., Bouillon, R. and Quesada, J. M. (2004) 'Calcitriol improves streptozotocin-induced diabetes and recovers bone mineral density in diabetic rats', *Calcif Tissue Int*, 75(6), 526-32.

Delmas, P. (1995) 'Biochemical markers for the assessment of bone turnover' in Rigg BL., M. L., ed., *Osteoporosis, etiology, diagnosis and management*, Philadelphia: Lippincott-Raven, 319-33.

Delmas, P. D. (1991) 'What do we know about biochemical bone markers?', *Baillieres Clin Obstet Gynaecol*, 5(4), 817-30.

Deltsidou, A. (2010) 'Age at menarche and menstrual irregularities of adolescents with type 1 diabetes', *J Pediatr Adolesc Gynecol*, 23(3), 162-7.

Department of Health (England) (2006) *Hospital Episode Statistics*.

Diab, T. and Vashishth, D. (2005) 'Effects of damage morphology on cortical bone fragility', *Bone*, 37(1), 96-102.

Diabetes Control and Complications Trial/ Epidemiology of Diabetes, I. and Complications Research Group (2016) 'Risk Factors for Cardiovascular Disease in Type 1 Diabetes', *Diabetes*, 65(5), 1370-9.

Diaz-Lopez, A., Bullo, M., Juanola-Falgarona, M., Martinez-Gonzalez, M. A., Estruch, R., Covas, M. I., Aros, F. and Salas-Salvado, J. (2013) 'Reduced serum concentrations of carboxylated and undercarboxylated osteocalcin are associated with risk of developing type 2 diabetes mellitus in a high cardiovascular risk population: a nested case-control study', *J Clin Endocrinol Metab*, 98(11), 4524-31.

Diederichs, G., Engelken, F., Marshall, L. M., Peters, K., Black, D. M., Issever, A. S., Barrett-Connor, E., Orwoll, E., Hamm, B., Link, T. M. and Osteoporotic Fractures in Men Research, G. (2011) 'Diffuse idiopathic skeletal hyperostosis (DISH): relation to vertebral fractures and bone density', *Osteoporos Int*, 22(6), 1789-97.

Dobnig, H., Piswanger-Solkner, J. C., Roth, M., Obermayer-Pietsch, B., Tiran, A., Strele, A., Maier, E., Maritschnegg, P., Sieberer, C. and Fahrleitner-Pammer, A. (2006) 'Type 2 diabetes mellitus in nursing home patients: effects on bone turnover, bone mass, and fracture risk', *J Clin Endocrinol Metab*, 91(9), 3355-63.

Dominguez, L. J., Davidoff, A. J., Srinivas, P. R., Standley, P. R., Walsh, M. F. and Sowers, J. R. (1996) 'Effects of metformin on tyrosine kinase activity, glucose transport, and intracellular calcium in rat vascular smooth muscle', *Endocrinology*, 137(1), 113-21.

Dooms, G. C., Fisher, M. R., Hricak, H., Richardson, M., Crooks, L. E. and Genant, H. K. (1985) 'Bone marrow imaging: magnetic resonance studies related to age and sex', *Radiology*, 155(2), 429-32.

Dorman, J. S., Laporte, R. E., Kuller, L. H., Cruickshanks, K. J., Orchard, T. J., Wagener, D. K., Becker, D. J., Cavender, D. E. and Drash, A. L. (1984) 'The Pittsburgh insulin-dependent diabetes mellitus (IDDM) morbidity and mortality study. Mortality results', *Diabetes*, 33(3), 271-6.

Dowling, R. J., Goodwin, P. J. and Stambolic, V. (2011) 'Understanding the benefit of metformin use in cancer treatment', *BMC Med*, 9, 33.

Downie, E., Craig, M. E., Hing, S., Cusumano, J., Chan, A. K. F. and Donaghue, K. C. (2011) 'Continued Reduction in the Prevalence of Retinopathy in Adolescents With Type 1 Diabetes', *Diabetes Care*, 34(11), 2368-2373.

Drucker, D. J. and Nauck, M. A. (2006) 'The incretin system: glucagon-like peptide-1 receptor agonists and dipeptidyl peptidase-4 inhibitors in type 2 diabetes', *Lancet*, 368(9548), 1696-705.

Ducy, P., Desbois, C., Boyce, B., Pinero, G., Story, B., Dunstan, C., Smith, E., Bonadio, J., Goldstein, S., Gundberg, C., Bradley, A. and Karsenty, G. (1996) 'Increased bone formation in osteocalcin-deficient mice', *Nature*, 382(6590), 448-52.

Ducy, P., Zhang, R., Geoffroy, V., Ridall, A. L. and Karsenty, G. (1997) 'Osf2/Cbfa1: a transcriptional activator of osteoblast differentiation', *Cell*, 89(5), 747-54.

Dulbecco, R. (1952) 'Production of Plaques in Monolayer Tissue Cultures by Single Particles of an Animal Virus', *Proc Natl Acad Sci U S A*, 38(8), 747-52.

Dulbecco, R. and Freeman, G. (1959) 'Plaque production by the polyoma virus', *Virology*, 8(3), 396-7.

Eagle, H. (1955) 'The growth requirements of two mammalian cell lines in tissue culture', *Trans Assoc Am Physicians*, 68, 78-81.

El-Mir, M. Y., Nogueira, V., Fontaine, E., Averet, N., Rigoulet, M. and Leverve, X. (2000) 'Dimethylbiguanide inhibits cell respiration via an indirect effect targeted on the respiratory chain complex I', *Journal of Biological Chemistry*, 275(1), 223-8.

Elbaz, A., Wu, X., Rivas, D., Gimble, J. M. and Duque, G. (2010) 'Inhibition of fatty acid biosynthesis prevents adipocyte lipotoxicity on human osteoblasts in vitro', *J Cell Mol Med*, 14(4), 982-91.

Eller-Vainicher, C., Zhukouskaya, V. V., Tolkachev, Y. V., Koritko, S. S., Cairoli, E., Grossi, E., Beck-Peccoz, P., Chiodini, I. and Shepelkevich, A. P. (2011) 'Low bone mineral density and its predictors in type 1 diabetic patients evaluated by the classic statistics and artificial neural network analysis', *Diabetes Care*, 34(10), 2186-91.

Elley, C. R., Robinson, T., Moyes, S. A., Kenealy, T., Collins, J., Robinson, E., Orr-Walker, B. and Drury, P. L. (2013) 'Derivation and validation of a renal risk score for people with type 2 diabetes', *Diabetes Care*, 36(10), 3113-20.

Emami, A., Mjoberg, B., Ragnarsson, B. and Larsson, S. (1996) 'Changing epidemiology of tibial shaft fractures. 513 cases compared between 1971-1975 and 1986-1990', *Acta Orthop Scand*, 67(6), 557-61.

Eriksen, E., Axelrod, D. and F., M. (1994) 'Bone histomorphometry' in, New York: Raven Press.

Ertl, D. A., Gleiss, A., Sagmeister, S. and Haeusler, G. (2014) 'Determining the normal range for IGF-I, IGFBP-3, and ALS: new reference data based on current internal standards', *Wien Med Wochenschr*, 164(17-18), 343-52.

Esser, N., Legrand-Poels, S., Piette, J., Scheen, A. J. and Paquot, N. (2014) 'Inflammation as a link between obesity, metabolic syndrome and type 2 diabetes', *Diabetes Res Clin Pract*, 105(2), 141-50.

Farlay, D., Armas, L. A., Gineyts, E., Akhter, M. P., Recker, R. R. and Boivin, G. (2016) 'Nonenzymatic Glycation and Degree of Mineralization Are Higher in Bone From Fractured Patients With Type 1 Diabetes Mellitus', *J Bone Miner Res*, 31(1), 190-5.

Farr, J. N., Amin, S., LeBrasseur, N. K., Atkinson, E. J., Achenbach, S. J., McCready, L. K., Joseph Melton, L., 3rd and Khosla, S. (2014a) 'Body composition during childhood and adolescence: relations to bone strength and microstructure', *J Clin Endocrinol Metab*, 99(12), 4641-8.

Farr, J. N., Drake, M. T., Amin, S., Melton, L. J., 3rd, McCready, L. K. and Khosla, S. (2014b) 'In vivo assessment of bone quality in postmenopausal women with type 2 diabetes', *J Bone Miner Res*, 29(4), 787-95.

Fatokun, A. A., Stone, T. W. and Smith, R. A. (2006) 'Hydrogen peroxide-induced oxidative stress in MC3T3-E1 cells: The effects of glutamate and protection by purines', *Bone*, 39(3), 542-51.

Faulkner, K. G. (2001) *Osteoporosis*, Academic Press.

Fazeli, P. K., Horowitz, M. C., MacDougald, O. A., Scheller, E. L., Rodeheffer, M. S., Rosen, C. J. and Klibanski, A. (2013) 'Marrow fat and bone--new perspectives', *J Clin Endocrinol Metab*, 98(3), 935-45.

Ferland-McCollough, D., Maselli, D., Spinetti, G., Sambataro, M., Sullivan, N., Blom, A. and Madeddu, P. (2018) 'MCP-1 Feedback Loop Between Adipocytes and Mesenchymal Stromal Cells Causes Fat Accumulation and Contributes to Hematopoietic Stem Cell Rarefaction in the Bone Marrow of Patients With Diabetes', *Diabetes*, 67(7), 1380-1394.

Ferrari, S., Rizzoli, R., Slosman, D. and Bonjour, J. P. (1998) 'Familial resemblance for bone mineral mass is expressed before puberty', *J Clin Endocrinol Metab*, 83(2), 358-61.

Ferron, M., Wei, J., Yoshizawa, T., Del Fattore, A., DePinho, R. A., Teti, A., Ducy, P. and Karsenty, G. (2010) 'Insulin signaling in osteoblasts integrates bone remodeling and energy metabolism', *Cell*, 142(2), 296-308.

Folkesson, J., Carballido-Gamio, J., Eckstein, F., Link, T. M. and Majumdar, S. (2010) 'Local bone enhancement fuzzy clustering for segmentation of MR trabecular bone images', *Med Phys*, 37(1), 295-302.

Fontaine, C., Cousin, W., Plaisant, M., Dani, C. and Peraldi, P. (2008) 'Hedgehog signaling alters adipocyte maturation of human mesenchymal stem cells', *Stem Cells*, 26(4), 1037-46.

Forbes, G. B. and Bruining, G. J. (1976) 'Urinary creatinine excretion and lean body mass', *Am J Clin Nutr*, 29(12), 1359-66.

Foretz, M., Hebrard, S., Leclerc, J., Zarrinpashneh, E., Soty, M., Mithieux, G., Sakamoto, K., Andreelli, F. and Viollet, B. (2010) 'Metformin inhibits hepatic gluconeogenesis in mice independently of the LKB1/AMPK pathway via a decrease in hepatic energy state', *Journal of Clinical Investigation*, 120(7), 2355-69.

Forst, T., Pfutzner, A., Kann, P., Schehler, B., Lobmann, R., Schafer, H., Andreas, J., Bockisch, A. and Beyer, J. (1995) 'Peripheral osteopenia in adult patients with insulin-dependent diabetes mellitus', *Diabet Med*, 12(10), 874-9.

Frassetto, L. A. and Sebastian, A. (2012) 'How metabolic acidosis and oxidative stress alone and interacting may increase the risk of fracture in diabetic subjects', *Med Hypotheses*, 79(2), 189-92.

Frazer, T. E., White, N. H., Hough, S., Santiago, J. V., McGee, B. R., Bryce, G., Mallon, J. and Avioli, L. V. (1981) 'Alterations in circulating vitamin D metabolites in the young insulin-dependent diabetic', *J Clin Endocrinol Metab*, 53(6), 1154-9.

Freshney, R. (2005) *Culture of Animal Cells: A Manual of Basic Technique*, 5th ed., Wiley & Sons.

Friedenstein, A. J., Gorskaja, U. F. and Kulagina, N. N. (1976) 'Fibroblast Precursors in Normal and Irradiated Mouse Hematopoietic Organs', *Experimental Hematology*, 4(5), 267-274.

Fryer, L. G., Parbu-Patel, A. and Carling, D. (2002) 'The Anti-diabetic drugs rosiglitazone and metformin stimulate AMP-activated protein kinase through distinct signaling pathways', *Journal of Biological Chemistry*, 277(28), 25226-32.

Fujii, N., Hayashi, T., Hirshman, M. F., Smith, J. T., Habinowski, S. A., Kaijser, L., Mu, J., Ljungqvist, O., Birnbaum, M. J., Witters, L. A., Thorell, A. and Goodyear, L. J. (2000)

'Exercise induces isoform-specific increase in 5'AMP-activated protein kinase activity in human skeletal muscle', *Biochem Biophys Res Commun*, 273(3), 1150-5.

Fukunaga, Y., Minamikawa, J., Inoue, D. and Koshiyama, H. (1997) 'Does insulin use increase bone mineral density in patients with non-insulin-dependent diabetes mellitus?', *Arch Intern Med*, 157(22), 2668-9.

Fulco, M., Cen, Y., Zhao, P., Hoffman, E. P., McBurney, M. W., Sauve, A. A. and Sartorelli, V. (2008) 'Glucose restriction inhibits skeletal myoblast differentiation by activating SIRT1 through AMPK-mediated regulation of Nampt', *Dev Cell*, 14(5), 661-73.

Fullerton, B., Jeitler, K., Seitz, M., Horvath, K., Berghold, A. and Siebenhofer, A. (2014) 'Intensive glucose control versus conventional glucose control for type 1 diabetes mellitus', *Cochrane Database Syst Rev*, 2014/02/15(2), CD009122.

Fulzele, K., Riddle, R. C., DiGirolamo, D. J., Cao, X. M., Wan, C., Chen, D. Q., Faugere, M. C., Aja, S., Hussain, M. A., Bruning, J. C. and Clemens, T. L. (2010) 'Insulin Receptor Signaling in Osteoblasts Regulates Postnatal Bone Acquisition and Body Composition', *Cell*, 142(2), 309-319.

Gale, E. A. (2002) 'The rise of childhood type 1 diabetes in the 20th century', *Diabetes*, 51(12), 3353-61.

Galindo, M., Pratap, J., Young, D. W., Hovhannisyan, H., Im, H. J., Choi, J. Y., Lian, J. B., Stein, J. L., Stein, G. S. and van Wijnen, A. J. (2005) 'The bone-specific expression of Runx2 oscillates during the cell cycle to support a G1-related antiproliferative function in osteoblasts', *Journal of Biological Chemistry*, 280(21), 20274-85.

Gao, Y., Xue, J., Li, X., Jia, Y. and Hu, J. (2008) 'Metformin regulates osteoblast and adipocyte differentiation of rat mesenchymal stem cells', *J Pharm Pharmacol*, 60(12), 1695-700.

Garber, A. and Samson, S. (2004) *Metformin and other biguanides: pharmacology and therapeutic usage*, 3rd ed., John Wiley and Sons.

Garcia-Martin, A., Rozas-Moreno, P., Reyes-Garcia, R., Morales-Santana, S., Garcia-Fontana, B., Garcia-Salcedo, J. A. and Munoz-Torres, M. (2012) 'Circulating levels of sclerostin are increased in patients with type 2 diabetes mellitus', *J Clin Endocrinol Metab*, 97(1), 234-41.

Gargano, V., Massaro, M., Morra, I., Formisano, C., Di Carlo, C., Nappi, C. (2008) 'Effects of two low-dose combined oral contraceptives containing drospirenone on bone turnover and bone mineral density in young fertile women: a prospective controlled randomized study', *Contraception*, 78(1):10-5

Garnero, P., Grimaux, M., Seguin, P. and Delmas, P. D. (1994) 'Characterization of immunoreactive forms of human osteocalcin generated in vivo and in vitro', *J Bone Miner Res*, 9(2), 255-64.

Gatehouse, P. D. and Bydder, G. M. (2003) 'Magnetic resonance imaging of short T-2 components in tissue', *Clinical Radiology*, 58(1), 1-19.

Gaudio, A., Pennisi, P., Bratengeier, C., Torrisi, V., Lindner, B., Mangiafico, R. A., Pulvirenti, I., Hawa, G., Tringali, G. and Fiore, C. E. (2010) 'Increased sclerostin serum levels associated with bone formation and resorption markers in patients with immobilization-induced bone loss', *J Clin Endocrinol Metab*, 95(5), 2248-53.

Gaudio, A., Privitera, F., Battaglia, K., Torrisi, V., Sidoti, M. H., Pulvirenti, I., Canzonieri, E., Tringali, G. and Fiore, C. E. (2012) 'Sclerostin levels associated with inhibition of the Wnt/beta-catenin signaling and reduced bone turnover in type 2 diabetes mellitus', *J Clin Endocrinol Metab*, 97(10), 3744-50.

Gennari, L., Merlotti, D., Valenti, R., Ceccarelli, E., Ruvio, M., Pietrini, M. G., Capodarca, C., Franci, M. B., Campagna, M. S., Calabro, A., Cataldo, D., Stolakis, K., Dotta, F. and Nuti, R. (2012) 'Circulating Sclerostin Levels and Bone Turnover in Type 1 and Type 2 Diabetes', *Journal of Clinical Endocrinology & Metabolism*, 97(5), 1737-1744.

Gheith, O., Farouk, N., Nampoory, N., Halim, M. A. and Al-Otaibi, T. (2016) 'Diabetic kidney disease: world wide difference of prevalence and risk factors', *J Nephropharmacol*, 5(1), 49-56.

Giangregorio, L. M., Leslie, W. D., Lix, L. M., Johansson, H., Oden, A., McCloskey, E. and Kanis, J. A. (2012) 'FRAX underestimates fracture risk in patients with diabetes', *J Bone Miner Res*, 27(2), 301-8.

Gilbert, L., He, X., Farmer, P., Boden, S., Kozlowski, M., Rubin, J. and Nanes, M. S. (2000) 'Inhibition of osteoblast differentiation by tumor necrosis factor-alpha', *Endocrinology*, 141(11), 3956-64.

Gilsanz, V., Chalfant, J., Kalkwarf, H., Zemel, B., Lappe, J., Oberfield, S., Shepherd, J., Wren, T. and Winer, K. (2011) 'Age at onset of puberty predicts bone mass in young adulthood', *J Pediatr*, 158(1), 100-5, 105 e1-2.

Glantschnig, H., Fisher, J. E., Wesolowski, G., Rodan, G. A. and Reszka, A. A. (2003) 'M-CSF, TNFalpha and RANK ligand promote osteoclast survival by signaling through mTOR/S6 kinase', *Cell Death and Differentiation*, 10(10), 1165-77.

Glorieux, F. H., Travers, R., Taylor, A., Bowen, J. R., Rauch, F., Norman, M. and Parfitt, A. M. (2000) 'Normative data for iliac bone histomorphometry in growing children', *Bone*, 26(2), 103-9.

Gluer, C. C. (1997) 'Quantitative ultrasound techniques for the assessment of osteoporosis: expert agreement on current status. The International Quantitative Ultrasound Consensus Group', *J Bone Miner Res*, 12(8), 1280-8.

Gluer, C. C., Wu, C. Y., Jergas, M., Goldstein, S. A. and Genant, H. K. (1994) 'Three quantitative ultrasound parameters reflect bone structure', *Calcif Tissue Int*, 55(1), 46-52.

Goldsmith, M., Damadian, R., Stanford, M. and Lipkowitz, M. (1977) 'NMR in cancer: XVIII. A superconductive NMR magnet for a human sample', *Physiol Chem Phys*, 9(1), 105-8.

Gortz, B. and Fassbender, W. J. (2001) '[Genetics of osteoporosis]', *Orthopade*, 30(7), 412-7.

Goulding, A. (2007) 'Risk factors for fractures in normally active children and adolescents', *Med Sport Sci*, 51, 102-20.

Gower, B. A., Pollock, N. K., Casazza, K., Clemens, T. L., Goree, L. L. and Granger, W. M. (2013) 'Associations of total and undercarboxylated osteocalcin with peripheral and hepatic insulin sensitivity and beta-cell function in overweight adults', *J Clin Endocrinol Metab*, 98(7), E1173-80.

Graeff, C., Timm, W., Nickelsen, T. N., Farrerons, J., Marin, F., Barker, C., Gluer, C. C. and Group, E. H. R. C. T. S. (2007) 'Monitoring teriparatide-associated changes in vertebral microstructure by high-resolution CT in vivo: results from the EUROFORS study', *J Bone Miner Res*, 22(9), 1426-33.

Granke, M., Makowski, A. J., Uppuganti, S., Does, M. D. and Nyman, J. S. (2015) 'Identifying Novel Clinical Surrogates to Assess Human Bone Fracture Toughness', *J Bone Miner Res*, 30(7), 1290-300.

Grey, A., Bolland, M., Gamble, G., Wattie, D., Horne, A., Davidson, J. and Reid, I. R. (2007) 'The peroxisome proliferator-activated receptor-gamma agonist rosiglitazone decreases bone formation and bone mineral density in healthy postmenopausal women: a randomized, controlled trial', *J Clin Endocrinol Metab*, 92(4), 1305-10.

Griffith, J. F., Yeung, D. K., Ma, H. T., Leung, J. C., Kwok, T. C. and Leung, P. C. (2012) 'Bone marrow fat content in the elderly: a reversal of sex difference seen in younger subjects', *Journal of Magnetic Resonance Imaging*, 36(1), 225-30.

Gunczler, P., Lanes, R., Paoli, M., Martinis, R., Villaroel, O. and Weisinger, J. R. (2001) 'Decreased bone mineral density and bone formation markers shortly after diagnosis of clinical type 1 diabetes mellitus', *J Pediatr Endocrinol Metab*, 14(5), 525-8.

Gunczler, P., Lanes, R., Paz-Martinez, V., Martins, R., Esaa, S., Colmenares, V. and Weisinger, J. R. (1998) 'Decreased lumbar spine bone mass and low bone turnover in children and adolescents with insulin dependent diabetes mellitus followed longitudinally', *J Pediatr Endocrinol Metab*, 11(3), 413-9.

Guntur, A. R., Gerencser, A. A., Le, P. T., DeMambro, V. E., Bornstein, S. A., Mookerjee, S. A., Maridas, D. E., Clemmons, D. E., Brand, M. D. and Rosen, C. J. (2018) 'Osteoblast-like MC3T3-E1 Cells Prefer Glycolysis for ATP Production but Adipocyte-like 3T3-L1 Cells Prefer Oxidative Phosphorylation', *J Bone Miner Res*, 33(6), 1052-1065.

Habinowski, S. A. and Witters, L. A. (2001) 'The effects of AICAR on adipocyte differentiation of 3T3-L1 cells', *Biochem Biophys Res Commun*, 286(5), 852-6.

Hahn, T. J., Westbrook, S. L., Sullivan, T. L., Goodman, W. G. and Halstead, L. R. (1988) 'Glucose transport in osteoblast-enriched bone explants: characterization and insulin regulation', *J Bone Miner Res*, 3(3), 359-65.

Ham, R. G. (1965) 'Clonal Growth of Mammalian Cells in a Chemically Defined, Synthetic Medium', *Proc Natl Acad Sci U S A*, 53, 288-93.

Hamada, Y., Fujii, H. and Fukagawa, M. (2009) 'Role of oxidative stress in diabetic bone disorder', *Bone*, 45 Suppl 1, S35-8.

Hamann, C., Picke, A. K., Campbell, G. M., Balyura, M., Rauner, M., Bernhardt, R., Huber, G., Morlock, M. M., Gunther, K. P., Bornstein, S. R., Gluer, C. C., Ludwig, B. and Hofbauer, L. C. (2014) 'Effects of parathyroid hormone on bone mass, bone strength, and bone regeneration in male rats with type 2 diabetes mellitus', *Endocrinology*, 155(4), 1197-206.

Hamed, E. A., Faddan, N. H., Elhafeez, H. A. and Sayed, D. (2011) 'Parathormone--25(OH)-vitamin D axis and bone status in children and adolescents with type 1 diabetes mellitus', *Pediatr Diabetes*, 12(6), 536-46.

Hampson, G., Evans, C., Petitt, R. J., Evans, W. D., Woodhead, S. J., Peters, J. R. and Ralston, S. H. (1998) 'Bone mineral density, collagen type 1 alpha 1 genotypes and bone turnover in premenopausal women with diabetes mellitus', *Diabetologia*, 41(11), 1314-20.

Hamrick, M. W., Della-Fera, M. A., Choi, Y. H., Pennington, C., Hartzell, D. and Baile, C. A. (2005) 'Leptin treatment induces loss of bone marrow adipocytes and increases bone formation in leptin-deficient ob/ob mice', *J Bone Miner Res*, 20(6), 994-1001.

Han, Y., Cowin, S. C., Schaffler, M. B. and Weinbaum, S. (2004) 'Mechanotransduction and strain amplification in osteocyte cell processes', *Proc Natl Acad Sci U S A*, 101(47), 16689-94.

Harada, H., Tagashira, S., Fujiwara, M., Ogawa, S., Katsumata, T., Yamaguchi, A., Komori, T. and Nakatsuka, M. (1999) 'Cbfa1 isoforms exert functional differences in osteoblast differentiation', *Journal of Biological Chemistry*, 274(11), 6972-8.

Hardie, D. G. (2007) 'AMP-activated/SNF1 protein kinases: conserved guardians of cellular energy', *Nat Rev Mol Cell Biol*, 8(10), 774-85.

Hardie, D. G., Carling, D. and Carlson, M. (1998) 'The AMP-activated/SNF1 protein kinase subfamily: metabolic sensors of the eukaryotic cell?', *Annu Rev Biochem*, 67, 821-55.

Hardie, D. G. and Pan, D. A. (2002) 'Regulation of fatty acid synthesis and oxidation by the AMP-activated protein kinase', *Biochem Soc Trans*, 30(Pt 6), 1064-70.

Harjutsalo, V., Maric-Bilkan, C., Forsblom, C., Groop, P. H. and FinnDiane Study, G. (2016) 'Age at menarche and the risk of diabetic microvascular complications in patients with type 1 diabetes', *Diabetologia*, 59(3), 472-80.

Harrison, R., Greenman, M., Franklin, P. and Jackson, C. (1907) 'Observations of the living developing nerve fiber', *The Anatomical Record*, 1(5), 116-128.

Hawley, S. A., Gadalla, A. E., Olsen, G. S. and Hardie, D. G. (2002) 'The antidiabetic drug metformin activates the AMP-activated protein kinase cascade via an adenine nucleotide-independent mechanism', *Diabetes*, 51(8), 2420-5.

Hawley, S. A., Pan, D. A., Mustard, K. J., Ross, L., Bain, J., Edelman, A. M., Frenguelli, B. G. and Hardie, D. G. (2005) 'Calmodulin-dependent protein kinase kinase-beta is an alternative upstream kinase for AMP-activated protein kinase', *Cell Metabolism*, 2(1), 9-19.

Hayflick, L. and Moorhead, P. S. (1961) 'The serial cultivation of human diploid cell strains', *Experimental Cell Research*, 25, 585-621.

Health Quality Improvement Partnership and Royal College of Paediatrics and Child Health (2015) *National Paediatric Diabetes Audit 2013-2014 Part 1: Care Processes and Outcomes* [online], available: http://www.rcpch.ac.uk/system/files/protected/page/2014%20NPDA%20Report%201%202014%20FINAL.pdf [accessed 17/10/2016].

Heaney, R. P., Abrams, S., Dawson-Hughes, B., Looker, A., Marcus, R., Matkovic, V. and Weaver, C. (2000) 'Peak bone mass', *Osteoporos Int*, 11(12), 985-1009.

Heap, J., Murray, M. A., Miller, S. C., Jalili, T. and Moyer-Mileur, L. J. (2004) 'Alterations in bone characteristics associated with glycemic control in adolescents with type 1 diabetes mellitus', *J Pediatr*, 144(1), 56-62.

Hegazy, S. K. (2015) 'Evaluation of the anti-osteoporotic effects of metformin and sitagliptin in postmenopausal diabetic women', *J Bone Miner Metab*, 33(2), 207-12.

Heilman, K., Zilmer, M., Zilmer, K. and Tillmann, V. (2009) 'Lower bone mineral density in children with type 1 diabetes is associated with poor glycemic control and higher serum ICAM-1 and urinary isoprostane levels', *J Bone Miner Metab*, 27(5), 598-604.

Heilman, K., Zilmer, M., Zilmer, K. and Tillmann, V. (2009) 'Lower bone mineral density in children with type 1 diabetes is associated with poor glycemic control and higher serum ICAM-1 and urinary isoprostane levels', *Journal of Bone and Mineral Metabolism*, 27(5), 598-604.

Heilmeier, U., Carpenter, D. R., Patsch, J. M., Harnish, R., Joseph, G. B., Burghardt, A. J., Baum, T., Schwartz, A. V., Lang, T. F. and Link, T. M. (2015) 'Volumetric femoral BMD, bone geometry, and serum sclerostin levels differ between type 2 diabetic postmenopausal women with and without fragility fractures', *Osteoporos Int*, 26(4), 1283-93.

Heilmeier, U., Hackl, M., Skalicky, S., Weilner, S., Schroeder, F., Vierlinger, K., Patsch, J. M., Baum, T., Oberbauer, E., Lobach, I., Burghardt, A. J., Schwartz, A. V., Grillari, J. and Link, T. M. (2016) 'Serum miRNA Signatures Are Indicative of Skeletal Fractures in Postmenopausal Women With and Without Type 2 Diabetes and Influence Osteogenic and Adipogenic Differentiation of Adipose Tissue-Derived Mesenchymal Stem Cells In Vitro', *J Bone Miner Res*, 31(12), 2173-2192.

Heuck, A. F., Block, J., Glueer, C. C., Steiger, P. and Genant, H. K. (1989) 'Mild versus definite osteoporosis: comparison of bone densitometry techniques using different statistical models', *J Bone Miner Res*, 4(6), 891-900.

Heuck, C., Skjaerbaek, C. and Wolthers, O. D. (1998) 'Diurnal rhythm of serum osteocalcin in normal children', *Acta Paediatr*, 87(9), 930-2.

Hind, K. and Burrows, M. (2007) 'Weight-bearing exercise and bone mineral accrual in children and adolescents: a review of controlled trials', *Bone*, 40(1), 14-27.

Ho, K. Y., Hu, H. H., Keyak, J. H., Colletti, P. M. and Powers, C. M. (2013) 'Measuring bone mineral density with fat-water MRI: comparison with computed tomography', *Journal of Magnetic Resonance Imaging*, 37(1), 237-42.

Hock, J. M., Centrella, M. and Canalis, E. (1988) 'Insulin-like growth factor I has independent effects on bone matrix formation and cell replication', *Endocrinology*, 122(1), 254-60.

Hofbauer, L. C., Brueck, C. C., Singh, S. K. and Dobnig, H. (2007) 'Osteoporosis in patients with diabetes mellitus', *J Bone Miner Res*, 22(9), 1317-28.

Hogler, W., Briody, J., Moore, B., Garnett, S., Lu, P. W. and Cowell, C. T. (2004) 'Importance of estrogen on bone health in Turner syndrome: a cross-sectional and longitudinal study using dual-energy X-ray absorptiometry', *J Clin Endocrinol Metab*, 89(1), 193-9.

Holmen, S. L., Zylstra, C. R., Mukherjee, A., Sigler, R. E., Faugere, M. C., Bouxsein, M. L., Deng, L., Clemens, T. L. and Williams, B. O. (2005) 'Essential role of beta-catenin in postnatal bone acquisition', *Journal of Biological Chemistry*, 280(22), 21162-8.

Hong, J., Hipp, J. A., Mulkern, R. V., Jaramillo, D. and Snyder, B. D. (2000) 'Magnetic resonance imaging measurements of bone density and cross-sectional geometry', *Calcif Tissue Int*, 66(1), 74-8.

Horcajada-Molteni, M. N., Chanteranne, B., Lebecque, P., Davicco, M. J., Coxam, V., Young, A. and Barlet, J. P. (2001) 'Amylin and bone metabolism in streptozotocin-induced diabetic rats', *J Bone Miner Res*, 16(5), 958-65.

Hothersall, E. J., Livingstone, S. J., Looker, H. C., Ahmed, S. F., Cleland, S., Leese, G. P., Lindsay, R. S., McKnight, J., Pearson, D., Philip, S., Wild, S. H. and Colhoun, H. M. (2014) 'Contemporary risk of hip fracture in type 1 and type 2 diabetes: a national registry study from Scotland', *J Bone Miner Res*, 29(5), 1054-60.

Hough, S., Avioli, L. V., Bergfeld, M. A., Fallon, M. D., Slatopolsky, E. and Teitelbaum, S. L. (1981) 'Correction of abnormal bone and mineral metabolism in chronic streptozotocin-induced diabetes mellitus in the rat by insulin therapy', *Endocrinology*, 108(6), 2228-34.

Hough, S., Russell, J. E., Teitelbaum, S. L. and Avioli, L. V. (1982) 'Calcium homeostasis in chronic streptozotocin-induced diabetes mellitus in the rat', *Am J Physiol*, 242(6), E451-6.

Hough, S., Slatopolsky, E. and Avioli, L. V. (1983) 'Hormonal alterations in experimental diabetes: role of a primary disturbance in calcium homeostasis', *Calcif Tissue Int*, 35(4-5), 615-9.

Hovind, P., Tarnow, L., Rossing, P., Jensen, B. R., Graae, M., Torp, I., Binder, C. and Parving, H. H. (2004) 'Predictors for the development of microalbuminuria and macroalbuminuria in patients with type 1 diabetes: inception cohort study', *BMJ*, 328(7448), 1105.

Hronik-Tupaj, M., Rice, W. L., Cronin-Golomb, M., Kaplan, D. L. and Georgakoudi, I. (2011) 'Osteoblastic differentiation and stress response of human mesenchymal stem cells exposed to alternating current electric fields', *Biomed Eng Online*, 10, 9.

http://www.revisemri.com/questions/pulse_sequences/se_ge_differences. [online], available: [accessed 28/10].

Ikeda, K., Matsumoto, T., Morita, K., Yamato, H., Takahashi, H., Ezawa, I. and Ogata, E. (1987) 'The role of insulin in the stimulation of renal 1,25-dihydroxyvitamin D synthesis by parathyroid hormone in rats', *Endocrinology*, 121(5), 1721-6.

in 't Anker, P. S., Noort, W. A., Scherjon, S. A., Kleijburg-van der Keur, C., Kruisselbrink, A. B., van Bezooijen, R. L., Beekhuizen, W., Willemze, R., Kanhai, H. H. and Fibbe, W. E. (2003) 'Mesenchymal stem cells in human second-trimester bone marrow, liver, lung, and spleen exhibit a similar immunophenotype but a heterogeneous multilineage differentiation potential', *Haematologica*, 88(8), 845-52.

in 'tAnker, P. S., Scherjon, S. A., Kleijburg-van der Keur, C., Noort, W. A., Claas, F. H. J., Willemze, R., Fibbe, W. E. and Kanhai, H. H. H. (2003) 'Amniotic fluid as a novel source of mesenchymal stem cells for therapeutic transplantation', *Blood*, 102(4), 1548-1549.

Inaba, M., Terada, M., Koyama, H., Yoshida, O., Ishimura, E., Kawagishi, T., Okuno, Y., Nishizawa, Y., Otani, S. and Morii, H. (1995) 'Influence of high glucose on 1,25-

dihydroxyvitamin D3-induced effect on human osteoblast-like MG-63 cells', *J Bone Miner Res*, 10(7), 1050-6.

Ingberg, C. M., Palmer, M., Aman, J., Arvidsson, B., Schvarcz, E. and Berne, C. (2004) 'Body composition and bone mineral density in long-standing type 1 diabetes', *J Intern Med*, 255(3), 392-8.

Irwin, R., LaPres, J. J., Kinser, S. and McCabe, L. R. (2007) 'Prolyl-hydroxylase inhibition and HIF activation in osteoblasts promotes an adipocytic phenotype', *Journal of Cellular Biochemistry*, 100(3), 762-72.

Isakovic, A., Harhaji, L., Stevanovic, D., Markovic, Z., Sumarac-Dumanovic, M., Starcevic, V., Micic, D. and Trajkovic, V. (2007) 'Dual antiglioma action of metformin: cell cycle arrest and mitochondria-dependent apoptosis', *Cellular and Molecular Life Sciences*, 64(10), 1290-302.

Issever, A. S., Link, T. M., Kentenich, M., Rogalla, P., Burghardt, A. J., Kazakia, G. J., Majumdar, S. and Diederichs, G. (2010) 'Assessment of trabecular bone structure using MDCT: comparison of 64- and 320-slice CT using HR-pQCT as the reference standard', *Eur Radiol*, 20(2), 458-68.

Ito, Y., Bae, S. C. and Chuang, L. S. (2015) 'The RUNX family: developmental regulators in cancer', *Nat Rev Cancer*, 15(2), 81-95.

Ivers, R. Q., Cumming, R. G., Mitchell, P., Peduto, A. J. and Blue Mountains Eye, S. (2001) 'Diabetes and risk of fracture: The Blue Mountains Eye Study', *Diabetes Care*, 24(7), 1198-203.

James, A. W., Leucht, P., Levi, B., Carre, A. L., Xu, Y., Helms, J. A. and Longaker, M. T. (2010) 'Sonic Hedgehog influences the balance of osteogenesis and adipogenesis in mouse adipose-derived stromal cells', *Tissue Eng Part A*, 16(8), 2605-16.

James, A. W., Pan, A., Chiang, M., Zara, J. N., Zhang, X., Ting, K. and Soo, C. (2011) 'A new function of Nell-1 protein in repressing adipogenic differentiation', *Biochem Biophys Res Commun*, 411(1), 126-31.

James, A. W., Pang, S., Askarinam, A., Corselli, M., Zara, J. N., Goyal, R., Chang, L., Pan, A., Shen, J., Yuan, W., Stoker, D., Zhang, X., Adams, J. S., Ting, K. and Soo, C. (2012) 'Additive effects of sonic hedgehog and Nell-1 signaling in osteogenic versus adipogenic differentiation of human adipose-derived stromal cells', *Stem Cells Dev*, 21(12), 2170-8.

Jang, W. G., Kim, E. J., Bae, I. H., Lee, K. N., Kim, Y. D., Kim, D. K., Kim, S. H., Lee, C. H., Franceschi, R. T., Choi, H. S. and Koh, J. T. (2011) 'Metformin induces osteoblast differentiation via orphan nuclear receptor SHP-mediated transactivation of Runx2', *Bone*, 48(4), 885-93.

Janghorbani, M., Van Dam, R. M., Willett, W. C. and Hu, F. B. (2007) 'Systematic review of type 1 and type 2 diabetes mellitus and risk of fracture', *American Journal of Epidemiology*, 166(5), 495-505.

Jansen, J. F. A., Backes, W. H., Nicolay, K. and Kooi, M. E. (2006) 'H-1 MR spectroscopy of the brain: Absolute quantification of metabolites', *Radiology*, 240(2), 318-332.

Jaramillo, D., Laor, T., Hoffer, F. A., Zaleske, D. J., Cleveland, R. H., Buchbinder, B. R. and Egglin, T. K. (1991) 'Epiphyseal marrow in infancy: MR imaging', *Radiology*, 180(3), 809-12.

Jeyabalan, J., Viollet, B., Smitham, P., Ellis, S. A., Zaman, G., Bardin, C., Goodship, A., Roux, J. P., Pierre, M. and Chenu, C. (2013) 'The anti-diabetic drug metformin does not affect bone mass in vivo or fracture healing', *Osteoporos Int*, 24(10), 2659-70.

Johansen, J. S., Giwercman, A., Hartwell, D., Nielsen, C. T., Price, P. A., Christiansen, C. and Skakkebaek, N. E. (1988) 'Serum bone Gla-protein as a marker of bone growth in children and adolescents: correlation with age, height, serum insulin-like growth factor I, and serum testosterone', *J Clin Endocrinol Metab*, 67(2), 273-8.

Johnell, O. and Kanis, J. A. (2006) 'An estimate of the worldwide prevalence and disability associated with osteoporotic fractures', *Osteoporos Int*, 17(12), 1726-33.

Johnell, O., Kanis, J. A., Oden, A., Johansson, H., De Laet, C., Delmas, P., Eisman, J. A., Fujiwara, S., Kroger, H., Mellstrom, D., Meunier, P. J., Melton, L. J., 3rd, O'Neill, T., Pols, H., Reeve, J., Silman, A. and Tenenhouse, A. (2005) 'Predictive value of BMD for hip and other fractures', *J Bone Miner Res*, 20(7), 1185-94.

Johnston, S. S., Conner, C., Aagren, M., Ruiz, K. and Bouchard, J. (2012) 'Association between hypoglycaemic events and fall-related fractures in Medicare-covered patients with type 2 diabetes', *Diabetes Obes Metab*, 14(7), 634-43.

Jones, I. E., Williams, S. M., Dow, N. and Goulding, A. (2002) 'How many children remain fracture-free during growth? a longitudinal study of children and adolescents participating in the Dunedin Multidisciplinary Health and Development Study', *Osteoporos Int*, 13(12), 990-5.

Jun, J. E., Lee, S. E., Lee, Y. B., Ahn, J. Y., Kim, G., Hur, K. Y., Lee, M. K., Jin, S. M. and Kim, J. H. (2019) 'Continuous glucose monitoring defined glucose variability is associated with cardiovascular autonomic neuropathy in type 1 diabetes', *Diabetes Metab Res Rev*, 35(2), e3092.

Kahn, B. B., Alquier, T., Carling, D. and Hardie, D. G. (2005) 'AMP-activated protein kinase: ancient energy gauge provides clues to modern understanding of metabolism', *Cell Metabolism*, 1(1), 15-25.

Kahn, S. E., Haffner, S. M., Heise, M. A., Herman, W. H., Holman, R. R., Jones, N. P., Kravitz, B. G., Lachin, J. M., O'Neill, M. C., Zinman, B., Viberti, G. and Group, A. S. (2006) 'Glycemic durability of rosiglitazone, metformin, or glyburide monotherapy', *N Engl J Med*, 355(23), 2427-43.

Kahn, S. E., Zinman, B., Lachin, J. M., Haffner, S. M., Herman, W. H., Holman, R. R., Kravitz, B. G., Yu, D. H., Heise, M. A., Aftring, R. P., Viberti, G. and Gr, P. T. A. S. (2008) 'Rosiglitazone-associated fractures in type 2 diabetes - An analysis from a diabetes outcome progression trial (ADOPT)', *Diabetes Care*, 31(5), 845-851.

Kanazawa, I., Yamaguchi, T. and Sugimoto, T. (2011) 'Serum insulin-like growth factor-I is a marker for assessing the severity of vertebral fractures in postmenopausal women with type 2 diabetes mellitus', *Osteoporos Int*, 22(4), 1191-8.

Kanazawa, I., Yamaguchi, T., Yano, S., Hayashi, K., Yamauchi, M. and Sugimoto, T. (2009) 'Inhibition of the mevalonate pathway rescues the dexamethasone-induced suppression of the mineralization in osteoblasts via enhancing bone morphogenetic protein-2 signal', *Horm Metab Res*, 41(8), 612-6.

Kanazawa, I., Yamaguchi, T., Yano, S., Yamauchi, M. and Sugimoto, T. (2008) 'Metformin enhances the differentiation and mineralization of osteoblastic MC3T3-E1 cells via AMP kinase activation as well as eNOS and BMP-2 expression', *Biochem Biophys Res Commun*, 375(3), 414-9.

Kanazawa, I., Yamaguchi, T., Yano, S., Yamauchi, M., Yamamoto, M. and Sugimoto, T. (2007) 'Adiponectin and AMP kinase activator stimulate proliferation, differentiation, and mineralization of osteoblastic MC3T3-E1 cells', *Bmc Cell Biology*, 8, 51.

Kanis, J. A. (2002) 'Diagnosis of osteoporosis and assessment of fracture risk', *Lancet*, 359(9321), 1929-36.

Kanis, J. A. and Gluer, C. C. (2000) 'An update on the diagnosis and assessment of osteoporosis with densitometry. Committee of Scientific Advisors, International Osteoporosis Foundation', *Osteoporos Int*, 11(3), 192-202.

Kanis, J. A., Johnell, O., Oden, A., Johansson, H. and McCloskey, E. (2008) 'FRAX and the assessment of fracture probability in men and women from the UK', *Osteoporos Int*, 19(4), 385-97.

Kanis, J. A., Oden, A., Johnell, O., Jonsson, B., de Laet, C. and Dawson, A. (2001) 'The burden of osteoporotic fractures: a method for setting intervention thresholds', *Osteoporos Int*, 12(5), 417-27.

Karaguzel, G., Ozdem, S., Boz, A., Bircan, I. and Akcurin, S. (2006) 'Leptin levels and body composition in children and adolescents with type 1 diabetes', *Clin Biochem*, 39(8), 788-93.

Karampinos, D. C., Ruschke, S., Gordijenko, O., Grande Garcia, E., Kooijman, H., Burgkart, R., Rummeny, E. J., Bauer, J. S. and Baum, T. (2015) 'Association of MRS-Based Vertebral Bone Marrow Fat Fraction with Bone Strength in a Human In Vitro Model', *J Osteoporos*, 2015, 152349.

Karim, L., Moulton, J., Van Vliet, M., Velie, K., Robbins, A., Malekipour, F., Abdeen, A., Ayres, D. and Bouxsein, M. L. (2018) 'Bone microarchitecture, biomechanical properties, and advanced glycation end-products in the proximal femur of adults with type 2 diabetes', *Bone*, 114, 32-39.

Kasai, T., Bandow, K., Suzuki, H., Chiba, N., Kakimoto, K., Ohnishi, T., Kawamoto, S., Nagaoka, E. and Matsuguchi, T. (2009) 'Osteoblast differentiation is functionally associated with decreased AMP kinase activity', *J Cell Physiol*, 221(3), 740-9.

Katagiri, T., Yamaguchi, A., Ikeda, T., Yoshiki, S., Wozney, J. M., Rosen, V., Wang, E. A., Tanaka, H., Omura, S. and Suda, T. (1990) 'The non-osteogenic mouse pluripotent cell line, C3H10T1/2, is induced to differentiate into osteoblastic cells by recombinant human bone morphogenetic protein-2', *Biochem Biophys Res Commun*, 172(1), 295-9.

Katayama, Y., Akatsu, T., Yamamoto, M., Kugai, N. and Nagata, N. (1996) 'Role of nonenzymatic glycosylation of type I collagen in diabetic osteopenia', *J Bone Miner Res*, 11(7), 931-7.

Kawai, M., Mushiake, S., Bessho, K., Murakami, M., Namba, N., Kokubu, C., Michigami, T. and Ozono, K. (2007) 'Wnt/Lrp/beta-catenin signaling suppresses adipogenesis by inhibiting mutual activation of PPARgamma and C/EBPalpha', *Biochem Biophys Res Commun*, 363(2), 276-82.

Keats, E. and Khan, Z. A. (2012) 'Unique responses of stem cell-derived vascular endothelial and mesenchymal cells to high levels of glucose', *PLoS One*, 7(6), e38752.

Kelly, D. J. and Jacobs, C. R. (2010) 'The role of mechanical signals in regulating chondrogenesis and osteogenesis of mesenchymal stem cells', *Birth Defects Res C Embryo Today*, 90(1), 75-85.

Kim, E. K., Lim, S., Park, J. M., Seo, J. K., Kim, J. H., Kim, K. T., Ryu, S. H. and Suh, P. G. (2012) 'Human mesenchymal stem cell differentiation to the osteogenic or adipogenic lineage is regulated by AMP-activated protein kinase', *J Cell Physiol*, 227(4), 1680-7.

Kim, J. E., Ahn, M. W., Baek, S. H., Lee, I. K., Kim, Y. W., Kim, J. Y., Dan, J. M. and Park, S. Y. (2008) 'AMPK activator, AICAR, inhibits palmitate-induced apoptosis in osteoblast', *Bone*, 43(2), 394-404.

Kim, K. M. and Lim, S. K. (2014) 'Role of miRNAs in bone and their potential as therapeutic targets', *Curr Opin Pharmacol*, 16, 133-41.

Kim, T. Y., Schwartz, A. V., Li, X., Xu, K., Black, D. M., Petrenko, D. M., Stewart, L., Rogers, S. J., Posselt, A. M., Carter, J. T., Shoback, D. M. and Schafer, A. L. (2017) 'Bone Marrow Fat Changes After Gastric Bypass Surgery Are Associated With Loss of Bone Mass', *J Bone Miner Res*, 32(11), 2239-2247.

Kjaer, K., Hagen, C., Sando, S. H. and Eshoj, O. (1992) 'Epidemiology of menarche and menstrual disturbances in an unselected group of women with insulin-dependent diabetes mellitus compared to controls', *J Clin Endocrinol Metab*, 75(2), 524-9.

Kliewer, S. A., Lenhard, J. M., Willson, T. M., Patel, I., Morris, D. C. and Lehmann, J. M. (1995) 'A prostaglandin J2 metabolite binds peroxisome proliferator-activated receptor gamma and promotes adipocyte differentiation', *Cell*, 83(5), 813-9.

Knox, S., Harris, J., Calton, L. and Wallace, A. M. (2009) 'A simple automated solid-phase extraction procedure for measurement of 25-hydroxyvitamin D3 and D2 by liquid chromatography-tandem mass spectrometry', *Ann Clin Biochem*, 46(Pt 3), 226-30.

Kobashigawa, L. C., Xu, Y. C., Padbury, J. F., Tseng, Y. T. and Yano, N. (2014) 'Metformin protects cardiomyocyte from doxorubicin induced cytotoxicity through an AMP-activated protein kinase dependent signaling pathway: an in vitro study', *PLoS One*, 9(8), e104888.

Kobayashi, H., Gao, Y., Ueta, C., Yamaguchi, A. and Komori, T. (2000) 'Multilineage differentiation of Cbfa1-deficient calvarial cells in vitro', *Biochem Biophys Res Commun*, 273(2), 630-6.

Komori, T. (2010) 'Regulation of bone development and extracellular matrix protein genes by RUNX2', *Cell Tissue Res*, 339(1), 189-95.

Komori, T., Yagi, H., Nomura, S., Yamaguchi, A., Sasaki, K., Deguchi, K., Shimizu, Y., Bronson, R. T., Gao, Y. H., Inada, M., Sato, M., Okamoto, R., Kitamura, Y., Yoshiki, S. and Kishimoto, T. (1997) 'Targeted disruption of Cbfa1 results in a complete lack of bone formation owing to maturational arrest of osteoblasts', *Cell*, 89(5), 755-64.

Korkusuz, F. (2015) *Musculoskeletal Research and Basic Science*, Springer.

Korula, S., Titmuss, A. T., Biggin, A. and Munns, C. F. (2015) 'A Practical Approach to Children with Recurrent Fractures', *Endocr Dev*, 28, 210-25.

Kowalski, K. C., Crocker, P. R. E. and Faulkner, R. A. (1997a) 'Validation of the physical activity questionnaire for older children', *Pediatric Exercise Science*, 9(2), 174-186.

Kowalski, K. C., Crocker, P. R. E. and Kowalski, N. P. (1997b) 'Convergent validity of the physical activity questionnaire for adolescents', *Pediatric Exercise Science*, 9(4), 342-352.

Krakauer, J. C., McKenna, M. J., Buderer, N. F., Rao, D. S., Whitehouse, F. W. and Parfitt, A. M. (1995) 'Bone loss and bone turnover in diabetes', *Diabetes*, 44(7), 775-82.

Krolewski, A. S., Kosinski, E. J., Warram, J. H., Leland, O. S., Busick, E. J., Asmal, A. C., Rand, L. I., Christlieb, A. R., Bradley, R. F. and Kahn, C. R. (1987) 'Magnitude and determinants of coronary artery disease in juvenile-onset, insulin-dependent diabetes mellitus', *Am J Cardiol*, 59(8), 750-5.

Krolewski, A. S., Warram, J. H., Christlieb, A. R., Busick, E. J. and Kahn, C. R. (1985) 'The changing natural history of nephropathy in type I diabetes', *Am J Med*, 78(5), 785-94.

Kudo, N., Barr, A. J., Barr, R. L., Desai, S. and Lopaschuk, G. D. (1995) 'High rates of fatty acid oxidation during reperfusion of ischemic hearts are associated with a decrease in malonyl-CoA levels due to an increase in 5'-AMP-activated protein kinase inhibition of acetyl-CoA carboxylase', *Journal of Biological Chemistry*, 270(29), 17513-20.

Kugel, H., Jung, C., Schulte, O. and Heindel, W. (2001) 'Age- and sex-specific differences in the 1H-spectrum of vertebral bone marrow', *Journal of Magnetic Resonance Imaging*, 13(2), 263-8.

Kume, S., Kato, S., Yamagishi, S., Inagaki, Y., Ueda, S., Arima, N., Okawa, T., Kojiro, M. and Nagata, K. (2005) 'Advanced glycation end-products attenuate human mesenchymal stem cells and prevent cognate differentiation into adipose tissue, cartilage, and bone', *J Bone Miner Res*, 20(9), 1647-58.

Kyriakou, A., Shepherd, S., Mason, A. and Ahmed, S. F. (2016) 'Prevalence of Vertebral Fractures in Children with Suspected Osteoporosis', *J Pediatr*, 179, 219-225.

Lachin, J. M., Genuth, S., Nathan, D. M., Zinman, B., Rutledge, B. N. and Group, D. E. R. (2008) 'Effect of glycemic exposure on the risk of microvascular complications in the diabetes control and complications trial--revisited', *Diabetes*, 57(4), 995-1001.

Laemmli, U. K. (1970) 'Cleavage of structural proteins during the assembly of the head of bacteriophage T4', *Nature*, 227(5259), 680-5.

Lagani, V., Chiarugi, F., Thomson, S., Fursse, J., Lakasing, E., Jones, R. W. and Tsamardinos, I. (2015) 'Development and validation of risk assessment models for diabetes-related complications based on the DCCT/EDIC data', *J Diabetes Complications*, 29(4), 479-87.

Landin, L. A. (1983) 'Fracture patterns in children. Analysis of 8,682 fractures with special reference to incidence, etiology and secular changes in a Swedish urban population 1950-1979', *Acta Orthop Scand Suppl*, 202, 1-109.

Lawson, M. L., Sochett, E. B., Chait, P. G., Balfe, J. W. and Daneman, D. (1996) 'Effect of puberty on markers of glomerular hypertrophy and hypertension in IDDM', *Diabetes*, 45(1), 51-5.

Lee, H., Kang, R., Bae, S. and Yoon, Y. (2011) 'AICAR, an activator of AMPK, inhibits adipogenesis via the WNT/beta-catenin pathway in 3T3-L1 adipocytes', *Int J Mol Med*, 28(1), 65-71.

Lee, J. O., Lee, S. K., Kim, J. H., Kim, N., You, G. Y., Moon, J. W., Kim, S. J., Park, S. H. and Kim, H. S. (2012) 'Metformin regulates glucose transporter 4 (GLUT4) translocation through AMP-activated protein kinase (AMPK)-mediated Cbl/CAP signaling in 3T3-L1 preadipocyte cells', *J Biol Chem*, 287(53), 44121-9.

Lee, N. K., Sowa, H., Hinoi, E., Ferron, M., Ahn, J. D., Confavreux, C., Dacquin, R., Mee, P. J., McKee, M. D., Jung, D. Y., Zhang, Z., Kim, J. K., Mauvais-Jarvis, F., Ducy, P. and Karsenty, G. (2007) 'Endocrine regulation of energy metabolism by the skeleton', *Cell*, 130(3), 456-69.

Lee, S., Cho, H. Y., Bui, H. T. and Kang, D. (2014) 'The osteogenic or adipogenic lineage commitment of human mesenchymal stem cells is determined by protein kinase C delta', *Bmc Cell Biology*, 15, 42.

Leger, J., Marinovic, D., Alberti, C., Dorgeret, S., Chevenne, D., Marchal, C. L., Tubiana-Rufi, N., Sebag, G. and Czernichow, P. (2006) 'Lower bone mineral content in children with type 1 diabetes mellitus is linked to female sex, low insulin-like growth factor type I levels, and high insulin requirement', *J Clin Endocrinol Metab*, 91(10), 3947-53.

Lehmann, J. M., Moore, L. B., Smith-Oliver, T. A., Wilkison, W. O., Willson, T. M. and Kliewer, S. A. (1995) 'An antidiabetic thiazolidinedione is a high affinity ligand for peroxisome proliferator-activated receptor gamma (PPAR gamma)', *Journal of Biological Chemistry*, 270(22), 12953-6.

Lenchik, L., Register, T. C., Hsu, F. C., Lohman, K., Nicklas, B. J., Freedman, B. I., Langefeld, C. D., Carr, J. J. and Bowden, D. W. (2003) 'Adiponectin as a novel determinant of bone mineral density and visceral fat', *Bone*, 33(4), 646-51.

Lenchik, L., Rochmis, P. and Sartoris, D. (1998) 'Optimised interpretation and reporting of dual X-ray absorptiometry (DXA) scans', *American Journal of Roentgenology*, 171(6), 1509-1520.

Leslie, W. D., Aubry-Rozier, B., Lamy, O., Hans, D. and Manitoba Bone Density, P. (2013) 'TBS (trabecular bone score) and diabetes-related fracture risk', *J Clin Endocrinol Metab*, 98(2), 602-9.

Lettgen, B., Hauffa, B., Mohlmann, C., Jeken, C. and Reiners, C. (1995) 'Bone mineral density in children and adolescents with juvenile diabetes: selective measurement of bone mineral density of trabecular and cortical bone using peripheral quantitative computed tomography', *Horm Res*, 43(5), 173-5.

Levy, J. R., Murray, E., Manolagas, S. and Olefsky, J. M. (1986) 'Demonstration of insulin receptors and modulation of alkaline phosphatase activity by insulin in rat osteoblastic cells', *Endocrinology*, 119(4), 1786-92.

Li, B. and Aspden, R. M. (1997) 'Composition and mechanical properties of cancellous bone from the femoral head of patients with osteoporosis or osteoarthritis', *J Bone Miner Res*, 12(4), 641-51.

Li, H., Xie, H., Liu, W., Hu, R., Huang, B., Tan, Y. F., Xu, K., Sheng, Z. F., Zhou, H. D., Wu, X. P. and Luo, X. H. (2009) 'A novel microRNA targeting HDAC5 regulates osteoblast differentiation in mice and contributes to primary osteoporosis in humans', *Journal of Clinical Investigation*, 119(12), 3666-77.

Li, X., Zhang, Y., Kang, H., Liu, W., Liu, P., Zhang, J., Harris, S. E. and Wu, D. (2005) 'Sclerostin binds to LRP5/6 and antagonizes canonical Wnt signaling', *Journal of Biological Chemistry*, 280(20), 19883-7.

Li, X. D., Cui, Q. J., Kao, C. H., Wang, G. J. and Balian, G. (2003) 'Lovastatin inhibits adipogenic and stimulates osteogenic differentiation by suppressing PPAR gamma 2 and increasing Cbfa1/Runx2 expression in bone marrow mesenchymal cell cultures', *Bone*, 33(4), 652-659.

Li, X. J., Kuo, D., Schafer, A. L., Porzig, A., Link, T. M., Black, D. and Schwartz, A. V. (2011) 'Quantification of Vertebral Bone Marrow Fat Content Using 3 Tesla MR Spectroscopy: Reproducibility, Vertebral Variation, and Applications in Osteoporosis', *Journal of Magnetic Resonance Imaging*, 33(4), 974-979.

Ljunggren, O., Bolinder, J., Johansson, L., Wilding, J., Langkilde, A. M., Sjostrom, C. D., Sugg, J. and Parikh, S. (2012) 'Dapagliflozin has no effect on markers of bone formation and resorption or bone mineral density in patients with inadequately controlled type 2 diabetes mellitus on metformin', *Diabetes Obes Metab*, 14(11), 990-9.

Loke, Y. K., Singh, S. and Furberg, C. D. (2009) 'Long-term use of thiazolidinediones and fractures in type 2 diabetes: a meta-analysis', *Canadian Medical Association Journal*, 180(1), 32-39.

Lombardo, F., Salzano, G., Crisafulli, G., Valenzise, M., Zirilli, G., Manzo, V., Aversa, T. and De Luca, F. (2009) 'Menarcheal timing in intensively treated girls with type 1 diabetes mellitus', *Nutr Metab Cardiovasc Dis*, 19(1), 35-8.

Longnus, S. L., Segalen, C., Giudicelli, J., Sajan, M. P., Farese, R. V. and Van Obberghen, E. (2005) 'Insulin signalling downstream of protein kinase B is potentiated by 5'AMP-activated protein kinase in rat hearts in vivo', *Diabetologia*, 48(12), 2591-601.

Loots, G. G., Kneissel, M., Keller, H., Baptist, M., Chang, J., Collette, N. M., Ovcharenko, D., Plajzer-Frick, I. and Rubin, E. M. (2005) 'Genomic deletion of a long-range bone enhancer misregulates sclerostin in Van Buchem disease', *Genome Res*, 15(7), 928-35.

Lopez-Ibarra, P. J., Pastor, M. M., Escobar-Jimenez, F., Pardo, M. D., Gonzalez, A. G., Luna, J. D., Requena, M. E. and Diosdado, M. A. (2001) 'Bone mineral density at time of clinical diagnosis of adult-onset type 1 diabetes mellitus', *Endocr Pract*, 7(5), 346-51.

Lorentzon, M. and Cummings, S. R. (2015) 'Osteoporosis: the evolution of a diagnosis', *J Intern Med*, 277(6), 650-61.

Lorentzon, M., Mellstrom, D. and Ohlsson, C. (2005) 'Age of attainment of peak bone mass is site specific in Swedish men--The GOOD study', *J Bone Miner Res*, 20(7), 1223-7.

Loro, M. L., Sayre, J., Roe, T. F., Goran, M. I., Kaufman, F. R. and Gilsanz, V. (2000) 'Early identification of children predisposed to low peak bone mass and osteoporosis later in life', *J Clin Endocrinol Metab*, 85(10), 3908-18.

Loureiro, M. B., Ururahy, M. A., Freire-Neto, F. P., Oliveira, G. H., Duarte, V. M., Luchessi, A. D., Brandao-Neto, J., Hirata, R. D., Hirata, M. H., Maciel-Neto, J. J., Arrais, R. F., Almeida, M. G. and Rezende, A. A. (2014) 'Low bone mineral density is associated to poor glycemic

control and increased OPG expression in children and adolescents with type 1 diabetes', *Diabetes Res Clin Pract*, 103(3), 452-7.

Lozano, D., de Castro, L. F., Dapia, S., Andrade-Zapata, I., Manzarbeitia, F., Alvarez-Arroyo, M. V., Gomez-Barrena, E. and Esbrit, P. (2009) 'Role of parathyroid hormone-related protein in the decreased osteoblast function in diabetes-related osteopenia', *Endocrinology*, 150(5), 2027-35.

Lumachi, F., Camozzi, V., Tombolan, V. and Luisetto, G. (2009) 'Bone mineral density, osteocalcin, and bone-specific alkaline phosphatase in patients with insulin-dependent diabetes mellitus', *Ann N Y Acad Sci*, 1173 Suppl 1, E64-7.

Luna, R., Garcia-Mayor, R. V., Lage, M., Andrade, M. A., Barreiro, J., Pombo, M., Dieguez, C. and Casanueva, F. F. (1999) 'High serum leptin levels in children with type 1 diabetes mellitus: contribution of age, BMI, pubertal development and metabolic status', *Clin Endocrinol (Oxf)*, 51(5), 603-10.

Lunt, H., Florkowski, C. M., Cundy, T., Kendall, D., Brown, L. J., Elliot, J. R., Wells, J. E. and Turner, J. G. (1998) 'A population-based study of bone mineral density in women with longstanding type 1 (insulin dependent) diabetes', *Diabetes Res Clin Pract*, 40(1), 31-8.

Lyons, R. A., Delahunty, A. M., Heaven, M., McCabe, M., Allen, H. and Nash, P. (2000) 'Incidence of childhood fractures in affluent and deprived areas: population based study', *BMJ*, 320(7228), 149.

Ma, L., Oei, L., Jiang, L., Estrada, K., Chen, H., Wang, Z., Yu, Q., Zillikens, M. C., Gao, X. and Rivadeneira, F. (2012) 'Association between bone mineral density and type 2 diabetes mellitus: a meta-analysis of observational studies', *Eur J Epidemiol*, 27(5), 319-32.

Ma, P., Gu, B., Ma, J., E, L., Wu, X., Cao, J. and Liu, H. (2010a) 'Glimepiride induces proliferation and differentiation of rat osteoblasts via the PI3-kinase/Akt pathway', *Metabolism-Clinical and Experimental*, 59(3), 359-66.

Ma, P., Gu, B., Ma, J. L., E, L. L., Wu, X., Cao, J. K. and Liu, H. C. (2010b) 'Glimepiride induces proliferation and differentiation of rat osteoblasts via the PI3-kinase/Akt pathway', *Metabolism-Clinical and Experimental*, 59(3), 359-366.

Madiraju, A. K., Erion, D. M., Rahimi, Y., Zhang, X. M., Braddock, D. T., Albright, R. A., Prigaro, B. J., Wood, J. L., Bhanot, S., MacDonald, M. J., Jurczak, M. J., Camporez, J. P., Lee, H. Y., Cline, G. W., Samuel, V. T., Kibbey, R. G. and Shulman, G. I. (2014) 'Metformin suppresses gluconeogenesis by inhibiting mitochondrial glycerophosphate dehydrogenase', *Nature*, 510(7506), 542-6.

Maggio, A. B., Ferrari, S., Kraenzlin, M., Marchand, L. M., Schwitzgebel, V., Beghetti, M., Rizzoli, R. and Farpour-Lambert, N. J. (2010) 'Decreased bone turnover in children and adolescents with well controlled type 1 diabetes', *J Pediatr Endocrinol Metab*, 23(7), 697-707.

Magland, J. F., Zhang, N., Rajapakse, C. S. and Wehrli, F. W. (2012) 'Computationally-optimized bone mechanical modeling from high-resolution structural images', *PLoS One*, 7(4), e35525.

Magnusson, P., Hager, A. and Larsson, L. (1995) 'Serum osteocalcin and bone and liver alkaline phosphatase isoforms in healthy children and adolescents', *Pediatr Res*, 38(6), 955-61.

Mai, Q. G., Zhang, Z. M., Xu, S., Lu, M., Zhou, R. P., Zhao, L., Jia, C. H., Wen, Z. H., Jin, D. D. and Bai, X. C. (2011) 'Metformin stimulates osteoprotegerin and reduces RANKL expression in osteoblasts and ovariectomized rats', *Journal of Cellular Biochemistry*, 112(10), 2902-9.

Majumdar, S., Genant, H., Grampp, S., Newitt, D., Truong, V., Lin, J. and Mathur, A. (1997) 'Correlation of Trabecular Bone Structure with Age, Bone Mineral Density, and Osteoporotic Status: In Vivo Studies in the Distal Radius Using High Resolution Magnetic Resonance Imaging', *Journal of Bone and Mineral Research*, 12(1), 111-118.

Majumdar, S., Newitt, D., Jergas, M., Gies, A., Chiu, E., Osman, D., Keltner, J., Keyak, J. and Genant, H. (1995) 'Evaluation of Technical Factors Affecting the Quantification of Trabecular Bone-Structure Using Magnetic-Resonance-Imaging', *Bone*, 17(4), 417-430.

Majumdar, S., Newitt, D., Mathur, A., Osman, D., Gies, A., Chiu, E., Lotz, J., Kinney, J. and Genant, H. (1996) 'Magnetic resonance imaging of trabecular bone structure in the distal radius: Relationship with X-ray tomographic microscopy and biomechanics', *Osteoporosis International*, 6(5), 376-385.

Makitie, O. (2013) 'Causes, mechanisms and management of paediatric osteoporosis', *Nat Rev Rheumatol*, 9(8), 465-75.

Malucelli, D. A., Malucelli, F. J., Fonseca, V. R., Zeigeboim, B., Ribas, A., Trotta, F. and Silva, T. P. (2012) 'Hearing loss prevalence in patients with diabetes mellitus type 1', *Braz J Otorhinolaryngol*, 78(3), 105-15.

Manavalan, J. S., Cremers, S., Dempster, D. W., Zhou, H., Dworakowski, E., Kode, A., Kousteni, S. and Rubin, M. R. (2012) 'Circulating osteogenic precursor cells in type 2 diabetes mellitus', *J Clin Endocrinol Metab*, 97(9), 3240-50.

Mangan, J. K. and Speck, N. A. (2011) 'RUNX1 mutations in clonal myeloid disorders: from conventional cytogenetics to next generation sequencing, a story 40 years in the making', *Crit Rev Oncog*, 16(1-2), 77-91.

Maor, G. and Karnieli, E. (1999) 'The insulin-sensitive glucose transporter (GLUT4) is involved in early bone growth in control and diabetic mice, but is regulated through the insulin-like growth factor I receptor', *Endocrinology*, 140(4), 1841-51.

Maratova, K., Soucek, O., Matyskova, J., Hlavka, Z., Petruzelkova, L., Obermannova, B., Pruhova, S., Kolouskova, S. and Sumnik, Z. (2018) 'Muscle functions and bone strength are impaired in adolescents with type 1 diabetes', *Bone*, 106, 22-27.

Marie, P. J. and Fromigue, O. (2006) 'Osteogenic differentiation of human marrow-derived mesenchymal stem cells', *Regen Med*, 1(4), 539-48.

Marshall, D., Johnell, O. and Wedel, H. (1996) 'Meta-analysis of how well measures of bone mineral density predict occurrence of osteoporotic fractures', *BMJ*, 312(7041), 1254-9.

Marsin, A. S., Bertrand, L., Rider, M. H., Deprez, J., Beauloye, C., Vincent, M. F., Van den Berghe, G., Carling, D. and Hue, L. (2000) 'Phosphorylation and activation of heart PFK-2 by AMPK has a role in the stimulation of glycolysis during ischaemia', *Curr Biol*, 10(20), 1247-55.

Martin, A., de Vittoris, R., David, V., Moraes, R., Begeot, M., Lafage-Proust, M. H., Alexandre, C., Vico, L. and Thomas, T. (2005) 'Leptin modulates both resorption and formation while preventing disuse-induced bone loss in tail-suspended female rats', *Endocrinology*, 146(8), 3652-9.

Martin, J. W., Zielenska, M., Stein, G. S., van Wijnen, A. J. and Squire, J. A. (2011) 'The Role of RUNX2 in Osteosarcoma Oncogenesis', *Sarcoma*, 2011, 282745.

Martin, R. and Burr, D. (1989) *The microscopic structure of bone*, New York: Raven Press.

Masse, P. G., Pacifique, M. B., Tranchant, C. C., Arjmandi, B. H., Ericson, K. L., Donovan, S. M., Delvin, E. and Caissie, M. (2010) 'Bone metabolic abnormalities associated with well-controlled type 1 diabetes (IDDM) in young adult women: a disease complication often ignored or neglected', *J Am Coll Nutr*, 29(4), 419-29.

Mastrandrea, L. D., Wactawski-Wende, J., Donahue, R. P., Hovey, K. M., Clark, A. and Quattrin, T. (2008) 'Young women with type 1 diabetes have lower bone mineral density that persists over time', *Diabetes Care*, 31(9), 1729-35.

Matikainen, T., Kakonen, S. M., Pettersson, K., Karp, M., Lovgren, T., Vaananen, H. and Hellman, J. (1999) 'Demonstration of the predominant urine osteocalcin fragments detectable by two-site immunoassays', *J Bone Miner Res*, 14(3), 431-8.

Maurin, A. C., Chavassieux, P. M., Frappart, L., Delmas, P. D., Serre, C. M. and Meunier, P. J. (2000) 'Influence of mature adipocytes on osteoblast proliferation in human primary cocultures', *Bone*, 26(5), 485-9.

Mayranpaa, M. K., Makitie, O. and Kallio, P. E. (2010) 'Decreasing incidence and changing pattern of childhood fractures: A population-based study', *J Bone Miner Res*, 25(12), 2752-9.

McBride, A. and Hardie, D. G. (2009) 'AMP-activated protein kinase--a sensor of glycogen as well as AMP and ATP?', *Acta Physiol (Oxf)*, 196(1), 99-113.

McCabe, L., Zhang, J. and Raehtz, S. (2011) 'Understanding the skeletal pathology of type 1 and 2 diabetes mellitus', *Crit Rev Eukaryot Gene Expr*, 21(2), 187-206.

McComb, C., Harpur, A., Yacoubian, C., Leddy, C., Anderson, G., Shepherd, S., Perry, C., Shaikh, M. G., Foster, J. and Ahmed, S. F. (2014a) 'MRI-based abnormalities in young adults at risk of adverse bone health due to childhood-onset metabolic & endocrine conditions', *Clinical Endocrinology*, 80(6), 811-817.

McComb, C., Harpur, A., Yacoubian, C., Leddy, C., Anderson, G., Shepherd, S., Perry, C., Shaikh, M. G., Foster, J. and Ahmed, S. F. (2014b) 'MRI-based abnormalities in young adults at risk of adverse bone health due to childhood-onset metabolic & endocrine conditions', *Clin Endocrinol (Oxf)*, 80(6), 811-7.

McDevitt, H. and Ahmed, S. F. (2007) 'Quantitative ultrasound assessment of bone health in the neonate', *Neonatology*, 91(1), 2-11.

McDonald, D. G., Kinali, M., Gallagher, A. C., Mercuri, E., Muntoni, F., Roper, H., Jardine, P., Jones, D. H. and Pike, M. G. (2002) 'Fracture prevalence in Duchenne muscular dystrophy', *Dev Med Child Neurol*, 44(10), 695-8.

McNair, P., Madsbad, S., Christiansen, C., Faber, O. K., Transbol, I. and Binder, C. (1978) 'Osteopenia in insulin treated diabetes mellitus. Its relation to age at onset, sex and duration of disease', *Diabetologia*, 15(2), 87-90.

Mehlem, A., Hagberg, C. E., Muhl, L., Eriksson, U. and Falkevall, A. (2013) 'Imaging of neutral lipids by oil red O for analyzing the metabolic status in health and disease', *Nat Protoc*, 8(6), 1149-54.

Melton, L. J., 3rd, Leibson, C. L., Achenbach, S. J., Therneau, T. M. and Khosla, S. (2008) 'Fracture risk in type 2 diabetes: update of a population-based study', *J Bone Miner Res*, 23(8), 1334-42.

Mergler, S., Evenhuis, H. M., Boot, A. M., De Man, S. A., Bindels-De Heus, K. G., Huijbers, W. A. and Penning, C. (2009) 'Epidemiology of low bone mineral density and fractures in children with severe cerebral palsy: a systematic review', *Dev Med Child Neurol*, 51(10), 773-8.

Meunier, P., Aaron, J., Edouard, C. and Vignon, G. (1971) 'Osteoporosis and the replacement of cell populations of the marrow by adipose tissue. A quantitative study of 84 iliac bone biopsies', *Clin Orthop Relat Res*, 80, 147-54.

Miao, J., Brismar, K., Nyren, O., Ugarph-Morawski, A. and Ye, W. (2005) 'Elevated hip fracture risk in type 1 diabetic patients: a population-based cohort study in Sweden', *Diabetes Care*, 28(12), 2850-5.

Miller, R. A., Chu, Q., Xie, J., Foretz, M., Viollet, B. and Birnbaum, M. J. (2013) 'Biguanides suppress hepatic glucagon signalling by decreasing production of cyclic AMP', *Nature*, 494(7436), 256-60.

Mills, L. A. and Simpson, A. H. (2013) 'The risk of non-union per fracture in children', *J Child Orthop*, 7(4), 317-22.

Miyamoto, S., Ochiai, A., Boku, N., Ohtsu, A., Tahara, M., Yoshida, S., Okabe, H., Takechi, T. and Fukushima, M. (2001) 'Discrepancies between the gene expression, protein expression,

and enzymatic activity of thymidylate synthase and dihydropyrimidine dehydrogenase in human gastrointestinal cancers and adjacent normal mucosa', *Int J Oncol*, 18(4), 705-13.

Miyata, T., Notoya, K., Yoshida, K., Horie, K., Maeda, K., Kurokawa, K. and Taketomi, S. (1997) 'Advanced glycation end products enhance osteoclast-induced bone resorption in cultured mouse unfractionated bone cells and in rats implanted subcutaneously with devitalized bone particles', *J Am Soc Nephrol*, 8(2), 260-70.

Molinuevo, M. S., Schurman, L., McCarthy, A. D., Cortizo, A. M., Tolosa, M. J., Gangoiti, M. V., Arnol, V. and Sedlinsky, C. (2010) 'Effect of metformin on bone marrow progenitor cell differentiation: in vivo and in vitro studies', *J Bone Miner Res*, 25(2), 211-21.

Monami, M., Cresci, B., Colombini, A., Pala, L., Balzi, D., Gori, F., Chiasserini, V., Marchionni, N., Rotella, C. M. and Mannucci, E. (2008) 'Bone fractures and hypoglycemic treatment in type 2 diabetic patients: a case-control study', *Diabetes Care*, 31(2), 199-203.

Monami, M., Dicembrini, I., Antenore, A. and Mannucci, E. (2011) 'Dipeptidyl peptidase-4 inhibitors and bone fractures: a meta-analysis of randomized clinical trials', *Diabetes Care*, 34(11), 2474-6.

Montazersaheb, S., Kabiri, F., Saliani, N., Nourazarian, A., Avci, C. B., Rahbarghazi, R. and Nozad Charoudeh, H. (2018) 'Prolonged incubation with Metformin decreased angiogenic potential in human bone marrow mesenchymal stem cells', *Biomed Pharmacother*, 108, 1328-1337.

Moreno D, Knecht E, Viollet B, Sanz P. (2008) 'A769662, a novel activator of AMP-activated protein kinase, inhibits non-proteolytic components of the 26S proteasome by an AMPK-independent mechanism', *FEBS Letter*, 582 (17):2650-4

Moreno-Navarrete, J. M., Ortega, F. J., Rodriguez-Hermosa, J. I., Sabater, M., Pardo, G., Ricart, W. and Fernandez-Real, J. M. (2011) 'OCT1 Expression in adipocytes could contribute to increased metformin action in obese subjects', *Diabetes*, 60(1), 168-76.

Morris, N. M. and Udry, J. R. (1980) 'Validation of a self-administered instrument to assess stage of adolescent development', *J Youth Adolesc*, 9(3), 271-80.

Mosekilde, L. (1990) 'Consequences of the remodelling process for vertebral trabecular bone structure: a scanning electron microscopy study (uncoupling of unloaded structures)', *Bone Miner*, 10(1), 13-35.

Mosenzon, O., Wei, C., Davidson, J., Scirica, B. M., Yanuv, I., Rozenberg, A., Hirshberg, B., Cahn, A., Stahre, C., Strojek, K., Bhatt, D. L. and Raz, I. (2015) 'Incidence of Fractures in Patients With Type 2 Diabetes in the SAVOR-TIMI 53 Trial', *Diabetes Care*, 38(11), 2142-50.

Motyl, K. J., Botolin, S., Irwin, R., Appledorn, D. M., Kadakia, T., Amalfitano, A., Schwartz, R. C. and McCabe, L. R. (2009) 'Bone inflammation and altered gene expression with type I diabetes early onset', *J Cell Physiol*, 218(3), 575-83.

Motyl, K. J. and McCabe, L. R. (2009) 'Leptin treatment prevents type I diabetic marrow adiposity but not bone loss in mice', *J Cell Physiol*, 218(2), 376-84.

Motyl, K. J., McCauley, L. K. and McCabe, L. R. (2012) 'Amelioration of type I diabetes-induced osteoporosis by parathyroid hormone is associated with improved osteoblast survival', *J Cell Physiol*, 227(4), 1326-34.

Motyl, K. J., Raetz, M., Tekalur, S. A., Schwartz, R. C. and McCabe, L. R. (2011) 'CCAAT/enhancer binding protein beta-deficiency enhances type 1 diabetic bone phenotype by increasing marrow adiposity and bone resorption', *Am J Physiol Regul Integr Comp Physiol*, 300(5), R1250-60.

Moustaki, M., Lariou, M. and Petridou, E. (2001) 'Cross country variation of fractures in the childhood population. Is the origin biological or "accidental"?', *Inj Prev*, 7(1), 77.

Moyer-Mileur, L. J., Dixon, S. B., Quick, J. L., Askew, E. W. and Murray, M. A. (2004) 'Bone mineral acquisition in adolescents with type 1 diabetes', *J Pediatr*, 145(5), 662-9.

Moyer-Mileur, L. J., Slater, H., Jordan, K. C. and Murray, M. A. (2008) 'IGF-1 and IGF-binding proteins and bone mass, geometry, and strength: relation to metabolic control in adolescent girls with type 1 diabetes', *J Bone Miner Res*, 23(12), 1884-91.

Muilerman, H. G., ter Hart, H. G. and Van Dijk, W. (1982) 'Specific detection of inactive enzyme protein after polyacrylamide gel electrophoresis by a new enzyme-immunoassay method using unspecific antiserum and partially purified active enzyme: application to rat liver phosphodiesterase I', *Anal Biochem*, 120(1), 46-51.

Mundlos, S., Otto, F., Mundlos, C., Mulliken, J. B., Aylsworth, A. S., Albright, S., Lindhout, D., Cole, W. G., Henn, W., Knoll, J. H., Owen, M. J., Mertelsmann, R., Zabel, B. U. and Olsen, B. R. (1997) 'Mutations involving the transcription factor CBFA1 cause cleidocranial dysplasia', *Cell*, 89(5), 773-9.

Muruganandan, S., Roman, A. A. and Sinal, C. J. (2009) 'Adipocyte differentiation of bone marrow-derived mesenchymal stem cells: Cross talk with the osteoblastogenic program', *Cellular and Molecular Life Sciences*, 66(2), 236-253.

Musi, N., Hirshman, M. F., Nygren, J., Svanfeldt, M., Bavenholm, P., Rooyackers, O., Zhou, G., Williamson, J. M., Ljunqvist, O., Efendic, S., Moller, D. E., Thorell, A. and Goodyear, L. J. (2002) 'Metformin increases AMP-activated protein kinase activity in skeletal muscle of subjects with type 2 diabetes', *Diabetes*, 51(7), 2074-81.

Naessen, T., Mallmin, H. and Ljunghall, S. (1995) 'Heel ultrasound in women after long-term ERT compared with bone densities in the forearm, spine and hip', *Osteoporos Int*, 5(3), 205-10.

Nakahara, H., Dennis, J. E., Bruder, S. P., Haynesworth, S. E., Lennon, D. P. and Caplan, A. I. (1991) 'Invitro Differentiation of Bone and Hypertrophic Cartilage from Periosteal-Derived Cells', *Experimental Cell Research*, 195(2), 492-503.

Nam, M., Lee, W. H., Bae, E. J. and Kim, S. G. (2008) 'Compound C inhibits clonal expansion of preadipocytes by increasing p21 level irrespectively of AMPK inhibition', *Arch Biochem Biophys*, 479(1), 74-81.

Napoli, N., Pedone, C., Pozzilli, P., Lauretani, F., Ferrucci, L. and Incalzi, R. A. (2010) 'Adiponectin and bone mass density: The InCHIANTI study', *Bone*, 47(6), 1001-5.

Napoli, N., Schwartz, A. V., Palermo, L., Jin, J. J., Wustrack, R., Cauley, J. A., Ensrud, K. E., Kelly, M. and Black, D. M. (2013) 'Risk factors for subtrochanteric and diaphyseal fractures: the study of osteoporotic fractures', *J Clin Endocrinol Metab*, 98(2), 659-67.

Napoli, N., Strotmeyer, E. S., Ensrud, K. E., Sellmeyer, D. E., Bauer, D. C., Hoffman, A. R., Dam, T. T., Barrett-Connor, E., Palermo, L., Orwoll, E. S., Cummings, S. R., Black, D. M. and Schwartz, A. V. (2014) 'Fracture risk in diabetic elderly men: the MrOS study', *Diabetologia*, 57(10), 2057-65.

Naressi, A., Couturier, C., Devos, J. M., Janssen, M., Mangeat, C., de Beer, R. and Graveron-Demilly, D. (2001) 'Java-based graphical user interface for the MRUI quantitation package', *Magnetic Resonance Materials in Physics Biology and Medicine*, 12(2-3), 141-152.

Nathan, D. M., Buse, J. B., Davidson, M. B., Ferrannini, E., Holman, R. R., Sherwin, R., Zinman, B., American Diabetes, A. and European Association for Study of, D. (2009) 'Medical management of hyperglycemia in type 2 diabetes: a consensus algorithm for the initiation and adjustment of therapy: a consensus statement of the American Diabetes Association and the European Association for the Study of Diabetes', *Diabetes Care*, 32(1), 193-203.

Nathan, D. M., Genuth, S., Lachin, J., Cleary, P., Crofford, O., Davis, M., Rand, L., Siebert, C. and on behalf of Diabetes Control Complications Trial Research Group (1993) 'The effect of intensive treatment of diabetes on the development and progression of long-term complications in insulin-dependent diabetes mellitus', *N Engl J Med*, 329(14), 977-86.

National Osteoporosis Society (2015) *The Osteoporosis Agenda England - Improving the lives of people with osteoporosis and fragility fractures*https://nos.org.uk/media/1959/agenda-for-osteoporosis-england-final.pdf.

Neumann, T., Lodes, S., Kastner, B., Franke, S., Kiehntopf, M., Lehmann, T., Muller, U. A., Wolf, G. and Samann, A. (2014) 'High serum pentosidine but not esRAGE is associated with prevalent fractures in type 1 diabetes independent of bone mineral density and glycaemic control', *Osteoporos Int*, 25(5), 1527-33.

Neumann, T., Samann, A., Lodes, S., Kastner, B., Franke, S., Kiehntopf, M., Hemmelmann, C., Lehmann, T., Muller, U. A., Hein, G. and Wolf, G. (2011) 'Glycaemic control is positively associated with prevalent fractures but not with bone mineral density in patients with Type 1 diabetes', *Diabet Med*, 28(7), 872-5.

Neve, A., Corrado, A. and Cantatore, F. P. (2011) 'Osteoblast physiology in normal and pathological conditions', *Cell Tissue Res*, 343(2), 289-302.

Nicodemus, K. K., Folsom, A. R. and Iowa Women's Health, S. (2001) 'Type 1 and type 2 diabetes and incident hip fractures in postmenopausal women', *Diabetes Care*, 24(7), 1192-7.

NIH Consensus Development Conference Panel (1993) 'Diagnosis, Prophylaxis and Treatment of Osteoporosis', *Am J Med*, 94(6), 646-50.

NIH Consensus Development Panel on Osteoporosis Prevention, D. and Therapy (2001) 'Osteoporosis prevention, diagnosis, and therapy', *JAMA*, 285(6), 785-95.

Nomoto, S., Kinoshita, T., Mori, T., Kato, K., Sugimoto, H., Kanazumi, N., Takeda, S. and Nakao, A. (2008) 'Adverse prognosis of epigenetic inactivation in RUNX3 gene at 1p36 in human pancreatic cancer', *Br J Cancer*, 98(10), 1690-5.

Nordwall, M., Abrahamsson, M., Dhir, M., Fredrikson, M., Ludvigsson, J. and Arnqvist, H. J. (2015) 'Impact of HbA1c, followed from onset of type 1 diabetes, on the development of severe retinopathy and nephropathy: the VISS Study (Vascular Diabetic Complications in Southeast Sweden)', *Diabetes Care*, 38(2), 308-15.

Nyman, J. S., Even, J. L., Jo, C. H., Herbert, E. G., Murry, M. R., Cockrell, G. E., Wahl, E. C., Bunn, R. C., Lumpkin, C. K., Jr., Fowlkes, J. L. and Thrailkill, K. M. (2011) 'Increasing duration of type 1 diabetes perturbs the strength-structure relationship and increases brittleness of bone', *Bone*, 48(4), 733-40.

Oakhill, J. S., Scott, J. W. and Kemp, B. E. (2009) 'Structure and function of AMP-activated protein kinase', *Acta Physiol (Oxf)*, 196(1), 3-14.

Ogawa, E., Inuzuka, M., Maruyama, M., Satake, M., Naito-Fujimoto, M., Ito, Y. and Shigesada, K. (1993) 'Molecular cloning and characterization of PEBP2 beta, the heterodimeric partner of a novel Drosophila runt-related DNA binding protein PEBP2 alpha', *Virology*, 194(1), 314-31.

Ogawa, N., Yamaguchi, T., Yano, S., Yamauchi, M., Yamamoto, M. and Sugimoto, T. (2007) 'The combination of high glucose and advanced glycation end-products (AGEs) inhibits the mineralization of osteoblastic MC3T3-E1 cells through glucose-induced increase in the receptor for AGEs', *Horm Metab Res*, 39(12), 871-5.

Oikawa, A., Siragusa, M., Quaini, F., Mangialardi, G., Katare, R. G., Caporali, A., van Buul, J. D., van Alphen, F. P., Graiani, G., Spinetti, G., Kraenkel, N., Prezioso, L., Emanueli, C. and Madeddu, P. (2010) 'Diabetes mellitus induces bone marrow microangiopathy', *Arterioscler Thromb Vasc Biol*, 30(3), 498-508.

Okazaki, K., Yamaguchi, T., Tanaka, K., Notsu, M., Ogawa, N., Yano, S. and Sugimoto, T. (2012) 'Advanced glycation end products (AGEs), but not high glucose, inhibit the osteoblastic differentiation of mouse stromal ST2 cells through the suppression of osterix expression, and inhibit cell growth and increasing cell apoptosis', *Calcif Tissue Int*, 91(4), 286-96.

Oskam, J., Kingma, J. and Klasen, H. J. (1998) 'Fracture of the distal forearm: epidemiological developments in the period 1971-1995', *Injury*, 29(5), 353-5.

Ostman, J., Lonnberg, G., Arnqvist, H. J., Blohme, G., Bolinder, J., Ekbom Schnell, A., Eriksson, J. W., Gudbjornsdottir, S., Sundkvist, G. and Nystrom, L. (2008) 'Gender differences and temporal variation in the incidence of type 1 diabetes: results of 8012 cases in the nationwide Diabetes Incidence Study in Sweden 1983-2002', *J Intern Med*, 263(4), 386-94.

Paccou, J., Penel, G., Chauveau, C., Cortet, B. and Hardouin, P. (2019) 'Marrow adiposity and bone: Review of clinical implications', *Bone*, 118, 8-15.

Padhi, D., Jang, G., Stouch, B., Fang, L. and Posvar, E. (2011) 'Single-dose, placebo-controlled, randomized study of AMG 785, a sclerostin monoclonal antibody', *J Bone Miner Res*, 26(1), 19-26.

Pantovic, A., Krstic, A., Janjetovic, K., Kocic, J., Harhaji-Trajkovic, L., Bugarski, D. and Trajkovic, V. (2013) 'Coordinated time-dependent modulation of AMPK/Akt/mTOR signaling and autophagy controls osteogenic differentiation of human mesenchymal stem cells', *Bone*, 52(1), 524-31.

Parfitt, A. M. (2002) 'Targeted and nontargeted bone remodeling: relationship to basic multicellular unit origination and progression', *Bone*, 30(1), 5-7.

Parfitt, A. M., Travers, R., Rauch, F. and Glorieux, F. H. (2000) 'Structural and cellular changes during bone growth in healthy children', *Bone*, 27(4), 487-94.

Parthasarathy, L. S., Khadilkar, V. V., Chiplonkar, S. A., Zulf Mughal, M. and Khadilkar, A. V. (2016) 'Bone status of Indian children and adolescents with type 1 diabetes mellitus', *Bone*, 82, 16-20.

Pascual, J., Argente, J., Lopez, M. B., Munoz, M., Martinez, G., Vazquez, M. A., Jodar, E., Perez-Cano, R. and Hawkins, F. (1998) 'Bone mineral density in children and adolescents with diabetes mellitus type 1 of recent onset', *Calcif Tissue Int*, 62(1), 31-5.

Pater, A., Sypniewska, G. and Pilecki, O. (2010) 'Biochemical markers of bone cell activity in children with type 1 diabetes mellitus', *J Pediatr Endocrinol Metab*, 23(1-2), 81-6.

Patsch, J. M., Burghardt, A. J., Yap, S. P., Baum, T., Schwartz, A. V., Joseph, G. B. and Link, T. M. (2013a) 'Increased cortical porosity in type 2 diabetic postmenopausal women with fragility fractures', *J Bone Miner Res*, 28(2), 313-24.

Patsch, J. M., Li, X. J., Baum, T., Yap, S. P., Karampinos, D. C., Schwartz, A. V. and Link, T. M. (2013b) 'Bone marrow fat composition as a novel imaging biomarker in postmenopausal women with prevalent fragility fractures', *Journal of Bone and Mineral Research*, 28(8), 1721-1728.

Peh, W. C. (2014) *Pitfalls in Diagnostic Radiology*, Springer.

Petrie, J. R., Chaturvedi, N., Ford, I., Brouwers, M., Greenlaw, N., Tillin, T., Hramiak, I., Hughes, A. D., Jenkins, A. J., Klein, B. E. K., Klein, R., Ooi, T. C., Rossing, P., Stehouwer, C. D. A., Sattar, N., Colhoun, H. M. and Group, R. S. (2017) 'Cardiovascular and metabolic effects of metformin in patients with type 1 diabetes (REMOVAL): a double-blind, randomised, placebo-controlled trial', *Lancet Diabetes Endocrinol*, 5(8), 597-609.

Pittenger, M. F., Mackay, A. M., Beck, S. C., Jaiswal, R. K., Douglas, R., Mosca, J. D., Moorman, M. A., Simonetti, D. W., Craig, S. and Marshak, D. R. (1999) 'Multilineage potential of adult human mesenchymal stem cells', *Science*, 284(5411), 143-147.

Porte, D., Tuckermann, J., Becker, M., Baumann, B., Teurich, S., Higgins, T., Owen, M. J., Schorpp-Kistner, M. and Angel, P. (1999) 'Both AP-1 and Cbfa1-like factors are required for the induction of interstitial collagenase by parathyroid hormone', *Oncogene*, 18(3), 667-78.

Pratap, J., Galindo, M., Zaidi, S. K., Vradii, D., Bhat, B. M., Robinson, J. A., Choi, J. Y., Komori, T., Stein, J. L., Lian, J. B., Stein, G. S. and van Wijnen, A. J. (2003) 'Cell growth regulatory role of Runx2 during proliferative expansion of preosteoblasts', *Cancer Res*, 63(17), 5357-62.

Pritchard, J. M., Giangregorio, L. M., Atkinson, S. A., Beattie, K. A., Inglis, D., Ioannidis, G., Gerstein, H., Punthakee, Z., Adachi, J. D. and Papaioannou, A. (2013) 'Changes in trabecular bone microarchitecture in postmenopausal women with and without type 2 diabetes: a two year longitudinal study', *BMC Musculoskelet Disord*, 14, 114.

Pritchard, J. M., Giangregorio, L. M., Atkinson, S. A., Beattie, K. A., Inglis, D., Ioannidis, G., Punthakee, Z., Adachi, J. D. and Papaioannou, A. (2012) 'Association of larger holes in the trabecular bone at the distal radius in postmenopausal women with type 2 diabetes mellitus compared to controls', *Arthritis Care Res (Hoboken)*, 64(1), 83-91.

Prockop, D. J. (1997) 'Marrow stromal cells as steam cells for nonhematopoietic tissues', *Science*, 276(5309), 71-74.

Puisto, V., Kaariainen, S., Impinen, A., Parkkila, T., Vartiainen, E., Jalanko, T., Pakarinen, M. P. and Helenius, I. (2010) 'Incidence of spinal and spinal cord injuries and their surgical treatment in children and adolescents: a population-based study', *Spine (Phila Pa 1976)*, 35(1), 104-7.

Pun, K. K. (1989) 'The importance of parathyroid hormone in inhibition of collagen synthesis and mitogenesis of osteoblastic cell', *J Biochem*, 106(6), 1090-3.

Quinn, J. M., Tam, S., Sims, N. A., Saleh, H., McGregor, N. E., Poulton, I. J., Scott, J. W., Gillespie, M. T., Kemp, B. E. and van Denderen, B. J. (2010) 'Germline deletion of AMP-activated protein kinase beta subunits reduces bone mass without altering osteoclast differentiation or function', *FASEB J*, 24(1), 275-85.

Radjenovic, A., Dall, B. J., Ridgway, J. P. and Smith, M. A. (2008) 'Measurement of pharmacokinetic parameters in histologically graded invasive breast tumours using dynamic contrast-enhanced MRI', *Br J Radiol*, 81(962), 120-8.

Rakic, V., Davis, W. A., Chubb, S. A., Islam, F. M., Prince, R. L. and Davis, T. M. (2006) 'Bone mineral density and its determinants in diabetes: the Fremantle Diabetes Study', *Diabetologia*, 49(5), 863-71.

Rasmussen, B. B. and Winder, W. W. (1997) 'Effect of exercise intensity on skeletal muscle malonyl-CoA and acetyl-CoA carboxylase', *J Appl Physiol (1985)*, 83(4), 1104-9.

Rauch, A., Haakonsson, A. K., Madsen, J. G. S., Larsen, M., Forss, I., Madsen, M. R., Van Hauwaert, E. L., Wiwie, C., Jespersen, N. Z., Tencerova, M., Nielsen, R., Larsen, B. D., Rottger, R., Baumbach, J., Scheele, C., Kassem, M. and Mandrup, S. (2019) 'Osteogenesis depends on commissioning of a network of stem cell transcription factors that act as repressors of adipogenesis', *Nat Genet*.

Rauch, F. (2003) 'Bone histomorphometry' in Glorieux FH., P. J., Jueppner H., ed., *Pediatric Bone*, San Diego: Academic Press.

Rauch, F. (2009) 'Bone biopsy: indications and methods', *Endocr Dev*, 16, 49-57.

Rauch, F., Schonau, E., Woitge, H., Remer, T. and Seibel, M. (1994) 'Urinary excretion of hydroxy-pyridinium cross-links of collagen reflects skeletal growth velocity in normal children', *Exp Clin Endocrinol*, 102(2), 94-7.

Rauch, F., Tutlewski, B., Fricke, O., Rieger-Wettengl, G., Schauseil-Zipf, U., Herkenrath, P., Neu, C. M. and Schoenau, E. (2001) 'Analysis of cancellous bone turnover by multiple slice analysis at distal radius: a study using peripheral quantitative computed tomography', *J Clin Densitom*, 4(3), 257-62.

Rauchenzauner, M., Schmid, A., Heinz-Erian, P., Kapelari, K., Falkensammer, G., Griesmacher, A., Finkenstedt, G. and Hogler, W. (2007) 'Sex- and age-specific reference curves for

serum markers of bone turnover in healthy children from 2 months to 18 years', *J Clin Endocrinol Metab*, 92(2), 443-9.

Rawshani, A., Sattar, N., Franzen, S., Rawshani, A., Hattersley, A. T., Svensson, A. M., Eliasson, B. and Gudbjornsdottir, S. (2018) 'Excess mortality and cardiovascular disease in young adults with type 1 diabetes in relation to age at onset: a nationwide, register-based cohort study', *Lancet*, 392(10146), 477-486.

Reseland, J. E., Syversen, U., Bakke, I., Qvigstad, G., Eide, L. G., Hjertner, O., Gordeladze, J. O. and Drevon, C. A. (2001) 'Leptin is expressed in and secreted from primary cultures of human osteoblasts and promotes bone mineralization', *J Bone Miner Res*, 16(8), 1426-33.

Rewers, M., Pihoker, C., Donaghue, K., Hanas, R., Swift, P. and Klingensmith, G. J. (2009) 'Assessment and monitoring of glycemic control in children and adolescents with diabetes', *Pediatr Diabetes*, 10 Suppl 12, 71-81.

Reyes-Garcia, R., Rozas-Moreno, P., Lopez-Gallardo, G., Garcia-Martin, A., Varsavsky, M., Aviles-Perez, M. D. and Munoz-Torres, M. (2013) 'Serum levels of bone resorption markers are decreased in patients with type 2 diabetes', *Acta Diabetol*, 50(1), 47-52.

Reznikoff, C. A., Brankow, D. W. and Heidelberger, C. (1973) 'Establishment and characterization of a cloned line of C3H mouse embryo cells sensitive to postconfluence inhibition of division', *Cancer Res*, 33(12), 3231-8.

Ricci, R., Bacci, A., Tugnoli, V., Battaglia, S., Maffei, M., Agati, R. and Leonardi, M. (2007) 'Metabolic findings on 3T 1H-MR spectroscopy in peritumoral brain edema', *AJNR Am J Neuroradiol*, 28(7), 1287-91.

Rico, H., Hernandez, E. R., Cabranes, J. A. and Gomez-Castresana, F. (1989) 'Suggestion of a deficient osteoblastic function in diabetes mellitus: the possible cause of osteopenia in diabetics', *Calcif Tissue Int*, 45(2), 71-3.

Ridgway, J. P. (2010) 'Cardiovascular magnetic resonance physics for clinicians: part I', *J Cardiovasc Magn Reson*, 12, 71.

Riggs, B. L., Melton, L. J., Robb, R. A., Camp, J. J., Atkinson, E. J., McDaniel, L., Amin, S., Rouleau, P. A. and Khosla, S. (2008) 'A population-based assessment of rates of bone loss at multiple skeletal sites: evidence for substantial trabecular bone loss in young adult women and men', *J Bone Miner Res*, 23(2), 205-14.

Riggs, B. L., Wahner, H. W., Dunn, W. L., Mazess, R. B., Offord, K. P. and Melton, L. J., 3rd (1981) 'Differential changes in bone mineral density of the appendicular and axial skeleton with aging: relationship to spinal osteoporosis', *J Clin Invest*, 67(2), 328-35.

Rivadeneira, F., Zillikens, M. C., De Laet, C. E., Hofman, A., Uitterlinden, A. G., Beck, T. J. and Pols, H. A. (2007) 'Femoral neck BMD is a strong predictor of hip fracture susceptibility in elderly men and women because it detects cortical bone instability: the Rotterdam Study', *J Bone Miner Res*, 22(11), 1781-90.

Robling, A. G., Niziolek, P. J., Baldridge, L. A., Condon, K. W., Allen, M. R., Alam, I., Mantila, S. M., Gluhak-Heinrich, J., Bellido, T. M., Harris, S. E. and Turner, C. H. (2008) 'Mechanical stimulation of bone in vivo reduces osteocyte expression of Sost/sclerostin', *Journal of Biological Chemistry*, 283(9), 5866-75.

Rodriguez, A., Griffiths-Jones, S., Ashurst, J. L. and Bradley, A. (2004) 'Identification of mammalian microRNA host genes and transcription units', *Genome Res*, 14(10A), 1902-10.

Roggen, I., Gies, I., Vanbesien, J., Louis, O. and De Schepper, J. (2013) 'Trabecular Bone Mineral Density and Bone Geometry of the Distal Radius at Completion of Pubertal Growth in Childhood Type 1 Diabetes', *Hormone Research in Paediatrics*, 79(2), 68-74.

Roggen, I., Gies, I., Vanbesien, J., Louis, O. and De Schepper, J. (2013) 'Trabecular bone mineral density and bone geometry of the distal radius at completion of pubertal growth in childhood type 1 diabetes', *Horm Res Paediatr*, 79(2), 68-74.

Rosen, C. J. (2004) 'Insulin-like growth factor I and bone mineral density: experience from animal models and human observational studies', *Best Pract Res Clin Endocrinol Metab*, 18(3), 423-35.

Rosen, E. D. and MacDougald, O. A. (2006) 'Adipocyte differentiation from the inside out', *Nat Rev Mol Cell Biol*, 7(12), 885-96.

Rosen, E. D. and Spiegelman, B. M. (2000) 'Molecular regulation of adipogenesis', *Annu Rev Cell Dev Biol*, 16, 145-71.

Ross, S. E., Hemati, N., Longo, K. A., Bennett, C. N., Lucas, P. C., Erickson, R. L. and MacDougald, O. A. (2000) 'Inhibition of adipogenesis by Wnt signaling', *Science*, 289(5481), 950-3.

Roszer, T. (2011) 'Inflammation as death or life signal in diabetic fracture healing', *Inflamm Res*, 60(1), 3-10.

Rzonca, S. O., Suva, L. J., Gaddy, D., Montague, D. C. and Lecka-Czernik, B. (2004) 'Bone is a target for the antidiabetic compound rosiglitazone', *Endocrinology*, 145(1), 401-406.

Safaei, H., Janghorbani, M., Aminorroaya, A. and Amini, M. (2007) 'Lovastatin effects on bone mineral density in postmenopausal women with type 2 diabetes mellitus', *Acta Diabetol*, 44(2), 76-82.

Saggese, G., Baroncelli, G. I. and Bertelloni, S. (2002) 'Puberty and bone development', *Best Pract Res Clin Endocrinol Metab*, 16(1), 53-64.

Saha, M. T., Sievanen, H., Salo, M. K., Tulokas, S. and Saha, H. H. (2009a) 'Bone mass and structure in adolescents with type 1 diabetes compared to healthy peers', *Osteoporosis International*, 20(8), 1401-1406.

Saha, M. T., Sievanen, H., Salo, M. K., Tulokas, S. and Saha, H. H. (2009b) 'Bone mass and structure in adolescents with type 1 diabetes compared to healthy peers', *Osteoporos Int*, 20(8), 1401-6.

Saito, M., Fujii, K., Mori, Y. and Marumo, K. (2006) 'Role of collagen enzymatic and glycation induced cross-links as a determinant of bone quality in spontaneously diabetic WBN/Kob rats', *Osteoporos Int*, 17(10), 1514-23.

Saitoh, M., Pullen, N., Brennan, P., Cantrell, D., Dennis, P. B. and Thomas, G. (2002) 'Regulation of an activated S6 kinase 1 variant reveals a novel mammalian target of rapamycin phosphorylation site', *J Biol Chem*, 277(22), 20104-12.

Salt, I.P., Celler, J. W., Hawley, S. A., Prescott, A., Woods, A., Carling, D. and Hardie, D. G. (1998) 'AMP-activated protein kinase: greater AMP dependence, and preferential nuclear localization, of complexes containing the alpha2 isoform', *Biochem J*, 334 (Pt 1), 177-87.

Salt, I. P., Johnson, G., Ashcroft, S. J. and Hardie, D. G. (1998) 'AMP-activated protein kinase is activated by low glucose in cell lines derived from pancreatic beta cells, and may regulate insulin release', *Biochem J*, 335 (Pt 3), 533-9.

Sambrook, J. and Russell, D. (2001) *Molecular cloning: A Laboratory Manual*, 3rd ed., Cold Spring harbor Laboratory Press.

Samelson, E. J., Broe, K. E., Xu, H., Yang, L., Boyd, S., Biver, E., Szulc, P., Adachi, J., Amin, S., Atkinson, E., Berger, C., Burt, L., Chapurlat, R., Chevalley, T., Ferrari, S., Goltzman, D., Hanley, D. A., Hannan, M. T., Khosla, S., Liu, C. T., Lorentzon, M., Mellstrom, D., Merle, B., Nethander, M., Rizzoli, R., Sornay-Rendu, E., Van Rietbergen, B., Sundh, D., Wong, A. K. O., Ohlsson, C., Demissie, S., Kiel, D. P. and Bouxsein, M. L. (2019) 'Cortical and trabecular bone microarchitecture as an independent predictor of incident fracture risk in older women and men in the Bone Microarchitecture International Consortium (BoMIC): a prospective study', *Lancet Diabetes Endocrinol*, 7(1), 34-43.

Sanguineti, R., Storace, D., Monacelli, F., Federici, A. and Odetti, P. (2008) 'Pentosidine effects on human osteoblasts in vitro', *Ann N Y Acad Sci*, 1126, 166-72.

Sauder, K. A., Stafford, J. M., Mayer-Davis, E. J., Jensen, E. T., Saydah, S., Mottl, A., Dolan, L. M., Hamman, R. F., Lawrence, J. M., Pihoker, C., Marcovina, S., D'Agostino, R. B., Jr., Dabelea, D. and Group, S. f. D. i. Y. S. (2019) 'Co-occurrence of early diabetes-related complications in adolescents and young adults with type 1 diabetes: an observational cohort study', *Lancet Child Adolesc Health*, 3(1), 35-43.

Sav, N. M., Kendirci, M., Akin, L. and Kurtoglu, S. (2017) 'Urinary levels of pyridinoline and deoxypyridinoline and bone mineral density in children with type 1 diabetes mellitus', *Endocr Res*, 42(4), 281-286.

Schade, D. S., Lorenzi, G. M., Braffett, B. H., Gao, X., Bainbridge, K. E., Barnie, A., Cruickshanks, K. J., Dalton, D., Diminick, L., Gubitosi-Klug, R., Kramer, J. R., Lachin, J. M., Larkin, M. E., Cowie, C. C. and Group, D. E. R. (2018) 'Hearing Impairment and Type 1 Diabetes in the Diabetes Control and Complications Trial/Epidemiology of Diabetes Interventions and Complications (DCCT/EDIC) Cohort', *Diabetes Care*, 41(12), 2495-2501.

Schellinger, D., Lin, C., Lim, J., Hatipoglu, H., Pezzullo, J. and Singer, A. (2004) 'Bone Marrow Fat and Bone Mineral Density on Proton MR Spectroscopy and Dual-Energy X-Ray Absorptiometry: Their Ratio as Indicator of Bone Weakening', *Am J Roentgenol*, 183, 1761-1765.

Schmid, C., Schlapfer, I., Peter, M., Boni-Schnetzler, M., Schwander, J., Zapf, J. and Froesch, E. R. (1994) 'Growth hormone and parathyroid hormone stimulate IGFBP-3 in rat osteoblasts', *Am J Physiol*, 267(2 Pt 1), E226-33.

Schmidt, A.M., Yan, S.D., Wautier, J.L., Stern, D. (1999) 'Activation of receptor for advanced glycation end products: a mechanism for chronic vascular dysfunction in diabetic vasculopathy and atherosclerosis' *Circ Res*, 84,489–497

Schnoke, M., Midura, S. B. and Midura, R. J. (2009) 'Parathyroid hormone suppresses osteoblast apoptosis by augmenting DNA repair', *Bone*, 45(3), 590-602.

Schoenau, E., Neu, C. M., Mokov, E., Wassmer, G. and Manz, F. (2000) 'Influence of puberty on muscle area and cortical bone area of the forearm in boys and girls', *J Clin Endocrinol Metab*, 85(3), 1095-8.

Schopfer, F. J., Lin, Y., Baker, P. R., Cui, T., Garcia-Barrio, M., Zhang, J., Chen, K., Chen, Y. E. and Freeman, B. A. (2005) 'Nitrolinoleic acid: an endogenous peroxisome proliferator-activated receptor gamma ligand', *Proc Natl Acad Sci U S A*, 102(7), 2340-5.

Schuit, S. C., van der Klift, M., Weel, A. E., de Laet, C. E., Burger, H., Seeman, E., Hofman, A., Uitterlinden, A. G., van Leeuwen, J. P. and Pols, H. A. (2004) 'Fracture incidence and association with bone mineral density in elderly men and women: the Rotterdam Study', *Bone*, 34(1), 195-202.

Schurman, L., McCarthy, A. D., Sedlinsky, C., Gangoiti, M. V., Arnol, V., Bruzzone, L. and Cortizo, A. M. (2008) 'Metformin reverts deleterious effects of advanced glycation end-products (AGEs) on osteoblastic cells', *Exp Clin Endocrinol Diabetes*, 116(6), 333-40.

Schwartz, A. V. (2003) 'Diabetes Mellitus: Does it Affect Bone?', *Calcif Tissue Int*, 73(6), 515-9.

Schwartz, A. V. (2008) 'TZDs and Bone: A Review of the Recent Clinical Evidence', *PPAR Res*, 2008, 297893.

Schwartz, A. V., Garnero, P., Hillier, T. A., Sellmeyer, D. E., Strotmeyer, E. S., Feingold, K. R., Resnick, H. E., Tylavsky, F. A., Black, D. M., Cummings, S. R., Harris, T. B., Bauer, D. C., Health, A. and Body Composition, S. (2009) 'Pentosidine and increased fracture risk in older adults with type 2 diabetes', *J Clin Endocrinol Metab*, 94(7), 2380-6.

Schwartz, A. V., Sellmeyer, D. E., Ensrud, K. E., Cauley, J. A., Tabor, H. K., Schreiner, P. J., Jamal, S. A., Black, D. M., Cummings, S. R. and Study of Osteoporotic Features

Research, G. (2001) 'Older women with diabetes have an increased risk of fracture: a prospective study', *J Clin Endocrinol Metab*, 86(1), 32-8.

Schwartz, A. V., Sellmeyer, D. E., Vittinghoff, E., Palermo, L., Lecka-Czernik, B., Feingold, K. R., Strotmeyer, E. S., Resnick, H. E., Carbone, L., Beamer, B. A., Park, S. W., Lane, N. E., Harris, T. B. and Cummings, S. R. (2006) 'Thiazolidinedione use and bone loss in older diabetic adults', *J Clin Endocrinol Metab*, 91(9), 3349-54.

Schwartz, A. V., Sigurdsson, S., Hue, T. F., Lang, T. F., Harris, T. B., Rosen, C. J., Vittinghoff, E., Siggeirsdottir, K., Sigurdsson, G., Oskarsdottir, D., Shet, K., Palermo, L., Gudnason, V. and Li, X. (2013) 'Vertebral bone marrow fat associated with lower trabecular BMD and prevalent vertebral fracture in older adults', *J Clin Endocrinol Metab*, 98(6), 2294-300.

Schwartz, A. V., Vittinghoff, E., Sellmeyer, D. E., Feingold, K. R., de Rekeneire, N., Strotmeyer, E. S., Shorr, R. I., Vinik, A. I., Odden, M. C., Park, S. W., Faulkner, K. A., Harris, T. B., Health, A. and Body Composition, S. (2008) 'Diabetes-related complications, glycemic control, and falls in older adults', *Diabetes Care*, 31(3), 391-6.

Scottish Diabetes Survery Monitoring Group NHS Scotland (2014) *Scottish Diabetes Survey 2013* [online], available: http://www.diabetesinscotland.org.uk/Publications/SDS2013.pdf [accessed 17/10/2016].

Seeliger, C., Karpinski, K., Haug, A. T., Vester, H., Schmitt, A., Bauer, J. S. and van Griensven, M. (2014) 'Five freely circulating miRNAs and bone tissue miRNAs are associated with osteoporotic fractures', *J Bone Miner Res*, 29(8), 1718-28.

Seeman, E. and Delmas, P. D. (2006) 'Bone quality--the material and structural basis of bone strength and fragility', *N Engl J Med*, 354(21), 2250-61.

Sernbo, I. and Johnell, O. (1993) 'Consequences of a hip fracture: a prospective study over 1 year', *Osteoporos Int*, 3(3), 148-53.

Shah, M., Kola, B., Bataveljic, A., Arnett, T. R., Viollet, B., Saxon, L., Korbonits, M. and Chenu, C. (2010) 'AMP-activated protein kinase (AMPK) activation regulates in vitro bone formation and bone mass', *Bone*, 47(2), 309-319.

Shah, V. N., Shah, C. S. and Snell-Bergeon, J. K. (2015) 'Type 1 diabetes and risk of fracture: meta-analysis and review of the literature', *Diabet Med*, 32(9), 1134-42.

Shanbhogue, V. V., Hansen, S., Frost, M., Jorgensen, N. R., Hermann, A. P., Henriksen, J. E. and Brixen, K. (2015) 'Bone Geometry, Volumetric Density, Microarchitecture, and Estimated Bone Strength Assessed by HR-pQCT in Adult Patients With Type 1 Diabetes Mellitus', *J Bone Miner Res*, 30(12), 2188-99.

Shanbhogue, V. V., Hansen, S., Frost, M., Jorgensen, N. R., Hermann, A. P., Henriksen, J. E. and Brixen, K. (2016) 'Compromised cortical bone compartment in type 2 diabetes mellitus patients with microvascular disease', *Eur J Endocrinol*, 174(2), 115-24.

Shaw, R. J., Kosmatka, M., Bardeesy, N., Hurley, R. L., Witters, L. A., DePinho, R. A. and Cantley, L. C. (2004) 'The tumor suppressor LKB1 kinase directly activates AMP-activated kinase and regulates apoptosis in response to energy stress', *Proc Natl Acad Sci U S A*, 101(10), 3329-35.

Shen, R., Wang, X., Drissi, H., Liu, F., O'Keefe, R. J. and Chen, D. (2006) 'Cyclin D1-cdk4 induce runx2 ubiquitination and degradation', *Journal of Biological Chemistry*, 281(24), 16347-53.

Shen, W., Chen, J., Gantz, M., Punyanitya, M., Heymsfield, S. B., Gallagher, D., Albu, J., Engelson, E., Kotler, D., Pi-Sunyer, X. and Gilsanz, V. (2012a) 'MRI-measured pelvic bone marrow adipose tissue is inversely related to DXA-measured bone mineral in younger and older adults', *Eur J Clin Nutr*, 66(9), 983-8.

Shen, W., Scherzer, R., Gantz, M., Chen, J., Punyanitya, M., Lewis, C. E. and Grunfeld, C. (2012b) 'Relationship between MRI-measured bone marrow adipose tissue and hip and spine bone

mineral density in African-American and Caucasian participants: the CARDIA study', *J Clin Endocrinol Metab*, 97(4), 1337-46.

Sheu, Y., Amati, F., Schwartz, A. V., Danielson, M. E., Li, X. J., Boudreau, R., Cauley, J. A. and MrOS, O. F. M. (2017) 'Vertebral bone marrow fat, bone mineral density and diabetes: The Osteoporotic Fractures in Men (MrOS) study', *Bone*, 97, 299-305.

Shifera, A. S. and Hardin, J. A. (2010) 'Factors modulating expression of Renilla luciferase from control plasmids used in luciferase reporter gene assays', *Anal Biochem*, 396(2), 167-72.

Shin, S., Hyun, B., Lee, A., SLee, S., Kong, H., Han, S., Song, Y. and Kim, K. (2013) 'Metformin reduces gene expression of adipogenesis and inflammatory cytokines through the modulation of T cell priming in obese-induced Type II diabetic mice', in The Journal of Immunology.

Silva, M. J., Brodt, M. D., Lynch, M. A., McKenzie, J. A., Tanouye, K. M., Nyman, J. S. and Wang, X. (2009) 'Type 1 diabetes in young rats leads to progressive trabecular bone loss, cessation of cortical bone growth, and diminished whole bone strength and fatigue life', *J Bone Miner Res*, 24(9), 1618-27.

Siris, E. S., Miller, P. D., Barrett-Connor, E., Faulkner, K. G., Wehren, L. E., Abbott, T. A., Berger, M. L., Santora, A. C. and Sherwood, L. M. (2001) 'Identification and fracture outcomes of undiagnosed low bone mineral density in postmenopausal women: results from the National Osteoporosis Risk Assessment', *JAMA*, 286(22), 2815-22.

Sjoberg, L., Pitkaniemi, J., Harjutsalo, V., Haapala, L., Tiitinen, A., Tuomilehto, J. and Kaaja, R. (2011) 'Menopause in women with type 1 diabetes', *Menopause*, 18(2), 158-63.

Slemenda, C. W., Hui, S. L., Longcope, C., Wellman, H. and Johnston, C. C., Jr. (1990) 'Predictors of bone mass in perimenopausal women. A prospective study of clinical data using photon absorptiometry', *Ann Intern Med*, 112(2), 96-101.

Smith P. K., R. I. Krohn, G. T. Hermanson, A. K. Mallia, F. H. Gartner, M. D.Provenzano, E. K. Fujimoto, N. M. Goeke, B. J. Olson and D. C. Klenk (1985). Measurement of protein using bicinchoninic acid. *Analytical Biochemistry* 150(1): 76-85.

Spranger, J., Kroke, A., Mohlig, M., Hoffmann, K., Bergmann, M. M., Ristow, M., Boeing, H. and Pfeiffer, A. F. (2003) 'Inflammatory cytokines and the risk to develop type 2 diabetes: results of the prospective population-based European Prospective Investigation into Cancer and Nutrition (EPIC)-Potsdam Study', *Diabetes*, 52(3), 812-7.

SR, C., DM, B., TM, V. and Group, f. t. F. R. (1996) 'Changes in BMD substantially underestimate the anti-fracture effects of alendronate and other antiresorptive drugs', *J Bone Miner Res*, 11, S102.

Stapleton, D., Mitchelhill, K. I., Gao, G., Widmer, J., Michell, B. J., Teh, T., House, C. M., Fernandez, C. S., Cox, T., Witters, L. A. and Kemp, B. E. (1996) 'Mammalian AMP-activated protein kinase subfamily', *Journal of Biological Chemistry*, 271(2), 611-4.

Stark, A. D., Bennet, G. C., Stone, D. H. and Chishti, P. (2002) 'Association between childhood fractures and poverty: population based study', *BMJ*, 324(7335), 457.

Starup-Linde, J. (2013) 'Diabetes, biochemical markers of bone turnover, diabetes control, and bone', *Front Endocrinol (Lausanne)*, 4, 21.

Starup-Linde, J., Eriksen, S. A., Lykkeboe, S., Handberg, A. and Vestergaard, P. (2014) 'Biochemical markers of bone turnover in diabetes patients--a meta-analysis, and a methodological study on the effects of glucose on bone markers', *Osteoporos Int*, 25(6), 1697-708.

Starup-Linde, J., Lykkeboe, S., Gregersen, S., Hauge, E. M., Langdahl, B. L., Handberg, A. and Vestergaard, P. (2016) 'Bone Structure and Predictors of Fracture in Type 1 and Type 2 Diabetes', *J Clin Endocrinol Metab*, 101(3), 928-36.

Stephens, T. J., Chen, Z. P., Canny, B. J., Michell, B. J., Kemp, B. E. and McConell, G. K. (2002) 'Progressive increase in human skeletal muscle AMPKalpha2 activity and ACC phosphorylation during exercise', *Am J Physiol Endocrinol Metab*, 282(3), E688-94.

Steppan, C. M., Crawford, D. T., Chidsey-Frink, K. L., Ke, H. and Swick, A. G. (2000) 'Leptin is a potent stimulator of bone growth in ob/ob mice', *Regul Pept*, 92(1-3), 73-8.

Strotmeyer, E. S., Cauley, J. A., Schwartz, A. V., Nevitt, M. C., Resnick, H. E., Bauer, D. C., Tylavsky, F. A., de Rekeneire, N., Harris, T. B. and Newman, A. B. (2005) 'Nontraumatic fracture risk with diabetes mellitus and impaired fasting glucose in older white and black adults: the health, aging, and body composition study', *Arch Intern Med*, 165(14), 1612-7.

Su, B., Sheng, H., Zhang, M., Bu, L., Yang, P., Li, L., Li, F., Sheng, C., Han, Y., Qu, S. and Wang, J. (2015) 'Risk of bone fractures associated with glucagon-like peptide-1 receptor agonists' treatment: a meta-analysis of randomized controlled trials', *Endocrine*, 48(1), 107-15.

Sun, H., Kim, J. K., Mortensen, R., Mutyaba, L. P., Hankenson, K. D. and Krebsbach, P. H. (2013) 'Osteoblast-targeted suppression of PPARgamma increases osteogenesis through activation of mTOR signaling', *Stem Cells.*, 31(10), 2183-92.

Szulc, P. and Delmas, P. D. (2008) 'Biochemical markers of bone turnover: potential use in the investigation and management of postmenopausal osteoporosis', *Osteoporos Int*, 19(12), 1683-704.

Taipaleenmaki, H., Abdallah, B. M., AlDahmash, A., Saamanen, A. M. and Kassem, M. (2011) 'Wnt signalling mediates the cross-talk between bone marrow derived pre-adipocytic and pre-osteoblastic cell populations', *Experimental Cell Research*, 317(6), 745-56.

Takahashi, N., Maeda, K., Ishihara, A., Uehara, S. and Kobayashi, Y. (2011) 'Regulatory mechanism of osteoclastogenesis by RANKL and Wnt signals', *Front Biosci (Landmark Ed)*, 16, 21-30.

Takeda, K., Ichiki, T., Tokunou, T., Funakoshi, Y., Iino, N., Hirano, K., Kanaide, H. and Takeshita, A. (2000) 'Peroxisome proliferator-activated receptor gamma activators downregulate angiotensin II type 1 receptor in vascular smooth muscle cells', *Circulation*, 102(15), 1834-9.

Tamura, T., Yoneda, M., Yamane, K., Nakanishi, S., Nakashima, R., Okubo, M. and Kohno, N. (2007) 'Serum leptin and adiponectin are positively associated with bone mineral density at the distal radius in patients with type 2 diabetes mellitus', *Metabolism-Clinical and Experimental*, 56(5), 623-8.

Tang, Q. Q., Otto, T. C. and Lane, M. D. (2004a) 'Commitment of C3H10T1/2 pluripotent stem cells to the adipocyte lineage', *Proc Natl Acad Sci U S A*, 101(26), 9607-11.

Tang, Q. Q., Otto, T. C. and Lane, M. D. (2004b) 'Commitment of C3H10T1/2 pluripotent stem cells to the adipocyte lineage', *Proceedings of the National Academy of Sciences of the United States of America*, 101(26), 9607-9611.

Tanji, N., Markowitz, G.S., Fu, C., Kislinger, T., Taguchi, A., Pischetsrieder, M., Stern, D., Schmidt, A.M., D'Agaiti, V.D. (2000) 'Expression of advanced glycation end products and their cellular receptor RAGE in diabetic nephropathy and nondiabetic renal disease. *J Am Soc Nephrol*, 11,1656–1666.

Taylor, A. K., Linkhart, S., Mohan, S., Christenson, R. A., Singer, F. R. and Baylink, D. J. (1990) 'Multiple osteocalcin fragments in human urine and serum as detected by a midmolecule osteocalcin radioimmunoassay', *J Clin Endocrinol Metab*, 70(2), 467-72.

The Diabetes Control and Complications Trial (DCCT) Research Group (1995) 'Effect of intensive diabetes management on macrovascular events and risk factors in the Diabetes Control and Complications Trial', *Am J Cardiol*, 75(14), 894-903.

Thomas, D. M., Hards, D. K., Rodgers, S. D., Ng, K. W. and Best, J. D. (1996a) 'Insulin receptor expression in bone', *Journal of Bone and Mineral Research*, 11(9), 1312-1320.

Thomas, D. M., Hards, D. K., Rogers, S. D., Ng, K. W. and Best, J. D. (1996b) 'Insulin receptor expression in bone', *J Bone Miner Res*, 11(9), 1312-20.

Thomsen, J. S., Ebbesen, E. N. and Mosekilde, L. (1998) 'Relationships between static histomorphometry and bone strength measurements in human iliac crest bone biopsies', *Bone*, 22(2), 153-63.

Thorn, L. M., Forsblom, C., Fagerudd, J., Thomas, M. C., Pettersson-Fernholm, K., Saraheimo, M., Waden, J., Ronnback, M., Rosengard-Barlund, M., Bjorkesten, C. G., Taskinen, M. R., Groop, P. H. and FinnDiane Study, G. (2005) 'Metabolic syndrome in type 1 diabetes: association with diabetic nephropathy and glycemic control (the FinnDiane study)', *Diabetes Care*, 28(8), 2019-24.

Thornton, C., Snowden, M. A. and Carling, D. (1998) 'Identification of a novel AMP-activated protein kinase beta subunit isoform that is highly expressed in skeletal muscle', *Journal of Biological Chemistry*, 273(20), 12443-50.

Thrailkill, K., Bunn, R. C., Lumpkin, C., Jr., Wahl, E., Cockrell, G., Morris, L., Kahn, C. R., Fowlkes, J. and Nyman, J. S. (2014) 'Loss of insulin receptor in osteoprogenitor cells impairs structural strength of bone', *J Diabetes Res*, 2014, 703589.

Tobiume, H., Kanzaki, S., Hida, S., Ono, T., Moriwake, T., Yamauchi, S., Tanaka, H. and Seino, Y. (1997) 'Serum bone alkaline phosphatase isoenzyme levels in normal children and children with growth hormone (GH) deficiency: a potential marker for bone formation and response to GH therapy', *J Clin Endocrinol Metab*, 82(7), 2056-61.

Today Study Group (2013) 'Treatment effects on measures of body composition in the TODAY clinical trial', *Diabetes Care*, 36(6), 1742-8.

Tofts, P. S. (1997) 'Modeling tracer kinetics in dynamic Gd-DTPA MR imaging', *Journal of Magnetic Resonance Imaging*, 7(1), 91-101.

Tomasek, J. J., Meyers, S. W., Basinger, J. B., Green, D. T. and Shew, R. L. (1994) 'Diabetic and age-related enhancement of collagen-linked fluorescence in cortical bones of rats', *Life Sci*, 55(11), 855-61.

Topaloglu, A. K., Yildizdas, D., Yilmaz, H. L., Mungan, N. O., Yuksel, B. and Ozer, G. (2005) 'Bone calcium changes during diabetic ketoacidosis: a comparison with lactic acidosis due to volume depletion', *Bone*, 37(1), 122-7.

Tothill, P., Hannan, W. J., Cowen, S. and Freeman, C. P. (1997) 'Anomalies in the measurement of changes in total-body bone mineral by dual-energy X-ray absorptiometry during weight change', *J Bone Miner Res*, 12(11), 1908-21.

Tsentidis, C., Gourgiotis, D., Kossiva, L., Marmarinos, A., Doulgeraki, A. and Karavanaki, K. (2016) 'Sclerostin distribution in children and adolescents with type 1 diabetes mellitus and correlation with bone metabolism and bone mineral density', *Pediatr Diabetes*, 17(4), 289-99.

Tsentidis, C., Gourgiotis, D., Kossiva, L., Marmarinos, A., Doulgeraki, A. and Karavanaki, K. (2017) 'Increased levels of Dickkopf-1 are indicative of Wnt/beta-catenin downregulation and lower osteoblast signaling in children and adolescents with type 1 diabetes mellitus, contributing to lower bone mineral density', *Osteoporos Int*, 28(3), 945-953.

Turnley, A. M., Stapleton, D., Mann, R. J., Witters, L. A., Kemp, B. E. and Bartlett, P. F. (1999) 'Cellular distribution and developmental expression of AMP-activated protein kinase isoforms in mouse central nervous system', *J Neurochem*, 72(4), 1707-16.

Tzameli, I., Fang, H., Ollero, M., Shi, H., Hamm, J. K., Kievit, P., Hollenberg, A. N. and Flier, J. S. (2004) 'Regulated production of a peroxisome proliferator-activated receptor-gamma ligand during an early phase of adipocyte differentiation in 3T3-L1 adipocytes', *Journal of Biological Chemistry*, 279(34), 36093-102.

Utting, J. C., Robins, S. P., Brandao-Burch, A., Orriss, I. R., Behar, J. and Arnett, T. R. (2006) 'Hypoxia inhibits the growth, differentiation and bone-forming capacity of rat osteoblasts', *Experimental Cell Research*, 312(10), 1693-702.

Valcourt, U., Merle, B., Gineyts, E., Viguet-Carrin, S., Delmas, P. D. and Garnero, P. (2007) 'Non-enzymatic glycation of bone collagen modifies osteoclastic activity and differentiation', *Journal of Biological Chemistry*, 282(8), 5691-703.

Valerio, G., del Puente, A., Esposito-del Puente, A., Buono, P., Mozzillo, E. and Franzese, A. (2002) 'The lumbar bone mineral density is affected by long-term poor metabolic control in adolescents with type 1 diabetes mellitus', *Horm Res*, 58(6), 266-72.

van Coeverden, S. C., Netelenbos, J. C., de Ridder, C. M., Roos, J. C., Popp-Snijders, C. and Delemarre-van de Waal, H. A. (2002) 'Bone metabolism markers and bone mass in healthy pubertal boys and girls', *Clin Endocrinol (Oxf)*, 57(1), 107-16.

van der Deen, M., Akech, J., Lapointe, D., Gupta, S., Young, D. W., Montecino, M. A., Galindo, M., Lian, J. B., Stein, J. L., Stein, G. S. and van Wijnen, A. J. (2012) 'Genomic promoter occupancy of runt-related transcription factor RUNX2 in Osteosarcoma cells identifies genes involved in cell adhesion and motility', *Journal of Biological Chemistry*, 287(7), 4503-17.

van Lierop, A. H., Hamdy, N. A., van der Meer, R. W., Jonker, J. T., Lamb, H. J., Rijzewijk, L. J., Diamant, M., Romijn, J. A., Smit, J. W. and Papapoulos, S. E. (2012) 'Distinct effects of pioglitazone and metformin on circulating sclerostin and biochemical markers of bone turnover in men with type 2 diabetes mellitus', *Eur J Endocrinol*, 166(4), 711-6.

Van Oss, C. J., Good, R. J. and Chaudhury, M. K. (1987) 'Mechanism of DNA (Southern) and protein (Western) blotting on cellulose nitrate and other membranes', *J Chromatogr*, 391(1), 53-65.

van Staa, T. P., Cooper, C., Leufkens, H. G. and Bishop, N. (2003) 'Children and the risk of fractures caused by oral corticosteroids', *J Bone Miner Res*, 18(5), 913-8.

van Staa, T. P., Dennison, E. M., Leufkens, H. G. and Cooper, C. (2001) 'Epidemiology of fractures in England and Wales', *Bone*, 29(6), 517-22.

Vande Berg, B. C., Malghem, J., Lecouvet, F. E. and Maldague, B. (1998) 'Magnetic resonance imaging of normal bone marrow', *Eur Radiol*, 8(8), 1327-34.

Vanhamme, L., van den Boogaart, A. and Van Huffel, S. (1997) 'Improved Method for Accurate and Efficient Quantification of MRS Data with Use of Prior Knowledge', *Journal of Magnetic Resonance Imaging*, 129, 35-43.

Vashishth, D., Gibson, G. J., Khoury, J. I., Schaffler, M. B., Kimura, J. and Fyhrie, D. P. (2001) 'Influence of nonenzymatic glycation on biomechanical properties of cortical bone', *Bone*, 28(2), 195-201.

Vasilkova, O., Mokhort, T., Sharshakova, T., Hayashida, N. and Takamura, N. (2011) 'Leptin is an independent determinant of bone mineral density in men with type 2 diabetes mellitus', *Acta Diabetol*, 48(4), 291-295.

Vatanparast, H., Baxter-Jones, A., Faulkner, R. A., Bailey, D. A. and Whiting, S. J. (2005) 'Positive effects of vegetable and fruit consumption and calcium intake on bone mineral accrual in boys during growth from childhood to adolescence: the University of Saskatchewan Pediatric Bone Mineral Accrual Study', *Am J Clin Nutr*, 82(3), 700-6.

Vavanikunnel, J., Charlier, S., Becker, C., Schneider, C., Jick, S. S., Meier, C. R. and Meier, C. (2019) 'Association between glycemic control and risk of fracture in diabetic patients: A nested case-control study', *J Clin Endocrinol Metab*, 104(5), 1645-1654

Vazquez-Martin, A., Oliveras-Ferraros, C. and Menendez, J. A. (2009) 'The antidiabetic drug metformin suppresses HER2 (erbB-2) oncoprotein overexpression via inhibition of the mTOR effector p70S6K1 in human breast carcinoma cells', *Cell Cycle.*, 8(1), 88-96.

Vella, S., Buetow, L., Royle, P., Livingstone, S., Colhoun, H. M. and Petrie, J. R. (2010) 'The use of metformin in type 1 diabetes: a systematic review of efficacy', *Diabetologia*, 53(5), 809-20.

Verborgt, O., Gibson, G. J. and Schaffler, M. B. (2000) 'Loss of osteocyte integrity in association with microdamage and bone remodeling after fatigue in vivo', *J Bone Miner Res*, 15(1), 60-7.

Verhaeghe, J., van Herck, E., Visser, W. J., Suiker, A. M., Thomasset, M., Einhorn, T. A., Faierman, E. and Bouillon, R. (1990) 'Bone and mineral metabolism in BB rats with long-term diabetes. Decreased bone turnover and osteoporosis', *Diabetes*, 39(4), 477-82.

Vestergaard, P. (2007) 'Discrepancies in bone mineral density and fracture risk in patients with type 1 and type 2 diabetes--a meta-analysis', *Osteoporos Int*, 18(4), 427-44.

Vestergaard, P., Rejnmark, L. and Mosekilde, L. (2005) 'Relative fracture risk in patients with diabetes mellitus, and the impact of insulin and oral antidiabetic medication on relative fracture risk', *Diabetologia*, 48(7), 1292-9.

Viegas, M., Costa, C., Lopes, A., Griz, L., Medeiro, M. A. and Bandeira, F. (2011) 'Prevalence of osteoporosis and vertebral fractures in postmenopausal women with type 2 diabetes mellitus and their relationship with duration of the disease and chronic complications', *J Diabetes Complications*, 25(4), 216-21.

Viollet, B., Guigas, B., Sanz Garcia, N., Leclerc, J., Foretz, M. and Andreelli, F. (2012) 'Cellular and molecular mechanisms of metformin: an overview', *Clin Sci (Lond)*, 122(6), 253-70.

Vogler, J. B., 3rd and Murphy, W. A. (1988) 'Bone marrow imaging', *Radiology*, 168(3), 679-93.

Vogt, J., Traynor, R. and Sapkota, G. P. (2011) 'The specificities of small molecule inhibitors of the TGFss and BMP pathways', *Cell Signal*, 23(11), 1831-42.

Vroegrijk, I. O. C. M., van Klinken, J. B., van Diepen, J. A., van den Berg, S. A. A., Febbraio, M., Steinbusch, L. K. M., Glatz, J. F. C., Havekes, L. M., Voshol, P. J., Rensen, P. C. N., van Dijk, K. W. and van Harmelen, V. (2013) 'CD36 Is Important for Adipocyte Recruitment and Affects Lipolysis', *Obesity*, 21(10), 2037-2045.

Wagner, E. R., He, B. C., Chen, L., Zuo, G. W., Zhang, W., Shi, Q., Luo, Q., Luo, X., Liu, B., Luo, J., Rastegar, F., He, C. J., Hu, Y., Boody, B., Luu, H. H., He, T. C., Deng, Z. L. and Haydon, R. C. (2010) 'Therapeutic Implications of PPARgamma in Human Osteosarcoma', *PPAR Res*, 2010, 956427.

Waitches, G., Zawin, J. K. and Poznanski, A. K. (1994) 'Sequence and rate of bone marrow conversion in the femora of children as seen on MR imaging: are accepted standards accurate?', *AJR Am J Roentgenol*, 162(6), 1399-406.

Walkey, C. J. and Spiegelman, B. M. (2008) 'A functional peroxisome proliferator-activated receptor-gamma ligand-binding domain is not required for adipogenesis', *Journal of Biological Chemistry*, 283(36), 24290-4.

Wang, A., Midura, R. J., Vasanji, A., Wang, A. J. and Hascall, V. C. (2014) 'Hyperglycemia diverts dividing osteoblastic precursor cells to an adipogenic pathway and induces synthesis of a hyaluronan matrix that is adhesive for monocytes', *Journal of Biological Chemistry*, 289(16), 11410-20.

Wang, E. A., Israel, D. I., Kelly, S. and Luxenberg, D. P. (1993) 'Bone morphogenetic protein-2 causes commitment and differentiation in C3H10T1/2 and 3T3 cells', *Growth Factors*, 9(1), 57-71.

Wang, P., Ma, T., Guo, D., Hu, K., Shu, Y., Xu, H. H. K. and Schneider, A. (2018) 'Metformin induces osteoblastic differentiation of human induced pluripotent stem cell-derived mesenchymal stem cells', *J Tissue Eng Regen Med*, 12(2), 437-446.

Wang, Y. H., Liu, Y., Buhl, K. and Rowe, D. W. (2005) 'Comparison of the action of transient and continuous PTH on primary osteoblast cultures expressing differentiation stage-specific GFP', *J Bone Miner Res*, 20(1), 5-14.

Warner, J. T., Cowan, F. J., Dunstan, F. D. J., Evans, W. D., Webb, D. K. H. and Gregory, J. W. (1998) 'Measured and predicted bone mineral content in healthy boys and girls aged 6–18 years: adjustment for body size and puberty', *Acta Paediatrica*, 87, 244-249.

Watts, N. B., Bilezikian, J. P., Usiskin, K., Edwards, R., Desai, M., Law, G. and Meininger, G. (2016) 'Effects of Canagliflozin on Fracture Risk in Patients With Type 2 Diabetes Mellitus', *J Clin Endocrinol Metab*, 101(1), 157-66.

Weatherholt, A. M., Fuchs, R. K. and Warden, S. J. (2012) 'Specialized connective tissue: bone, the structural framework of the upper extremity', *J Hand Ther*, 25(2), 123-31; quiz 132.

Weber, D. R., Haynes, K., Leonard, M. B., Willi, S. M. and Denburg, M. R. (2015) 'Type 1 diabetes is associated with an increased risk of fracture across the life span: a population-based cohort study using The Health Improvement Network (THIN)', *Diabetes Care*, 38(10), 1913-20.

Wehrli, F. W. (2007) 'Structural and functional assessment of trabecular and cortical bone by micro magnetic resonance imaging', *Journal of Magnetic Resonance Imaging*, 25(2), 390-409.

Wehrli, F. W., Hopkins, J. A., Hwang, S. N., Song, H. K., Snyder, P. J. and Haddad, J. G. (2000) 'Cross-sectional study of osteopenia with quantitative MR imaging and bone densitometry', *Radiology*, 217(2), 527-38.

Weinberg, E., Maymon, T. and Weinreb, M. (2014) 'AGEs induce caspase-mediated apoptosis of rat BMSCs via TNFalpha production and oxidative stress', *J Mol Endocrinol*, 52(1), 67-76.

Weinstock, R. S., Goland, R. S., Shane, E., Clemens, T. L., Lindsay, R. and Bilezikian, J. P. (1989) 'Bone mineral density in women with type II diabetes mellitus', *J Bone Miner Res*, 4(1), 97-101.

Wendt, T.M., Harja, E., Bucciarelli, L., Qu, W., Lu, Y., Rong, L.L., Jenkins, D.G., Stein, G., Schmidt, A.M., Yan, S.F. (2006) 'RAGE modulates vascular inflammation and atherosclerosis in a murine model of type 2 diabetes' *Atherosclerosis*, 185,70–77

Wendt, T.M., Tanji, N., Guo, J., Kislinger, T.R., Qu, W., Lu, Y., Bucciarelli, L.G., Rong, L.L., Moser, B., Markowitz, G.S., Stein, G., Bierhaus, A., Liliensiek, B., Arnold, B., Nawroth, P.P., Stern, D.M., D'Agati, V.D., Schmidt, A.M. (2003) 'RAGE drives the development of glomerulosclerosis and implicates podocyte activation in the pathogenesis of diabetic nephropathy' *Am J Pathol*,162,1123–1137

Wergedal, J. E. and Baylink, D. J. (1984) 'Characterization of cells isolated and cultured from human bone', *Proc Soc Exp Biol Med*, 176(1), 60-9.

Westbrook, C., Roth, C. and J, T. (2011) *MRI in Practice*, Wiley-Blackwell.

Whiting, S. J., Vatanparast, H., Baxter-Jones, A., Faulkner, R. A., Mirwald, R. and Bailey, D. A. (2004) 'Factors that affect bone mineral accrual in the adolescent growth spurt', *J Nutr*, 134(3), 696S-700S.

WHO Study Group (1994) *Assessment of fracture risk and its application to screening for postmenopausal osteoporosis. Report of a WHO Study Group*, 843World Health Organization.

Williams, G. A., Wang, Y., Callon, K. E., Watson, M., Lin, J. M., Lam, J. B., Costa, J. L., Orpe, A., Broom, N., Naot, D., Reid, I. R. and Cornish, J. (2009) 'In vitro and in vivo effects of adiponectin on bone', *Endocrinology*, 150(8), 3603-10.

Winder, W. W. and Hardie, D. G. (1996) 'Inactivation of acetyl-CoA carboxylase and activation of AMP-activated protein kinase in muscle during exercise', *Am J Physiol*, 270(2 Pt 1), E299-304.

Wolff, S. P., Jiang, Z. Y. and Hunt, J. V. (1991) 'Protein glycation and oxidative stress in diabetes mellitus and ageing', *Free Radic Biol Med*, 10(5), 339-52.

Woods, A., Salt, I., Scott, J., Hardie, D. G. and Carling, D. (1996) 'The alpha1 and alpha2 isoforms of the AMP-activated protein kinase have similar activities in rat liver but exhibit differences in substrate specificity in vitro', *FEBS Lett*, 397(2-3), 347-51.

Wren, T. A., Shepherd, J. A., Kalkwarf, H. J., Zemel, B. S., Lappe, J. M., Oberfield, S., Dorey, F. J., Winer, K. K. and Gilsanz, V. (2012) 'Racial disparity in fracture risk between white and nonwhite children in the United States', *J Pediatr*, 161(6), 1035-40.

Wu, Y., Hrovat, M. I., Ackerman, J. L., Reese, T. G., Cao, H., Ecklund, K. and Glimcher, M. J. (2010) 'Bone matrix imaged in vivo by water- and fat-suppressed proton projection MRI (WASPI) of animal and human subjects', *Journal of Magnetic Resonance Imaging*, 31(4), 954-63.

Wu, Y., Tu, Q., Valverde, P., Zhang, J., Murray, D., Dong, L. Q., Cheng, J., Jiang, H., Rios, M., Morgan, E., Tang, Z. and Chen, J. (2014) 'Central adiponectin administration reveals new regulatory mechanisms of bone metabolism in mice', *Am J Physiol Endocrinol Metab*, 306(12), E1418-30.

Yamaguchi, N., Kukita, T., Li, Y. J., Kamio, N., Fukumoto, S., Nonaka, K., Ninomiya, Y., Hanazawa, S. and Yamashita, Y. (2008) 'Adiponectin inhibits induction of TNF-alpha/RANKL-stimulated NFATc1 via the AMPK signaling', *FEBS Lett*, 582(3), 451-6.

Yamamoto, M., Yamaguchi, T., Nawata, K., Yamauchi, M. and Sugimoto, T. (2012) 'Decreased PTH levels accompanied by low bone formation are associated with vertebral fractures in postmenopausal women with type 2 diabetes', *J Clin Endocrinol Metab*, 97(4), 1277-84.

Yamamoto, M., Yamaguchi, T., Yamauchi, M., Kaji, H. and Sugimoto, T. (2009) 'Diabetic patients have an increased risk of vertebral fractures independent of BMD or diabetic complications', *J Bone Miner Res*, 24(4), 702-9.

Yamamoto, M., Yamaguchi, T., Yamauchi, M., Sugimoto, T. (2009) 'Low serum level of the endogenous secretory receptor for advanced glycation end products (esRAGE) is a risk factor for prevalent vertebral fractures independent of bone mineral density in patients with type 2 diabetes' *Diabetes Care*, 32(12),2263–8

Yamamoto, M., Yamaguchi, T., Yamauchi, M., Yano, S. and Sugimoto, T. (2008) 'Serum pentosidine levels are positively associated with the presence of vertebral fractures in postmenopausal women with type 2 diabetes', *J Clin Endocrinol Metab*, 93(3), 1013-9.

Yamamoto, T., Ozono, K., Miyauchi, A., Kasayama, S., Kojima, Y., Shima, M. and Okada, S. (2001) 'Role of advanced glycation end products in adynamic bone disease in patients with diabetic nephropathy', *American Journal of Kidney Diseases*, 38(4 Suppl 1), S161-4.

Yan, J., Dong, L., Zhang, B. and Qi, N. (2010) 'Effects of extremely low-frequency magnetic field on growth and differentiation of human mesenchymal stem cells', *Electromagn Biol Med*, 29(4), 165-76.

Yang, D. C., Tsay, H. J., Lin, S. Y., Chiou, S. H., Li, M. J., Chang, T. J. and Hung, S. C. (2008) 'cAMP/PKA Regulates Osteogenesis, Adipogenesis and Ratio of RANKL/OPG mRNA Expression in Mesenchymal Stem Cells by Suppressing Leptin', *PLoS One*, 3(2).

Yang, L. and Grey, V. (2006) 'Pediatric reference intervals for bone markers', *Clin Biochem*, 39(6), 561-8.

Yarwood, S. J., Sale, E. M., Sale, G. J., Houslay, M. D., Kilgour, E. and Anderson, N. G. (1999) 'Growth hormone-dependent differentiation of 3T3-F442A preadipocytes requires Janus kinase/signal transducer and activator of transcription but not mitogen-activated protein kinase or p70 S6 kinase signaling', *J Biol Chem.*, 274(13), 8662-8.

Yee, C. S., Xie, L., Hatsell, S., Hum, N., Murugesh, D., Economides, A. N., Loots, G. G. and Collette, N. M. (2016) 'Sclerostin antibody treatment improves fracture outcomes in a Type I diabetic mouse model', *Bone*, 82, 122-34.

Yki-Jarvinen, H. (2004) 'Drug therapy: Thiazolidinediones', *New England Journal of Medicine*, 351(11), 1106-1118.

Young, I. and Bydder, G. (2003) 'Magenetic resonance: new approach to imaging of the musculoskeletal system', *Physiological Measurement*, 24, 1-23.

Yu, E. W., Greenblatt, L., Eajazi, A., Torriani, M. and Bredella, M. A. (2017) 'Marrow adipose tissue composition in adults with morbid obesity', *Bone*, 97, 38-42.

Yu, P. B., Hong, C. C., Sachidanandan, C., Babitt, J. L., Deng, D. Y., Hoyng, S. A., Lin, H. Y., Bloch, K. D. and Peterson, R. T. (2008) 'Dorsomorphin inhibits BMP signals required for embryogenesis and iron metabolism', *Nat Chem Biol*, 4(1), 33-41.

Yu, W., Gluer, C. C., Grampp, S., Jergas, M., Fuerst, T., Wu, C. Y., Lu, Y., Fan, B. and Genant, H. K. (1995) 'Spinal bone mineral assessment in postmenopausal women: a comparison between dual X-ray absorptiometry and quantitative computed tomography', *Osteoporos Int*, 5(6), 433-9.

Zayzafoon, M., Stell, C., Irwin, R. and McCabe, L. R. (2000) 'Extracellular glucose influences osteoblast differentiation and c-Jun expression', *Journal of Cellular Biochemistry*, 79(2), 301-10.

Zebaze, R. M., Ghasem-Zadeh, A., Bohte, A., Iuliano-Burns, S., Mirams, M., Price, R. I., Mackie, E. J. and Seeman, E. (2010) 'Intracortical remodelling and porosity in the distal radius and post-mortem femurs of women: a cross-sectional study', *Lancet*, 375(9727), 1729-36.

Zhang, M., Xuan, S., Bouxsein, M. L., von Stechow, D., Akeno, N., Faugere, M. C., Malluche, H., Zhao, G., Rosen, C. J., Efstratiadis, A. and Clemens, T. L. (2002) 'Osteoblast-specific knockout of the insulin-like growth factor (IGF) receptor gene reveals an essential role of IGF signaling in bone matrix mineralization', *Journal of Biological Chemistry*, 277(46), 44005-12.

Zhang, X., Yang, M., Lin, L., Chen, P., Ma, K. T., Zhou, C. Y. and Ao, Y. F. (2006) 'Runx2 overexpression enhances osteoblastic differentiation and mineralization in adipose - derived stem cells in vitro and in vivo', *Calcif Tissue Int*, 79(3), 169-178.

Zhang, Y., Papasian, C. J. and Deng, H. W. (2011) 'Alteration of vitamin D metabolic enzyme expression and calcium transporter abundance in kidney involved in type 1 diabetes-induced bone loss', *Osteoporos Int*, 22(6), 1781-8.

Zhao, J. X., Yue, W. F., Zhu, M. J. and Du, M. (2011) 'AMP-activated protein kinase regulates beta-catenin transcription via histone deacetylase 5', *Journal of Biological Chemistry*, 286(18), 16426-34.

Zhao, L., Li, G., Chan, K. M., Wang, Y. and Tang, P. F. (2009) 'Comparison of multipotent differentiation potentials of murine primary bone marrow stromal cells and mesenchymal stem cell line C3H10T1/2', *Calcif Tissue Int*, 84(1), 56-64.

Zhen, D., Chen, Y. and Tang, X. (2010) 'Metformin reverses the deleterious effects of high glucose on osteoblast function', *J Diabetes Complications*, 24(5), 334-44.

Zhou, G. C., Myers, R., Li, Y., Chen, Y. L., Shen, X. L., Fenyk-Melody, J., Wu, M., Ventre, J., Doebber, T., Fujii, N., Musi, N., Hirshman, M. F., Goodyear, L. J. and Moller, D. E. (2001) 'Role of AMP-activated protein kinase in mechanism of metformin action', *Journal of Clinical Investigation*, 108(8), 1167-1174.

Zhu, Z. N., Jiang, Y. F. and Ding, T. (2014) 'Risk of fracture with thiazolidinediones: an updated meta-analysis of randomized clinical trials', *Bone*, 68, 115-23.

Zhukouskaya, V. V., Eller-Vainicher, C., Vadzianava, V. V., Shepelkevich, A. P., Zhurava, I. V., Korolenko, G. G., Salko, O. B., Cairoli, E., Beck-Peccoz, P. and Chiodini, I. (2013) 'Prevalence of morphometric vertebral fractures in patients with type 1 diabetes', *Diabetes Care*, 36(6), 1635-40.

Zinman, B., Haffner, S. M., Herman, W. H., Holman, R. R., Lachin, J. M., Kravitz, B. G., Paul, G., Jones, N. P., Aftring, R. P., Viberti, G., Kahn, S. E. and Group, A. S. (2010) 'Effect of rosiglitazone, metformin, and glyburide on bone biomarkers in patients with type 2 diabetes', *J Clin Endocrinol Metab*, 95(1), 134-42.

Zuk, P. A., Zhu, M., Ashjian, P., De Ugarte, D. A., Huang, J. I., Mizuno, H., Alfonso, Z. C., Fraser, J. K., Benhaim, P. and Hedrick, M. H. (2002) 'Human adipose tissue is a source of multipotent stem cells', *Molecular Biology of the Cell*, 13(12), 4279-4295.

Appendices

Clinical Study Documentation

Appendix A Study Protocol

Appendix B Case Report Form for Cases

Appendix C Case Report Form for Controls

Appendix D Consent/Assent Form for Cases

Appendix E Consent/Assent Form for Controls

Appendix F Physical Activity Questionnaire (Under 14 years old)

Appendix G Physical Activity Questionnaire (14-19 years old)

Publications

Appendix H Abdalrahman N, **Chen SC**, Wang JR, Ahmed SF. An update on diabetes related skeletal fragility. *Expert Review of Endocrinology & Metabolism* 2015;10:193-210

Appendix I **Chen SC**, Brooks R, Houskeeper J, Bremner SK, Dunlop J, Viollet B, Logan PJ, Salt IP, Ahmed SF, Yarwood SJ. Metformin suppresses adipogenesis through both AMP-activated protein kinase (AMPK)-dependent and AMPK-independent mechanisms. *Mol Cell Endocrinol* 2017;440:57-68; Corrigendum *Mol Cell Endocrinol* 2017;443:176

Appendix J **Chen SC**, Shepherd S, McMillan M, McNeilly J, Foster J, Wong SC, Robertson KJ, Ahmed SF. Skeletal fragility & its clinical determinants in children with type 1 diabetes. *J Clin Endocrinol Metab*. 2019 Mar 8. pii: jc.2019-00084. doi: 10.1210/jc.2019-00084

STUDY PROTOCOL

TITLE	The Effects of Type 1 Diabetes Mellitus on the Bone Health of Children and Adolescents
VERSION	Version 3.0
DATE	10/12/2014
SPONSOR	NHS Greater Glasgow and Clyde (GGC)
FUNDER	Glasgow Children's Hospital Charity
QUALIFICATION AIM	MD, University of Glasgow

This study will be performed according to the Research Governance Framework for Health and Community Care (Second edition, 2006) and World Medical Association Declaration of Helsinki Ethical Principles for Medical Research Involving Human Subjects 1964

CONTACTS PAGE

INVESTIGATORS

CHIEF INVESTIGATOR
Professor S Faisal Ahmed
Samson Gemmell Chair of Child Health
Royal Hospital for Children,
Glasgow G51 4TF
Email faisal.ahmed@glasgow.ac.uk

CO-INVESTIGATOR(S)
Dr Jarod Wong Sze Choong
Senior Research Fellow
Developmental Endocrinology Research Group
Royal Hospital for Children
Glasgow G51 4TF
Email jarod.wong@glasgow.ac.uk

Dr S Ching Chen
Clinical Research Fellow
Developmental Endocrinology Research Group
Royal Hospital for Children
Glasgow G51 4TF
Email suetching.chen1@nhs.net

TECHNICAL SUPPORT

MRI PHYSICIST
Ms Christie McComb
Clinical Scientist
MRI Department, Clinical Research Facility
Royal Hospital for Children
Glasgow G51 4TF
Email christie.mccomb@nhs.net

BONE DENSITOMETRY
Dr Sheila Shepherd (nee Khanna) (PhD)
Paediatric Bone Densitometry Service Manager
Developmental Endocrinology Research Group
Royal Hospital for Children
Glasgow G51 4TF
Email s.khanna@nhs.net

LABORATORY
Mr Martin McMillan
Research Scientist
Developmental Endocrinology Research Group
Royal Hospital for Children
Glasgow G51 4TF
Email martin.mcmillan@glasgow.ac.uk

COLLABORATING CLINICAL STAFF

Dr Kenneth Robertson
Consultant Paediatrician and Diabetes
Ward 6B, West Ambulatory Care Hospital
Glasgow G3 8SJ
Email kjr@diabetes-scotland.org

Dr M Guftar Shaikh
Consultant Paediatric Endocrinology
Developmental Endocrinology Research Group
Royal Hospital for Children
Glasgow G51 4TF
Email guftar.shaikh@nhs.net

TABLE OF CONTENTS

Appendix A

ABBREVIATIONS

ALP	alkaline phosphatase
Bic	bicarbonate
BMC	bone mineral content
BMD	bone mineral density
BV/TV	ratio of bone volume over total volume of area scanned
Ca^{2+}	calcium
CRF	Clinical Research Facility
CTX	carboxyl-terminal cross-linked telopeptide of Type1 collagen
DXA	dual X-ray absorptiometry
GGC	Greater Glasgow and Clyde
GH	growth hormone
H^+	hydrogen ions
HbA1C	glycated haemoglobin
IGF1	insulin-like growth factor 1
IGFBP	insulin-like growth factor binding protein
ALS	acid labile subunit
IRR	incidence rate ratio
MRI	magnetic resonance imaging
MRS	magnetic resonance spectroscopy
NHS	National Health Service
PO_4	phosphate
PTH	parathyroid hormone
RHC	Royal Hospital for Children, Glasgow
T1DM	Type 1 Diabetes Mellitus

STUDY SYNOPSIS

Title of study	The Effects Of Type 1 Diabetes Mellitus On The Bone Health Of Children And Adolescents
Study Centre	Royal Hospital for Children, Glasgow
Duration of Study	24 months
Objectives	To use novel methods of microMRI and MRS in assessing bone health of children with T1DM
Primary Objective	To establish the prevalence of abnormal bone health in children with newly diagnosed and established T1DM, comparing cases and controls
Secondary Objective	To assess the relationship of abnormal bone health to disease and treatment factors
Methodology	Prospective study in the newly diagnosed T1DM children over 14 month period from diagnosis Cross sectional study in established diagnosed cases of T1DM
Sample size	<u>Newly Diagnosed Diabetes Study</u> Estimated 30 cases, based on annual incidence of T1DM in NHS GGC Paediatric Diabetes service <u>Established Diabetes Study</u> 30 cases, based on power calculation and previous studies <u>Controls</u> Estimated 30 controls, based on power calculation and previous studies but final numbers may vary
Inclusion criteria	<u>Newly Diagnosed Diabetes Study</u> • First presentation of T1DM during study period • Age ≥10 and ≤18 yrs <u>Established Diabetes Study</u> • Children with T1DM of ≥3 yrs duration • Age ≥10 and ≤18 yrs <u>Controls</u> • Healthy children age ≥10 and ≤18 yrs • No contraindications for MRI

Exclusion criteria	<u>All potential participants (including controls)</u> • Age ≥19 years • Significant other chronic diseases • On medication known to affect bone health (e.g glucocorticoids, bone protective therapy) <u>Established Diabetes Study</u> • Age <10 years • Disease duration <3 years <u>MRI exclusion criteria</u> • Contraindications for MRI (e.g cardiac pacemaker, metallic clip in body etc)
Study involvement	<u>Assessment of bone health by:</u> • Dietary, exercise & fracture history • Biochemical markers of bone metabolism • Serum GH/IGF1 axis and adipokines • Dual energy X-ray Absorptiometry (DXA) • MRI to assess bone microarchitecture • MRS to assess vertebral bone marrow adiposity <u>Assessment of T1DM disease by:</u> • Degree of acidosis at presentation • Glycated haemoglobin(HbA1c) & C-peptide • Insulin dose (unit/kg) • Presence of other microvascular complications
Primary Outcome	Quantitative measurements of trabecular bone (bone volume/total volume) obtained from microMRI images in cases versus controls
Secondary Outcome	1) Measure of bone marrow adiposity by MRS 2) Relationship of markers of bone health (including DXA) to markers of T1DM disease 3) Change in bone and adiposity markers over first year of diagnosis
Statistical Analysis	Inter-group comparison to be performed by non-parametric analyses of difference and assessment of correlation between continuous variables by univariate and multivariate regression analysis

STUDY FLOW CHART: Newly Diagnosed Diabetes Study

	Study Period		
	Visit 1 (To be completed within 10 days of discharge)	Visit 2 (6-8 months from diagnosis)	Visit 3 (12-14 months from diagnosis)
Obtain informed consent	x		
Personal and demographic data	x		
Medical, surgical and medication history	x		
Review inclusion and exclusion criteria	x		
Physical examination	x		
Pubertal assessment	x	x	x
Height (cm) and weight (kg)	x	x	x
BMI calculation (kg/m^2)	x	x	x
Study bloods			
• HbA1c* and C-peptide	x	x	x
• Laboratory blood glucose*	x		
• Degree of acidosis (H^+, Bic)*	x		
• Markers of bone metabolism	x	x	x
• Serum GH/IGF1 axis and adipokines	x	x	x
Urinalysis*	x		
MRI scan	x		x

* Routinely performed for clinical purpose

STUDY FLOW CHART: Established Diabetes Cases

	Study Period		
	Routine clinic visit for initial approach	Visit 1 (Next clinic visit when screening bloods due)	Visit 2 (MRI attendance)
Obtain informed consent		x	
Personal and demographic data		x	
Medical, surgical and medication history		x	
Review inclusion and exclusion criteria	x		
Physical examination		x	
Pubertal assessment		x	
Height (cm) and weight (kg)*		x	
BMI calculation (kg/m^2)*		x	
Study bloods			
• HbA1c*		x	
• Markers of bone metabolism		x	
• Serum GH/IGF1 axis and adipokines		x	
DXA scan		x	
MRI scan			x

* Routinely performed for clinical purpose

1.0 INTRODUCTION

1.1 Overview

Bone health in diabetes has become an increasing focus of interest as the association between fractures and Type 1 diabetes mellitus (T1DM) becomes increasingly recognised (Nicodemus 2001, Forsen 1999). Patients with Type 1 diabetes have reduced bone mineral density (BMD) as assessed by dual energy X-ray absorptiometry but patients with T2DM have increased BMD (Bouillon 1991, Vestergaard 2006), yet both groups have increased risk of fragility fractures. With a modest degree of reduced BMD, T1DM should have a predicted relative fracture risk of one and a half fold when compared with age-matched non-diabetics, yet a meta-analysis of several large cohort studies (Janghorbani 2007) have demonstrated a disproportionately increased risk of hip fractures by seven-fold.

Such disparities between DXA-derived bone mineral density and actual fracture risk in T1DM suggest that there are other factors contributing to overall bone health. This is acknowledged by the National Institute of Health (NIH) Consortium on Osteoporosis which recognises the importance of bone microarchitecture as a factor determining bone health. Bone microMRI technique is able to distinguish between cortical and trabecular bone hence confer the necessary information of bone microarchitecture to more accurately assess the fracture risk in diabetes patients. Recent evidence has also suggested increasing bone marrow adiposity in osteoporotic bones (Rosen 2006), providing another insight into bone health amenable to attractive treatment options targeting bone marrow adipogenesis.

1.2 Literature background

Earlier studies suggested that the defect in bone mass accretion in T1DM appears quite early on in the course of the disease, with evidence of osteopenia as early as two years after the diagnosis (McNair 1978, Gunczler 1998). More recent studies have shown that children with T1DM have decreased lumbar spine BMD within the first few months of diagnosis (Gunczler 2001). This osteopenia doubles in children with disease duration of more than three months but stabilises out with no further correlation between longer disease duration and BMD (Gunczler 2001).

The mechanisms underlying the abnormalities of bone health may involve:

1) Alteration in bone remodelling, and/or
2) Lack of anabolic action of insulin, and/or
3) Toxic effects of hyperglycaemia or diabetes ketoacidosis

1.2.1) Understanding the changes in biochemical bone markers can provide insight into the pathophysiology of osteopenia in T1DM. Bone formation is a tightly regulated process characterized by a sequence of events starting with commitment of osteoprogenitor cells, and their differentiation into pre-osteoblasts and then into mature osteoblasts, which express high levels of alkaline phosphatase (ALP) and osteocalcin, both of which are markers of bone formation. Experimental and animal models with T1DM have suggested a defect in bone formation with reduction in osteoblastic numbers and function (Rico 1989, Verhaeghe 1990, Hie 2011). Clinical studies in children and young adult with T1DM have shown a reduction in biochemical markers of bone formation

(Bouillon 1995, Gunczler 1998, Lappin 2009, Pater 2010) thought to be most likely secondary to the maturation defect described above. The degree of bone resorption contributing to the osteopenia remains somewhat more controversial with suggestions of decreased (Pater 2010) but also increased osteoclastic activity (Gunczler 2001) in children with T1DM.

1.2.2) T1DM is a condition of insulinopenia and insulin has an anabolic effect on the bone, both directly and indirectly. In vitro studies have demonstrated insulin as an anabolic agent in osteoblastogenesis as cultured osteoblasts proliferate successfully in response to physiological doses of insulin (Wergedal 1984). In insulin deficient state, immature mesenchymal cells do not differentiate into mature osteoblasts, likely due to altered gene expression of proosteoblastic proteins (Lu 2003). Insulin also exerts indirect but synergistic effects with other anabolic agents in bone, such as parathyroid hormone (PTH) (Hickman 1990) and IGF-1 (Conover 1996). Rats with T1DM rendered insulin-deficient by the chemical streptozotocin (STZ) have non-osmotic hypercalciuria resulting in a negative calcium balance which may indirectly affect bone integrity (Ward 2001).

1.2.3) Animal studies have also shown that the degree of overall glycaemic control correlates with fracture healing (Follak 2004, Follak 2005). Many studies in human have investigated the association of metabolic control in T1DM (as measured by HbA1c) and bone mineral density with some suggesting benefit in good glycaemic control (Valerio 2002, Heap 2004, Pater 2010) whilst others do not (Gunczler 1998, Ersoy 1999). Pater et al showed that HbA1c was inversely correlated to osteocalcin but *only* at the onset of diagnosis and not later on in the disease process, suggesting that factors other than hyperglycaemia also exert toxic effect on bones in T1DM. One other proposed diabetes-related factor is the effect of acidosis during DKA on bone mineral density. Metabolic acidosis is known to result in negative calcium balance in bone through a reduction in osteoblastic formation, increase in osteoclastic resoption and bone mineral resolution (Krieger 1992, Bushinsky 1993, Frick 1997). Topaloglu et al have suggested that the decreased osteoblastic activity in DKA is solely due to effect of acidosis without additional influences from other diabetes related-factors such as hyperglycaemia and hypoinsulinaemia (Topaloglu 2005).

1.3 Preliminary data from our group

Preliminary data from a recent study performed on the Scottish national diabetes database has not only confirmed that T1DM patients have a substantially increased relative risk of hip fractures (IRR 3.28 in men, 3.54 in women) compared with age-matched non-diabetics, but also revealed that this increased fracture risk is greatest in younger men and women in their second and third decade of life (Hothersall 2013).

In previous pilot studies, the Developmental Endocrinology Research Group led by Professor Ahmed have developed a method to assess bone microarchitecture using microMRI and demonstrated that this method is sensitive in differentiating between healthy adult volunteers and volunteers with osteogenesis imperfecta as well as growth hormone deficiency (McComb 2013). These studies which employed a 3T-MRI to assess bone microarchitecture and combined this with MR

spectroscopy to assess BMA clearly showed that, in healthy adults, there is an age dependent degradation in bone microarchitecture which is accompanied by increased BMA (McComb 2013). Whilst both groups of cases, OI and GHD, had a reduction in trabecular bone (Fig.1), it was only the GHD cases who showed an increase in BMA. This technique was later applied to young adult women at risk of adverse bone health with childhood onset T1DM. This group has shown that affected women had a lower number of trabeculae and lower BV/TV and these abnormalities were more likely in those patients who were diagnosed at an early age or had a longer duration of disease. These abnormalities were also more profound in those who had retinopathy (Fig.2).

Fig. 1

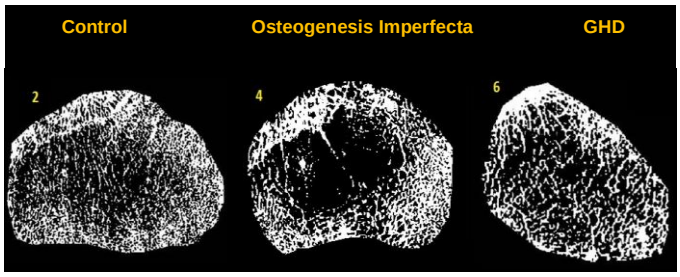

Fig. 2

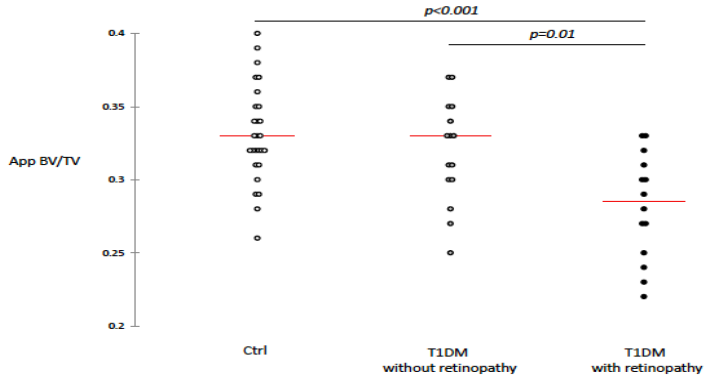

1.4 Research Strategy

The aim of the current proposal is to explore the use of these novel methods (microMRI and MRS) in children to improve our understanding of the prevalence of early abnormal bone health in conditions such as T1DM.

This research will be dependent on close collaboration between colleagues in endocrinology and diabetes, as well as expertise of the MRI physicists, bone densitometry service and support from laboratory contacts, all of whom have worked together successfully in previous collaborations.

2.0 STUDY OBJECTIVES

The objective of this research is to use novel methods of microMRI and MRS in assessing bone health of children with T1DM.

2.1 Primary Objective
To establish the prevalence of abnormal bone health in children with newly diagnosed and established T1DM, comparing cases and controls

2.2 Secondary Objective
To assess the relationship of abnormal bone health to disease (age at diagnosis, severity at disease presentation, duration of disease) and treatment factors (insulin dose, overall glycaemic control)

2.3 Null Hypotheses
2.3.1 Children and adolescent with T1DM have normal bone health
2.3.2 Severity of disease (degree of acidosis and HbA1C) at presentation has no correlation to underlying bone microarchitecture of children with T1DM
2.3.3 Poor diabetes control has no effect on bone health in children with established T1DM

3.0 STUDY DESIGN
This research is divided into:

3.1 Newly Diagnosed Diabetes Cases
A prospective study of bone health in newly diagnosed T1DM children over 14 month period from diagnosis

3.1.1 Setting
Recruitment for the study will be conducted over a period of 18 months between June 2014 – Nov 2015 at Royal Hospital for Children, Glasgow within NHS GGC Paediatric Diabetes Service Network

3.1.2 Subject selection and recruitment
All newly diagnosed T1DM patients between age 10 (inclusive) to 18 years old (inclusive) within these three hospitals will be eligible for recruitment into the study. Recruited subjects will undergo the full study involving blood samples, DXA and MRI scans. The annual T1DM incidence in 2012 within the NHS GGC Health Board is 80, of which 35 are ≥10 years of age.

Patients who are newly diagnosed with T1DM will be identified by the NHS GGC Paediatric Diabetes Service and information leaflet of the study provided. The researcher (also part of diabetes clinical team) will be informed and will make contact and meet with the patients and families in the ward to invite them to take part in the study. There will be opportunities to ask questions, which will be answered comprehensively in the best interest of the patients.

To be enrolled into this study, a child must meet the following **inclusion criteria**:
- Newly diagnosed case of T1DM
- Age ≥10 and ≤18 yrs old

- Be able and willing to participate in the study as evidence by a parent/guardian signing a valid written informed consent and the patient signing to show their consent/assent (competence appropriate)
- Child and parents must be able to understand English either directly or through interpreters

A child is not eligible for the study if any of the following **exclusion criteria** apply:

- Age <10 or >19 years old
- Has significant other co-morbidities (e.g prematurity, congenital heart disease, inflammatory bowel disease etc)
- On medication known to affect bone health (e.g glucocorticoids, bone protective therapy)

A child will not be eligible for a MRI study if any of the following exclusion criteria apply:

- Age <10 years old
- Has contraindications for MRI scan (e.g cardiac pacemaker, metallic clip in body etc)

3.1.3 Consent/Assent

Written informed consent will be obtained by the researcher from the family whilst inpatient prior to conducting any study procedures. Informed consent will be obtained in accordance with the Declaration of Helsinki (World Medical Organisation, 2008). The research group is aware that following the new diagnosis of a chronic health problem in children, parents may need more time to assimilate information and this will be respected. In such cases, parents/guardian/young person will be approached again prior to discharge from hospital.

All participation in our study will be consented by the child or young person (ideally with parental consent as well), if deemed competent, or consented by the parents or legal guardian with assent from the child or young person. Consent will be obtained from the study participants, if competent, as assessed by the researcher, according to the guidance from the Scottish Children Research Network (ScotCRN) and the Ethics Working Group of the Confederation of the European Specialists in Paediatrics (CESP). Assent will be obtained from the young person when consent is not appropriate for reasons of competence.

Copies of the consent and/or assent form(s) will be given to the parents/guardian and child respectively, and placed within the child's medical record. The original(s) will be placed in the site file or subject file, as appropriate.

3.1.4 Schedule of events

Visit 1

Visit 1 is the first contact between the researcher and the patient/family. This will be undertaken whilst patient is still in the ward. After obtaining informed consent, each participant will be screened for eligibility according to the inclusion and exclusion criteria. Other components for the first contact will consist of:

- Medical, surgical and medication information inc. dietary, exercise & fracture history
- Physical examination and pubertal assessment undertaken preferably by examination (or self-reporting if preferred)
- Information on severity of disease at presentation, laboratory glucose, HbA1C and urinalysis result will be collected from medical record
- Study bloods (C-peptide, biochemical markers of bone metabolism, GH/IGF1 axis and adipokines) will be requested on excess blood samples collected during initial routine sampling on admission (if available) or obtained from venepuncture if insufficient and patient agreeable
- Baseline MRI scan will be organised within 10 days of discharge

Visit 2

Visit 2 will be timed with routine diabetes clinic visit at 6 months from diagnosis, where the researcher will meet with participant and family. Components for this contact will consist of:

- Medical, surgical and medication information inc. dietary, exercise & fracture history and severe hypoglycaemia history
- Height and weight
- Pubertal assessment
- Study bloods (not routine) will be obtained for HbA1C, C-peptide, biochemical markers of bone metabolism, GH/IGF1 axis and adipokines

Visit 3

Visit 3 will be timed with routine diabetes clinic visit at 12-14 months from diagnosis where the researcher will meet with participant and family. This visit will involve:

- Medical, surgical and medication information inc. dietary, exercise & fracture history and severe hypoglycaemia history
- Height and weight
- Pubertal assessment
- Study bloods (not routine) will be obtained for HbA1C, C-peptide, biochemical markers of bone metabolism, GH/IGF1 axis and adipokines
- DXA scan at RSC
- An MRI scan will be arranged for the same day at the Clinical Research Facility at RHC, thereafter participant will have completed the study

3.1.5 Controls

In the first instance, age-matched controls from the controls recruited for established children with T1DM will be used. In the event that there are no suitable age-matched controls from the established cohort, more controls will be recruited from healthy age-matched friends or siblings of index cases, children of staff members and from other clinics in RHC**.** Friends of index cases may be interested to volunteer as controls, and in such instances, parents of the index case may share with the other parents the study information sheet for controls obtained directly from the researchers. If they are keen to know more about the study or proceed to participate, they will respond directly by contacting the researcher (contact details on study information sheet). Children of staff members who are interested to volunteer as controls may also do so. Control participants will only be recruited if they are willing and able to either assent or consent to participation.

All controls will undergo anthropometry, dietary, exercise and fracture history, pubertal assessment and a single MRI scan at the RHC.

3.2 Established Diabetes Cases

A cross sectional case control study of bone health in children with established T1DM

3.2.1 Setting

Recruitment for the study will be conducted over a period of 12 months between June 2014 – May 2015 at the Royal Hospital for Children, Glasgow.

3.2.2 Subject selection and recruitment

A total of 30 patients will be recruited and enrolled (numbers based on power calculation in Section 3.5), along with a group of healthy age-matched controls involving friends or siblings of cases and children of staff members.

All current patients with T1DM of ≥3 years duration will be identified by the researcher from the SCI-Diabetes database and subdivided into three groups based on their glycaemic control (HbA1c ranges: <59mmol/mol, 59-74mmol/mol, >74mmol/mol). The researcher will arrange to meet these potential participants at their next routine clinic appointments to verbally explain the study to them. An information leaflet will be provided by the researcher or another member of the diabetes team to interested participants. There will be opportunities to ask questions, which will be answered comprehensively in the best interest of the patients. This will be considered the initial approach (see Study Flow Chart for Established Diabetes Cases). It is expected that over a period of 3-4 months all interested and eligible patients would have been identified. From this group of willing participants, 30 subjects with 10 subjects from each HbA1c bracket will be recruited into the study based on first come first serve basis.

To be enrolled in the study, a child must meet the following **inclusion criteria**:

- Diagnosed with T1DM for at least three years
- Age ≥ 10 years and ≤18 years old
- Be able and willing to participate in the study as evidence by a parent/guardian signing a valid written informed consent and the patient signing to show their consent/assent (competence appropriate)
- Child and parents must be able to understand English either directly or through interpreters

A child is not eligible for the study if any of the following **exclusion criteria** apply:

- Age <10 or >19 years
- Duration of T1DM less than 3 years
- Has contraindications for MRI scan (e.g. cardiac pacemaker, metallic clip in body etc)
- Has significant other chronic diseases (e.g prematurity, congenital heart disease, inflammatory bowel disease etc)
- On medication known to affect bone health (e.g glucocorticoids, bone protective therapy)

Should any participants decide to withdraw from the study before completion, the next eligible and willing participant with a HbA1c within the same range would be recruited.

3.2.3 Consent/Assent

Written informed consent will be obtained by researcher prior to conducting any study procedures at Visit 1. Informed consent will be obtained in accordance with the Declaration of Helsinki (World Medical Organisation, 2008). All participation in our study will be consented by the child or young person (ideally with parental consent as well), if deemed competent, or consented by the parents or legal guardian with assent from the child or young person. Consent will be obtained from the study participants, if competent, as assessed by the researcher, according to the guidance from the Scottish Children Research Network (ScotCRN) and the Ethics Working Group of the Confederation of the European Specialists in Paediatrics (CESP). Assent will be obtained from the young person when consent is not appropriate for reasons of competence.

Copies of the consent and/or assent form(s) will be given to the parents/guardian and child respectively, and placed within the child's medical record. The original(s) will be placed in the site file or subject file, as appropriate.

3.2.4 Schedule of Events

Initial Approach

The researcher will meet with the potential participants at their routine clinic visit at RHC to verbally explain the study to them. An information

leaflet will be provided to participants who satisfy the recruitment criteria. There will be opportunities to ask questions, which will be answered comprehensively in the best interest of the patients. If the patient and family are happy to participate, arrangements will be made to obtain informed consent at Visit 1.

Visit 1
This visit will coincide with the eligible patient's next routine visit to the diabetes clinic at RHC when their routine screening blood is due. The researcher will meet with the participant and undertake the following:

- Informed consent
- Height and weight
- Physical examination and pubertal assessment undertaken preferably by examination (or self-reporting if preferred)
- Study bloods for HbA1C, C-peptide, biochemical markers of bone metabolism, GH/IGF1 axis and adipokines will be performed at the same time as the routine screening bloods
- DXA scan will be performed if possible prior to patient leaving the hospital that day

Visit 2
This visit will be within 10 weeks of Visit 1. Participant will be requested to attend for an MRI scan, thereafter participant will have completed the study.

3.2.5 Controls

30 healthy age-matched controls will be recruited from friends or siblings of index cases, children of staff members and from other clinics in RHC. Friends of index cases may be interested to volunteer as controls, and in such instances, parents of the index case may share with the other parents the study information sheet for controls obtained directly from the researchers. If they are keen to know more about the study or proceed to participate, they will respond directly by contacting the researcher (contact details on study information sheet). Children of staff members who are interested to volunteer as controls may also do so. Control participants will only be recruited if they are willing and able to either assent or consent to participation.

All controls will undergo anthropometry, dietary, exercise and fracture history, pubertal assessment and a single MRI scan.

3.3 Study blood samples

All participants will have blood samples taken at the appropriate intervals according to the schedule of events. Research bloods will involve:

- HbA1c to assess glycaemic control
- C-peptide to assess residual pancreatic beta-cell function
- Biochemical markers of bone metabolism (osteocalcin, BALP, CTX)
- Serum markers of GH/IGF1 axis (IGF-1, IGFBP-3, IGFBP-2, ALS) and adipokines (leptin)

Excluding the HbA1c which is obtained for routine clinical purpose, the total volume of research blood required will be 5mls per collection. At all times possible, study bloods will be timed with routine screening bloods.

All newly diagnosed T1DM patients in Greater Glasgow and Clyde (GGC) have a standard number of blood tests collected at the point of first intravenous access or venous sampling as part of a routine protocol. In order to minimise burden on patient with an extra venepuncture, excess blood samples available from this initial routine collection will be accessed if the patient and parents consent to participate in the study. Once consented, the NHS lab will be contacted by the researcher within a week of discharge, to release the samples for research, all of which will then be stored at the University of Glasgow freezer at RHC. These will be processed in batches at the University of Glasgow lab.
The Research Group has also created its own reference data for markers of bone turnover and GH/IGF-1 axis.

3.4 Study imaging

3.4.1 DXA scan

This will be performed at the bone densitometry unit at RHC involving whole body, AP spine and femoral neck. The total maximum dose per scan is 3microSv, which is equivalent to less than half a day of natural background radiation in the UK.

The Research Group has normative DXA BMC data for 150 school age boys and girls in Glasgow for LS, TB and FN as well as manufacturer's reference data for LS and TB BMC which are very similar to the Glasgow data. DXA data shall be analysed as per the recommendations of the recent ISCD guidelines as well as following correction for bone area. LS and FN BMC data shall also be mathematically transformed into volumetric data by calculating bone mineral apparent density.

There is a possibility that we might find something unexpected (incidental finding) in the participant's images. If this happens, the child will be referred to the appropriate specialist for further investigation. All DXA scans will be reviewed by the Bone Densitometry Service as part of the research collaboration. Parents are made aware that they may then have to disclose such findings in future applications for health-related insurance.

3.4.2 MRI/MRS scan

Participants will need to attend dedicated sessions for MRI. The 3T-MRI scanner is based at the RHC Glasgow. Whilst some participants will be able to have the scan on the same day when they are attending the diabetes clinic, it is highly likely they will also need to devote additional time to attend for this. Participants shall be provided with gift vouchers worth £10 per scan visit for this inconvenience and all taxi fares paid for in full from base hospital, or home if no hospital appointment on the day. Base hospital is defined as the local hospital where the patients attends for routine diabetes follow-up.

Participants will be taken through an MRI safety checklist, as per standard MRI practice prior to entering room. The maximum duration of the MRI scan will be one hour, and during this time both microMRI of the tibia and MRS of the lumbar spine will be performed. Participants will be advised to attend for a whole morning or an afternoon so that all the assessments can be performed.

There is a possibility that we might find something unexpected (incidental finding) in the participant's images. If this happens, the child will be referred to the appropriate specialist for further investigation. All MRI scan images will be clinically reviewed by Dr Ruth Allen, Consultant Paediatric Radiologist, solely for this purpose as part of paid research service. Parents are made aware that they may then have to disclose such findings in future applications for health-related insurance.

3.5 Statistical consideration and power calculation

All data will be presented as medians (ranges) if they are not normally distributed. Group differences will be compared by non-parametric tests and Chi-square test for categorical variable. Repeated measures of ANOVA will be used to test the quantitative measurements of bone health, bone marrow adiposity and metabolic status. Multiple logistic regression analysis will be used to adjust for confounding variables.

Intra-operator repeatability of microMRI and MRS is high with an average CoV of 1% and 2.5%, respectively. The primary hypothesis was that children with T1DM would have a lower appBV/TV compared to healthy children. In our previous work in adult T1DM of 30 cases and control and in adults with OI, which is a more severe osteopathy, the estimated coefficient of variation (CoV) for appBV/TV was less than 5%. in our previous work. Based on this a 7.5% difference at $p<0.05$ with a power of 0.8 would require at least 25 subjects in each arm.

4.0 STUDY OUTCOMES

4.1 Primary Outcome

The primary outcome of the study is the quantitative measurements of bone microarchitecture (apparent BV/TV, apparent trabecular thickness, apparent trabecular number and apparent trabecular separation) obtained from microMRI in cases and controls. Additional measures of bone microarchitecture will also be explored including measures of connectivity (branch density, nodal density)

4.2 Secondary Outcome

The secondary outcome measures include:

- Measure of bone marrow adiposity as assessed by MR spectroscopy
- Relationship of markers of bone health (including DXA) to markers of T1DM disease (duration of disease, age of onset, insulin dose, HbA1C and microvascular complications)
- Change in bone and adiposity markers over first year of diagnosis

5.0 DATA MANAGEMENT

Quantitative data will be collected from a variety of sources – blood and urine samples, questionnaire results, imaging including DXA, MRI and MRS. Data quality will be ensured with repeat measurements taken where appropriate to ensure consistency and regular calibration checks on all equipments used. Only one trained DXA and MRI staff respectively will be used to ensure consistency of results. All personal data will be treated as strictly confidential. Each participant will be given a unique study identifier to preserve anonymity of data stored. All study questionnaires will be filed on site in a security-coded office and results data stored on the researcher's university computer which is password protected. Personal data will be stored only until completion of assessments and all data anonymised for analysis. All data will be curated responsibly subjected to the University of Glasgow guidance on managing research records. http://www.gla.ac.uk/services/dpfoioffice/guidanceonresearch/

6.0 STUDY TIMELINE

This study will take 24 months to complete from the point of ethics and R&D approval, with timelines as follows:

Months -6 to 0	Design study protocol
Months -3 to 0	Obtain ethics and R&D approval
Months 0 to 1	Identify suitable participants for established T1DM cases
Months 1-18	Recruit participants, begin assessments and follow-up to completion, with interim analysis at 6 months
Months 16-20	Perform full data analysis
Months 20-24	Prepare final thesis

7.0 FUNDING

This study is funded by Glasgow Hospital Children's Charity, for a one-year full time clinical research fellow with £10,000 for consumables and the Medical Fund of the University of Glasgow for a further £10,000 for consumables. Consumables will include cost of scans, study blood sampling and processing, patient travel and gift vouchers.

The research costs of the proposed study over 2 years are outlined as follows.

<u>Established diabetes study</u> (30 cases and 30 controls)		
- Biochemical markers (@£25) x 30 samples	£ 750	
- Minor consumables (purchase of blood bottles, etc)	£ 200	
- DXA scan (@£50) x 30 scans	£ 1,500	
- MRI scan (@£250) x 60 scans including controls	£15,000	
- MRI review for incidental findings (@£12.50 X 60 scans)	£ 750	
- Patient reimbursement (@20) x 60 visits for MRI	£ 1,200	
Total		£19,400

<u>Newly diagnosed diabetes study</u> (estimated 30 patients)	
- Biochemical markers (@£25) x 90 sample	£ 2,250
- Minor consumables top-up	£ 100
- DXA scan (@£50) x 60 scans	£ 3,000
- MRI scan (@£250) x 60 scans	£15,000
- MRI review for incidental findings (@£12.50 X 60 scans)	£ 750
- Patient reimbursement (@20) x 60 visits for MRI	£ 1,200

Total	£22,300
There will also be NHS support costs for obtaining informed consent from NHS patients as per the AcoRD Cost Attribution Guidance 2012 (@£71.08 x90)	£6,397

Total consumable costs = £48,097

Additional fundings will be sourced for the full cost of the research and applications have been submitted to NovoNordisk UK Research Foundation and the Chief Scientist Office (CSO).

8.0 PROTOCOL AMENDMENTS

Any change in the study protocol will require an amendment. Any proposed protocol amendment will be submitted to a) the Sponsor for approval, b) REC for favourable opinion and c) R&D for acknowledgement. The sponsor will determine whether an amendment is substantial or non-substantial. The chief investigator will sign and file any amended versions of the protocol before this can be implemented.

9.0 REFERENCES

Bouillon R, M Bex, E Van Herck, J Laureys, L Dooms, E Lesaffre, and E Ravussin Influence of age, sex, and insulin on osteoblast function: osteoblast dysfunction in diabetes mellitus. JCEM 1995 80: 1194-202

Bushinsky DA, Wolbach W, Sessler NE, Mogilevsky R, Levi-Setti R. Physiochemical effects of acidosis on bone calcium flux and surface ion composition. J Bone Miner Res 1993;8:93-101

Conover CA, Lee PD, Riggs BL, Powell DR. Insulin-like growth factor-binding protein-1 expression in cultured human bone cells: regulation by insulin and glucocorticoid. Endocrinology 1996;137:3295-3301

Ersoy B, Goksen D, Darcan S, Mavi E, Ozturk C. Evaluation of bone mineral density in children with diabetes mellitus. Indian J Pediatr 1999;66:375-379

Follak N, Kloting I, Wolf E, Merk H. Delayed remodeling in the early period of fracture healing spontaneously diabetic BB/OK rats depending on the diabetic metabolic state. Histol Histopathol 2004;19:473-486

Follak N, Kloting I, Merk H. Influence of diabetic metabolic state on fracture healing in spontaneously diabetic rats. Diabetes Metab Res Rev 2005;21:288-296

Forsen L, Meyer HE, Midthjell K et al. Diabetes mellitus and the incidence of hip fracture: results from the Nord-Trondelag Health Survey. Diabetologica 1999;42:920-5

Frick KK, Jiang L, Bushinsky DA. Acute metabolic acidosis inhibits the induction of osteoblastic egr-1 and type 1 collagen. Am J Physiol 1997;272:1450-1456

Gunczler P, Lanes R, Paz-Martinez V et al. Decreased lumbar spine bone mass and low bone turnover in children and adolescents with IDDM followed longitudinally J Pediatr Endocrinol Metab 1998;11:413-419

Gunczler P, Lanes R, Paoli M, et al. Decreased Bone Mineral Density and Bone Formation Markers shortly after Diagnosis of Clinical Type 1 DM
J Pediatr Endocrinol Metab 2001;14:525-528

Janghorbani M, Van Dam RM, Willett WC, Hu FB. Systematic review of Type 1 and Type 2 Diabetes Mellitus and Risk of Fracture. Am J Epidemiol 2007;166:495-505

Heap J, Murray MA, Miller SC, Jalili T, Moyer-Mileur LJ. Alterations in bone characteristics associated with glycemic control in adolescents with type 1 diabetes mellitus. J Pediatr 2004;144:56-62

Hickman J, McElduff A. Insulin sensitizes a cultured rat osteogenic sarcoma cell lines to hormones which activate adenylate cyclase. Calcif Tissue Int 1990;46:401-405

Hie M, Iitsuka N, Otsuka T, Tsukamoto I. Insulin-dependent diabetes mellitus decreases osteoblastogenesis associated with the inhibition of Wnt signaling through increased expression of Sost and Dkk1 and inhibition of Akt activation. Int J Mol Med 2011;28:455-462

Krieger NS, Sessler NE, Bushinsky DA. Acidosis inhibits osteoclastic and stimulates osteclastic activity in vitro. Am J Physiol: Renal, Fluid Electrolyte Physiol 1992;31:442-448

Hothersall EJ, Livingstone SJ, Looker HC, Ahmed SF, Cleland S, Leese GP, Lindsay RS,McKnight J, Pearson D, Philip S, Wild SH, Colhoun HM. Contemporary risk of Hip fracture in Type 1 and Type 2 Diabetes: a national registry study from Scotland. J Bone Miner Res 2013 (Epub doi 10.1002/jbmr 2118)

Lappin DF, Eapen B, Robertson D, Young J, Hodge PJ. Markers of bone destruction and formation and periodontitis in Type 1 Diabetes Mellitus. J Clin Periodontol 2009;36:634-41

Lu H, Krant D, Gerstenfeld LC, Graves DT. Diabetes interferes with the bone formation by affecting the expression of transcription factors that regulate osteoblast differentiation. Endocrinology 2003;144:346-352

McComb C, Harpur A, Yacoubian, Leddy C, Anderson G, Shepherd S, Perry C, Shaikh MG, Foster J, Ahmed SF. Clin Endo 2013 (Epub doi 10 10.1111/cen 12367)

McNair P, Madsbad S, Christiansen C, Faber OK, Transbol I, Binder C. Osteopenia in insulin treated diabetes mellitus. Diabetologica 1978;15:87-90

Nicodemus KK, Folsom AR. Type 1 and Type 2 diabetes and incidence of hip fractures in postmenopausal women. Diabetes Care 2001;24:1192-1197

Pater A, Sypniewska G, Pilecki O. Biochemical Markers of Bone Cell Activity in Children with T1DM. J Pediatr Endocrinol Metab 2010;23:81-86

Rico H, Hernandez ER, Cabranes JA, Gomez-Castresana F. Suggestions of the deficient osteoblastic function in diabetes mellitus: the possible cause of osteopenia in diabetes. Calcif Tissue Int. 1989;45:71-73

Rosen CJ and Bouxsein ML. Mechanisms of Disease: is osteoporosis the obesity of bone? Nature Clinical Practice of Rheumatology. 2006;2:35-43

Topaloglu AK, Yildizdas D, Yilmaz HL, Mungan NO, Yuksel B, Ozer G. Bone calcium changes during diabetic ketoacidosis: A comparison with lactic acidosis due to volume depletion. Bone 2005;37:122-127

Valerio G, Esposito-del Puente A, Buono P, Mozzillo E, Franzese A. The lumbar bone mineral density is affected by long-term poor metabolic control in adolescents with Type 1 diabetes mellitus. Horm Res 2002;58:266-272

Verhaeghe J, Van Herck E, Visser WJ, Suiker AMH, Thomasset M, Einhorn TA, Faierman E, Bouillon R. Bone and mineral metabolism in BB rats with long term diabetes: decreased bone turnover and osteoporosis. Diabetes 1990;39:477-482

Vestergaard P. Discrepancies in bone mineral density and fracture risk in patients with type 1 and type 2 diabetes- a meta-analysis. Osteoporos Int 2007;18:427-444

Ward DT, Yau SK, Mee AP, Mawer EB, Miller CA, Garland HO, Riccardi D. Functional, molecular and biochemical characterization of strepzotocin-induced diabetes. J Am Soc Nephrol 2001;12:779-790

Wergedal JE, Baylink DJ. Characterization of cells isolated and cultured from human bone. Proc Soc Exp Biol Med 1984;176:60-69

Appendix B

ESTABLISHED DIABETES STUDY

Case Report Form

Study number:

Information Sheet given: Yes / No

Date of consent:

GP Letter sent: Yes / No

Visit 1

Date of Visit 1:

Demographic and anthropometric data:

Patient initials	**Sex:**	**Date of birth**	**Height=**
Tel number:	**Female** ☐	**Age in year**	**Weight=**
	Male ☐		

Details of diabetes:

Age at diagnosis:

Disease duration:

Severity at presentation:

Walking wounded	**DKA**

H+ **Bic** **Lab glucose** **%dehydration** **HbA1c**

Total insulin dose:

Pump or injection:

Current HbA1c:

Available HbA1C results in the 2 years:

Date	HbA1C (mmol/mol)

Average HbA1C in the last 2 years:
Average HbA1C in the last year:

Category of HbA1C control:

Good (<59)	Moderate (59-75)	Poor (>75)

Health behaviour and diet

How often do you eat dairy products? (please circle one)

Never	Once a week	2-3times a week	More than 3 times a week

Calcium (mg/day):

Vitamin D (IU/day):

Multivitamin use:

Smoking: (please circle one)

Current	(number/day)	Past	Never

Physical activity (hrs/week): see Physical Activity Questionaire **Completed:**

Appendix B

Medical/Surgical History

Patient History (inc Birth Hx)	**Diabetes complications**
Gestation: **Birth weight:** **PMHx:** **Med Hx:** **Previous surgery:** **Orthopaedic:** **Joint problems** **Fracture history:** Number Location Age	**Previous DKAs (details)** 1. 2. 3. **Thyroid disorder:** Last TFT at ……/ ……/…… Result **Renal complication (Microalbuminuria):** Date ……/……/…… Result **Retinopathy:** Last follow up at ……/……/…… Result **Neuropathy:** **……**
	Family History **Family history of T1DM:** **Family history of osteoporosis:** **Family history of fracture:**

Reproductive history and examination

Onset of puberty (years): **Menarche (years):** **Puberty status:**

Appendix B

Blood Investigations:

Blood tests	Date done	Date processed	Results
HbA1C			
C-peptide			
25VitD			
PTH			
B-ALP			
Osteocalcin			
CTX			
IGF1			
Leptin			
Adiponectin			
Others:			

Storage inform: _____

DXA	Date	Notes
Total body (TB)		
Femoral neck (FN)		
Lumbar spine (LS)		

Visit 2 (Within 6 weeks of Visit 1)

Date of Visit 2:

Taxi organised:

PICU informed: Yes / No

CRF nurses organisation- CM/RW informed : Yes / No

Radiological Investigation:

MRI/MRS		
Proximal tibia		
Abdominal fat		
Lumbar spine		

Study Completed

Appendix C

BONE HEALTH IN DIABETES STUDY

Case Report Form (CONTROL)

Study number:

Information Sheet given: Yes / No

Date of consent:

Visit 1

Date of Visit 1:

Demographic and anthropometric data:

Patient initials	**Sex:**	**Date of birth**	**Height=**
	Female ☐		**Weight=**
Tel number:		**Age in year**	
	Male ☐		

Health behaviour and diet

How often do you eat dairy products? (please circle one)

Never	Once a week	2-3times a week	More than 3 times a week

Calcium (mg/day):

Vitamin D (IU/day):

Multivitamin use:

Smoking: (please circle one)

Current	(number/day)	Past	Never

Physical activity (hrs/week): see Physical Activity Questionaire

Appendix C

Medical/Surgical History

Patient History (inc Birth Hx)	**Clinical Examination**
Gestation: **Birth weight:** **Past Medical History:** **Orthopaedic:** **Joint problems** **Fracture history:** Number Location Age	**Family History** **Family history of T1DM:** **Family history of osteoporosis:** **Family history of fracture:**

Reproductive history and examination

Onset of puberty (years): **Menarche (years):** **Pubertal status:**

Radiological Investigation:

MRI/MRS	Date	Notes
Proximal tibia		
Abdominal fat		
Lumbar spine		

Study Completed

Appendix D

For advice on this study
Dr S Ching Chen
Royal Hospital for Children
Glasgow
Tel 0141 201 0709

For independent advice
Dr Martina Rodie
Royal Hospital for Children
Glasgow
Tel 0141 201 0236

ESTABLISHED DIABETES STUDY

STUDY OF BONE HEALTH IN CHILDREN WITH ESTABLISHED TYPE 1 DIABETES MELLITUS (T1DM)

Consent Form – Case

Study Number:……

Participant's Name (Block Capitals):……

Please initial boxes

1.	I confirm that I have read and understood the Study Information Sheet for Participant/Parent/Legal Guardian (Case) (Version 3, 16/06/14). I have had the opportunity to consider the information, ask questions and had these questions answered to my satisfaction	☐
2.	I understand that my child's participation is voluntary and that I am free to withdraw at any time, without giving a reason, without my child's medical care or legal rights being affected	☐
3.	I understand that my child's GP will be informed that I/he/she am/is participating in this study	☐
4.	I allow access for the research team and sponsor representatives to my child's medical records and patient identifiable information	☐
5.	I understand that if anything unexpected is demonstrated on my child's scan, I/he/she will be referred to the appropriate specialist for further investigation	☐
6.	I agree for my child to take part in this study	☐

Name of Participant/Parent/Guardian: ……

Signature of Participant/Parent/Guardian: …… Date:……

Signature of Researcher:…… Date:……

Appendix D

For advice on this study
Dr S Ching Chen
Royal Hospital for Sick Children
Yorkhill, Glasgow
Tel 0141 201 0709

For independent advice
Dr Martina Rodie
Royal Hospital for Sick Children
Yorkhill, Glasgow
Tel 0141 201 0236

ESTABLISHED DIABETES STUDY

STUDY OF BONE HEALTH IN CHILDREN WITH ESTABLISHED TYPE 1 DIABETES MELLITUS (T1DM)

Assent Form – Case

Study Number:……

Participant's Name (Block Capitals): ……..

Please initial boxes

1.	I confirm that I have read and understood the Study Information Sheet for Participant (Case) (Version 3, 16/06/14)	☐
2.	I have had the time to think about this and ask questions	☐
3.	I understand that I do not have to take part if I do not want to	☐
4.	I agree to take part in this study	☐

Signature of Participant: …….. Date:……..

Signature of Researcher:…….. Date:……

Appendix E

For advice on this study
Dr S Ching Chen
Royal Hospital for Children
Glasgow
Tel 0141 201 0709

For independent advice
Dr Martina Rodie
Royal Hospital for Children
Glasgow
Tel 0141 201 0236

ESTABLISHED DIABETES STUDY

STUDY OF BONE HEALTH IN CHILDREN WITH ESTABLISHED TYPE 1 DIABETES MELLITUS (T1DM)

Consent Form for Parent/Legal Guardian – Control

Study Number:……

Name of Participant (Block Capitals):……..

Please initial boxes

1.	I confirm that I have read and understood the Information Sheet for Parent/Legal Guardian (Control) dated 10/12/14 (Version 4) for the above study. I have had the opportunity to consider the information, ask questions and had these questions answered to my satisfaction	☐
2.	I understand that my child's participation is voluntary and that I am free to withdraw at any time, without giving a reason, without my child's medical care or legal rights being affected	☐
3.	I understand that my child's GP will be informed that he/she is participating in this study	☐
4.	I understand that if anything unexpected is demonstrated on my child's scan, he/she will be referred to the appropriate specialist for further investigation	☐
5.	I agree for my child to take part in this study	☐

Name of Parent/Guardian: …….. Date:…….. Signature: ……

Name of Researcher:…… Date: …….. Signature: ……

Appendix E

For advice on this study
Dr S Ching Chen
Royal Hospital for Children
Glasgow
Tel 0141 201 0709

For independent advice
Dr Martina Rodie
Royal Hospital for Children
Glasgow
Tel 0141 201 0236

University of Glasgow
NHS Greater Glasgow and Clyde

ESTABLISHED DIABETES STUDY

STUDY OF BONE HEALTH IN CHILDREN WITH ESTABLISHED TYPE 1 DIABETES MELLITUS (T1DM)

Consent Form for Young Person – Control

Study Number:……

Please initial boxes

1.	I confirm that I have read and understood the Information Sheet for Participant (Control) dated 10/12/14 (Version 4) for the above study	☐
2.	I have had a chance to discuss this study and ask questions	☐
3.	I have received satisfactory answers to all of my questions	☐
4.	I have received enough information about the study	☐
5.	I understand that my participation is voluntary and I am free to withdraw at any time, without giving any reason, without my medical care or legal rights being affected	☐
6.	I understand that sections of my medical notes may be looked at by the research team where it is relevant to my taking part in the research. I give my permission for the research team to have access to my records	☐
7.	I agree to take part in the above study	☐

Name of Participant: …… Date: …… Signature: ……

Name of Parent/Guardian: …… Date:…… Signature: ……

Name of Researcher:…… Date: …… Signature: ……

Appendix E

For advice on this study
Dr S Ching Chen
Royal Hospital for Children
Glasgow
Tel 0141 201 0709

For independent advice
Dr Martina Rodie
Royal Hospital for Children
Glasgow
Tel 0141 201 0236

University of Glasgow
NHS Greater Glasgow and Clyde

ESTABLISHED DIABETES STUDY

STUDY OF BONE HEALTH IN CHILDREN WITH ESTABLISHED TYPE 1 DIABETES MELLITUS (T1DM)

Assent Form for Young Person – Control

Study Number:……

Please circle your answers:

Have you read (or had read to you) about this project?	Yes / No
Has somebody else explained this project to you?	Yes / No
Do you understand what this project is about?	Yes / No
Have you asked all the questions you want?	Yes / No
Have your questions been answered in a way that you understand?	Yes / No
Do you understand that it's OK to stop taking part at any time?	Yes / No
Are you happy to take part?	Yes / No

If <u>any</u> answers are 'no' or you don't want to take part, don't sign your name!

If you <u>do</u> want to take part, you can sign your name below

Your name _____

Signature _____

Date _____

The doctor who explained this project to you needs to sign too:

Print Name _____

Signature _____

Date _____

Thank you for your help

(To be completed by the child and their parent/guardian)

Appendix F

Physical Activity Questionnaire (<14 years old)

Name:_____ Age:_____

Sex: M_____ F_____ Grade:_____

We are trying to find out about your level of physical activity from ***the last 7 days*** (in the last week). This includes sports or dance that make you sweat or make your legs feel tired, or games that make you breathe hard, like tag, skipping, running, climbing, and others.

Remember:
1. There are no right and wrong answers — this is not a test
2. Please answer all the questions as honestly and accurately as you can — this is very important

1. Physical activity in your spare time: Have you done any of the following activities in the past 7 days (last week)? If yes, how many times? (Check only one box per row)

	No	1-2	3-4	5-6	≥7
Aerobics					
Badminton					
Baseball, softball					
Basketball					
Bicycling					
Dance					
Football					
Hockey					
In-line/Ice skating					
Jogging or running					
Rowing/canoeing					
Rugby					
Skateboarding					
Skipping					
Swimming					
Tag					
Volleyball					
Walking for exercise					
Other(s): _____					

2. In the last 7 days, during your physical education (PE) classes, how often were you very active (playing hard, running, jumping)? (Check one only)

- I don't do PE ☐
- Hardly ever ☐
- Sometimes ☐
- Quite often ☐
- Always ☐

3. In the last 7 days, what did you do most of the time at recess? (Check one only)

- Sat down (talking, reading, doing schoolwork) ☐
- Stood around or walked around ☐
- Ran or played a little bit ☐
- Ran around and played quite a bit ☐
- Ran and played hard most of the time ☐

4. In the last 7 days, what did you normally do at lunch (besides eating lunch)?
(Check one only)

- Sat down (talking, reading, doing schoolwork) ☐
- Stood around or walked around ☐
- Ran or played a little bit ☐
- Ran around and played quite a bit ☐
- Ran and played hard most of the time ☐

5. In the last 7 days, on how many days right after school, did you do sports, dance, or play games in which you were very active?
(Check one only)

- None ☐
- 1 time last week ☐
- 2 or 3 times last week ☐
- 4 or 5 last week ☐
- 6 or 7 times last week ☐

6. In the last 7 days, on how many evenings did you do sports, dance, or play games in which you were very active? (Check one only)

- None ☐
- 1 time last week ☐
- 2 or 3 times last week ☐
- 4 or 5 last week ☐
- 6 or 7 times last week ☐

7. On the last weekend, how many times did you do sports, dance, or play games in which you were very active? (Check one only)

- None ☐
- 1 time ☐
- 2 — 3 times ☐
- 4 — 5 times ☐
- 6 or more times ☐

8. Which one of the following describes you best for the last 7 days?
Read all five statements before deciding on the one answer that describes you.

A. All or most of my free time was spent doing things that involve little physical effort ☐
B. I sometimes (1 — 2 times last week) did physical things in my free time ☐
(e.g. played sports, went running, swimming, bike riding, did aerobics)
C. I often (3 — 4 times last week) did physical things in my free time ☐
D. I quite often (5 — 6 times last week) did physical things in my free time ☐
E. I very often (7 or more times last week) did physical things in my free time ☐

9. Mark how often you did physical activity (like playing sports, games, doing dance, or any other physical activity) for each day last week.

	None	A bit	Medium	Often	Very often
Monday					
Tuesday					
Wednesday					
Thursday					
Friday					
Saturday					
Sunday					

10. Were you sick last week, or did anything prevent you from doing your normal physical activities? (Check one)

Yes
No
If Yes, what prevented you? _____

Physical Activity Questionnaire (14-19 years old)

Name:_____ Age:_____

Sex: M_____ F_____ Grade:_____

We are trying to find out about your level of physical activity from ***the last 7 days*** (in the last week). This includes sports or dance that make you sweat or make your legs feel tired, or games that make you breathe hard, like tag, skipping, running, climbing, and others.

Remember:
1. There are no right and wrong answers — this is not a test
2. Please answer all the questions as honestly and accurately as you can — this is very important

1. Physical activity in your spare time: Have you done any of the following activities in the past 7 days (last week)? If yes, how many times? (Check only one box per row)

	No	1-2	3-4	5-6	≥7
Aerobics					
Badminton					
Baseball, softball					
Basketball					
Bicycling					
Dance					
Football					
Hockey					
In-line/Ice skating					
Jogging or running					
Rowing/canoeing					
Rugby					
Skateboarding					
Skipping					
Swimming					
Tag					
Volleyball					
Walking for exercise					
Other(s):					
_____					
_____					

2. In the last 7 days, during your physical education (PE) classes, how often were you very active (playing hard, running, jumping)?
(Check one only)

- I don't do PE ☐
- Hardly ever ☐
- Sometimes ☐
- Quite often ☐
- Always ☐

3. In the last 7 days, what did you normally do at lunch (besides eating lunch)? (Check one only)

- Sat down (talking, reading, doing schoolwork) ☐
- Stood around or walked around ☐
- Ran or played a little bit ☐
- Ran around and played quite a bit ☐
- Ran and played hard most of the time ☐

4. In the last 7 days, on how many days right after school, did you do sports, dance, or play games in which you were very active? (Check one only)

- None ☐
- 1 time last week ☐
- 2 or 3 times last week ☐
- 4 or 5 last week ☐
- 6 or 7 times last week ☐

5. In the last 7 days, on how many evenings did you do sports, dance, or play games in which you were very active? (Check one only)

- None ☐
- 1 time last week ☐
- 2 or 3 times last week ☐
- 4 or 5 last week ☐
- 6 or 7 times last week ☐

6. On the last weekend, how many times did you do sports, dance, or play games in which you were very active? (Check one only)

- None ☐
- 1 time ☐
- 2 — 3 times ☐
- 4 — 5 times ☐
- 6 or more times ☐

7. Which one of the following describes you best for the last 7 days?
Read all five statements before deciding on the one answer that describes you.

A. All or most of my free time was spent doing things that involve little physical effort ☐
B. I sometimes (1 — 2 times last week) did physical things in my free time ☐
(e.g. played sports, went running, swimming, bike riding, did aerobics)
C. I often (3 — 4 times last week) did physical things in my free time ☐
D. I quite often (5 — 6 times last week) did physical things in my free time ☐
E. I very often (7 or more times last week) did physical things in my free time ☐

8. Mark how often you did physical activity (like playing sports, games, doing dance, or any other physical activity) for each day last week.

	None	A bit	Medium	Often	Very often
Monday					
Tuesday					
Wednesday					
Thursday					
Friday					
Saturday					
Sunday					

9. Were you sick last week, or did anything prevent you from doing your normal physical activities? (Check one.)

Yes
No
If Yes, what prevented you? _____

Molecular and Cellular Endocrinology 440 (2017) 57–68

Contents lists available at ScienceDirect

Molecular and Cellular Endocrinology

journal homepage: www.elsevier.com/locate/mce

Metformin suppresses adipogenesis through both AMP-activated protein kinase (AMPK)-dependent and AMPK-independent mechanisms

Suet Ching Chen [a, b], Rebecca Brooks [a], Jessica Houskeeper [b], Shaun K. Bremner [b], Julia Dunlop [b], Benoit Viollet [d], Pamela J. Logan [c], Ian P. Salt [c], S. Faisal Ahmed [a], Stephen J. Yarwood [e, *]

[a] The Developmental Endocrinology Research Group, School of Medicine, University of Glasgow, Glasgow G51 4TF, UK
[b] Institute of Molecular, Cell and Systems Biology, University Avenue, University of Glasgow, Glasgow G12 8QQ, UK
[c] Institute of Cardiovascular and Medical Sciences, University Avenue, University of Glasgow, Glasgow G12 8QQ, UK
[d] INSERM, U1016, Institut Cochin, Paris, France, CNRS, UMR8104, Paris, France, Université Paris Descartes, Sorbonne Paris Cité, France
[e] Institute of Biological Chemistry, Biophysics and Bioengineering, Edinburgh Campus, Heriot-Watt University, Edinburgh EH14 4AS, UK

ARTICLE INFO

Article history:
Received 12 April 2016
Received in revised form
11 November 2016
Accepted 12 November 2016
Available online 14 November 2016

Keywords:
Adipogenesis
Osteogenesis
Metformin
Diabetes
AMPK
Mesenchymal stem cells

ABSTRACT

People with Type 2 diabetes mellitus (T2DM) have reduced bone mineral density and an increased risk of fractures due to altered mesenchymal stem cell (MSC) differentiation in the bone marrow. This leads to a shift in the balance of differentiation away from bone formation (osteogenesis) in favour of fat cell development (adipogenesis). The commonly used anti-diabetic drug, metformin, activates the osteogenic transcription factor Runt-related transcription factor 2 (Runx2), which may suppress adipogenesis, leading to improved bone health. Here we investigate the involvement of the metabolic enzyme, AMP-activated protein kinase (AMPK), in these protective actions of metformin. The anti-adipogenic actions of metformin were observed in multipotent C3H10T1/2 MSCs, in which metformin exerted reciprocal control over the activities of Runx2 and the adipogenic transcription factor, PPARγ, leading to suppression of adipogenesis. These effects appeared to be independent of AMPK activation but rather through the suppression of the mTOR/$p70^{S6K}$ signalling pathway. Basal AMPK and mTOR/$p70^{S6K}$ activity did appear to be required for adipogenesis, as demonstrated by the use of the AMPK inhibitor, compound C. This observation was further supported by using AMPK knockout mouse embryo fibroblasts (MEFs) where adipogenesis, as assessed by reduced lipid accumulation and expression of the adipogeneic transcription factor, C/EBPβ, was found to display an absolute requirement for AMPK. Further activation of AMPK in wild type MEFS, with either metformin or the AMPK-specific activator, A769662, was also associated with suppression of adipogenesis. It appears, therefore, that basal AMPK activity is required for adipogenesis and that metformin can inhibit adipogenesis through AMPK-dependent or -independent mechanisms, depending on the cellular context.

1. Introduction

Type 2 diabetes mellitus (T2DM) is characterized by chronic elevation of blood glucose levels because of systemic insulin resistance. In addition to the reduction of insulin sensitivity in muscle, adipose tissue and the liver, it has been noted recently that people with diabetes have increased risk of bone fractures (Janghorbani et al., 2007,Kilpadi et al., 2014,Hothersall et al., 2013). Furthermore, the use of the thiazolidinedione (TZD) antidiabetic drug class, which includes pioglitazone and rosiglitazone, has been shown to increase the risk of bone fractures and secondary osteoporosis (Lecka-Czernik, 2009,Grey et al., 2007,Schwartz et al., 2006).

TZDs act as agonists for the nuclear receptor peroxisome proliferator-activated receptor gamma (PPARγ) which is considered to be the master regulator of fat cell development (adipogenesis) (Tontonoz et al., 1994a). It is therefore thought that the detrimental

* Corresponding author. Rm 3William Perkin Building, Institute of Biological Chemistry, Biophysics and Bioengineering, Edinburgh Campus, Heriot-Watt University, Edinburgh EH14 4AS UK.
E-mail address: S.Yarwood@hw.ac.uk (S.J. Yarwood).

http://dx.doi.org/10.1016/j.mce.2016.11.011

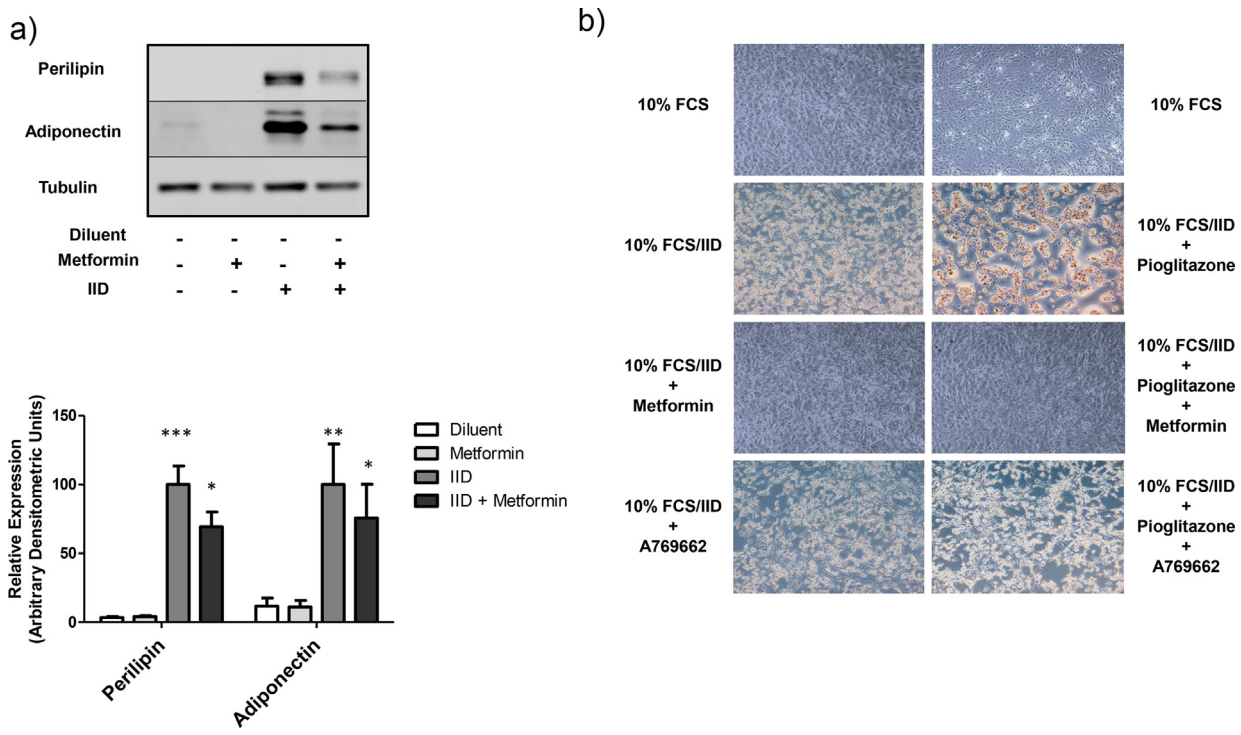

Fig. 1. Metformin and the AMPK-activator, A769662, suppress adipogenesis of CH3H10T1/2 MSCs.
A) Confluent CH3H10T1/2 MSCs were induced to differentiate by addition 10% foetal calf serum (FCS) in the presence or absence of adipogenic IID medium (insulin, isobutylmethylxanthine and dexamethasone) and/or 10 μM pioglitazone (PIO), 500 μM metformin or 100 μM A769662. After 5 days cells were fixed with formalin and stained with Oil Red O to detect neutral lipid accumulation. Representative micrographs from an experiment carried out on three separate occasions with similar results are shown.
B) Confluent CH3H10T1/2 MSCs were induced to differentiate by addition 10% FCS in the presence or absence of IID medium and/or 500 μM metformin. Cell extracts were then prepared after 5 days and immunoblotted with antibodies to perilipin, adiponectin and tubulin. Representative immunoblots from an experiment carried out on three separate occasions with similar results are shown. Densitometric analysis of three immunoblots are shown as means ± SEM in the *lower panel*. Significant increases relative to control are indicated, $^{*}p < 0.05$ and ***, $p < 0.001$.

effects of TZDs on bone health is through the activation of PPARγ in mesenchymal stem cells (MSCs) causing adipogenesis and, consequently, suppressing bone development (osteogenesis) (Lecka-Czernik et al., 2007,Shockley et al., 2009). Adipogenesis is regulated by a temporally induced cascade involving PPARγ and members of the CCAAT/enhancer binding protein (C/EBP) transcription factor family. In the initial stages of adipogenesis there is a transient accumulation of C/EBPβ and C/EBPδ proteins, leading to a later accumulation of C/EBPα and PPARγ (Cao et al., 1991,Yeh et al., 1995). C/EBPα and PPARγ then promote gene expression characteristic of an adipocyte phenotype and their expression remains elevated for the life of the differentiated cell (Tontonoz et al., 1994b).

Metformin has been used clinically for the treatment of T2DM since the 1960s and it is thought to function primarily through the inhibition of hepatic gluconeogenesis (Cusi et al., 1996). Metformin interferes with oxidative phosphorylation in the mitochondria by inhibiting complex I in the electron transport chain, although the exact mechanism of inhibition is not yet known (El-Mir et al., 2000,Lantier et al., 2014). Metformin has also been shown to stimulate osteogenic differentiation of MSCs towards osteoblasts *in vitro* through the trans-activation of Runt-related transcription factor 2 (Runx2), the key regulatory transcription factor for osteogenic differentiation (Jang et al., 2011) and, unlike TZDs, has been shown to be associated with a reduced risk of fractures. Osteoblast differentiation has been proposed to be dependent on the cellular energy sensor AMP-activated protein kinase (AMPK), as the expression of various osteogenic genes has been shown to be inhibited by compound C, a chemical inhibitor of AMPK, and a dominant negative form of AMPK (Banerjee et al., 1997). Furthermore, metformin stimulates AMPK activation through the inhibition of oxidative phosphorylation in hepatocytes (Zhou et al., 2001).

AMPK is a heterotrimeric serine/threonine protein kinase that acts as a cellular energy sensor due to its ability to be activated by an increase in the AMP-ATP ratio, which leads to phosphorylation of Thr172 on AMPKα by liver kinase B1 (LKB1) (Hardie, 2015,Woods et al., 2003). AMPK can also be phosphorylated and activated at Thr172 by calcium/calmodulin-dependent protein kinase kinase (CaMKK) in a Ca^{2+}-dependent, AMP-independent manner (Hawley et al., 2005). AMPK functions to inhibit ATP consuming pathways and at the same time activate catabolic pathways to re-establish cellular energy homeostasis. It has also been shown that AMPK has an array of non-metabolic functions including promotion of nitric oxide synthesis and numerous anti-inflammatory actions (Jones et al., 2005,Reihill et al., 2007,Salminen et al., 2011,Morrow et al., 2003, Salt and Palmer, 2012). Recently, it has been shown that AMPK functions in cell differentiation by promoting osteogenic differentiation while suppressing adipogenic differentiation (Kanazawa et al., 2008,Vila-Bedmar et al., 2010), however, the role of AMPK in cell commitment to differentiation remains unclear. Therefore, the main aim of the current study is to determine the effect of metformin on adipogenesis and, in particular, to understand the role of the AMPK signalling pathway in these processes.

2. Materials and methods

2.1. Cell culture and induction of differentiation

AMPK α1/α2 knockout mouse embryonic fibroblasts (MEFs), C3H10T1/2 mouse mesenchymal stem cells (Clone 9; ATCC CCL-

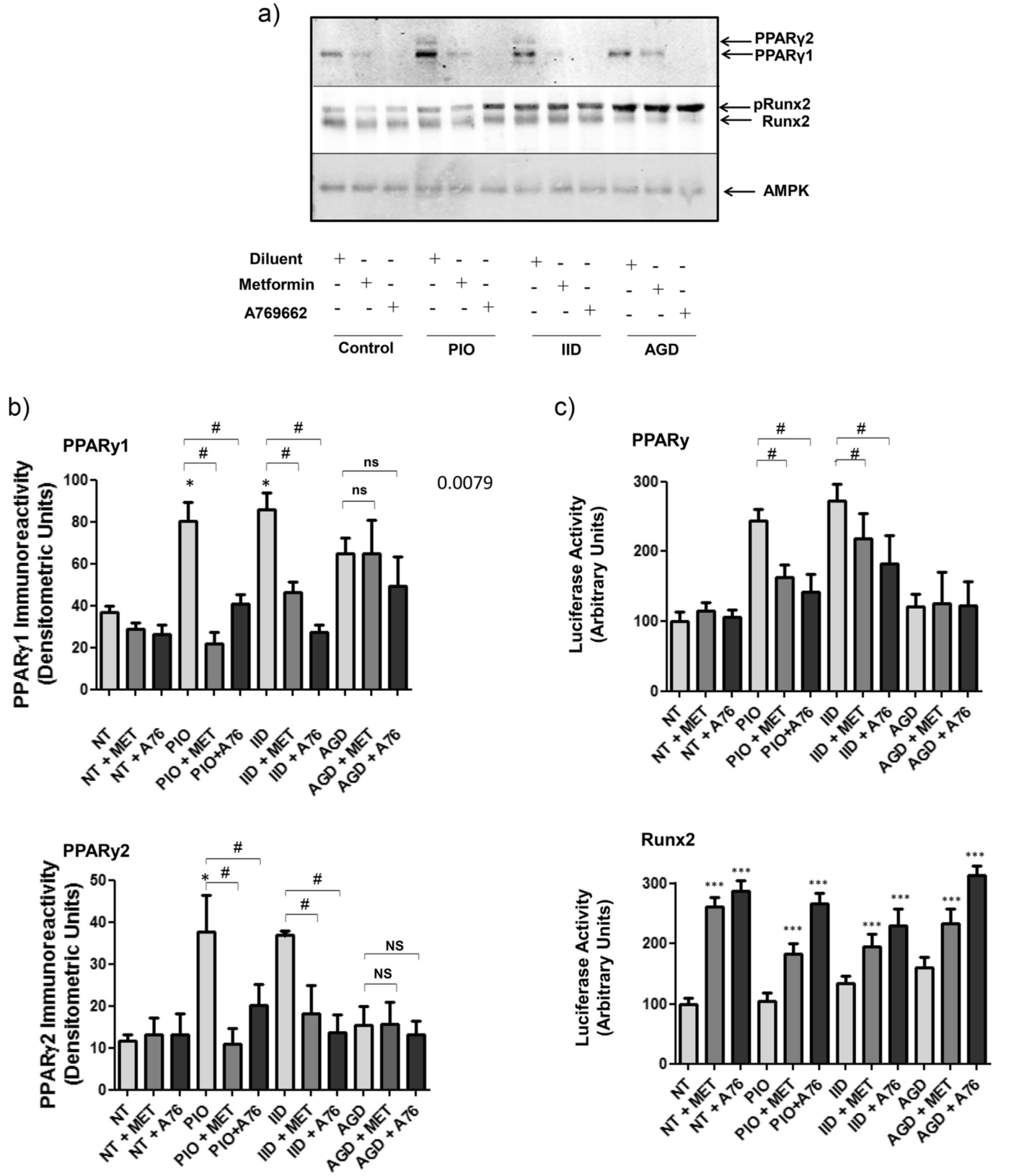

Fig. 2. Effects of Metformin and the AMPK-activator, A769662, on early markers of differentiation in C3H10T1/2 cells.

A) Confluent CH3H10T1/2 cells were stimulated for 5 days with 10 μM pioglitazone (PIO) or an adipogenic (IID) or osteogenic (AGD) cocktail, in the presence or absence of 500 μM metformin or 100 μM A769662. Cell extracts were then prepared and immunoblotted with antibodies to PPARγ, Runx2 and AMPK. The phosphorylation-dependent electrophoretic mobility shift of Runx2 induced by AGD treatment is indicated (pRunx2). Representative immunoblots from an experiment carried out on three separate occasions with similar results are shown.

B) Densitometric analysis of PPARγ1 (*upper panel*) and PPARγ2 (*lower panel*) levels relative to Runx2 are shown as means ± SEM. Significant increases (*, $p < 0.05$) relative to control, and significant decreases relative to PIO-stimulated cells (#, $p < 0.05$), are indicated (n = 3). Non-significant changes are also indicated (ns).

C) Confluent C3H10T1/2 cells were transfected with a PPARγ (*upper panel*) and Runx2 (*lower panel*) luciferase gene reporter constructs, together with control *Renilla* luciferase vector, and then stimulated for two days with 500 μM metformin or 100 μM A769662, in the presence or absence of 10 μM pioglitazone (PIO), adipogenic medium (IID) or osteogenic medium (AGD). Cell extracts were then prepared and luciferase activities were measured using a dual luciferase reporter assay. Luciferase activities from three separate experiments are shown as means ± SEM. Significant increases in luciferase activity are indicated; *, $p < 0.05$, **, $p < 0.01$ and ***, $p < 0.001$, as are significant decreases in activity, #, $p < 0.05$ (n = 3). Non significance is also indicated (ns).

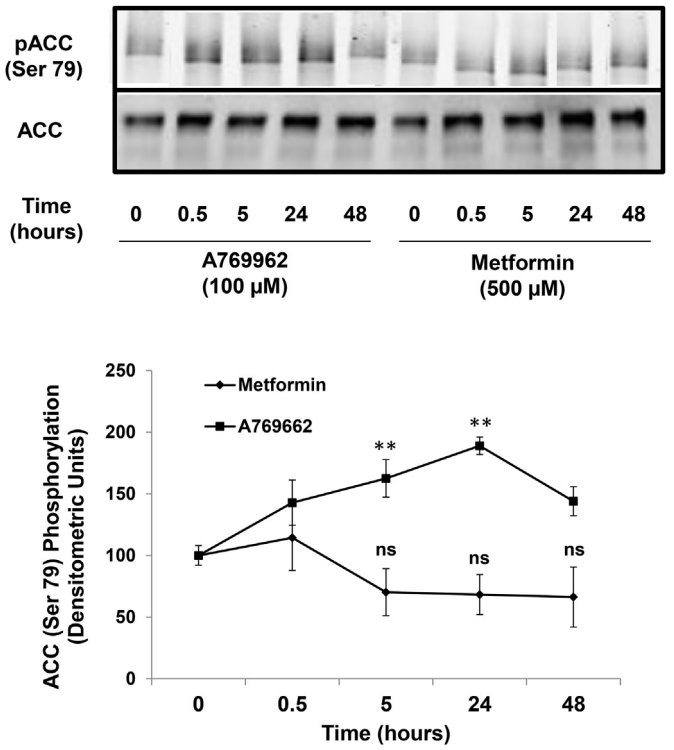

Fig. 3. The AMPK activator, A769662, but not metformin activates AMPK in C3H10T1/2 cells.
Confluent C3H10T1/2 cells were stimulated for the indicated times with 100 μM A769662 or 500 μM metformin. Cell extracts were then prepared and immunoblotted with antibodies towards the phosphorylated form of the AMPK substrate, ACC, or total ACC, as indicated in the *upper panel*. Densitometric values were obtained from immunoblots from three separate experiments and are shown as means ± SEM in the line graph in the *lower panel*. Significant increases in pACC are indicated; **, $p < 0.01$ ($n = 3$). Non significance is also indicated (ns).

226) and 3T3-L1 preadipocytes were maintained in DMEM (41965–039, Sigma-Aldrich Ltd, Gillingham, Dorset, UK) containing 10% (v/v) FCS, 2 mM glutamine, 100 U/mL penicillin and 100 μg/ml streptomycin. To promote adipogenic differentiation, cells were cultured in the standard media supplemented with either 10 μM pioglitazone alone or in combination with 100 nM insulin, 500 μM 3-isobutyl-1-methylxanthine (IBMX) and 10 μM dexamethasone (IID medium). For osteogenic differentiation, cells were cultured in standard media supplemented with 284 μmol/L ascorbic acid, 10 mM β-glycerophosphate and 10 nM dexamethasone (AGD medium). Differentiation media was changed every 3 days.

2.2. Preparation of cell extracts

For the preparation of cell extracts from MEFs, the media was aspirated and then cells were washed with ice cold PBS (137 mM NaCl, 2.7 mM KCl, 10 mM Na_2HPO_4, 1.8 mM KH_2PO_4) and then either 100 μl of ice cold Triton-X100 lysis buffer (50 mM Tris-HCl pH 7.4, 50 mM NaF, 1 mM $Na_4P_2O_7$, 1 mM EDTA, 1 mM EGTA, 250 mM mannitol, 1% (v/v) triton X-100, 0.1 mM phenylmethanesulphonylfluoride (PMSF), 0.1 mM benzamidine, 5 μg/ml soybean trypsin inhibitor, 1 mM dithiothreitol (DTT), 1 mM Na_3VO_4) or 1× Laemmli-sample buffer (50 mM Tris-HCl pH 6.8, 2% (w/v) SDS, 10% (v/v) glycerol, 0.1% (w/v) bromophenol blue, 50 mM DTT) was added and then cells were harvested by scraping. Lysates exracted with Triton-X100 were cleared by centrifugation (24 100 × *g*, for 5 min at 4 °C) and the supernatant stored at −20 °C. Samples lysed using 1× Laemmli-sample buffer were incubated in a sonicating water bath at 60 °C for 30 min prior to storage at −20 °C. C3H10T1/2 MSCs were harvested and nuclear extracts prepared using the Nuclear Extraction kit from Active Motif, Belgium. Briefly, the media was aspirated and cells were harvested in ice-cold PBS containing phosphatase inhibitors and centrifuged (200 × *g*, for 5 min at 4 °C) to obtain a cell pellet. The cell pellet was re-suspended in complete lysis buffer containing 10 mM DTT and phosphatase inhibitor cocktail and then centrifuged (14 000 × *g*, for 10 min at 4 °C) to obtain nuclear and supernatant fractions.

2.3. Western blotting

Protein samples were separated by SDS-PAGE and then transferred electrophoretically onto nitrocellulose membranes. Membranes were blocked with 5% (w/v) Marvel milk powder in TBS (20 mM Tris-HCl pH 7.5, 150 mM NaCl) for 1 h. Membranes were then incubated with primary antibodies overnight at 4 °C. Following washes with TBST (TBS supplemented with 0.5% (v/v) Tween-20), membranes were incubated with secondary antibodies for 1 h at room temperature. Antibodies were diluted to the required concentration in 50% (v/v) Sea Block (Thermo Scientific) and 50% (v/v) TBST. The primary antibodies included those purchased from Cell Signalling Technologies (CST), Danvers, MA and included perilipin, peroxisome proliferator-activated receptor gamma (PPARγ; marker for adipogenesis), Runt-related transcription factor 2 (Runx2; marker for osteogenesis), phosphorylated-ACC (P-ACC (Ser79); marker for AMPK activity), phosphorylated AMPKα (P- AMPKα (Thr172); detects active AMPK) and phosphorylated-$p70^{S6K}$ (P-$p70^{S6K}$ (Thr389); upstream regulator of mTOR signalling). The rabbit polyclonal adiponectin antibody was generated in house and the tubulin antibody was bought from Abcam, Cambridge, UK. Antibodies were detected using a LI-COR® Odyssey Infrared Imaging systems and densitometric analysis was carried out using ImageJ software (National Institute of Health, UK) software Version 1.47.

2.4. Oil Red O staining

Cells were incubated with adipogenic IID media in the presence or absence of either 10 μM pioglitazone, 500 μM metformin, 100 μM of the AMPK-activator, A769662, or 10 μM of the $p70^{S6K}$-inhibitor, rapamycin. Following differentiation, media was aspirated and cells were fixed to cell culture plates with 10% (v/v) neutral buffered formalin for 30 min. The formalin was then aspirated and staining was carried out with the addition of 0.3% (w/v) Oil Red O in isopropanol:water (60:40) for 5 min in room temperature. The Oil Red O was then aspirated and wells washed with distilled water four times. Imaging was carried out using a Zeiss Axiovert 25 microscope with QImaging camera and supporting software.

2.5. AMPK activity assays

AMPK activity was determined in AMPK α1 plus AMPK α2 immuno-complexes through phosphorylation of the peptide HMRSAMSGLHLVKRR [SAMS], as previously described (Morrow et al., 2003). Briefly, the AMPK immunoprecipitates were re-suspended in 20 μl of HEPES Brij-35 buffer. Reaction mixtures (20 μl) containing 5 μl of HEPES Brij-35 buffer, 5 μl of 1 mM SAMS peptide in HEPES Brij-35 buffer, 5 μl of 1 mM AMP in HEPES Brij- 35 buffer and 5 μl of immunoprecipitate re-suspended in HEPES Brij-35 buffer, were prepared in 1.5 ml microcentrifuge tubes on ice and the reaction initiated by the addition of 5 μl of MgATP solution (1 mM [γ-^{32}P] ATP, 250–500 c.p.m./pmol; 25 mM MgCl2 in HEPES Brij-35 buffer). Reaction mixtures were then incubated on a vibrating platform in an air incubator at 30 °C for 10 min. Assay mixtures (15 μl) were spotted onto P81 phosphocellulose paper, and rinsed, with gentle stirring to remove free ATP, for 5 min in 1% (v/v)

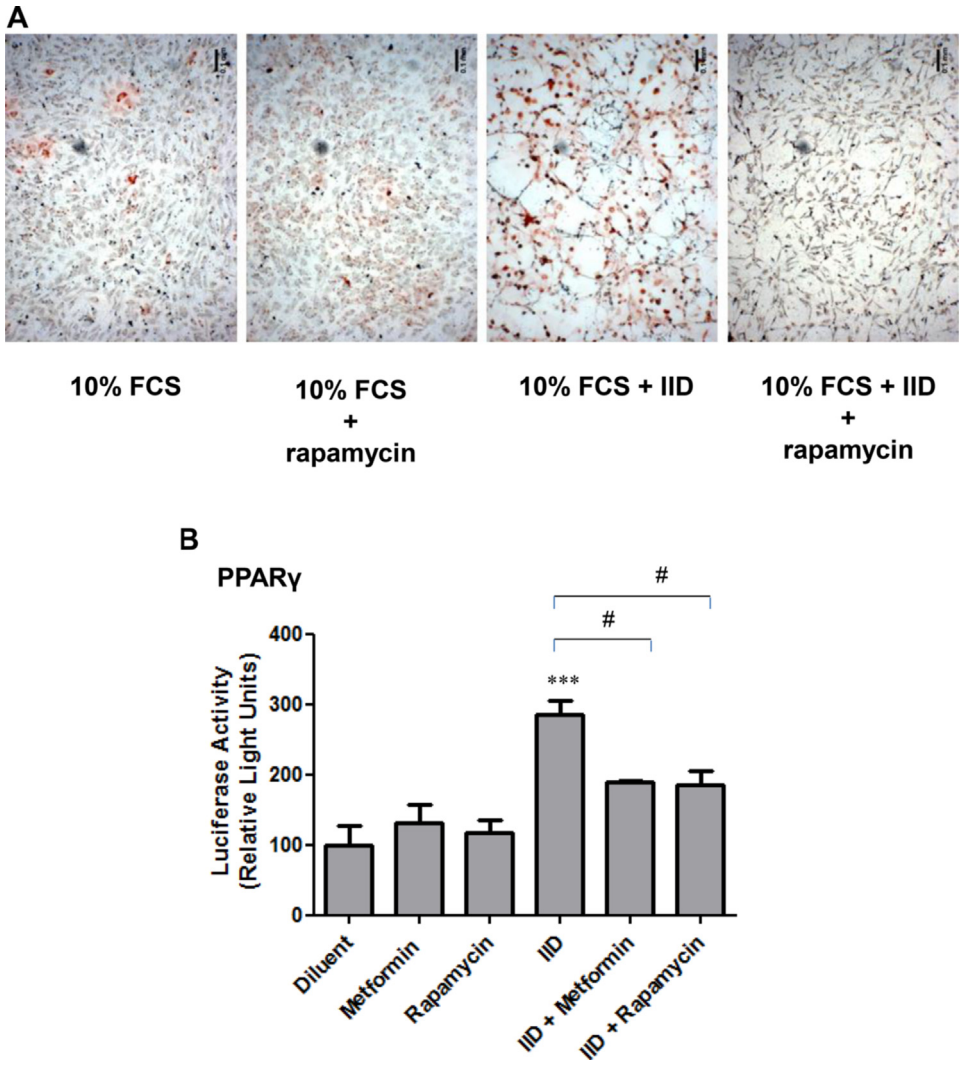

Fig. 4. The mTOR inhibitor, rapamycin, suppresses adipogenesis of C3H10T1/2 cells.
A) Confluent CH3H10T1/2 cells were induced to differentiate by addition of 10% foetal calf serum (FCS) supplemented with adipogenic cocktail (IID), in the presence or absence of the mTOR inhibitor, 10 μM rapamycin. After 5 days cells were fixed with formalin and stained with Oil Red O to detect neutral lipid accumulation. Representative micrographs from an experiment carried out on three separate occasions with similar results are shown.
B) Confluent C3H10T1/2 cells were transfected with PPARγ luciferase gene reporter construct, together with control *Renilla* luciferase vector and then stimulated for two days with 500 μM metformin or 10 μM rapamycin, in the presence or absence of IID. Cell extracts were then prepared and luciferase activity was measured using a dual luciferase reporter assay. Luciferase activities from three separate experiments are shown as means ± SEM. Significant increases in PPARγ activity are indicated ***, $p < 0.001$, as are significant decreases in PPARγ activity, #, $p < 0.05$, relative to IID-stimulated cells (n = 3).

phosphoric acid. A further 2 × 5 min water washes were performed on the phosphocellulose paper, before a final 5 min wash with 1% (v/v) phosphoric acid. A Beckman Multi-Purpose scintillation counter LS 6500 was used to measure [^{32}P]-labelled substrate. 3 ml of scintillation fluid was used per sample. Results were corrected for radioactivity recovered in blank reactions lacking the SAMS peptide. One unit of AMPK activity is that required to incorporate 1 nmol of ^{32}P into the SAMS substrate peptide/min/mg protein.

2.6. Transient transfection and luciferase assay

C3H10T1/2 cells were transfected with the indicated plasmids in 6-well plates, with 1.125 μg/well PPRE (PPARγ reporter, purchased from Adgene) and 6xOSE reporter constructs (Runx2 reporter, supplied by Jian Huang, Rush Medical Centre, Chicago, USA) using Lipofectamine 2000 reagent (Invitrogen, Carlsbad, CA) and then treated with metformin, A769662 or rapamycin with and without adipogenic differentiation media. Cells were then harvested 48 h after transfection and assayed using the Luciferase reporter assay system (Promega, Madison, WI) according to manufacturer's instructions. As a transfection control, the *Renilla* plasmid 0.125 μg/well was co-transfected in each transfection experiment, and the luciferase activity was normalised to the *Renilla* activity.

2.7. Statistical analysis

All experiments were performed in triplicate and statistical analysis was performed using Student's t-test or one-way ANOVA. Results are expressed as mean ± standard error (SEM) and differences with $p < 0.05$ were considered statistically significant.

3. Results

3.1. Metformin suppresses adipogenesis in C3H10T1/2 MSCs

It has been previously reported that treatment of preadipocyte cell lines with AMPK activators inhibits their conversion to fat cells (Lee et al., 2011, Habinowski and Witters, 2001). Paradoxically,

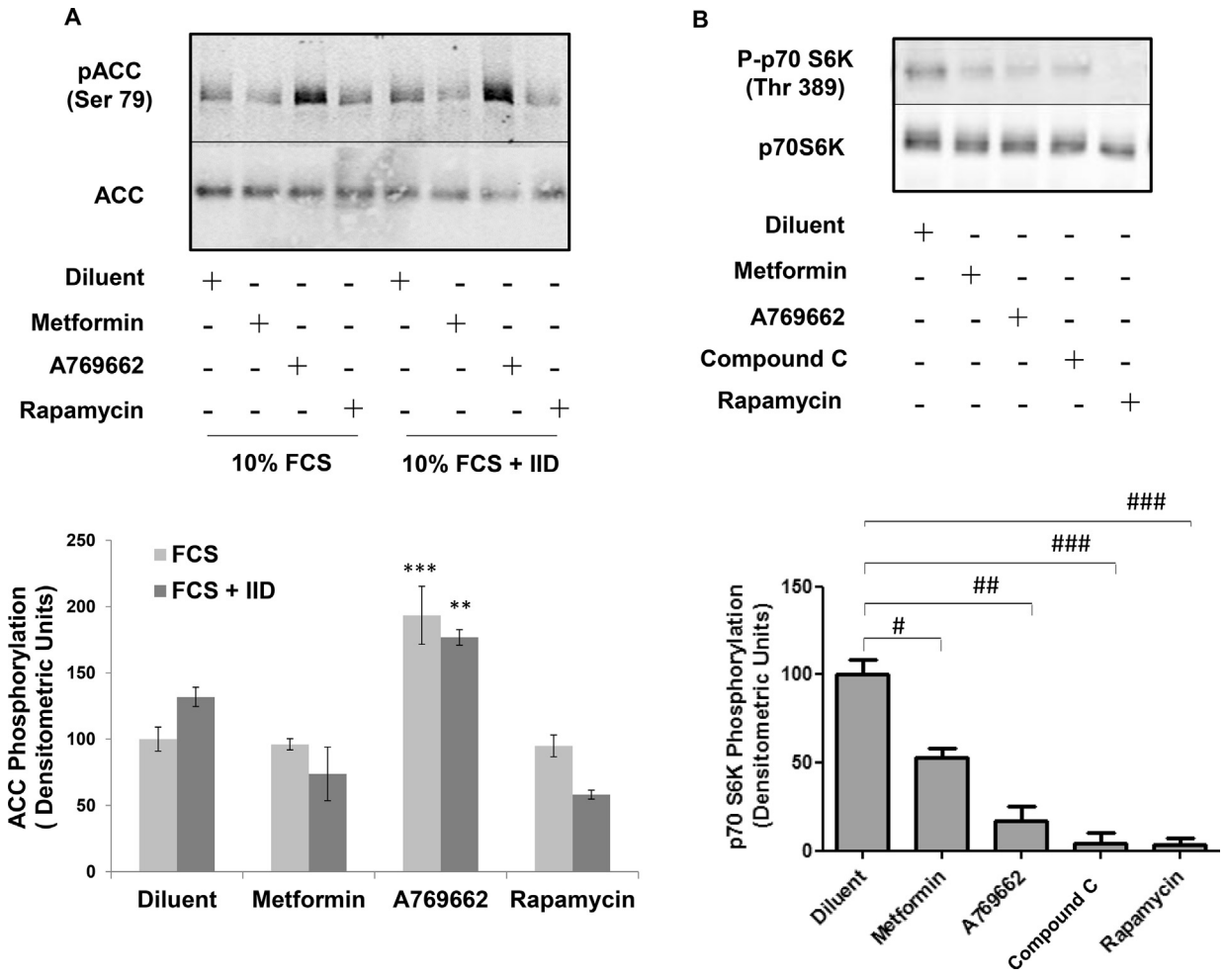

Fig. 5. Effects of rapamycin on AMPK and p70^{S6K} activities in C3H10T1/2 cells.
A) Confluent CH3H10T1/2 cells were stimulated for 5 days with IID, in the presence or absence of 500 μM metformin, 100 μM A769662, 10 μM rapamycin or the AMPK inhibitor, 10 μM compound C. Cell extracts were then prepared and immunoblotted with antibodies to phosphorylated ACC (Ser 79). Representative immunoblots from an experiment carried out on three separate occasions with similar results are shown (*upper panel*). Densitometric values from 3 separate experiments are shown in the *lower panel* as means ± SEM. Significant increases relative to control are indicated, **, $p < 0.01$ and ***, $p < 0.001$ (n = 3).
B) Confluent CH310T1/2 cells were stimulated for 5 days with IID, in the presence or absence of 500 μM metformin, 100 μM A769662, 10 μM compound C or 10 μM rapamycin. Cell extracts were then prepared and immunoblotted with antibodies to phosphorylated p70^{S6K} and total p70^{S6K}. Representative immunoblots from an experiment carried out on three separate occasions with similar results are shown in the *upper panel*. Densitometric analysis of mean ± SEM p70^{S6K} phosphorylation from 3 separate experiments are shown in the *lower panel*. Significant increases (*, $p < 0.05$) relative to control, and significant decreases relative to IID-stimulated cells (##, $p < 0.01$ and ###, $p < 0.001$), are indicated (n = 3).

however, the widely used AMPK inhibitor, compound C, has also been reported to inhibit adipogenesis of preadipocyte cell lines (Nam et al., 2008). To try and address this apparent contradiction and to further investigate the role of AMPK in the control of adipogenesis of multipotent mesenchymal stem cells (MSCs), we stimulated murine C3H10T1/2 MSCs with two known activators of AMPK, metformin (500 μM) and A769662 (100 μM). Confluent cultures of C3H10T1/2 MSCs were treated for 5 days with medium containing 10% foetal calf serum (FCS) supplemented with either an insulin-containing, adipogenic medium (IID) and/or the anti-diabetic drug, pioglitazone (PIO), which is a known agonist of the adipogenic transcription factor, PPARγ (Day and Bailey, 2007). Cells were also incubated with 10% FCS alone, as negative control for differentiation. After 5 days of treatment, cells were fixed and then stained with the neutral lipid stain, Oil Red O, to monitor lipid accumulation, which is a widely used late marker of adipogenesis (Fig. 1a). We found that treatment of cells with IID-containing medium stimulated lipid accumulation in C3H10T1/2 MSCs, an effect that was further enhanced by co-treatment of cells with PIO (Fig. 1a). We also found that treatment of cells with either metformin or A769662 suppressed adipogenesis promoted by IID alone or by a combination of IID plus PIO (Fig. 1A), with metformin being a more effective inhibitor of lipid accumulation (Fig. 1A). The effects of metformin on the suppression of adipogensis was confirmed by western blotting for two late markers of fat cell conversion, adiponectin and perilipin, the expression of which were strongly induced following IID treatment, but were suppressed in the presence of metformin (Fig. 1B).

These results suggest that AMPK activators inhibit adipogenesis of C3H10T1/2 MSCs. To further elucidate the mechanisms of action of metformin and A769662 in these cells, we next treated cells with 10% FCS, supplemented with either IID or PIO, and measured the protein expression levels of the transcription factor, PPARγ, which is a widely used early marker of adipogenesis (Fig. 2A and B). To complement these experiments, we also measured the activation of PPARγ transcriptional activity, by transfecting C3H10T1/2 cells with PPARγ-responsive luciferase reporter construct (Fig. 2C). We found that treatment of cells for 5 days with 10% FCS in the presence of either IID or PIO, induced a significant increase in the two PPARγ splice variants, PPARγ1 and PPARγ2 (Fig. 2A and B), which correlated with a significant increase in PPARγ transcriptional activity, as determined by luciferase assay (Fig. 2c). In agreement with the Oil

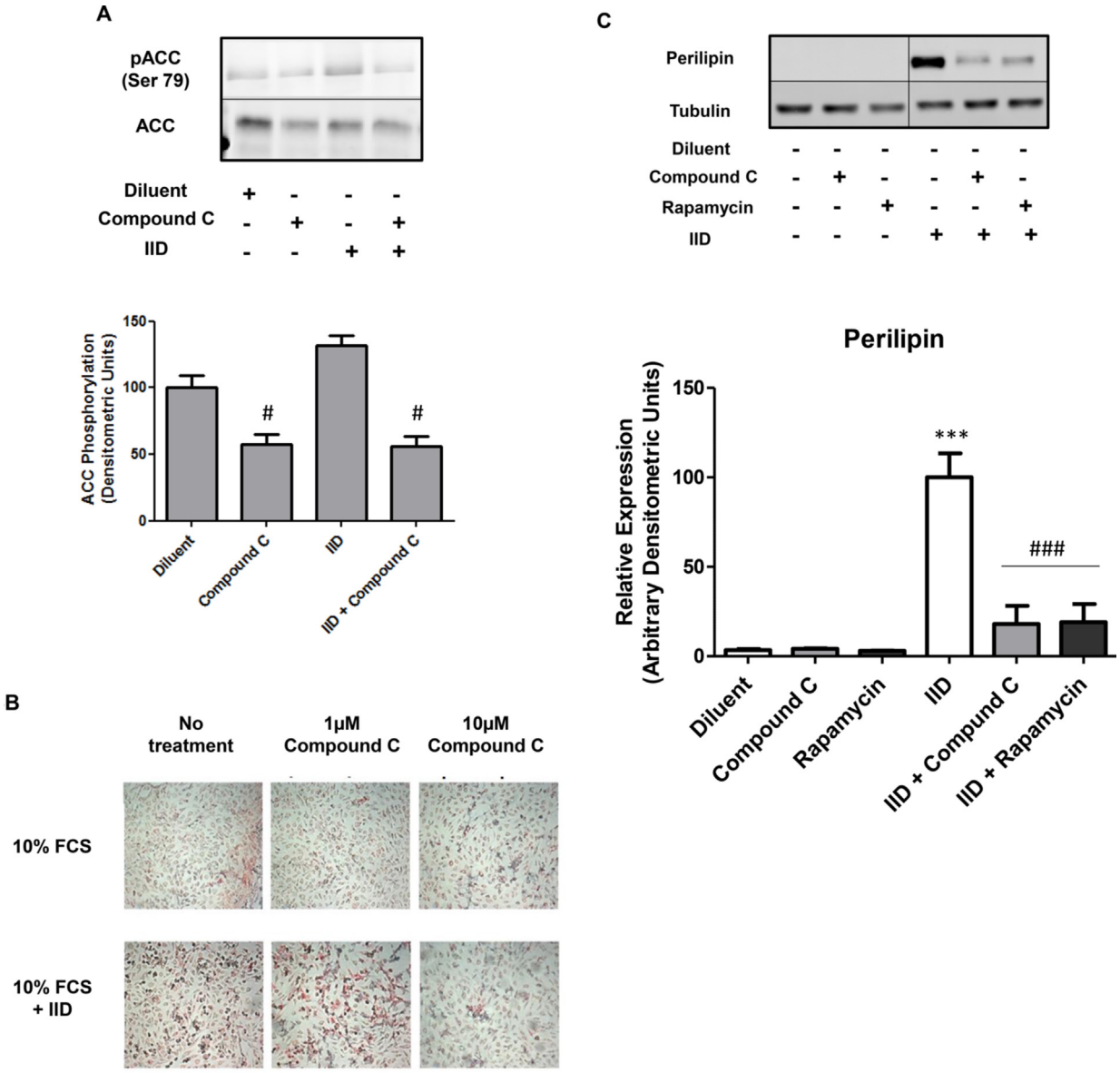

Fig. 6. Compound C inhibits adipogenesis of C3H10T1/2 cells.

A) Confluent CH3H10T1/2 cells were stimulated for 5 days with IID, in the presence or absence of the AMPK inhibitor, 10 μM compound C. Cell extracts were then prepared and immunoblotted with antibodies to phosphorylated ACC (Ser 79). Representative immunoblots from an experiment carried out on three separate occasions with similar results are shown (*upper panel*). Densitometric values from 3 separate experiments are shown in the *lower panel* as means ± SEM. Significant decreases relative to control are indicated, #, $p < 0.05$.

B) Confluent CH3H10T1/2 cells were treated with 10% FCS supplemented with adipogenic cocktail (IID), in the presence or absence of the indicated concentrations of compound C. After 5 days cells were fixed with formalin and stained with Oil Red O to detect neutral lipid accumulation. Representative micrographs from an experiment carried out on three separate occasions with similar results are shown.

C) Confluent CH3H10T1/2 MSCs were induced to differentiate by addition 10% FCS in the presence or absence of IID medium and/or 10 μM Compound C or 10 μM rapamycin. Cell extracts were then prepared after 5 days and immunoblotted with antibodies to perilipin and tubulin. Representative immunoblots from an experiment carried out on three separate occasions with similar results are shown. Densitometric analysis of three immunoblots are shown as means ± SEM in the *lower panel*. Significant increases relative to control are indicated, ***$p < 0.001$ and significant decreases with respect to IID-treated cells are indicated, ###, $p < 0.001$.

Red O staining experiments in Fig. 1, we found that treatment of cells with either metformin or A769662 effectively suppressed IID- and PIO-stimulated increases in PPARγ protein levels (Fig. 2A and B), as well as IID- and PIO-stimulated PPARγ activity (Fig. 2C), as determined by gene reporter assays. Given that increases in PPARγ activity during the early stages of adipogenesis are necessary and sufficient to promote terminal fat cell development (Rosen and Spiegelman, 2000), it appears that the ability of metformin and A769662 to inhibit adipogenesis of C3H10T1/2 MSCs is linked to their ability to suppresses increases in PPARγ protein levels promoted by treatment of cells with either IID or PIO. Moreover, given that the PPARγ luciferase reporter assays were carried out after only two days of differentiation, it appears that the suppressive actions of metformin and A769662 occur at a very early stage of the adipogenic process.

The control of differentiation of MSCs into fat and bone is thought to be controlled through reciprocal regulation of PPARγ and the osteogenic transcription factor, Runx2 (Jeon et al., 2003,Muruganandan et al., 2009), during the commitment stage of differentiation. We therefore also examined Runx2 protein levels (Fig. 2A and B) and activity (Fig. 2C). As a positive control for these experiments, cells were incubated with 10% FCS supplemented

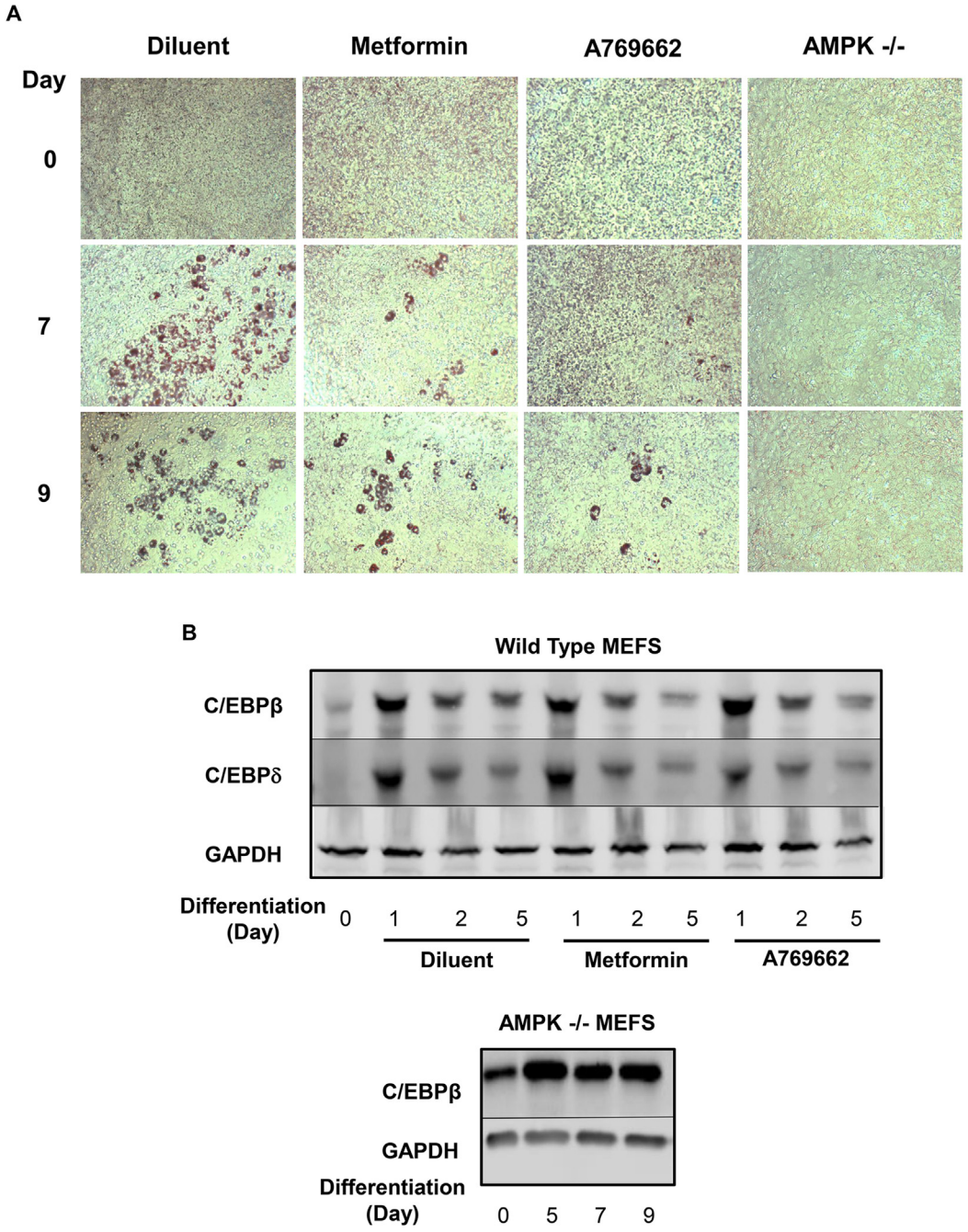
A
Diluent
Metformin
A769662
AMPK -/-
Day
0
7
9
B
Wild Type MEFS
C/EBPβ
C/EBPδ
GAPDH
Differentiation (Day)
0 1 2 5 1 2 5 1 2 5
Diluent
Metformin
A769662
AMPK -/- MEFS
C/EBPβ
GAPDH
Differentiation (Day)
0 5 7 9
C
#
***
**
***
ns
0 days
5 days
C/EBPβ expression (Densitometric units)
400
350
300
250
200
150
100
50
0
Diluent
Metformin
A769662
AMPK -/-
pACC (Ser 79)
pAMPK (Thr 172)
GAPDH
0 0.5 1 2 24 A769662
Metformin (hours)
*
*
ACC Phosphorylation (Densitometric Units)
400
300
200
100
0
0 0.5 1 2 24 A769662
Time (hours)

with a widely used osteogenic medium (AGD) (Shea et al., 2003) to induce Runx2 activity. We found that treatment of cells with 10% FCS plus AGD for 5 days did not significantly affect PPARγ protein levels (Fig. 2A and B) or activity (Fig. 2C). However, AGD treatment alone did promote a noticeable phosphorylation band-shift of Runx2 protein in treated cells (Fig. 2A), which correlated with an increase in Runx2 activity, as determined by a Runx2 gene reporter assay (Fig. 2C). Treatment with either metformin or A769662 significantly increased Runx2 activity in C3H10T1/2 cells (Fig. 2C), which did not correlate with an increase in AGD-promoted phospho-Runx2 levels, as determined by band-shift (Fig. 2A). Since osteogenesis and adipogenesis of MSCs are thought to be reciprocally regulated by the PPARγ:Runx2 activation ratio (Chen et al., 2016), we can conclude that the inhibitory actions of metformin and A769662 on the adipogenesis of C3H10T1/2 MSCs can partly be explained by reciprocal control of PPARγ and Runx2 activity, thereby favouring an osteogenic lineage. In addition, whereby the actions of metformin and A769662 appear to be through the suppression of adipogenic-dependent increases in PPARγ expression, the actions on Runx2 activity remain to be determined, but appear to be independent of osteogenic-linked increases in Runx2 phosphorylation (Fig. 2A).

3.2. Metformin suppresses adipogenesis in C3H10T1/2 MSCs through the inhibition of the p70^{S6K} signalling pathway and not through the activation of AMPK

Both metformin and A769662 are reported to activate AMPK in a variety of cell types (Zhou et al., 2001,Cool et al., 2006). Given the inhibitory effects of these two compounds on early and late markers of adipogenesis of C3H10T1/2 MSCs (Figs. 1 and 2), we next tested their ability to activate AMPK in these cells. We did this by measuring the phosphorylation of a known AMPK substrate, Ser 79 of acetyl coenzyme carboxylase (ACC), using phospho-specific antibodies. Intriguingly, although A769662 provoked a robust and rapid phosphorylation of ACC, which was maintained for up to 48 h, metformin did not induce a significant phosphorylation of ACC, even after 48 h stimulation (Fig. 3). It is likely, therefore, that while metformin is an effective inhibitor of the adipogenic differentiation of C3H10T1/2 MSCs, in response to insulin-containing IID medium, or activation of PPARγ by PIO, this occurs through mechanisms that are independent of AMPK activation. Recent work, however, has shown that the control of osteogenesis is regulated through interactions between PPARγ and the mTOR/p70^{S6K} signalling pathway (Sun et al., 2013). Moreover, metformin has been shown to inhibit the activation of the p70^{S6K} pathway independently of AMPK (Vazquez-Martin et al., 2009) in tumour cells and p70^{S6K} has been shown to be required for the growth hormone-dependent adipose conversion of 3T3-F442A preadipocytes (Yarwood et al., 1999). We therefore examined the role of the p70^{S6K} pathway on IID-induced adipogenesis of C3H10T1/2 cells by incubating cells with the mTOR/p70^{S6K} inhibitor, rapamycin. We found that incubation of differentiating cells with rapamycin dramatically inhibited lipid accumulation associated with adipogenesis, as determined by Oil Red O staining (Fig. 4A). Furthermore, rapamycin also suppressed PPARγ activity, as determined by gene reporter assays, indicating that the mTOR/p70^{S6K} pathway is required for adipogenesis of C3H10T1/2 cells (Fig. 4B). We found that the effects of rapamycin were specific to inhibition of mTOR/p70^{S6K}, since rapamycin treatment had no significant effect of phospho-ACC levels (Fig. 5A), indicating no effect on AMPK activity, but, rather, significantly inhibited phosphorylation of p70^{S6K} on Thr 389 (Fig. 5B), which is the mTOR phosphorylation site critical for kinase function (Saitoh et al., 2002). Importantly, both metformin and A769662 also inhibited p70^{S6K} phosphorylation (Fig. 5B), indicating that suppression of adipogenesis of C3H10T1/2 MSCs by these compounds may involve suppression of mTOR/p70^{S6K} signalling at early stages of commitment to differentiation.

Although we found that metformin inhibits mTOR/p70^{S6K} signalling apparently independently of AMPK activation (Figs. 3 and 5A), this does not rule out a role for AMPK in the control of p70^{S6K} activation. In fact, it has been reported that AMPK inhibits mTOR/p70^{S6K} signalling, which is thought to underlie the actions of metformin in a range of cellular contexts (Viollet et al., 2012,Dowling et al., 2011). To determine whether the same relationship exists in C3H10T1/2 MSCs, we incubated cells with the AMPK inhibitor, compound C, and determined its action on ACC (Ser 79) and p70^{S6K} (Thr 389) phosphorylation (Fig. 5A and B, respectively). We found that compound C significantly inhibited both basal p70^{S6K} (Thr 389; Fig. 5B) and ACC (Ser 79; Fig. 6A) phosphorylation, suggesting that AMPK is linked to the activation of mTOR/p70^{S6K} signalling in these cells. We also found that 10 μM compound C was able to inhibit adipogenesis of C3H10T1/2 cells treated with IID, as determined by lipid accumulation (Fig. 6B) and expression of the adipogeneic marker, perilipin (Fig. 6C), as well as suppressing AMPK activation in the presence or absence of IID (Fig. 6A). This suggests that basal levels of AMPK activity, perhaps acting through the mTOR/p70^{S6K} pathway (Fig. 5B), are important for supporting adipose conversion of these cells.

3.3. AMPK plays a dual role in regulating the adipogenesis of mouse embryonal fibroblasts (MEFs)

Our findings in C3H10T1/2 cells may provide the explanation for the apparently conflicting, previous reports that both activation AMPK and inhibition of AMPK block adipogenesis of 3T3-L1 preadipocytes (Lee et al., 2011, Habinowski and Witters, 2001,Nam et al., 2008). This has been suggested to be a result of AMPK exerting differential control during the process of differentiation; due to AMPK exerting different control at early time points versus late time points. Instead, we hypothesise there is a threshold level of AMPK activity required for adipogenesis, above which further activation leads to a break on the process. Indeed, it is worth noting that AMPK activity levels do not change significantly during

Fig. 7. Metformin suppresses adipogenesis in MEFs.

A) Wild type and AMPK knockout (−/−) mouse embryonic fibroblasts (MEFs) were treated with IID plus 10 μM pioglitazone (PIO) for 7 or 9 days as indicated. Wild type MEFs were also stimulated in the presence or absence of 1 mM metformin or 100 μM A769662. Cells were then stained with Oil Red O. Representative micrographs from an experiment carried out on three separate occasions with similar results are shown.

B) Confluent wild-type (*upper panel*) and AMPK−/− (*lower panel*) MEFs were stimulated for the indicated times with 10 μM pioglitazone (PIO) plus (IID) and, for wild-type MEFs, in the presence or absence of 1 mM metformin or 100 μM A769662. Cell extracts were then prepared and immunoblotted with antibodies to C/EBPβ and/or C/EBPδ, as indicated. Representative immunoblots from experiments carried out on three separate occasions with similar results are shown.

C) Densitometric values taken at day 5 from the experiment carried out in Fig. 7B are shown in the *lower panel* as means ± SEM. Significant increases in expression are indicated, **, $p < 0.01$ and ***, $p < 0.001$. Significant decreases relative to control are also indicated, #, $p < 0.05$. Non-significance is also indicated (ns).

D) Wild type MEFs were incubated with 1 mM metformin for the times indicated or with 100 μM A769662 for 30 min. Cells were then lysed and the lysates were immunoblotted with antibodies specific to the indicated proteins (*upper panel*). Results from densitometric analysis of three separate immunoblots are shown in the *lower panel* as means ± SEM. Significant increases relative to t = 0 are indicated, *, $p < 0.05$.

adipogeneis of 3T3-L1 preadipocytes (Supplementary Fig. 1) and C3H10T1/2 MSCs (unpublished observations) indicating that AMPK activity must be kept under stringent control to allow the differentiation of these cells. To investigate this relationship further, we next examined the effects of metformin and A769662 and adipogenesis in wild type and AMPKα knockout (−/−) mouse embryonal fibroblasts (MEFs). We first incubated wild type or AMPKα (−/−) MEFs with 10% FCS, in the presence or absence of a combination of adipogenic medium (IID) plus PIO, (Fig. 7A). Cells were then fixed and stained with Oil Red O at days 7 and 9, to monitor late-stage triglyceride accumulation (Fig. 7A), and cell extracts were prepared at days 1, 2 and 5, to detect levels of the early marker of differentiation, the transcription factor C/EBPβ, by western blotting (Fig. 7B). We found that a combination of IID and PIO promoted a large increase in lipid accumulation in wild type MEFs but not AMPKα (−/−) MEFs, at days 7 and 9 (Fig. 7A). We also found that after an initial increase in the expression of C/EBPβ and C/EBPδ at day 1 in wild type MEFs, following IID and PIO treatment, levels fell by day 5 but remained significantly above basal (Fig. 7B). This was not the case in AMPKα (−/−) MEFs, where C/EBPβ levels returned to basal by day 5 and remained at that level for up to 9 days of treatment with differentiation medium (Fig. 7B). These results suggest that a basal level of AMPKα is required for adipogenesis of MEFs and exerts actions on both early and late markers of adipose conversion. We next examine the effects of metformin and A769662 on adipogenesis of MEFs in response to IID and PIO treatment. We found that treatment of wild type MEFs with either metformin or A769662 led to a reduction in lipid accumulation (Fig. 7A) and C/EBPβ protein levels (Fig. 7B), indicating that both compounds are anti-adipogenic in these cells. We also found that both metformin (1 mM) and A769662 (100 μM) significantly increased phosphorylation of ACC at (Ser 79; Fig. 7C), indicating that they both exert their anti-adipogenic actions through the activation of AMPK. Together with the results obtained from CH310T1/2 MSCs this suggests that the role of AMPK in the control of adipogensis is complex, suggesting both positive and negative regulation that may depend on the cellular context. Moreover, the anti-adipogenic actions of the anti-diabetic drug, metformin, may be both AMPK-dependent and AMPK-independent, again depending on the cellular context.

4. Discussion

Previous work has shown that AMPK activation reduces adipogenesis in favour of osteogenesis in adipocyte-derived human MSCs (hMSCs) and bone marrow-derived MSCs (Kim et al., 2012,Lee et al., 2014). In the present work, we found that the AMPK activators, metformin and A769662, inhibited adipogenesis in murine C3H10T1/2 MSCs and in wild type MEFs. Both AMPK activators promoted a significant activation of AMPK in wild type MEFs, although, interestingly, we found that metformin, did not promote AMPK activation in C3H10T1/2 cells (Fig. 3). Metformin has been shown to activate AMPK in many different cell types; however a requirement of AMPK for the therapeutic actions of metformin has been questioned following genetic loss of function experiments that demonstrated AMPK-independent mechanisms of action of metformin during the inhibition of hepatic gluconeogenesis (Foretz et al., 2010). The AMPK-independent action of metformin on the inhibition of adipogenesis reported here might be due to cell type specific effects or stage-specific effects during the differentiation process. For example, most of the studies demonstrating an AMPK-dependent action of metformin were conducted in more differentiated cell lines, such as pre-osteoblasts (Jang et al., 2011, Kanazawa et al., 2008,Cortizo et al., 2006), pre-adipocytes (Moreno-Navarrete et al., 2011,Lee et al., 2012), myoblasts (Longnus et al., 2005,Kobashigawa et al., 2014,Fulco et al., 2008) and neuronal mouse cell lines (Bang et al., 2014), instead of the more primitive cell progenitors investigated here.

With regards to stage-specific effects, Pantovic et al. (Pantovic et al., 2013) demonstrated that there is a coordinated time-dependent activation of different signalling pathways during the osteogenic differentiation of hMSCs, which is AMPK-dependent in the early stages of differentiation followed by late stage activation of the Akt/mTOR signalling pathway. Given the results presented here, it could be argued that similar mechanisms might regulate adipogenesis in murine MSCs. For example, we find an overall requirement for basal levels of AMPK activity for adipogenesis of C3H10T1/2 cells, as demonstrated by the use of the AMPK inhibitor compound C (Fig. 6B) and verified by the use of AMPK knockout (−/−) MEFs (Fig. 7A). It should be noted, however, that AMPK activity levels remain constant throughout the process of adipogenesis, as determined by AMPK activation assays (Supplementary Fig. 1) and phosphorylation of ACC on Ser 79 (results not shown). Despite this, the ability of metformin to inhibit adipogenesis was found to be due to a reduction in the PPARγ:Runx2 activation ratio (Fig. 2C) and this was linked to the inhibition of mTOR/p70^{S6K} signalling (Fig. 4). This suggests that the ability of metformin to control the commitment of MSCs to differentiate into either osteoblasts or adipocytes is governed at an early stage through the inhibition of mTOR/p70^{S6K} signalling. Moreover, wild type MEFs were observed to accumulate lipid and increase expression of C/EBPβ in response to an adipogenic cocktail of IID plus PIO (Fig. 7). These effects were blocked in AMPK (−/−) MEFs, which may indicate that AMPK is required for efficient, late stage lipid accumulation or, since AMPK is involved in mitochondrial biogenesis, altered mitochondrial function (Bergeron et al., 2001).

Overall, our work suggests that metformin exerts multiple effects to inhibit adipogenesis in different cell types. Therefore, the overriding view that metformin exerts its effects on adipogenesis simply by promoting AMPK activation may therefore need some revision. In particular, the role of AMPK itself appears to be complex, in that it appears to exert both positive and negative effects during the adipogenic conversion of MEFs and C3H10T1/2 MSCs. In conclusion, further investigation into how metformin suppresses signalling through the mTOR/p70^{S6K} pathway may lead to new therapeutic intervention strategies to prevent unwanted bone marrow adipogenesis associated with diseases, such as T2DM, where bone health is impaired.

Acknowledgements

This work was funded by a research project grant from Tenovus Scotland (grant number S13/15), awarded to SJY, IPS and SFA, a Diabetes UK Equipment Grant (grant number BDA: 11/0004309), awarded to SJY and IPS, and a British Heart Foundation Project Grant (grant number PG/15/15/31316) awarded to SJY.

Appendix A. Supplementary data

Supplementary data related to this article can be found at http://dx.doi.org/10.1016/j.mce.2016.11.011.

References

Banerjee, C., McCabe, L.R., Choi, J.Y., Hiebert, S.W., Stein, J.L., Stein, G.S., Lian, J.B., 1997. Runt homology domain proteins in osteoblast differentiation: AML3/CBFA1 is a major component of a bone-specific complex. J. Cell Biochem. 66, 1–8.

Bang, S., Chen, Y., Ahima, R.S., Kim, S.F., 2014. Convergence of IPMK and LKB1-AMPK signaling pathways on metformin action. Mol. Endocrinol. 28, 1186–1193.

Bergeron, R., Ren, J.M., Cadman, K.S., Moore, I.K., Perret, P., Pypaert, M., Young, L.H.,

Semenkovich, C.F., Shulman, G.I., 2001. Chronic activation of AMP kinase results in NRF-1 activation and mitochondrial biogenesis. Am. J. Physiol. Endocrinol. Metab. 281, E1340–E1346.
Cao, Z., Umek, R.M., McKnight, S.L., 1991. Regulated expression of three C/EBP isoforms during adipose conversion of 3T3-L1 cells. Genes Dev. 5, 1538–1552.
Chen, Q., Shou, P., Zheng, C., Jiang, M., Cao, G., Yang, Q., Cao, J., Xie, N., Velletri, T., Zhang, X., Xu, C., Zhang, L., Yang, H., Hou, J., Wang, Y., Shi, Y., 2016. Fate decision of mesenchymal stem cells: adipocytes or osteoblasts? Cell Death Differ. 0000023, 1128–1139.
Cool, B., Zinker, B., Chiou, W., Kifle, L., Cao, N., Perham, M., Dickinson, R., Adler, A., Gagne, G., Iyengar, R., Zhao, G., Marsh, K., Kym, P., Jung, P., Camp, H.S., Frevert, E., 2006. Identification and characterization of a small molecule AMPK activator that treats key components of type 2 diabetes and the metabolic syndrome. Cell Metab. 3, 403–416.
Cortizo, A.M., Sedlinsky, C., McCarthy, A.D., Blanco, A., Schurman, L., 2006. Osteogenic actions of the anti-diabetic drug metformin on osteoblasts in culture. Eur. J. Pharmacol. 536, 38–46.
Cusi, K., Consoli, A., DeFronzo, R.A., 1996. Metabolic effects of metformin on glucose and lactate metabolism in noninsulin-dependent diabetes mellitus. J. Clin. Endocrinol. Metab. 81, 4059–4067.
Day, C., Bailey, C.J., 2007. Pioglitazone a2-enna, S.J. xPharm. In: Bylund, D.B. (Ed.), The Comprehensive Pharmacology Reference. Elsevier, New York, pp. 1–4.
Dowling, R.J., Goodwin, P.J., Stambolic, V., 2011. Understanding the benefit of metformin use in cancer treatment. BMC Med. 9, 33.
El-Mir, M.Y., Nogueira, V., Fontaine, E., Averet, N., Rigoulet, M., Leverve, X., 2000. Dimethylbiguanide inhibits cell respiration via an indirect effect targeted on the respiratory chain complex I. J. Biol. Chem. 275, 223–228.
Foretz, M., Hebrard, S., Leclerc, J., Zarrinpashneh, E., Soty, M., Mithieux, G., Sakamoto, K., Andreelli, F., Viollet, B., 2010. Metformin inhibits hepatic gluconeogenesis in mice independently of the LKB1/AMPK pathway via a decrease in hepatic energy state. J. Clin. Invest. 120, 2355–2369.
Fulco, M., Cen, Y., Zhao, P., Hoffman, E.P., McBurney, M.W., Sauve, A.A., Sartorelli, V., 2008. Glucose restriction inhibits skeletal myoblast differentiation by activating SIRT1 through AMPK-mediated regulation of Nampt. Dev. Cell. 14, 661–673.
Grey, A., Bolland, M., Gamble, G., Wattie, D., Horne, A., Davidson, J., Reid, I.R., 2007. The peroxisome proliferator-activated receptor-gamma agonist rosiglitazone decreases bone formation and bone mineral density in healthy postmenopausal women: a randomized, controlled trial. J. Clin. Endocrinol. Metab. 92, 1305–1310.
Habinowski, S.A., Witters, L.A., 2001. The effects of AICAR on adipocyte differentiation of 3T3-L1 cells. Biochem. Biophys. Res. Commun. 286, 852–856.
Hardie, D.G., 2015. AMPK: positive and negative regulation, and its role in whole-body energy homeostasis. Curr. Opin. Cell Biol. 33, 1–7.
Hawley, S.A., Pan, D.A., Mustard, K.J., Ross, L., Bain, J., Edelman, A.M., Frenguelli, B.G., Hardie, D.G., 2005. Calmodulin-dependent protein kinase kinase-beta is an alternative upstream kinase for AMP-activated protein kinase. Cell Metab. 2, 9–19.
Hothersall, E.J., Livingstone, S.J., Looker, H.C., Ahmed, S.F., Cleland, S., Leese, G.P., Lindsay, R.S., McKnight, J., Pearson, D., Philip, S., Wild, S.H., Colhoun, H.M., 2013. Contemporary risk of hip fracture in type 1 and type 2 diabetes: a national registry study from Scotland. J. Bone Min. Res.
Jang, W.G., Kim, E.J., Bae, I.H., Lee, K.N., Kim, Y.D., Kim, D.K., Kim, S.H., Lee, C.H., Franceschi, R.T., Choi, H.S., Koh, J.T., 2011. Metformin induces osteoblast differentiation via orphan nuclear receptor SHP-mediated transactivation of Runx2. Bone 48, 885–893.
Janghorbani, M., Van Dam, R.M., Willett, W.C., Hu, F.B., 2007. Systematic review of type 1 and type 2 diabetes mellitus and risk of fracture. Am. J. Epidemiol. 166, 495–505.
Jeon, M.J., Kim, J.A., Kwon, S.H., Kim, S.W., Park, K.S., Park, S.W., Kim, S.Y., Shin, C.S., 2003. Activation of peroxisome proliferator-activated receptor-gamma inhibits the Runx2-mediated transcription of osteocalcin in osteoblasts. J. Biol. Chem. 278, 23270–23277.
Jones, R.G., Plas, D.R., Kubek, S., Buzzai, M., Mu, J., Xu, Y., Birnbaum, M.J., Thompson, C.B., 2005. AMP-activated protein kinase induces a p53-dependent metabolic checkpoint. Mol. Cell. 18, 283–293.
Kanazawa, I., Yamaguchi, T., Yano, S., Yamauchi, M., Sugimoto, T., 2008. Metformin enhances the differentiation and mineralization of osteoblastic MC3T3-E1 cells via AMP kinase activation as well as eNOS and BMP-2 expression. Biochem. Biophys. Res. Commun. 375, 414–419.
Kilpadi, K.L., Eldabaje, R., Schmitz, J.E., Ehler, B., Thames, T.A., Joshi, A.P., Simmons 3rd, J.W., Michalek, J.E., Fajardo, R.J., 2014. Type 2 diabetes is associated with vertebral fractures in a sample of clinic- and hospital-based Latinos. J. Immigr. Minor Health 16, 440–449.
Kim, E.K., Lim, S., Park, J.M., Seo, J.K., Kim, J.H., Kim, K.T., Ryu, S.H., Suh, P.G., 2012. Human mesenchymal stem cell differentiation to the osteogenic or adipogenic lineage is regulated by AMP-activated protein kinase. J. Cell Physiol. 227, 1680–1687.
Kobashigawa, L.C., Xu, Y.C., Padbury, J.F., Tseng, Y.T., Yano, N., 2014. Metformin protects cardiomyocyte from doxorubicin induced cytotoxicity through an AMP-activated protein kinase dependent signaling pathway: an in vitro study. PLoS One 9, e104888.
Lantier, L., Fentz, J., Mounier, R., Leclerc, J., Treebak, J.T., Pehmoller, C., Sanz, N., Sakakibara, I., Saint-Amand, E., Rimbaud, S., Maire, P., Marette, A., Ventura-Clapier, R., Ferry, A., Wojtaszewski, J.F., Foretz, M., Viollet, B., 2014. AMPK controls exercise endurance, mitochondrial oxidative capacity, and skeletal muscle integrity. Faseb J. 28, 3211–3224.
Lecka-Czernik, B., 2009. Bone as a target of type 2 diabetes treatment. Curr. Opin. Investig. Drugs 10, 1085–1090.
Lecka-Czernik, B., Ackert-Bicknell, C., Adamo, M.L., Marmolejos, V., Churchill, G.A., Shockley, K.R., Reid, I.R., Grey, A., Rosen, C.J., 2007. Activation of peroxisome proliferator-activated receptor gamma (PPARgamma) by rosiglitazone suppresses components of the insulin-like growth factor regulatory system in vitro and in vivo. Endocrinology 148, 903–911.
Lee, H., Kang, R., Bae, S., Yoon, Y., 2011. AICAR, an activator of AMPK, inhibits adipogenesis via the WNT/beta-catenin pathway in 3T3-L1 adipocytes. Int. J. Mol. Med. 28, 65–71.
Lee, J.O., Lee, S.K., Kim, J.H., Kim, N., You, G.Y., Moon, J.W., Kim, S.J., Park, S.H., Kim, H.S., 2012. Metformin regulates glucose transporter 4 (GLUT4) translocation through AMP-activated protein kinase (AMPK)-mediated Cbl/CAP signaling in 3T3-L1 preadipocyte cells. J. Biol. Chem. 287, 44121–44129.
Lee, S., Cho, H.Y., Bui, H.T., Kang, D., 2014. The osteogenic or adipogenic lineage commitment of human mesenchymal stem cells is determined by protein kinase C delta. BMC Cell Biol. 15, 42.
Longnus, S.L., Segalen, C., Giudicelli, J., Sajan, M.P., Farese, R.V., Van Obberghen, E., 2005. Insulin signalling downstream of protein kinase B is potentiated by 5'AMP-activated protein kinase in rat hearts in vivo. Diabetologia 48, 2591–2601.
Moreno-Navarrete, J.M., Ortega, F.J., Rodriguez-Hermosa, J.I., Sabater, M., Pardo, G., Ricart, W., Fernandez-Real, J.M., 2011. OCT1 Expression in adipocytes could contribute to increased metformin action in obese subjects. Diabetes 60, 168–176.
Morrow, V.A., Foufelle, F., Connell, J.M., Petrie, J.R., Gould, G.W., Salt, I.P., 2003. Direct activation of AMP-activated protein kinase stimulates nitric-oxide synthesis in human aortic endothelial cells. J. Biol. Chem. 278, 31629–31639.
Muruganandan, S., Roman, A.A., Sinal, C.J., 2009. Adipocyte differentiation of bone marrow-derived mesenchymal stem cells: cross talk with the osteoblastogenic program. Cell Mol. Life Sci. 66, 236–253.
Nam, M., Lee, W.H., Bae, E.J., Kim, S.G., 2008. Compound C inhibits clonal expansion of preadipocytes by increasing p21 level irrespectively of AMPK inhibition. Arch. Biochem. Biophys. 479, 74–81.
Pantovic, A., Krstic, A., Janjetovic, K., Kocic, J., Harhaji-Trajkovic, L., Bugarski, D., Trajkovic, V., 2013. Coordinated time-dependent modulation of AMPK/Akt/mTOR signaling and autophagy controls osteogenic differentiation of human mesenchymal stem cells. Bone 52, 524–531.
Reihill, J.A., Ewart, M.A., Hardie, D.G., Salt, I.P., 2007. AMP-activated protein kinase mediates VEGF-stimulated endothelial NO production. Biochem. Biophys. Res. Commun. 354, 1084–1088.
Rosen, E.D., Spiegelman, B.M., 2000. Molecular regulation of adipogenesis. Annu. Rev. Cell Dev. Biol. 16, 145–171.
Saitoh, M., Pullen, N., Brennan, P., Cantrell, D., Dennis, P.B., Thomas, G., 2002. Regulation of an activated S6 kinase 1 variant reveals a novel mammalian target of rapamycin phosphorylation site. J. Biol. Chem. 277, 20104–20112.
Salminen, A., Hyttinen, J.M., Kaarniranta, K., 2011. AMP-activated protein kinase inhibits NF-kappaB signaling and inflammation: impact on healthspan and lifespan. J. Mol. Med. Berl. 89, 667–676.
Salt, I.P., Palmer, T.M., 2012. Exploiting the anti-inflammatory effects of AMP-activated protein kinase activation. Expert Opin. Investig. Drugs 21, 1155–1167.
Schwartz, A.V., Sellmeyer, D.E., Vittinghoff, E., Palermo, L., Lecka-Czernik, B., Feingold, K.R., Strotmeyer, E.S., Resnick, H.E., Carbone, L., Beamer, B.A., Park, S.W., Lane, N.E., Harris, T.B., Cummings, S.R., 2006. Thiazolidinedione use and bone loss in older diabetic adults. J. Clin. Endocrinol. Metab. 91, 3349–3354.
Shea, C.M., Edgar, C.M., Einhorn, T.A., Gerstenfeld, L.C., 2003. BMP treatment of C3H10T1/2 mesenchymal stem cells induces both chondrogenesis and osteogenesis. J. Cell Biochem. 90, 1112–1127.
Shockley, K.R., Lazarenko, O.P., Czernik, P.J., Rosen, C.J., Churchill, G.A., Lecka-Czernik, B., 2009. PPARgamma2 nuclear receptor controls multiple regulatory pathways of osteoblast differentiation from marrow mesenchymal stem cells. J. Cell Biochem. 106, 232–246.
Sun, H., Kim, J.K., Mortensen, R., Mutyaba, L.P., Hankenson, K.D., Krebsbach, P.H., 2013. Osteoblast-targeted suppression of PPARgamma increases osteogenesis through activation of mTOR signaling. Stem Cells 31, 2183–2192.
Tontonoz, P., Hu, E., Graves, R.A., Budavari, A.I., Spiegelman, B.M., 1994. mPPAR gamma 2: tissue-specific regulator of an adipocyte enhancer. Genes Dev. 8, 1224–1234.
Tontonoz, P., Hu, E., Spiegelman, B.M., 1994. Stimulation of adipogenesis in fibroblasts by PPAR gamma 2, a lipid-activated transcription factor. Cell 79, 1147–1156.
Vazquez-Martin, A., Oliveras-Ferraros, C., Menendez, J.A., 2009. The antidiabetic drug metformin suppresses HER2 (erbB-2) oncoprotein overexpression via inhibition of the mTOR effector p70S6K1 in human breast carcinoma cells. Cell Cycle 8, 88–96.
Vila-Bedmar, R., Lorenzo, M., Fernandez-Veledo, S., 2010. Adenosine 5'-monophosphate-activated protein kinase-mammalian target of rapamycin cross talk regulates brown adipocyte differentiation. Endocrinology 151, 980–992.
Viollet, B., Guigas, B., Sanz Garcia, N., Leclerc, J., Foretz, M., Andreelli, F., 2012. Cellular and molecular mechanisms of metformin: an overview. Clin. Sci. (Lond) 122, 253–270.
Woods, A., Johnstone, S.R., Dickerson, K., Leiper, F.C., Fryer, L.G., Neumann, D., Schlattner, U., Wallimann, T., Carlson, M., Carling, D., 2003. LKB1 is the upstream kinase in the AMP-activated protein kinase cascade. Curr. Biol. 13, 2004–2008.

Yarwood, S.J., Sale, E.M., Sale, G.J., Houslay, M.D., Kilgour, E., Anderson, N.G., 1999. Growth hormone-dependent differentiation of 3T3-F442A preadipocytes requires Janus kinase/signal transducer and activator of transcription but not mitogen-activated protein kinase or p70 S6 kinase signaling. J. Biol. Chem. 274, 8662–8668.

Yeh, W.C., Cao, Z., Classon, M., McKnight, S.L., 1995. Cascade regulation of terminal adipocyte differentiation by three members of the C/EBP family of leucine zipper proteins. Genes Dev. 9, 168–181.

Zhou, G., Myers, R., Li, Y., Chen, Y., Shen, X., Fenyk-Melody, J., Wu, M., Ventre, J., Doebber, T., Fujii, N., Musi, N., Hirshman, M.F., Goodyear, L.J., Moller, D.E., 2001. Role of AMP-activated protein kinase in mechanism of metformin action. J. Clin. Invest. 108, 1167–1174.

Molecular and Cellular Endocrinology 443 (2017) 176

Contents lists available at ScienceDirect

Molecular and Cellular Endocrinology

journal homepage: www.elsevier.com/locate/mce

Corrigendum

Corrigendum to "Metformin suppresses adipogenesis through both AMP-activated protein kinase (AMPK)-dependent and AMPK-independent mechanisms" [Mol. Cell. Endocrinol. 440 15 January 2017 57–68]

S.C. Chen [a, d], R. Brooks [a], J. Houskeeper [b], S.K. Bremner [b], J. Dunlop [b], B. Viollet [c, d, e], P.J. Logan [f], I.P. Salt [f], S.F. Ahmed [a], S.J. Yarwood [g, *]

[a] The Developmental Endocrinology Research Group, School of Medicine, University of Glasgow, Glasgow G51 4TF, UK
[b] Institute of Molecular, Cell and Systems Biology, University Avenue, University of Glasgow, Glasgow G12 8QQ, UK
[c] INSERM, U1016, Institut Cochin, Paris, France
[d] CNRS, UMR8104, Paris, France
[e] Université Paris Descartes, Sorbonne Paris Cité, France
[f] Institute of Cardiovascular and Medical Sciences, University Avenue, University of Glasgow, Glasgow G12 8QQ, UK
[g] Institute of Biological Chemistry, Biophysics and Bioengineering, Edinburgh Campus, Heriot-Watt University, Edinburgh EH14 4AS, UK

The authors regret that the crop lines in the western blot in Figure 6c were put in the wrong place when the figure was prepared. The corrected version of the figure is:

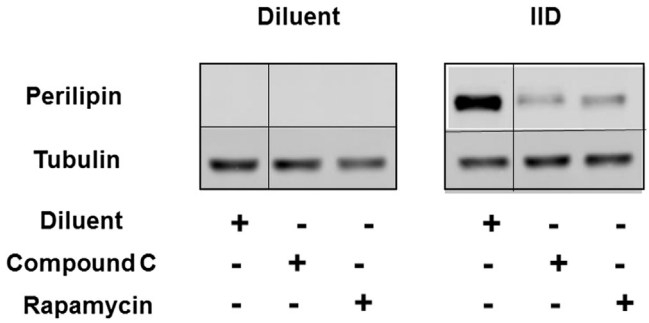

Revising the figure does not alter the densitometry measurements we made or change the conclusions we draw from the data. The authors would like to apologise for any inconvenience caused.

DOI of original article: http://dx.doi.org/10.1016/j.mce.2016.11.011.
* Corresponding author.
E-mail address: S.Yarwood@hw.ac.uk (S.J. Yarwood).

http://dx.doi.org/10.1016/j.mce.2017.01.049
0303-7207